AN ABSTRACT OF THE THESIS OF

Thomas Dean Yager for the degree of Doctor of Philosophy in Biochemistry and Biophysics, presented on September 28, 1984.

Title: Nucleosome Instabilities in Physiological Salt.

Redacted for Privacy

Abstract approved: _____

K.E. van Holde

Part 1 of this thesis reviews the known dynamical processes of DNA, histones and nucleosomes.

Part 2 presents research on salt-induced nucleosome dissociation. In elevated [NaCl], dissociation occurs within minutes to hours, to generate free DNA. Dissociation is reversible (or nearly so), and is enhanced by nucleosome dilution; thus it appears to be an equilibrium phenomenon.

Upon exposure of nucleosome core particles to 0.35-0.75 M NaCl, a second reversible transition is observed, on a much faster time-scale (thesis, part 3). This fast transition results in a 15% decrease in $s_{20,w}$. It also involves an increase in circular dichroism around 280 nm, amounting to

35-40% of the difference in CD between free DNA and native core particles. The fast transition is interpreted in terms of a two-state model: the core particle is envisioned to move from the native state into a new state, where some portion of its DNA is now more like the solution "B" form. The CD increase (assayed in 0.65 M NaCl) is temperature independent over 5-35 C. This is interpreted (via the two-state model) to mean that the fast transition is entropy-driven.

From a consideration of both these data and published studies, we suggest that the fast transition involves the release of two 25-30 bp DNA "termini" from the histone core. Under this model, we calculate that 5-7 DNA/histone bonds are broken in the release of each terminus. From oligopeptide/DNA binding data, we calculate these bonds to be at least as strong as oligoarginine/DNA bonds; thus they probably have substantial non-electrostatic character.

Part 4 of this thesis describes a test system with which to monitor the sliding of histone cores along DNA. Single-end-labelled 195 bp <u>Lytichinus variegatus</u> 5S rDNA (+ flanking regions) serves as a DNA substrate upon which nucleosomes are reconstituted in a uniquely phased arrangement. A quantitative analysis of the loss of phasing expected from core sliding is presented.

# Nucleosome Instabilities in Physiological Salt

by

Thomas D. Yager

A THESIS

submitted to

Oregon State University

in partial fulfillment of
the requirements for the
degree of

Doctor of Philosophy

Completed September 28, 1984

Commencement June 1985

APPROVED:

Redacted for Privacy

Professor of Biochemistry and Biophysics in charge of major

Redacted for Privacy

Chairman of Department of Biochemistry and Biophysics

Redacted for Privacy

Dean of Graduate School

Redacted for Privacy

Date thesis presented

Typed by Nanette C. Cardon for Thomas D. Yager

Acknowledgements

I would like to thank many people for comments, criticism and advice: G. Ackers, K. Ahern, G. Bailey, E.M. Bradbury, D. Brooker, J. Davie, H. Eisenberg, E. Farifield, G. Fasman, G. Felsenfeld, R. Harrington, G. Ide, I. Isenberg, W.C. Johnson, D. Lohr, C. McMurray, P. Meagher, D. Ornstein, A. Paton, J. Proffitt, G. Riedel, C. Saunders, M. Schimerlik, H. Schaup, R.T. Simpson, M. Soumpasis, L. Ulanovsky, P.H. von Hippel, S. Weber, H. Wickman, F. Ziemer. Thanks also are due to E. Gillman, R. Moyer, C. Poklemba and G. Riedel for expert technical help on various experimental problems, and to I. Isenberg, P. Meagher, T. Tibbitts and M. Zephus for computer programs used in data analysis.

I would like to express appreciation to Deborah Brooker, for much patience and moral support.

I am most grateful to have had the opportunity to work under Ken van Holde, a man of uncommon brilliance and humanity.

This thesis is dedicated to the memory of my parents, and to the memory of Irv Isenberg.

TABLE OF CONTENTS

Page

Part 1

A review of nucleosome dynamics 1

I. The nucleosome as a changeable structure. 1. An emerging perspective 2

II. The dynamics of B-DNA 4

A. Intrinsic DNA motions 6

1. Motions within the "B" form 6

a. Motions deduced from the analysis of x-ray diffraction patterns 7

b. Motions predicted by potential energy-vs.-conformation models 9

c. Motions deduced from spectroscopic measurements 13

2. Transitions out of the "B" form 17

a. Rupture of hydrogen bonds between complementary bases 18

b. Highly localized transitions from B- to other DNA forms 19

B. The dynamics of solvent bound to DNA 20

1. A view of the dynamics of DNA-bound solvent, with emphasis on hydration 21

a. Definitions of hydration 21

b. The structure of the hydration layer(s) of DNA 24

2. A view of the dynamics of DNA-bound solvent, with emphasis on ions 25

Page

a. A brief review of counterion condensation theory 26

b. The effect of bulk salt concentration on the condensed layer of counterions 28

3. Attempts at integrating hydration- and ion-binding data 29

C. The interaction of DNA with its bound solvent 29

1. DNA flexibility 29

2. The sensitivity of DNA winding to concentration and type of salt 32

3. The (putative) B-to-C transition 35

4. The B-to-A transition 36

5. The B-to-Z transition 36

6. The relevance of counterion condensation theory to chromatin studies 38

III. The dynamics of the (purified) histone core 39

A. Rapid motions of the core 39

B. Changes in the hydration of the core 41

C. Equilibria between the histones of the core 41

1. The monomer/tetramer equilibrium of H3 and H4 42

2. The monomer/dimer equilibrium of H2A and H2B 44

3. The "mixed" equilibria of H2A and H3, H2B and H3, H2A and H4, and H2B and H4 45

4. The association of the (H3.H4)2 tetramer with (H2A.H2B) dimers 47

IV. The nucleosome as a changeable structure. 2. Five principles of nucleosome structure which delimit and predict nucleosome dynamics 51

Page

A. The differential stabilities of different bonding domains within the histone core 52

1. High stability of bonding domains within the (H3.H4)2 tetramer 52

2. High stability of bonding domains within the (H2A.H2B) dimer 55

3. Marginal stability of bonding domains between the (H3.H4)2 tetramer and the (H2A.H2B) dimer 56

B. The torsional stress placed upon the DNA and the histone core from bending the DNA about the core 58

C. The electrostatic repulsion between adjacent loops of DNA in a nucleosome 59

D. The release of bound counterions from the DNA (and possibly also from the histone core), upon binding the DNA to the core 61

E. The "degeneracy" of the domain of bonding between the DNA and the histone core 63

V. The nucleosome as a changeable structure. 3. Specific dynamical processes which have been reported in the literature 64

A. Nucleosome dynamics leaving the histone/histone and histone/DNA bonding domains virtually intact 65

1. Changes in hydration 65

2. Small changes in the structure of the histone core 66

3. Small changes in DNA structure, and in the DNA/core bonding pattern 67

a. The view, from electrostatics, of DNA/core bonding 68

b. The chemical nature of the bonds between the DNA and the histone core 70

c. The topographic arrangement of the bonds

Page

between the DNA and the histone core: the "cell" model 73

d. Predictions of dynamical processes 80

e. Observed dynamical processes 81

B. Nucleosome dynamics involving major changes in the histone/histone and histone/DNA bonding domains 83

1. The (putative) transition of DNA from B- to other forms, in nucleosomes 83

2. Nucleosome "unfolding" 85

a. Low-salt unfolding 85

b. Transcriptional unfolding 86

c. Unfolding in the presence of "environmental perturbants" 87

d. Unfolding after trypsinization of the core histones 87

e. High-salt unfolding 88

f. Unfolding because of histone acetylation 89

3. Unbinding of DNA "tails" 90

4. Nucleosome Dissociation 96

a. Documentation of the phenomenon; potential problems of study 96

b. The thermodynamics of dissociation 98

c. The mechanism of dissociation 100

VI. The nucleosome as a changeable structure. 4. An approach to a broader context: the specific binding of additional proteins to nucleosomes 105

A. The binding of additional inner histones to nucleosomes 107

B. The binding of H1 to nucleosomes 108

Page

C. The binding of high mobility group proteins (HMGs) to nucleosomes 111

1. The binding of HMGs 14 and 17 111

2. The binding of HMGs 1 and 2 116

D. The binding of topoisomerase to nucleosomes 117

E. The binding of DNA polymerase to nucleosomes 119

F. The (possible) binding of specific proteins to nucleosomes, in transcriptionally active chromatin 120

G. The binding of RNA polymerase to nucleosomes 122

1. E. coli RNA polymerase 122

2. Eukaryotic RNA polymerase II 123

3. Eukaryotic RNA polymerase III 130

H. The (putative) binding of nucleoplasmin to "octamers" of the inner histones, and (transiently) to nucleosome-like structures 132

VII. Summary 134

Part 2.

The dynamics and equilibria of nucleosomes at elevated ionic strength 136

I. Abstract 137

II. Introduction 137

III. Materials and Methods 141

A. Initial preparation of chromatin 141

B. Purification of mononucleosomes 145

C. Crosslinking of the histone core 147

Page

D. Gel electrophoresis 148

E. Analytical centrifugation 150

F. Data analysis 150

IV. Results and Discussion 153

A. Characterization of the nucleosomes 153

1. Distribution of DNA lengths 153

2. Absence of proteins other than core histones 153

3. Nucleosomes with crosslinked histone cores 160

B. Dissociation of nucleosomes in salt 165

1. Moderate salt leads to the reversible generation of a slowly sedimenting species 165

2. In moderate salt, nucleosomes dissociate to yield free DNA 171

3. Dissociation in low salt 180

4. Crosslinking of the histone core with dimethyl suberimidate changes the salt-dependence of nucleosome dissociation 188

C. Nucleosome unfolding: does It occur? 189

V. Summary 192

VI. Acknowledgements 194

VII. List of abbreviations 195

Part 3

The release of DNA tails from nucleosome core particles at elevated ionic strength 196

I. Abstract 197

II. Introduction 198

Page

III. Materials and methods 198

A. Preparation of core particles 198

B. Electrophoresis 203

C. Sedimentation velocity measurements 204

D. Circular dichroism measurements 205

IV. Results 207

A. Characterization of the core particles 207

B. Sedimentation studies of the effects of ionic strength on core particle structure 217

C. Circular dichroism studies 224

D. Thermodynamic analysis 242

V. Discussion 248

A. The fast conformational change involves the release of DNA tails 248

B. Estimates of the number of bonds holding the DNA tails to the histone core 261

C. The strength of the bonds holding DNA tails to the core 264

D. The problem of DNA topology in the core particle 275

E. The relationship between tail release and dissociation 276

VI. Appendix - evaluation of a temperature-correction term in the CD equations 279

VII. Acknowledgements 280

VIII. List of abbreviations 281

Part 4

A Quantitative assay for nucleosome sliding 282

Page

I. Introduction 283

II. Preparation of plasmid pLV405-10 285

A. Procedure for isolation of crude plasmid 285

B. Removal of contaminants 286

C. Estimated potential yield of the 260 bp Eco RI fragment 288

III. Characterization of the plasmid 288

A. Extent of RNA contamination 289

B. Variability of the pattern of plasmid bands; identities of the bands 289

C. Extent of genomic DNA contamination 297

D. Estimated nicking of the 260 bp Eco RI fragment within the amplified plasmid 298

E. Estimated ribose-substitution in the 260 bp Eco RI fragment within the amplified plasmid 308

IV. Preparation of the 260 bp Eco RI fragment 320

V. End-labelling and secondary restriction of the 260 bp Eco RI fragment; purification and characterization of the 195 bp Eco RI - Nci I fragment 327

A. 3' End labelling 327

1. End-filling with [α-32P]-dATP 327

2. End-filling with [α-35S]-dATP 329

3. The potential generation of microheterogeneity in the end-filling reaction 330

B. 5' end labelling 334

C. Preparation for the secondary restriction step 335

D. Secondary restriction; purification

Page

of the 195 bp Eco RI - Nci I fragment 338

E. The stability of the 195 bp Eco RI - Nci I fragment 347

VI. Reconstitution of nucleosomes 363

A. The "histone transfer from core particles" method 364

B. Dependence of reconstitution yield upon the concentration of core particles 367

C. Dependence of reconstitution yield upon the concentration of labelled DNA 375

D. Joint dependence of reconstitution yield upon core particle concentration and radiolabelled DNA concentration 383

E. The effects of dialysis geometry on nucleosome reconstitution 384

VII. Analysis of the phasing of reconstituted nucleosomes 390

A. Outline of theory 390

B. Technical problems encountered in practice 391

1. The choice of a gel system for analyzing nuclease digestion patterns 391

2. The need to optimize the radioautographic process 393

3. Calibration markers 399

4. Background problems 400

C. The DNAase I digestion pattern expected for phased nucleosomes 401

1. The global features of the pattern 401

2. The fine structure of the pattern 402

3. A reexamination of Lutter's DNAase I digestion patterns 403

Page

4. A mathematical description of Lutter's data 407

5. A technical comment on the foregoing mathematical description 418

D. Analysis of preliminary phasing data 427

VIII. Possible approaches to detecting core movement 450

A. General requirements of a "sliding" assay 450

B. Mapping of sliding by digestion with MNase and restriction enzymes 452

C. Mapping of sliding by DNAase I digestion 455

D. Mapping of sliding by digestion with lambda exonuclease 457

IX. List of abbreviations 459

Bibliography 461

LIST OF FIGURES


| | | Page |
|---|---|---|
| Figure I.1 | The Pattern of Histone-DNA Contacts in the Nucleosome Core Particle | 75 |
| Figure II.1A | Gel Electrophorsis of Mononucleosomal DNA | 154 |
| Figure II.1B | Distribution of Mononucleosomal DNA Lengths | 156 |
| Figure II.2A | Gel Electrophoresis of Chromatin Proteins, with Staining by Coomassie Blue | 158 |
| Figure II.2B | Gel Electrophoresis of Chromatin Proteins, with Staining by Silver | 161 |
| Figure II.3 | SDS Gel Electrophoresis of the Crosslinked Histone Core | 163 |
| Figure II.4A | Sedimentation of Mononucleosomes in Moderate Salt | 167 |
| Figure II.4B | Nucleosomes Approach the Same State, if Jumped to the Same Salt Concentration from Different Directions | 169 |
| Figure II.5A | Particle Gel Analysis of Mononucleosomes in 0.6 M Salt | 172 |
| Figure II.5B | Integral Distribution of S, for Nucleosomes or DNA in Salt | 174 |
| Figure II.5C | Dissociation of Nucleosomes is Enhanced by Their Dilution | 178 |
| Figure II.5D | Free DNA from Nucleosomes, in Low Salt: Particle Gel | 183 |
| Figure II.5E | Free DNA from Nucleosomes, in Low Salt: Scan of Particle Gel | 185 |
| Figure III.1A | Characterization of Nucleosome Core Particles and Core Particle DNA, by Gel Electrophoresis | 208 |

| | | Page |
|---|---|---|
| Figure III.1B | Characterization of Nucleosome Core Particle Histones, by Gel Electrophoresis. Coomassie Blue Stain | 212 |
| Figure III.1C | Characterization of Nucleosome Core Particle Histones, by Gel Electrophoresis. Silver Stain | 214 |
| Figure III.2 | Time-Dependence of Core Particle Dissociation in 0.75 M NaCl | 219 |
| Figure III.3 | Core Particle Dissociation, as a Function of Salt Concentration and Time of Incubation | 221 |
| Figure III.4 | Decrease in Sedimentation Coefficient of the Fast (Nucleosomal) Centrifuge Boundary, With Increasing NaCl Concentration | 225 |
| Figure III.5 | Detail of the Integral Distribution of s20,w Analysis, for the Centrifuge Data of Figure III.2 | 227 |
| Figure III.6 | Time-Dependent Changes in the Circular Dichroism of Core Particles, at Elevated NaCl Concentrations | 231 |
| Figure III.7 | The Salt-Induced Rapid Increase in Circular Dichroism of Core Particles | 237 |
| Figure III.8 | Reversibility of the Salt-Induced Rapid Increase in Circular Dichroism of Core Particles | 240 |
| Figure III.9 | Salt-Dependence of the Observed Equilibrium Constant for the Binding of DNA Tails to the Histone Core | 245 |
| Figure III.10 | The Temperature-Dependence of the Unbinding of DNA Tails for the Histone Core, in 0.65 M NaCl | 249 |
| Figure III.11A | Hydrodynamic Model for the Unbinding of DNA Tails from the Histone Core | 253 |
| Figure III.11B | Quantitative Predictions of | |

| | | Page |
|---|---|---|
| | the Hydrodynamic Model of Figure III.11A | 256 |
| Figure III.12A | Theoretical Curves for the Salt-Dependent Binding of DNA to Oligolysines | 269 |
| Figure III.12B | Theoretical Curves for the Salt-Dependent Binding of DNA to Oligoarginines | 273 |
| Figure IV.1A | Preparation I of plasmid pLV405-10 (and contaminating RNA), before RNAase treatment. The effect of alkaline heat treatment | 290 |
| Figure IV.1B | Purified plasmid of preparation I, after RNAase treatment. 7% supercoiled form | 292 |
| Figure IV.1C | Purified plasmid of preparation II, after RNAase treatment. 47% supercoiled form; no contaminant DNAs | 295 |
| Figure IV.2A | Probability density functions for nicking in the plasmids of preparation I and II. 1. The distribution of nicks throughout the entire plasmid molecule | 302 |
| Figure IV.2B | Probability Density Functions for Nicking in the Plasmids of Preparations I and II. 2. The distribution of nicks in the 2600 bp insert | 305 |
| Figure IV.2C | Probability Density Functions for Nicking in the Plasmids of Preparations I and II. 3. The distribution of nicks in the 260 bp repeat | 309 |
| Figure IV.3A | Probability density functions for ribosylation in the plasmid of preparation I. 1. The distribution of ribosylation events throughout the entire plasmid molecule | 313 |
| Figure IV.3B | Probability density functions for ribosylation in the plasmid | |

Page

of preparation I. 2. The distribution of ribosylation events throughout the 2600 bp insert 315

Figure IV.3C Probability density functions for ribosylation in the plasmid of preparation I. 2. The distribution of ribosylation events throughout the 260 bp repeat 317

Figure IV.4A The digestion of plasmid pLV405-10 with Eco RI. 1. Intermediate timepoint in the digestion. Proof that the cloned insert is comprised of 10 tandem repeats of a 260 bp unit 322

Figure IV.4B The digestion of plasmid pLV405-10 with Eco RI. 2. purified Eco RI fragment, 260 bp in length, on a 3.5% polyacrylamide "E" gel. Ethidium-fluorescence photograph. 325

Figure IV.5A Purified 195 bp Eco RI - Nci I fragment, labelled with $^{32}P$ at the Eco RI end, on a 3.5 % polyacrylamide "E" gel. 1. Ethidium-fluorescence photograph 342

Figure IV.5B Purified 195 bp Eco Ri - Nci I fragment, labelled with $^{32}P$ at the Eco RI end, on a 3.5% polyacrylamide "E" gel. 2. Radioautograph 344

Figure IV.6A Stability of the end-labelled 195 bp fragment. 1. Stability over 3 days' incubation in buffer. Polyacrylamide "E" gel; ethidium fluorescence photograph 348

Figure IV.6B Stability of the end-labelled 195 bp fragment. 1. Stability over 3 days' incubation in buffer. Polyacrylamide "E" gel; radioautograph 351

Figure IV.6C Stability of the end-labelled 195 bp fragment. 2. Stability over 3 days' incubation in buffer, followed by 5 min heating at 100 °C. "SS" gel; ethidium fluorescence photograph 354

Figure IV.6D Stability of the end-labelled 195 bp

Page

fragment. 2. Stability over 3 days' incubation in buffer, followed by 5 min heating at 100°C. "SS" gel; radioautograph 356

Figure IV.6E Stability of the end-labelled 195 bp fragment. 3. Stability over 13 days' incubation in buffer at 0 or 22 °C, or over 3 days' incubation in buffer at 27 °C, followed by 10 days' incubation in solid form at 37 °C. Polyacrylamide "E" gel; ethidium fluorescence photograph 359

Figure IV.6F Stability of the end-labelled 195 bp fragment. 3. Stability over 13 days' incubation in buffer at 0 or 22°C, or over 3 days' incubation in buffer at 27°C, followed by 10 days' incubation in solid form at 37°C. Polyacrylamide "E" gel; radioautograph 361

Figure IV.7A Reconstitution of nucleosomes, by the method of "histone transfer from (unlabelled) core particles". 1. The effect of changing the concentration of the core particles. "Native" gel; ethidium-fluorescence photograph 368

Figure IV.7B Reconstitution of nucleosomes, by the method of "histone transfer from (unlabelled) core particles". 1. The effect of changing the concentration of the core particles. "Native" gel; radioautograph 370

Figure IV.7C Reconstitution of nucleosomes, by the method of "histone transfer from (unlabelled) core particles". 1. The effect of changing the concentration of the core particles. Quantitation of the radioautograph of Figure 7B. 373

Figure IV.8A Reconstitution of nucleosomes by the method of "histone transfer from (unlabelled) core particles". 2. Effect of changing the concentration of radiolabelled DNA. "Native" gel;

| | | Page |
|---|---|---|
| | ethidium-fluorescence photograph | 377 |
| Figure IV.8B | Reconstitution of nucleosomes by the method of "histone transfer from (unlabelled) core particles". 2. Effect of changing the concentration of radiolabelled DNA. "Native" gel; radioautograph | 379 |
| Figure IV.8C | Reconstitution of nucleosomes by the method of "histone transfer from (unlabelled) core particles". 2. Effect of changing the concentration of radiolabelled DNA. Quantitation of the radioautograph of Figure 8B. | 381 |
| Figure IV.9A | The effect of dialysis geometry on the reconstitution reaction. Ethidium-fluorescence photograph | 385 |
| Figure IV.9B | The effect of dialysis geometry on the reconstitution reaction. Radioautograph | 388 |
| Figure IV.10 | Film geometry is a critical variable in the radioautography of gels of DNAase I digestion fragments. | 394 |
| Figure IV.11A | Fine structure of radioautographs of phased nucleosomes: the problem of microheterogeneity. 1. Lutter' radioautograph of the DNAase I digestion of double-end-labelled core particles. | 404 |
| Figure IV.11B | Fine structure of radioautographs of phased nucleosomes: the problem of microheterogeneity. 2. Frequency distributions of cutting within the "S1" and "S2" sites of double-end-labelled core particles, computed from Lutter's data. | 408 |
| Figure IV.11C | Fine structure of radioautographs of phased nucleosomes: the problem of microheterogeneity. 3. Frequency distributions for DNAase I cutting within the "S1" and "S2" sites of | |

Page

Lutter's double-end-labelled core particles, graphed under the assumption of a constant "fall-off ratio". 412

Figure IV.11D Fine structure of radioautographs of phased nucleosomes: the problem of microheterogeneity. 4. Predicted frequency distributions for cutting within "S1" and "S2", for single-end-labelled mononucleosomes which are uniformly phased. Effect of varying the selectivity of DNAase I (source I of variance). 416

Figure IV.11E Fine structure of radioautographs of phased nucleosomes: the problem of microheterogeneity. 5. Predicted frequency distributions for cutting within "S1" and "S2", for single-end-labelled mononucleosomes having different amounts of microheterogeneity with respect to phasing position (source II of variance). DNAase I selectivity assumed maximal (k = 1 in "central region"). 419

Figure IV.11F Fine structure of radioautographs of phased nucleosomes: the problem of microheterogeneity. 6. Four Statistics, Defined on the Basis of the Data of Figure IV.11 E, Which are Sensitive to the Existance of Phasing Microheterogeneity. 421

Figure IV.12A Analysis of preliminary data on phasing in reconstituted nucleosomes. 1. Time-course of DNAase I digestion. "SS" gel; ethidium-fluorescence photograph 428

Figure IV.12B Analysis of preliminary data on phasing in reconstituted nucleosomes. 2. Time-course of DNAase I digestion. "SS" gel; close-up of ethidium-fluorescence photograph 430

Figure IV.12C Analysis of preliminary data on phasing in reconstituted nucleosomes.

| | | Page |
|---|---|---|
| | 3. Time-course of DNAase I digestion. "SS" gel; radioautograph | 432 |
| Figure IV.12D | Analysis of preliminary data on phasing in reconstituted nucleosomes. 4. Low-Resolution Scan of Individual Lanes of the Radioautograph of Figure 12C; Preliminary Assignment of Bands. | 435 |
| Figure IV.12E | Analysis of preliminary data on phasing in reconstituted nucleosomes. 5. Plot of Band Mobility versus ln(# of Nucleotides), for the DNAase I - Digested Cold Carrier Nucleosomes and Single-End-Labelled Nucleosomes of Figure 12 C. Band Sizes Assigned on the Basis of Lutter's Proposal for the Positions of Cutting Sites. | 438 |
| Figure IV.12F | Analysis of preliminary data on phasing in reconstituted nucleosomes. 6. The Zero DNAase I Scan and 2 hour Scan from Figure 12 D, with Proposed Baselines; Scans Cut into 41 "Channels" each, for Purposes of a "Difference" calculation. | 442 |
| Figure IV.12G | Analysis of preliminary data on phasing in reconstituted nucleosomes. 7. Normalized Scans from Figure 12F. | 444 |
| Figure IV.12H | Analysis of preliminary data on phasing in reconstituted nucleosomes. 8. Calculated Difference Between the 2 h DNAase I- and Zero DNAase I- Scans of Figure 12 G. "Difference" Calculation with Either Full Weight or Half Weight Assigned to the Zero DNAase I Scan. | 446 |

# Nucleosome Instabilities in Physiological Salt

## Part 1

## A Review of Nucleosome Dynamics

by

Thomas Dean Yager
Department of Biochemistry and Biophysics
Oregon State University
Corvallis, OR 97331

## I. The nucleosome as a changeable structure. 1. An emerging perspective.

The elucidation of the structure of the basic unit of chromatin - the nucleosome - has provided deep insight into understanding the nature of the chromosome itself (Elgin and Weintraub, 1975; van Holde and Isenberg, 1975; Kornberg, 1977; Chambon, 1977; Felsenfeld, 1978; Dubochet and Noll, 1978; Olins and Olins, 1978; Isenberg, 1979; Lilley and Pardon, 1979; Kornberg, 1980; Lasky and Earnshaw, 1980; Mirzabekov, 1980; McGhee and Felsenfeld, 1980a; Lewin, 1980; Cartwright et al., 1981; Sperling and Wachtel, 1981; Igo-Kemenes et al., 1982; Nicolini, 1983; van Holde, 1986). Soon, the structure of the nucleosome will be known to a resolution of several angstroms (Finch et al., 1977; Klug et al., 1980; Finch et al., 1981; Bentley et al., 1981; Lattman et al., 1982; Burlingame et al., 1984).

Because the nucleosome is so well-defined, there has been a tendency to view it as immutable, or at least as extremely stable. This tendency leads, however, to ad hoc proposals that nucleosomes can sometimes become unstable, so that transcription, replication, repair, recombination and other physiological processes can occur.

In this essay, I hope to describe a new view of the nucleosome which is emerging. A growing literature reports that

nucleosomes can undergo many profound structural changes under "physiological" conditions. When carried to its logical conclusion, this view sees the nucleosome in vivo as a highly dynamic, changing entity.

Besides arguing generally for the viewpoint that, in vivo, the nucleosome is dynamic, this essay attempts to reach three more specific goals. The first is that of evaluating critically the literature on each known type of nucleosome instability. The second is that of defining a complete set of elementary dynamic, or mechanistic processes, into which any of these instabilities may be resolved. (In the spirit of this second goal, I hope, for example, to be able to resolve the complex process of histone core sliding into the elementary processes of histone/DNA bond breakage and reformation, rapid DNA oscillatory motions, etc.) The third goal is that of determining the fundamental thermodynamic driving forces underlying each of the elementary processes, and thus underlying the observed instabilities. It should become clear, upon reading this review, that the instabilities of nucleosomes which have been observed are rather complex processes. Their precise discussion will require knowledge concerning (i) DNA structure and dynamics, (ii) protein structure and dynamics, and (iii) the interactions of DNA and solvent, of protein and solvent, and of DNA and protein.

So that subsequent discussion will be unambiguous, I will

attempt to delineate here the ranges of salt concentration and temperature within which a nucleosome instability must fall, to be considered in this essay. The temperature range is that bounded roughly by 0 $^{o}$C and 40 $^{o}$C. These limits seem reasonable, inasmuch as (i) aquaeous solution chemistry must change fundamentally at or near the freezing point of water, and (ii) 40 C approaches the empirical upper temperature for viability of most eukaryotic cells. The range of bulk ionic strength is that lying above roughly 1-10 mM (hence above the low salt transition for core particles [see section V B, 2]), and below roughly 2-4 M (where, for an equimolar mixture of the inner histones, the histone/histone equilibria are shifted to strongly favor the existance of the (H2A.H2B)2:(H3.H4)2 octamer [see section III C]).

## II. The dynamics of B-DNA

From a variety of experimental approaches, it has been established that the DNA in nucleosomes has a form which is "condensed", but which is still in many respects like the B-form (Fasman, 1979; Wang, 1982). Since a great body of work and considerable insight exists on the dynamics of B-DNA, it seems reasonable to begin a discussion of nucleosome dynamics by reviewing what is known about this more modest problem. The review will attempt to ask whether a particular dynamical

process that is observed for free B-DNA can also occur for DNA that is bound up in nucleosomes.

My review of B-DNA dynamics will be divided into three sections. The first section will deal with the "intrinsic" motions of B-DNA - those motions which occur regardless of the properties of the surrounding medium. Such motions are in essence the vibrational modes displayed by a semi-rigid mechanical structure (the DNA molecule), as it takes up and releases thermal energy through collision with solvent molecules and ions. This section complements portions of an earlier review (Record et al., 1981).

The second section focuses exclusively on changes occurring in the "layers" of hydration and counterions that are bound to the surface of the DNA. The innermost of these layers, at least, has considerable structure and thermodynamic stability, due to the many hydrogen- and electrostatic bonds between itself and the DNA, and between its constituent particles. It is of considerable interest to learn how the internal structure of this layer changes with environmental conditions.

The third section takes a more holistic, or interactive viewpoint. Here, the DNA and its layers of bound hydration and counterions are viewed as two interacting subsystems, which comprise a larger single entity. As the literature reviewed in this section will demonstrate, changes in the structure of the layers of hydration and counterions can cause transitions in

DNA structure, and vice-versa. This third point of view is of increasing prominence in the literature.

## A. Intrinsic DNA motions

### 1. Motions within the "B" form

In analysis of the x-ray diffraction pattern from a single crystal of a DNA dodecamer, it was found that the individual DNA base pairs, while all approximately B-form, actually display a number of well-defined deviations from the canonical B structure (Wing et al., 1980; Drew et al., 1981; Drew et al., 1982).

What are the broad consequences of this finding? It appears that one should not view DNA simply as a uniform "B structure". Rather, one probably should view the individual base pairs in the DNA molecule as constituting many different "near-B" conformational isomers, close to each other in a continuum of "near-B structure", and of approximately equal potential energy. Also, one probably should view each particular base pair as oscillating about a "preferred conformation" during the course of thermal vibration.

The prediction that "B" DNA is a dynamic structure - implicit in the above analysis - has been confirmed by a number of studies (see below). Perhaps the most direct confirmation

was obtained through analysis of x-ray crystallographic thermal parameters. Support has also been received from (theoretical) potential energy calculations, and from several different kinds of spectroscopy. It is to a discussion of these types of data that I now turn.

a. Motions deduced from the analysis of X-ray diffraction patterns

Holbrook and Kim (1984) have developed a general method of analyzing the thermal noise inherent in the x-ray diffraction pattern of a single macromolecular crystal. Their method proposes a "segmented rigid body" model as a representation of the macromolecule under study; in this view, the macromolecule is made of rigid groups, which undergo coupled translations and vibrations.

This method has been applied to x-ray diffraction data from single crystals of both DNA (data of Wing et al. [1980] and Drew et al. [1981]), and RNA (data of Sussman et al. [1972], Suck et al. [1976], Seeman et al. [1976], and Rosenberg et al. [1976]). In either case, the nucleic acid is divided into base, sugar and phosphate groups. For either nucleic acid, five modes of motion are observed for the aromatic bases. The three major modes are propeller twisting between paired bases, rocking of base pairs as units (along the same axes involved in propeller

twisting), and buckling of the base pairs (resulting in a change in the angles of the hydrogen bonds between the paired bases). The two minor modes of motion are sliding of the bases in the plane of the base pairs, and local fluctuations in the twist of the DNA or RNA (due to rotation of base pairs about the macromolecule's long axis). Several classes of sugar motions were also observed, apparently strongly coupled to the first three of the above base motions, and weakly coupled to the remaining two base motions. Finally, there was considerable movement of the phosphate groups, probably due to rotations about the phosphodiester bonds.

This analysis, which is of a very high resolution, provides direct information about the magnitudes and directions of all short-range motions in DNA. I note that, in principle, the same approach may be taken to study the motions of DNA in nucleosomes, when crystallographic data of sufficiently high resolution (less than 2.0 angstroms) are finally obtained.

I note that a recent paper from Dickerson's group may call into question some of the detailed conclusions of this analysis. In this paper (Drew et al., 1982), DNA crystals were cooled to 16 K (very slowly, to avoid ice formation), and crystallography done. It was discovered that a significant component of the noise in the electron density map was relatively temperature-insensitive. It was suggested that this component of the noise, previously thought due to internal DNA

motions(s) (which should be temperature-sensitive), was actually due to disorder in the packing of adjacent DNA molecules. Thus it seems that, for greater certainty of conclusions, the analysis of Holbrook and Kim should be carried out on x-ray data collected at several temperatures (preferably from the same sample).

Besides this technical point, I note that the analysis has several more fundamental limitations. First, it can say nothing about the rates of the motions. Second, it is possible that the short-range motions of DNA in solution may be different from those in a crystal. Third, the analysis is unable to focus on the longer-range harmonics of these motions, involving perhaps quite extensive regions of the DNA. To address some of these further complexities, I now turn to potential energy calculations, and to various spectroscopic methods of detecting motion.

b. Motions predicted by potential energy-vs.-conformation models

Four different approaches have evolved for the theoretical study of B-DNA motion. In the first, a molecule of DNA is treated as a semi-rigid rod, and its behavior deduced by solving the equations of motion of classical mechanics. This approach is based on the early treatment by Landau and

Lifschitz (1958) of the general problem in mechanics of small uniform deformations of a thin elastic rod. Various applications to DNA, each emphasizing different aspects of the problem, have been made (Tao, 1969; Schellman, 1974; Shore and Zwanzig, 1975; Harrington, 1977; Riemer and Bloomfield, 1978; Barkley and Zimm, 1979; Robinson et al., 1980; Hurley et al., 1982). This approach predicts (not unexpectedly) that a DNA molecule should tumble anisotropically in solution; perhaps more surprisingly, it also predicts the DNA to bend and twist. In these last two motions, a DNA molecule is characterized by the respective coefficients of "stiffness" and "torsional rigidity". Calculations suggest that the bending motions increase the potential energy of the DNA "rod" a great deal, and so are not favored. The twisting motions, however, involve much smaller increases of potential energy, and so are predicted to be common. For a 200 bp piece of DNA, the dominant twisting modes are predicted to have time constants ranging from 0.1 nsec to 100 nsec.

There is some experimental evidence in support of the above theoretical predictions (Millar et al., 1980; Hogan et al., 1982; Ashikawa et al., 1983a, 1983b). In these experiments, an aromatic, fluorescent dye molecule is allowed to intercalate between the base pairs of the DNA, and the depolarization of its fluorescence is observed. If the dye is behaving similarly to the base pairs, its polarized fluorescence should have quite

a different decay curve from that predicted for a dye molecule rigidly attached to a rigid rod (which just tumbles in solution). To a fair approximation, the polarized fluorescence follows the decay curve predicted by the "semi-rigid rod" theory. I note that, in experiments of this type, there is always some uncertainty about how much the dye molecule restricts DNA motion (Hogan and Jardetzsky, 1980), and also about how much the dye molecule "wobbles" (Wang et al., 1982).

I note that experiments of the above type have also been done on DNA that is bound up in nucleosomes (Wang et al., 1982; Hurley et al., 1982; Ashikawa et al., 1983a; 1983b). The interpretation of such nucleosome experiments is considerably more subtle than the interpretation of the analogous DNA experiments, and will be deferred to section V A, 3.

The remaining three theoretical approaches to B-DNA motion are similar in that they are based, not upon an approximate representation of the DNA molecule, but rather upon a detailed atomic model of DNA structure deriving from x-ray crystallography.

In the "energy minimization" approach (Levitt, 1978; Sussman and Trifonov, 1978; Keepers et al., 1982; Tidor et al., 1983), an initial DNA structure is obtained from crystallography. It is then subjected to arbitrary virtual deformations, and the resultant potential energy calculated (through use of a potential function). This provides

information on how much the variants of "B" conformation (discussed above) differ in energy from each other.

In the "molecular dynamics" approach (Tidor et al., 1983), the classical equations of motion are combined with a potential function to calculate, for a short DNA fragment, the positions and velocities of all the constituent atoms as functions of time, over 10-60 psec of thermal vibration. This approach is used to study very small, very rapid deformations of individual atoms during thermal vibration.

In the "harmonic dynamics" approach (Tidor et al., 1983), a potential energy function is used to obtain time-independent (eigenstate) solutions to the classical equations of motion, for the each of the atoms of a short DNA fragment. These solutions represent the normal vibrational modes of the DNA.

These three approaches suggest very strongly that all the atoms in the DNA undergo very rapid (psec) motions, involving deformations on the order of 0.1 angstrom. In addition, a number of vibrational modes exist. The main ones are: smooth bending of the entire molecule; twisting of the base pairs in planes perpendicular to the central axis of the DNA; fluctuation of the distance between adjacent base pairs; fluctuation of the distance between adjacent phosphates; movement of base pairs away from the central axis of the DNA; propeller twisting of the base pairs; buckling of the base pairs. An important point is that most of these vibrational

modes are the same as the modes deduced in the crystallographic analysis of Holbrook and Kim (1984), above.

c. Motions deduced from spectroscopic measurements

In NMR, the linewidth of the resonance peak of a particular type of atomic nucleus within a macromolecule will decrease, as that type of nucleus becomes more mobile. The exact relationship between the (observable) linewidth and the (theoretical) longitudinal and transverse relaxation times T1 and T2 (for the loss of magnetic resonance energy) is well-known (see, for example, Cantor and Schimmel [1980]). Typically, after measuring the linewidth and calculating T1 and T2 for a particular type of nucleus, one then attempts to make inferences about the motions, within a macromolecule, of the chemical group(s) containing that type of nucleus. Clearly, the path of reasoning that leads from the (observed) linewidth and T1/T2 values to the (inferred) intramolecular mobilities must always proceed through a theoretical structural model, which relates T1 and T2 to molecular motions.

An early quantitative model of the motions of an arbitrary small molecule was developed by Woessner (1962). This model has proved to be the paradigm upon which all subsequent treatments are based. In Woessner's model, a particular atomic nucleus is assumed to lose magnetic resonance energy through dipolar

interactions, both with nearby nuclei and with the applied magnetic field. (Other mechanisms for the loss of resonance energy probably also operate, but are ignored in this treatment; see below.) All nuclei within the molecule are assumed stationary; the entire molecule is assumed to tumble in solution, either isotropically as a sphere, or anisotropically as an ellipsoid.

In an analysis based on Woessner's model, one looks for a discrepancy between the T1 and T2 values calculated for such a rigid tumbling body, and the T1 and T2 values actually obtained from linewidth measurements. If the experimentally obtained values are lower that the theoretically calculated ones, this indicates that the resonance energy is dissipated faster than expected. This in turn suggests some motion of the atomic nuclei within the molecule, in addition to the overall tumbling of the entire molecule.

Woessner's model, which was derived originally for treatment of isolated small molecules, has been applied, with varying degrees of rigor, to the motions of (partially immobilized) chemical groups in the DNA (see, for example, Early and Kearns [1979], and Hogan and Jardetzsky [1979]). As might be expected, difficulties of interpretation are encountered in this profound extrapolation of Woessner's original model. It therefore seems best, in this context, to view NMR results as being only qualitative, or at most

semi-quantitative.

One general problem with the extrapolation of Woessner's model arises because a chemical group in DNA is not freely tumbling, but is connected to the main body of the macromolecule by a chemical bond. The presence of the bond restricts the universe of possible motions that the chemical group can experience (i.e. decreases the group's number of degrees of freedom). Also, the bond causes the thermal motions of the remainder of the macromolecule to be "communicated" to the chemical group (McCammon, 1984). In my opinion, neither of these complications has been treated adequately.

A second general problem lies in the fact that the individual members of a class of chemical group within a macromolecule probably all have slightly different motions and environments. This implies an inherent heterogeneity in any resonance signal from DNA, which is lacking in the signal from a small molecule. An attempt has been made to treat this complication quantitatively, but still from within the context of the "tumbling body" model of Woessner (Shindo, 1980). Under the assumption that the DNA behaves as a semiflexible chain of repeating units, Shindo replaces each single rotational correlation time in his "tumbling equations" with a probability distribution of correlation times. (Here, the term "tumbling equations" is used to mean a set of equations which predicts relaxation times T1 and T2 from a model of the internal and

overall motions of the DNA.) I note that this approach is helpful only to the extent that the "tumbling body" model really is applicable to chemical groups within a macromolecule.

A third general problem arises because Woessner, in his original derivation, considered only two mechanisms for nuclear spin relaxation. In fact, at least seven relaxation mechanisms are known, and each can contribute to the shape of a resonance peak (see Hull and Sykes [1975]). These are: (i) dipolar interaction with another nuclear spin; (ii) dipolar interaction with the external magnetic field; (iii) dipolar interaction with an unpaired electron spin ("paramagnetic relaxation"); (iv) chemical shift anisotropy (a mechanism involving interaction of a nuclear spin with its surrounding electron cloud, when the latter is not spherically symmetrical); (v) interaction of a (quadrupolar) nucleus with the electric field gradients of its chemical bonds; (vi) spin rotation (the interaction of a nuclear spin with the angular momentum of the entire molecule of which it is a part); and (vii) scalar, or hyperfine coupling (an interaction of the nucleus with an unpaired electron, mediated through a [perhaps transitory] chemical bond [Dwek, 1973]). For 1H studies on DNA, perhaps only relaxation mechanisms (i) and (ii) need be considered; however, for 13C or 31P studies, at least the chemical shift anisotropy mechanism (iv) must also be considered (Shindo, 1980; Yuhasz et al., 1984).

Despite these complications, a number of studies seem to show, in the DNA, at least four classes of rapid motion. These involve: (i) the backbone phosphates (Hogan and Jardetzsky, 1979; Shindo, 1980); the non-exchangeable ring protons (Early and Kearns, 1979); the hydrogen-bonded protons between the base pairs (Early and Kearns, 1979); and the hydroxyl protons on the deoxyribose groups (Early and Kearns, 1979). I suspect, however, that NMR cannot say much without ambiguity about the directions or magnitudes of these motions, about the rigidity of bonds within particular chemical groups, about the movement of other (unexamined) atomic nuclei and chemical groups, or about harmonic coupling of the various types of motion.

Although, in NMR, the quantitative theory of absolute DNA motion is fraught with difficulties, one can easily make a qualitative comparison of the mobilities of free- and nucleosome-bound DNA. (Note, however, that for unambiguous interpretation, an NMR-based comparison must be related to more absolute information - for example, information from a Holbrook/Kim-type analysis of crystal x-ray diffraction [see above].) In this vein, Shindo and McGhee (1980) have shown with $^{31}P$ NMR that, if rapid phosphate motion occurs in free DNA, then motion very much like it must also occur for the DNA in core particles.

2. Transitions out of the "B" form

The DNA motions described above have the common feature of not appreciably disrupting the B-form structure of the DNA. I turn now to a consideration of motions which lead to a loss of "B" structure.

a. Rupture of hydrogen bonds between complementary bases

One mode in which thermal energy is dissipated by the mechanical structure of the DNA is through the transitory breakage and reformation of the hydrogen bonds between complementary bases. The breakage of a base pair "opens up" the DNA in a local region, thus causing a local loss of B-type structure (Mandel et al., 1979; Early et al., 1981; Zuiderweg et al., 1981; Patel et al., 1982).

There are three salient characteristics of hydrogen bond rupture (for review, see Bloomfield et al. [1974]). First, GC base pairs, which have three hydrogen bonds, are stronger than AT base pairs, which have only two bonds; thus the former have less of a tendency to rupture. Second, base pair formation and stabilization is a highly cooperative process, due to stacking interactions between adjacent base pairs. Thus the base pairs at the ends of the DNA, which have only half the stacking interaction, rupture more easily than base pairs within the DNA. (The difference in stability is quite large: at 20 C,

rupture at the ends ["fraying"] occurs with an average frequency of 10,000/sec, while internal rupture ["breathing"] has an average frequency of only 1/sec [Kallenbach et al., 1980]. Third, B-form DNA is a right-handed helix. Supercoiling of this structure in a left-handed direction therefore causes a destabilization of base pairing (Vologodskii et al., 1979), and an increase in DNA "breathing" (Bendel and James, 1983).

b. Highly localized transitions from B- to other DNA forms

As described above, a rupture of base pairing in one or a few adjacent bases may be regarded as a local and transient loss of structure. I turn now to cases where it is believed that, in a local region, B structure is not simply transiently lost, but instead is replaced by a fundamentally different type of structure.

A highly hypothetical mechanism for a localized B-to-A transition has been proposed on the basis of computer-aided systematic distortion of three-dimensional DNA models (Sobell, 1980). Acoustical phonon waves, arising through thermal fluctuations (as in the "semi-rigid rod" model of DNA motion, above), are envisioned to resonate on the DNA, in many modes. Occasionally the waves may superimpose at particular points on the DNA, resulting in the sudden localization of a large amount of strain energy. These rare events should force the DNA in

these localized regions from the B-form into a "beta-kinked" intermediate, and then into the A-form. Such a local discontinuity of structure would be of relatively high potential energy, and thus would have a short lifetime. (Note: another, entirely different mechanism for the B-to-A transition, which involves DNA/solvent interactions, has also been proposed; see section II C, 3).

B-DNA is believed to also undergo transitions to other right- and left-handed helical forms. These transitions are best explained through an interaction of the DNA with solvent (see section II C).

B. The dynamics of solvent bound to DNA

Both on structural and on thermodynamic grounds, it seems plausible to believe that the two phenomena of binding water to DNA, and of binding ions to DNA are inextricably linked. However (perhaps in an attempt to reduce this joint binding problem to manageable proportions), most of the studies in the literature have focused on one of these two aspects, to the partial or complete neglect of the other.

In the initial portion of my review of DNA/solvent dynamics, I will follow this "separatist" convention, to give the reader an appreciation of the degree to which it is entrenched in the literature. One should of course suspect that

the conceptual separation of water binding and ion binding may be simplistic or even misleading, and that a fundamental theory of DNA solvation would treat the two phenomena as aspects of a larger whole. Therefore in the final portion of the review, I will discuss the few studies which attempt to integtate the two perspectives.

1. A view of the dynamics of DNA-bound solvent that emphasizes hydration

Relatively little is known of the structure and dynamics of the layer(s) of hydration surrounding the DNA. A fundamental theory should be able to predict at least the following: (i) the energetically most favorable arrangement of water molecules about a given DNA sequence, and how this arrangement fluctuates in thermal motion through time; (ii) how bound water molecules influence the natural stability and motions of the DNA; and (iii) how such a "layer" of water molecules is affected by the presence of other small molecules and ions (especially the group IA and group IIA cations).

In the absence of a fundamental theory, some insight may be gained by examining individual papers.

a. Definitions of hydration

The first problem one encounters in reading the literature on DNA hydration dynamics, is one of definition. "DNA hydration" has been defined operationally in at least very three different ways: (i) as a variable in classical thermodynamics, related to the (thermodynamic) activity of the water in a DNA solution; (ii) as a parameter in transport equations which describe the movement of DNA through solution, either by diffusion or under the influence of external fields; and (iii) as the three-dimensional distribution of tightly bound water molecules, in x-ray diffraction studies, high-resolution spectroscopic analyses, in statistical thermodynamic calculations.

The thermodynamic hydration of DNA is defined as the number of moles of water which must be added to a solution of very large volume containing one mole of nucleotide (incorporated in DNA), to keep the chemical potential of the water constant (Hearst and Vinograd, 1961). The thermodynamic hydration of DNA is a calculated quantity, which derives ultimately from an observable such as the bouyant density of the DNA in a solution of a certain salt composition. A plot of thermodynamic hydration versus bulk salt concentration is a parabola, which tends to infinity at low salt, and to zero at high salt. From the fact that the curve is unbounded at low salt, it is clear that the thermodynamic definition of hydration carries little information about the internal structure of the layer of water

immobilized about a DNA molecule. Therefore it will not be of further interest in this discussion.

Transport hydration may be defined as the mass of water carried along with one unit mass of dry DNA, when the latter diffuses or is forced through solution (Wang, 1954a, 1954b, 1955). Here again, hydration is a derived quantity; the observable which underlies it is the DNA's translational frictional coefficient, or some similar parameter. This definition begins to approach the type of structural knowledge sought about bound water: it suggests, for example, that certain water molecules may be bound tightly, to form an inner hydration shell, while other water molecules may be bound in a more diffuse way, gradully becoming indistinguishable from free water.

To obtain a true molecular-level picture of DNA hydration, one must turn to either x-ray diffraction, various types of high-resolution spectroscopy, or statistical thermodynamic calculations. Such investigative techniques, in conjunction with a quantum-mechanical view of the hydrogen bonding between DNA and water molecules, begin to approach a fundamental view of DNA hydration.

With this introduction, I am now almost ready to summarize what has been learned about the fine structure of DNA hydration (in the spirit of definition [iii], above). Before the summary, though, it is important to state a fundamental problem one

encounters in comparing information from different high-resolution investigative techniques. Presumeably the degree of order in the DNA's hydration layer(s) (and the fluctuation in that order) varies from one type of chemical group to another on the DNA, and also varies from the surface of the DNA to radially more distant positions. Different investigative techniques, being focused on different regions of the DNA and its environment, will thus "see" different levels of structure and stability, in the hydration layer(s). It may therefore be difficult to integrate information from different techniques into a single coherent picture.

b. The structure of the hydration layer(s) of the DNA

From transport studies of the diffusion of radiolabelled water through (low salt) solutions of B-DNA (Wang, 1954a, 1955), it was deduced that, in solution, water associates with B-DNA in two "layers": a tightly bound, highly oriented layer, and a loosely bound layer which, with increasing radial distance, loses structure and "degenerates" into free water.

High-resolution infrared spectroscopy of DNA fibres (Falk et al., 1963a, 1963b) revealed that, in the "tightly bound layer", there are four regions of the DNA which bind water molecules rather independently of each other. These are (in order of decreasing affinity for water): the O-P-O and C-O-P

regions of the phosphates; the C-O-C region of the furanose rings; the C=N-C, N-CO-C, and N-CO-N regions of the heterocyclic rings; and the -NH2 region of the guanine residues. (Note: in the macroscopic fibres of DNA used in these studies, the "salt concentration" was not precisely known, and may not even have been precisely defineable. Thus it was not determined how sensitive the "affinity for water" of these five structures was to the presence of nearby ions.)

Recently, Dickerson and coworkers have conducted a careful analysis of the x-ray diffraction pattern of a (hydrated) DNA dodecamer crystal (see Kopka et al. [1983]). The electron density maps which they obtain are of high enough resolution to include bound water molecules. It was found that the water molecules in the minor groove of the DNA form a stable, extensively hydrogen-bonded structure. The dissolution of this structure was proposed to underlie the B-A transition (see section II C, 4; also, see section II A, 2 for an alternative explanation of the B-A transition). (Note: as in the case of hydrated DNA fibres, considerable difficulty is met in measuring or even defining the "salt concentration" in crystals of hydrated DNA.)

2. A view of the dynamics of DNA-bound solvent that emphasizes ions

a. A brief review of counterion condensation theory

Counterions have been observed to "condense" about the DNA to form a highly concentrated surface layer, which is largely unaffected by changes in bulk salt concentration (evidence reviewed in Manning [1978, 1979]). Why does this occur? Condensation is predicted unambiguously in mathematical terms, when the Debye-Huckel theory of ionic interactions is extended from treating the ion cloud about a very-widely-spaced array of point charges, to treating the ion cloud about a closely-spaced array of point charges (Manning, 1978, 1979). However, people often have difficulty in understanding intuitively why it is that counterions should condense about the close array, and not about the wide array.

In the Debye-Huckel theory, condensation arises as a consequence of the superpositioning of the electrostatic (Couloumb) fields of neighboring point charges in the array. For the case of a closely-spaced array (e.g. DNA), the point charges create a "potential well" near the array's surface that is both "deep" and "steep". A high concentration of counterions "fall" into this well and become "trapped". For an array of widely-separated point charges, the potential well is more "shallow". Thus, for the latter array, a lower concentration of counterions is held, and in a much more diffuse way.

For DNA, it is important to learn whether the cations in

the condensed layer are bound rigidly to particular phosphates and thus largely dehydrated, or whether they are loosely bound, thus retaining some or all of their own hydration. Not surprisingly, "tightness" or "looseness" of binding is found to depend on the nature of the cation. For two cases of biological interest - $K^+$ and $Mg^{2+}$ - the binding turns out to be loose and nonspecific. Thus it seems most realistic to view at least these cations as remaining highly hydrated, and being able to "slide" along the isopotential surface of the DNA, from phosphate to phosphate (Manning, 1978).

What are the variables which strongly affect the "concentration" of cations in the condensed layer? The three most important ones are the linear spacing of the phosphates on the DNA (as explained above), the valence of the cation, and the bulk salt concentration. The particular chemical nature of the cation is of only secondary importance, and has been ignored in theoretical treatments to date.

Besides the condensed layer of cations, there is an outer ionic layer, or "screening" layer about the DNA, which contains both cations and anions. In this outer layer, the ions obey a Debye-Huckel-type limiting law for sensitivity to bulk salt (Manning, 1978; Record et al., 1978; van Holde, 1984). This outer ion shell is characterized by a "reciprocal ion atmosphere radius", which is proportional to the square root of the bulk ionic strength (van Holde, 1984). The outer ionic

layer is diffuse and extended at low ionic strengths, while at high ionic strengths, it is shrunken tightly about the DNA.

In terms of affecting such properties of the DNA as its intrinsic flexibility, the inner condensed layer is much more important than the outer "screening" layer (Manning, 1978). Therefore it is to the salt-dependence of the structure of the condensed layer that I now turn.

b. The effect of bulk salt concentration on the condensed layer of counterions

The "concentration" of counterions in the inner, "condensed" layer has a dependence on bulk salt concentration which at first seems counter-intuitive, or surprising. For monovalent salts, the situation is as follows. As the bulk salt concentration is increased from zero to about 100 uM, cations move from solution onto the surface of the DNA. At 100 uM bulk salt concentration, the "concentration" of cations in the screening layer has risen to about 1.2 M. It remains roughly invariant at 1.2 M (corresponding to a phosphate neutralization of about 77%) as the bulk salt concentration is raised up to 0.1 M. Above 0.1 M, though, its concentration begins again to increase, but only very slowly. (For example, it rises from 1.20 M only to 1.26 M, as the bulk concentration is raised from 0.1 M to 1.2 M [Manning, 1978].)

### 3. Attempts at integrating hydration and ion binding data

It is well known that DNA hydration, as defined in the thermodynamic sense, decreases with an increase in bulk salt concentration (see, for example, Hearst and Vinograd [1961]). This indicates that, as the salt is increased, the hydrogen bonding interactions between water and DNA are "screened" - i.e. are replaced by water/ion and DNA/counterion interactions. Two studies that attempt to elucidate the structural basis of this "screening" are those of Hearst (1965), and Wolf and Hanlon (1975).

## C. The interaction of DNA with its bound solvent

A unified theory of DNA dynamics, which would relate changes in DNA structure to changes in the solvation layer(s) (hydration and ions), does not yet exist. Nonetheless, it is instructive to focus on the several cases for which the outlines of such a theory are being drawn.

### 1. DNA flexibility

DNA is an inherently "stiff" structure. The electrostatic basis of this "stiffness" lies in the fact that the DNA's

numerous negative charges are arranged helically at a positive radial distance from its central axis. The argument is as follows. The force of repulsion between two adjacent phosphates in the DNA is inversely proportional to the square of the distance between them. Thus if the DNA is bent, adjacent phosphates on the inner perimeter of the curved DNA surface will experience an increase in repulsive force. The increase will be large because the inner phosphates will be brought very close together. In contrast, adjacent phosphates on the outer perimeter of the curved DNA surface will experience a decrease in repulsive force. This decrease, however, will be relatively small, because the "outer" phosphates will not be moved as far apart as the "inner" phosphates are moved together. In bending of the DNA, the sum of phosphate-phosphate repulsive forces will be increased by the "inside" phosphates more than it will be decreased by the "outside" phosphates. In consequence, the state of lowest potential energy will be that of a straight rod. (Note: if the DNA's phosphates were spaced uniformly along the central axis [at radial distance zero], the distinction between "inside" phosphates and "outside" phosphates would disappear; the DNA in consequence would be much more flexible.)

A complication is introduced in the above analysis when one admits that counterions are actually condensed about the DNA, and that they screen the phosphate-phosphate repulsions. Manning (1978) has used counterion condensation theory to

relate the stiffness of the DNA to the extent of neutralization (by cations in the condensed layer) of the backbone phosphates.

His theoretical argument, along with my comments on available experimental data, is as follows.

(i) Consider the situation that must exist when the concentration of counterions in the condensation layer is approximately zero (implying that the bulk salt concentration is zero). The phosphates of a B-DNA structure, which lie only 1.7 Å apart (roughly the distance between unlike charges in an ionic bond), repel each other very strongly, and so the DNA is stiff. (Note: operationally, the stiffness of the DNA must be defined by a measureable parameter such as the persistence length. A zero-salt state may be in practice unattainable for B-DNA, because of: (a) the need to work at a finite DNA [hence counterion] concentration [if measurements are to be made], (b) the resistance of the condensed cationic layer to being removed, and (c) the [well-known] instability of the B form of DNA relative to the denatured form, in very low bulk concentrations of salt [see Manning, 1978]. Thus the "stiffness" of B-form DNA in zero salt may be in practice unmeasureable, and deducible only as the extrapolation to a limit.)

(ii) As the bulk salt increases from 0 to 100 uM, condensation theory predicts a rapid increase in the extent of phosphate neutralization, and thus a large decrease in DNA

stiffness. (Note: the persistence length of the DNA has not been measured over this range of bulk salt concentration.)

(iii) From 10 uM to 0.1 M bulk salt, condensation theory predicts that the phosphate neutralization, hence DNA stiffness should be constant. (Note: the persistence length of the DNA has not been measured over this range of salt concentration, either.)

(iv) As the bulk salt is raised further above 0.1 M, condensation theory predicts that phosphate neutralization should should slowly increase, and thus that DNA stiffness should decrease. It is well known that the persistence length of B-DNA decreases with bulk salt concentration over the range 0.1-3.0 M (see, for example, Harrington [1978]; Borochov et al. [1981]; Kam et al. [1981]; for summary and commentary, see Record et al. [1981]). The form of the observed persistence-length decrease is in reasonable accord with Manning's predictions.

From the above discussion, it appears that the nature of DNA flexibility may successfully be explained by counterion condensation theory. However, further experimental testing of the theory seems necessary, especially at concentrations of bulk salt below 0.1 M.

2. The sensitivity of DNA winding to the type and concentration of salt

Anderson and Bauer (1978) have studied the effects of different types and concentrations of monovalent (and, in one instance, divalent) neutral salts on the winding angle (i.e. the duplex rotation angle) of the DNA. Their procedure was the following. (i) Unnicked circular (PM2) DNA molecules were placed in various concentrations (0.05-0.3 M) of different monovalent salts; (ii) the molecules were allowed to relax topologically through the action of "nicking/closing enzyme"; (iii) the molecules were transferred to a low (I=0.005) salt buffer; (iv) the frequency distribution of linking number topoisomers was analyzed by agarose gel electrophoresis.

For all monovalent cations, the winding angle of the DNA was found to increase approximately linearly with the logarithm of the bulk salt concentration. The following explanation of this logarithmic dependence has been offered (see Record et al., 1981). When the winding angle increases, the axial spacing of the phosphates on the DNA also increases (see Table I of Record et al. [1981]). Therefore the extent of counterion condensation decreases (see section II B, 2). This release of formerly bound counterions, and their consequent dilution, increases the entropy of the solution. Entropy of dilution, though, is known to increase in proportion to the logarithm of the bulk salt concentration. From this chain of reasoning, one therefore expects the DNA winding angle to increase in

proportion to the logarithm of the bulk salt concentration.

These workers also found that the winding angle of the DNA depends upon counterion type, increasing according to the progression $Na^+, K^+, Li^+, Rb^+, Cs^+, NH_4^+$. (Note: this order of increase is the same as the order of effectiveness of the cations in depressing the positive CD band of the DNA, in an aqueous solution [Chan et al., 1979]. It differs slightly from the order of effectiveness of positive band depression in a mixed aquaeous/methanol solvent, the order here being $Li^+, Na^+, K^+, Rb^+, Cs^+$ [Ivanov et al., 1973]. It is worth noting that the difference between the two CD studies lies solely in the aberrant behavior of $Li^+$. The CD depression is interpreted as being due to an increase in DNA winding [Chan et al., 1979; Fasman, 1979].)

The ability of an arbitrary monovalent cation to increase the DNA winding angle is directly correlated with its strength of binding, as inferred from a $[23]Na^+$ NMR assay designed to measure competition with $Na^+$ in binding to DNA (Bleam et al., 1980; Bleam et al., 1983). (In this assay, the relative binding affinity of the cations to DNA increases in the order $Na^+, Li^+, K^+, Cs^+, NH_4^+$. From comparing this progression to those above, $Li^+$ is again found to act anomalously.)

In a very brief extension of their study to divalent cations, Anderson and Bauer found that $Mg^{2+}$ increases the DNA winding angle to about the same extent as does $Cs^+$, but at

roughly 1 order of magnitude lower bulk concentration.

3. The (putative) B-to-C transition

DNA can be condensed into fibers containing a low degree of hydration (e.g. 60-70%), and a high concentration of monovalent salt (e.g. 5M LiCl). When x-ray diffraction is done on such fibers, the molecular parameters for the DNA double helix are found to be quite different from the canonical B-form parameters (obtained from fibers in high hydration, and in low salt). Thus the low-hydration, high-salt fibers are believed to contain a qualitatively new DNA form (see Fasman [1979] for discussion). This "C" form of DNA is characterized by a 5-10% increase in winding angle, over the "B" form (see Record et al. [1981] for a tabulation of molecular parameters.)

The duplex rotation angle of B-DNA in solution has been shown unambiguously to increase monotonically with increasing salt concentration (see section II C, 2). One might therefore predict that, in solution, a large enough increase in salt concentration might cause the conversion of (soluble) DNA from the B form to the C form. There have been several attempts to test this prediction, using circular dichroism to monitor structural changes in soluble DNA (see Fasman, 1979). However, in principle, many different changes in DNA structure can give rise to the same change in CD spectrum. This fact makes

interpretation of CD results highly uncertain. A less ambiguous technique for the study of DNA structural changes in solution is x-ray scattering. Bram amd coworkers have shown convincingly by this technique that, in solutions containing up to 5M monovalent salt, the B-form persists (see Bram, 1971; Bram and Beerman, 1971; Carlson, 1973; Bram et al, 1977). Thus it seems likely that the B-to-C transition cannot occur under the solution conditions ( < 2.5 - 4 M monovalent salt) of interest in this essay.

4. The B-to-A transition

Dickerson and coworkers have proposed that the stability of B-form DNA is in large part determined by the existance of a highly structured "spine" of water molecules, bound to $-NH_2$ groups of guanines in the minor groove (see Kopka et al. [1983]). They propose that, in the absence of this "spine", the A-form of DNA is more stable than the B-form. Therefore, they predict that any change in the solvent which tends to disrupt the "spine" will induce the B-to-A transition. (For an alternative view of the B-to-A transition, see section II A, 2.)

5. The B-to-Z Transition

Soumpasis (1984) has shown, with a theoretical model from statistical mechanics, that the phosphate backbone of the DNA, which contains a relatively rigid three-dimensional arrangement of (-) charges, will undergo the B-to-Z transition as the bulk monovalent salt concentration is raised above 2-3 M. Soumpasis' model takes no account of the presence of the nucleotide bases, but only of the DNA's backbone structure. Apparently, this indicates that the potentiality for the B-to-Z transition is carried within the backbone of the DNA. Thus the base sequence may not define this potentiality, but may merely modify its tendency to occur.

The B-to-Z transition has apparently been observed in poly(dC.dG):poly(dC.dG) (Pohl and Jovin, 1972; Peck and Wang, 1983), poly(dG.m$^5$dC):poly(dG.m$^5$dC) (Behe and Felsenfeld, 1981; Chen et al., 1984) and poly(dA.dC):poly(dT.dG) (Arnott et al., 1980).

Ordinarily, poly(dG.dC):poly(dG.dC) can undergo the transition only above 2 M NaCl, or above 0.7 M $MgCl_2$ (Pohl and Jovin, 1972). Peck and Wang (1983), however, have forced it to occur in low bulk concentrations of monovalent salt, by adding negative supercoiling tension to a closed circle of B-DNA which contained a poly(dC.dG):poly(dC.dG) sequence. Using an analysis from statistical mechanics, they conclude that the free energy change for the formation of the initial stretch of Z-DNA (one d(pCpG):d(pCpG) unit, involving two B/Z junctions) is 10

Kcal/mol, and that the free energy change for recruitment of each additional d(pCpG):d(pCpG) unit to the Z-form is only 0.66 Kcal/mol. This predicts a very high degree of cooperativity for the B-to-Z transition. Such cooperativity is in fact observed, in the extreme sensitivity of the transition upon the linking number of the plasmid (see Peck and Wang [1983]).

Upon methylating the cytosines in poly(dG.dC):poly(dG.dC) at the 5 position, the transition appears to occur spontaneously in physiological salt (0.7 M NaCl, or 50 mM NaCl + 0.6 mM MgCl2) (Behe and Felsenfeld, 1981). Titrations of the transition in poly(dG.$m^5$dC):poly(dG.$m^5$dC) with mono-, di-, tri-, and tetra-valent ions have also been made (Chen et al., 1984). Fujii et al. (1982) have offered a molecular explanation of how the methyl group of $m^5$dC promotes Z formation.

There is currently a controversy about whether Z-DNA can exist, and whether the B-to-Z transition can occur, within nucleosomes. This will be reviewed in section V A, 4.

6. The relevance of counterion condensation theory to chromatin studies

Counterion condensation theory promises to explain many of the basic solution properties of many polyelectrolytes, DNA included (Manning, 1978, 1979). A fundamental question is whether this theory can be applied to DNA that is associated

with the histones, in chromatin. A tentative guess, based on the successes this theory has had in explaining other DNA/protein interactions (see Record et al., 1978), is that it can be so applied. A more complete consideration of this question, especially in regard to chromatin dynamics, will be taken up in a later section.

## III. The dynamics of the (purified) histone core

In a nucleosome, the histone core is surrounded by approximately two coils of DNA. Therefore a fundamental question concerns the nature of histone core dynamics within these enwrapping DNA coils. What little is known about histone core dynamics inside the nucleosome will be reviewed in sections IV and V. Here, I will be concerned with a simpler problem - that of model studies on the stability of the isolated histone core.

It is worthwhile, first, to mention several lines of inquiry which have been pursued using other protein systems. These studies are of a very general nature, and their conclusions probably are directly applicable to the histone core.

### A. Rapid motions of the core

The subject of rapid motions in proteins has, within the past few years, come under both experimental and theoretical scrutiny. Most of the generalizations which have been formulated in a recent review (McCammon, 1984) seem applicable to the case of the histone core:

(i) The peptidyl linkages between adjacent amino acids, and the aromatic sidechains of phenylalanine, tyrosine and tryptophan constitute the relatively rigid dynamical elements in a protein molecule. The thermal motions within a protein are dominated by the torsional oscillations of these groups about the single bonds linking them together.

(ii) The (small-amplitude) motions which are calculated to occur on a very short time-scale ( $<$ 0.5 psec) have similarities to molecular motions in liquids. Thus a particular (rigid) chemical group in a protein may be envisioned as vibrationally colliding with the "walls" of a "cage" which consists of neighboring chemical groups (and solvent molecules). The amplitudes of such rapid "collisional" motions are on the order of 0.01 - 0.5 angstrom.

(iii) Many distinct types of motion exist on larger time-scales, also (1 psec - 1 msec). These motions have characteristics one typically associates with solid bodies. Thus the rotation or libration of a chemical group which is buried in a protein produces a strain in the remaining, connected portion of the protein molecule; this strain then

acts as a force resisting the continued motion of the group in question. "Solid-body"-like motions such as this have amplitudes on the order of 0.5 - 10 angstrom.

(iv) The motional displacements of atoms and groups in a protein are larger at the surface of the protein than in its interior.

(v) On the slower time scales, anharmonic contributions may be more dominant than harmonic contributions, in determining the nature of the overall motion.

B. Changes in the hydration of the core

It is well known that proteins are hydrated (for reviews, see Edsall [1953], Steinhardt and Reynolds [1969], Kuntz and Kauzmann [1974], Cantor and Schimmel [1980]). It is also known that protein hydration decreases with increasing NaCl concentration (Kuntz and Kauzmann, 1974). It is reasonable to expect the same type of behavior for the histone core.

C. Equilibria between the histones of the core

The various equilibria between the inner histones have received considerable study. For some of the equilibria, quite good data exist; for other (putative) equilibria, some ambiguities remain.

1. The monomer/tetramer equilibrium of H3 and H4

The dominant equilibrium, in terms of establishing the "kernel" of histone core structure, seems to be a very strong monomer-tetramer association, involving two copies of histone H3 and two copies of histone H4.

That an equilibrium really exists in this case was rigorously demonstrated by D'Anna and Isenberg (1974a). Their investigation was based upon an earlier study of H3/H4 association by Kornberg and Thomas (1974). D'Anna and Isenberg showed, with fluorescence anisotropy, CD, and light scattering techniques, that H3 or H4 slowly aggregate when present separately in solution, but do not aggregate when mixed in equimolar ratios. By varying the relative molar amounts of H3 and H4 in their CD and light scattering experiments, and by analysis of equilibrium sedimentation data, these workers were able to determine both the stoichiometry of the association reaction, and also a value for the equilibrium constant. In 16 mM phosphate, pH 7.0, Keq = 0.7 ($10^{21}$) $M^{-3}$. Another careful study, reporting a significantly lower (10- to 100-fold lower) value of the equilibrium constant, is that of Roark et al. (1974). The study of Roark et al. indicates that, at least at lower histone concentrations, there may be some dimer-tetramer equilibrium as well.

D'Anna and Isenberg did not investigate the salt-dependence of the association of H3 and H4. The association appears to be relatively insensitive to salt, though. For example, Moss et al. (1976) report, by velocity- and equilibrium sedimentation in the analytical centrifuge, that, in an equimolar mixture of H3 and H4 in a 50 mM acetate/ 50 mM bisulfite buffer, the stable species appears to be the tetramer ($s_{20,w}$ at infinite dilution = 2.54 +- 0.05 S; M = 41,000). Also, Rubin and Moudrianakis (1975) report that the H3/H4 "complex" present in 1.2 M NaCl contains equimolar amounts of the two proteins, and has approximately the correct sedimentation coefficient for a tetramer ($s_{20,w}$ = about 4, by sucrose gradient analysis). Finally, Ruiz-Carillo and Jorcano (1979) argue, from sucrose gradient sedimentation and gel filtration, that the H3/H4 "complex" present in 2 M NaCl is a tetramer (having equimolar amounts of H3 and H4, an apparent s value of 3.2 S, and an apparent molecular weight of 55,000). I note that, in the above three studies, the demonstration of equilibrium and stoichiometry is not as rigorous as in the study of D'Anna and Isenberg, and numerical values of the association constant are not reported. Also, there are great inconsistencies in $s_{20,w}$ and M between the three studies. Finally, in the studies of Rubin and Moudrianakis (1975) and of Moss et al. (1976), considerable aggregation was observed. Thus there is the worrisome uncertainty that the H3/H4 "complex" that has been

reported for all these disparate conditions may not in all cases be a homogeneous $(H3.H4)_2$ tetramer.

From the above studies, I put forth the tentative conclusion that the H3/H4 tetramer is the dominant stable species over the 16 mM - 2 M salt range. It therefore seems reasonable to suppose that, because of this insensitivity to ionic strength, the association equilibrium is not governed by ionic interactions, but rather by hydrophobic interactions.

2. The monomer/dimer equilibrium of H2A and H2B

Early suggestions of a 1:1 stoichiometric complex between H2A and H2B were given by Skadrani et al. (1972), and by Kelley (1973). A rigorous investigation of the interaction of these two histones was then made by D'Anna and Isenberg (1974b). Using fluorescence anisotropy and CD techniques as in their H3/H4 study above, these workers demonstrated an equilibrium association reaction between H2A and H2B, in approximately a 1:1 stoichiometry. Equilibrium centrifugation analysis suggested that the association product was a dimer (M=28,500 +- 800). However (unlike in these workers' earlier study of H3,H4 association), there was some self-aggregation in portions of the spectroscopic experiments, and considerable aggregation in the ultracentrifugation experiment. Thus the conclusion that a 1:1 dimeric complex is formed is slightly uncertain.

The spectroscopic studies of D'Anna and Isenberg (1974b) were done in either 3 mM phosphate, 16 mM phosphate, or 0.2 M NaCl + 6 mM cacodylate, always at pH 7.0. Under all conditions, calculated equilibrium constants were approximately the same, at the value $K = 1.6\ (10^{6})\ M^{-1}$. Due to the relatively large error in measurement, an estimate of the salt-dependence of the equilibrium constant is difficult to make. The constant does not seem to be very ionic-strength-dependent, though, at least over the 3 mM - 0.2 M salt range.

3. The "mixed" equilibria between H2B and H4, between H2A and H4, between H2B and H3, and between H2A and H3

The earliest rigorous demonstration of a "cross-complex" between histones was that given by D'Anna and Isenberg (1973), for H2B and H4. These workers observed that H4 undergoes an apparently indefinite aggregation with time, when present alone in moderate ionic strength solution. Addition of an equimolar amount of H2B prevents this aggregation. Applying the method of continuous variations to CD and fluorescence anisotropy measurements, a 1:1 stoichiometric equilibrium between these two species was demonstrated. It was suggested (but not proved) that the complex was a dimer. An apparent equilibrium constant of $0.3\text{-}3\ \ 10^{6}\ M^{-1}$ was estimated, under conditions of 3-240 mM ionic strength (pH 7.0).

By applying the method of continuous variations to CD measurements, D'Anna and Isenberg (1974a) also observed an apparent equilibrium between H2A and H4, in 7 mM phosphate, pH 7.0. The interaction between these two histones, however, appeared to be quite weak (i.e. comparable in magnitude to the self-aggregation tendencies displayed by the histones individually). A 1:1 stoichiometry was observed, and an apparent equilibrium constant of about $4\ 10^{4}\ M^{-1}$ was calculated (assuming a dimeric association product).

D'Anna and Isenberg (1974b) observed a third "cross-complexing reaction" to occur, in this case between H2A and H3. Complex formation was studied in 15 mM phosphate, pH 7.0. By applying the method of continuous variations to fluorescence anisotropy measurements, it was determined that a 1:1 stoichiometric complex was formed. An apparent equilibrium constant of $10^{5} - 10^{6}\ M^{-1}$ was estimated (assuming a dimeric complex to have formed).

Finally, D'Anna and Isenberg (1974b) observed that the addition of an equimolar amount of H2B to a low-ionic-strength solution of H3 prevented the latter species' self-aggregation. This suggested the formation of a specific complex between the two histones. However, it proved impossible to use the method of continuous variations to study complex formation, because there was little or no change in the fluorescence anisotropy or CD upon complex formation. Thus the stoichiometry of

association and the equilibrium association constant were not determined.

In none of the above cases was the salt-dependence of the association examined. Thus much remains to be learned about the stabilities of these complexes under physiological conditions.

4. The association of the $(H3\ H4)_2$ tetramer with (H2A H2B) dimers

From the above discussion, it is clear that the $(H3\ H4)_2$ tetramer and the (H2A H2B) dimer are stable species, perhaps over a range of ionic strengths as broad as 0.016 - 2.0 M. If these species are mixed together, will they retain their identities, and perhaps associate to produce $(H3\ H4)_2$ : (H2A H2B) hexamers, and $(H3\ H4)_2$ : $(H2A\ H2B)_2$ octamers? In investigating this question, one must consider certain alternatives - in particular, the hypothesis that, when mixed together, new sets of inter-histone interactions become favored, so that the heterotypic tetramer (H2A H2b H3 H4) becomes the stable species (see Weintraub et al. [1976] for a phrasing of this hypothesis).

Much work has been done attempting to investigate the equilibria that arise when the inner histones are mixed together in equimolar ratios. In spite of this body of work, however, even the identities of the equilibria were until very

recently quite controversial. This controversy persisted because of the many experimental artifacts that tended to occur in study, particularly when hydrodynamic techniques were used (see Stein and Page [1980] for a good discussion of some of these artifacts).

An example of just one subtle type of difficulty is that given in a paper by Philip et al. (1979). This work relied upon a very gentle isolation procedure, in which a complex of the inner histones was obtained in a high concentration of NaCl, at neutral pH and at atmospheric pressure. At 2-6 mg/ml total histone concentration, 2 M NaCl + 25 mM phosphate, pH 7.0, and a centrifugal field strength less than 60,000 x g, the complex appeared identifiable as an octamer of core histones, by extrapolating $S_{20,w}/D_{20,w}$ measurments to infinite dilution and atmospheric pressure. These workers, however, observed a sharp decrease in the sedimentation coefficient as the centrifugal field strength was raised through the 63,000 - 75,000 x g range. They suggested that this was due to an irreversible (denaturing) transition.

Perhaps the most experimentally rigorous work to date on the problem of equilibria in equimolar mixtures of the inner histones is that from the laboratory of E. Moudrianakis. Godfrey et al. (1980) have prepared a histone complex in 2 M NaCl, pH 7.0, at atmospheric pressure. They then performed a very careful equilibrium sedimentation study of this complex in

2.0 M NaCl, 10 mM Tris, pH 7.5. Data were analyzed according to a "mixed associating system" model. In this model, an $(H3\ H4)_2$ tetramer and an (H2A H2B) dimer can associate to form an $(H3H4)_2$ : (H2A H2B) hexamer (described by an equilibrium constant K1); also, the hexamer can associate with an additional (H2A H2B) dimer, to produce an $(H3\ H4)_2$ : $(H2A\ H2B)_2$ octamer (described by an equilibrium constant K2). They found that the data fit the above model statistically well, and they concluded that K1 and K2 were approximately equal, at the value 8.2 +- 1 ($10^5$) $M^{-1}$. (Note: the equilibrium centrifugation was carried out at fairly high centrifugal field strengths (for example, at r=6.8 cm, a field strength of 51,000 x g was present). Thus conditions toward the bottom of the centrifuge cell approached those where Philip et al. observed the pressure-dependent decrease in S for the (putative) histone octamer (see above). Thus caution may be necessary in extrapolating the conclusions of Godfrey et al. to atmospheric pressure.)

The data of Godfrey et al. exclude models invoking the existance of a "heterotypic tetramer". Thus it seems reasonable to conclude that the (H2A.H2B) dimer and the $(H3.H4)_2$ tetramer remain stable species when mixed together. In other words, the interactions holding the (H2A.H2B) dimer or the $(H3.H4)_2$ tetramer together are strong, relative to the interactions holding either of the (H2A.H2B) dimers to the $(H3.H4)_2$

tetramer.

The work of Godfrey et al. (1980) was followed by a calorimetric study from the laboratories of Moudrianakis and Ackers. In this later study, Benedict et al. (1984) observed a slight cooperativity for the binding of the two (H2A.H2B) dimers to the $(H3.H4)_2$ tetramer; thus the second association was measured to have a four-fold greater value for the equilibrium constant than the first association had. From studying the association reaction in different buffers, a small proton release upon octamer formation was inferred. This was studied further in a subsequent publication (McCarthy et al., 1984).

It is worth noting that the "mixed associating system" model of Godfrey et al. is consistent with earlier experiments in which the histone octamer was isolated in 2 M NaCl, was dialyzed into various concentrations of NaCl, and was then examined on a gel filtration column (Eickbush and Moudrianakis, 1978; Ruiz-Carillo and Jorcano, 1979). The separate peaks which eluted from the column were analyzed directly on denaturing protein gels, to determine their histone stoichiometries. The peaks' elution positions (relative to markers) and histone stoichiometries suggested that their identities were in fact the (H2A.H2B) dimer, the $(H3.H4)_2$ tetramer, the $(H2A.H2B):(H3.H4)_2$ hexamer, and the $(H2A.H2B)_2:(H3.H4)_2$ octamer.

This concludes my brief review of the known dynamical processes of free DNA and (purified) histone cores. With this background, it becomes possible to discuss in a fashion that is not naive the instabilities of the complete nucleosome core particle. Below, an attempt will be made to understand the instabilities of core particles in terms of the dynamics of the constituent DNA and histone core. As will be shown, this reductionist viewpoint yields considerable insight into nucleosome instabilities.

IV. The nucleosome as a changeable structure. 2. Five principles of nucleosome structure which delimit and predict nucleosome dynamics.

It is my belief that a great deal about the dynamics of nucleosomes can be predicted from an understanding of five principles of structure. These principles deal with: (A) the differential stabilities of the various domains of bonding between the histones of the nucleosome's core; (B) the conformational "strain" placed on the DNA (and, in a complementary way, placed on the histone core as well) by bending the DNA about the core; (C) the potential energy of repulsion between adjacent loops of DNA in a nucleosome, which arises as the length of DNA in the nucleosome increases above about 80 bp; (D) the unbinding and release of counterions from

the DNA (and possibly from the histone core as well), which occurs as the DNA and the histone core come together to form the nucleosome; and (E) the "degeneracy" of the domain of bonding between the DNA and the histone core. Below, I attempt to state the principles in such a way as to emphasize their predictive ability concerning nucleosome dynamics.

A. The Differential Stabilities of Different Bonding Domains Within the Histone Core

1. High stability of bonding domains within the $(H3.H4)_2$ tetramer

From studies on mixtures of purified histones, it appears that the H3,H4 monomer/tetramer equilibrium is relatively insensitive to changes in ionic strength, at least in the range of 0.016 to 2.0 M (see section III C). This suggests that the domains of bonding in the $(H3.H4)_2$ tetramer are primarily hydrophobic in nature. Thus one might predict that, when nucleosomes are placed under "physiological" conditions of salt and temperature, a dominant feature governing their ensuing dynamics should be an inherent stability of the $(H3.H4)_2$ tetramer.

In the presence of the (H2A.H2B) dimer, the $(H3.H4)_2$ tetramer seems to retain an integrity of its own, entering as a

unitary entity into association reactions with the dimer, and showing no enhanced tendency to split apart (as reviewed in section III C).

Is the $(H3.H4)_2$ tetramer a stable species also in the presence of DNA? Some structural stability is indicated by the fact that equimolar H3 and H4 can induce (-) supercoils in closed circular DNA (Bina-Stein and Simpson, 1977; Jorcano and Ruiz-Carillo, 1979), and can confer upon linear DNA a DNase I protection pattern which appears to be a rudimentary form of the "10 bp ladder" so well known for authentic nucleosomes (Sollner-Webb et al., 1976). No firm conclusion, however, can be drawn concerning the integrity of the $(H3.H4)_2$ tetramer in the presence of DNA, until more information is obtained about the nature of the H3/H4/DNA "complexes" in the above studies.

Cary et al. (1978) have investigated the stability of the $(H3.H4)_2$ tetramer within core particles, over a range of bulk salt concentration. These workers carefully monitored portions of the 1H NMR spectrum of a 10 mg/ml (A260 = 100) solution of core particles, as the concentration of NaCl was varied from 0 to 0.6 M. They observed no changes in the linewidths of resonances from aromatic amino acids in the hydrophobic regions of the $(H3.H4)_2$ tetramer. (Their assignment of resonances was based on numerous previous 1H NMR studies of sequenced histone fragments.) Thus, when in contact with (H2A.H2B) dimers and DNA in a core particle, the $(H3.H4)_2$ tetramer appears to remain as

a stable complex in response to changes in bulk salt concentration.

The hypothesis that the $(H3.H4)_2$ tetramer remains a very stable entity within the nucleosome receives additional (although somewhat more indirect) support from the following data. (i) The sulfhydryl groups of the H3 histones in non-acetylated core particles are unreactive to bulky thiol reagents below about 1M salt (Zama et al., 1977; Wong and Candido, 1978; Bode and Wagner, 1980; Bode et al., 1980). (Note, however, that acetylation of H3 and H4 seems to make these thiols much more reactive, for somewhat uncertain reasons [Bode et al., 1980; Bode et al., 1983].) (ii) No changes in the pattern of histone/histone crosslinking within core particles are observed over the 0.01 - 0.6 M salt range (Wilhelm and Wilhelm, 1980). (iii) There is virtually no change in either the intensity or anisotropy of the fluorescence of the histone core's tyrosines, as core particles are examined over the 0.01 - 0.6 M KCl range (Libertini and Small, 1982).

From all the above data, I propose that, in dynamical processes of nucleosomes, the integrity of the $(H3.H4)_2$ tetramer is maintained, because of hydrophobic interactions between the monomers of the tetramer. This proposal, when treated as a working hypothesis, has great predictive power. For example, it predicts that, at elevated temperatures or salt concentrations, the core particle will not unfold to produce

the "double hemisome" postulated by Weintraub et al. (1976), or the "linearized nucleosome" postulated by Dieterich et al. (1979) and Zayetz et al. (1981).

2. High stability of bonding domains within the (H2A.H2B) dimer

From studies on mixtures of purified histones, it appears that the monomer/dimer equilibrium between purified H2A and H2B is relatively insensitive to bulk salt concentration, at least from 0.003 M to 0.2 M (and possibly up to 2 M; see section III C).

Just as for the above case of the H3/H4 equilibrium, this salt-independence suggests that the domains of bonding in the (H2A.H2B) dimer are principally hydrophobic. Thus I predict that another dominant feature governing the dynamics of the nucleosome under physiological conditions will be an inherent stability of the (H2A.H2B) dimer.

Knowledge is rather incomplete concerning the stability of the (H2A.H2B) dimer in the presence of the other components of the nucleosome. Apparently nothing is known about the stability of the (H2A.H2B) dimer in the presence of DNA alone. In the presence of the $(H3.H4)_2$ tetramer, the (H2A.H2B) dimer seems to retain an integrity of its own, entering as a unitary entity into association reactions with the tetramer, and showing no

enhanced tendency to split apart (as reviewed in section III C. The stability of the (H2A.H2B) dimer in the presence of both DNA and equimolar H3,H4 has not been directly investigated. H2A and H2B are known to dissociate from long chromatin fragments in elevated salt (Burton et al., 1978, 1979); however, their state(s) of association during release from the chromatin is not known. Apparently, no analogous studies have been done to determine the association state(s) of H2A and H2B released during the salt-induced dissociation of mononucleosomes.

3. Marginal stability of bonding domains between the (H3.H4)2 tetramer and the (H2A.H2B) dimer

It is becoming increasingly clear that (in the absence of DNA) the dissociation of the histone octamer is dominated by the stabilities of the $(H3.H4)_2$ tetramer and the (H2A.H2B) dimer (see section III C). The tetramer-hexamer-octamer equilibrium involved in this dissociation seems to be highly salt-dependent, although the stabilities of the $(H3.H4)_2$ tetramer and the (H2A.H2B) dimer do not seem to be (see section III C).

The fact that the tetramer-hexamer-octamer equilibrium is highly salt-dependent suggests that the free energy of bonding of (H2A.H2B) dimers to the $(H3.H4)_2$ tetramer has a substantial electrostatic component. Presumeably, if the salt-dependencies

of the association constants were known, conclusions could be drawn about the number of electrostatic interactions which are involved. This line of reasoning suggests a third principle governing nucleosome dynamics under physiological conditions: that the tendency for rupture of the bonding domain between the $(H3.H4)_2$ tetramer and each of the (H2A.H2B) dimers helps determine which dynamical processes can actually occur.

Little is known with certainty about how the tetramer-hexamer-octamer equilibrium is affected by the presence of free DNA. One view which has been put forth is that the DNA bonds to the $(H3.H4)_2$ tetramer, as well as to the $(H3.H4)_2.(H2A.H2B)_2$ octamer (Sollner-Webb et al., 1976; Thomas and Oudet, 1979). In this view, the presence of the DNA does not disrupt the tetramer-hexamer-octamer equilibrium, but merely superimposes upon it additional equilibria of the tetramer and octamer (and possibly also the hexamer) with the DNA. This view must admit, however, that the presence of DNA in effect shifts the tetramer-hexamer-octamer equilibrium to favor states of high association. Thus one never observes the release of one or two (H2A.H2B) dimers from the $(H3.H4)_2$ tetramer in a nucleosome, during moderate-salt nucleosome dissociation (see section VB, 3).

A radically different view is that, in the presence of the DNA, the tetramer-hexamer-octamer equilibrium is eliminated, and replaced with an equilibrium between an intact nucleosome

and a "double hemisome" (Weintraub et al., 1976), or a "linearized" structure in which all the histones are separated, but are still bound to the DNA (Dieterich et al., 1979; Zayetz et al., 1981). Recently, a third proposal has been put forth (Ellison and Pulleyblank, 1983a, 1983b, 1983c). In this third view, in the presence of DNA the H3:H3 and H4:H4 bonding domains become unstable, and (H3.H4) dimers are released from nucleosomes as stable entities. Recalling the apparently high and salt-independent stabilities of the $(H3.H4)_2$ tetramer and the (H2A.H2B) dimer, the first view seems to me more plausible than either the second or the third. Nonetheless, more study is necessary to finally settle this point.

The ultimate conclusions of this discussion, then, can be phrased as follows. It seems that a dominant feature governing nucleosome instabilities in elevated salt and temperature may be the tendency for various equilibria to occur between complexes of the histones. To be more explicit, dynamical processes may be strongly influenced, or even determined by the tendency of the $(H3.H4)_2$ tetramer and the (H2A.H2B) dimer to remain intact as unitary entities, and by the tendency of the (H2A.H2B) dimers to split off from the $(H3.H4)_2$ tetramer.

B. The Torsional Stress Placed upon the DNA and the Histone Core from Bending the DNA About the Core

Under physiological conditions, the free energy of a 150 bp length of B-DNA is increased considerably when it is bent into a superhelix about the histone core. (The exact magnitude of the increase is uncertain, but probably lies between 20 and 120 Kcal/mol; some calculations are reviewed in part 3 of this thesis.) Thus, in a nucleosome, the DNA is under considerable torsional stress to straighten back out.

It is worth noting that, in a situation of structural equilibrium, in addition to the DNA's torsional stress, there will be an equal but opposite stress on the histone core. Thus the histone core in a nucleosome, due to interaction with the (unfavorably bent) DNA, may have a somewhat "strained" or "deformed" shape, relative to its shape when free in solution.

Since (at least in low to moderate bulk salt) the nucleosome is a stable entity, the above discussion implies that the DNA must be firmly "anchored" to the histone core, at least at its termini. Any reaction tending to break terminal bonds between the core and the DNA will therefore have the effect of causing DNA "tails" to straighten out and project off the surface of the core. Also, the straightening of any portion of the DNA in a nucleosome may be a driving force in nucleosome unfolding and dissociation (see sections VB,1 and VB,3 respectively).

C. The electrostatic repulsion between adjacent loops of

DNA in a nucleosome

According to the x-ray diffraction map of Klug et al. (1980), the central 80 bp of DNA in the nucleosome comprises one complete turn of a superhelix of 27 A pitch; any additional DNA in the nucleosome is viewed as forming two identical "tails" which extend off the ends of the central "coil". As a consequence of this geometry, any segment of DNA outside the central coil must, of necessity, approach fairly closely another segment of DNA lying in the same radial position on the superhelix, but 80 bp before or ahead of it.

The above model leads naturally to the problem of estimating the energy of repulsion between the two adjacent loops of (negatively charged) DNA. In an approximate analysis (Yager and van Holde [1984], unpublished), the phosphates on the loops are modelled as point charges 1.7 Å apart, on two parallel straight lines separated by 27 Å. Each point charge is assumed subject to Debeye-Huckel screening by the solvent (see Manning, 1978). Because of the simple geometry, a general formula for the net electrostatic repulsion is easily written. There is a fundamental difficulty in using this formula, though - that of fixing a numerical value to the dielectric constant. Indeed, it is not entirely clear what physical meaning should be ascribed to the concept of a "dielectric constant", for the region between two adjacent coils of DNA on the surface of a

nucleosome. This difficulty precludes computing a numerical value for the electrostatic repulsion energy. (Assuming the "dielectric constant" to be a meaningful concept, and assigning the constant some arbitrary value, the calculation may be done anyway. When it is done, the result emerges that the repulsive energy is linearly proportional to the number of point charges in the region of overlap between the two coils.)

The fact that the two adjacent coils repel each other leads to several predictions concerning nucleosome dynamics. First it predicts that, in "stripping off" the DNA from the histone core, the central 80 bp should be the most stably bound. This may underlie the observed "plateau effect" in the release of DNA tails from the histone core, both in the low-salt thermal denaturation of core particles, and in the "fast structural transition" induced in core particles by elevated salt (see section V B, 2). Second, it predicts that an "unfolded nucleosomal state", in which the apposed coils are far apart, may be more stable than a "compact nucleosomal state", under some conditions (see section V B, 1).

D. The release of bound counterions from the DNA (and possibly also from the histone core), upon binding the DNA to the core

It was only about a decade ago that the theory of

protein/DNA interactions was finally placed on a rigorous theoretical basis. Two breakthroughs in understanding allowed this to occur. First, McGhee and von Hippel [1974] correctly understood that, for any nucleic acid lattice that nonspecifically binds a protein, an overlapping degeneracy of protein-binding sites is a fundamental property. They modified the traditional Scatchard-type analysis to include this insight. This theoretical development will be applied to nucleosomal DNA/core interactions in the next section (IV E).

The second breakthrough was made by T. Record and coworkers (see Record et al. [1978]). These workers began with a standard binding-polynomial-type description of a protein-nucleic acid interaction, and then incorporated into it a description of the nucleic acid based on Manning's counterion condensation theory. The significance of this analysis is the following. It points out that a fundamental driving force for the binding of a protein to DNA is the entropy increase caused by diluting into the surrounding medium the counterions which were formerly bound to the DNA and the protein.

The binding of DNA to an intact octamer of the core histones probably can be described by Record's type of thermodynamic formalism. For the analysis to be accurate, however, one must also take account of the facts that: (i) the octamer itself can dissociate (cf. section IV A); (ii) the DNA must bend, in addition to forming bonds with the octamer (cf.

section IV B); (iii) adjacent coils of DNA closely appose each other (cf. section IV C); and (iv) there is degeneracy in the domain of DNA/core bonding (cf. section IV E). One attempt to apply a Record-type analysis to DNA/core interactions has been made by Yager et al. (part 3 of this thesis), in connection with the release of DNA "tails" from the core in elevated salt (see section V B, 2).

E. The "degeneracy" of the domain of bonding between the DNA and the histone core

The degeneracy "principle" or, more accurately, hypothesis simply states that, in a nucleosome, the DNA can sit on the histone core in a large number of energetically equivalent ways. A simple calculation illustrates this hypothesis. According to the model of Klug et al. (1980), the histone core can accomodate about two full turns of DNA (i.e. about 166 bp). In a core particle, however, the DNA is only about 146 bp long. Assuming therefore that, on the core, all binding sites for the DNA are equivalent, one predicts about 20 equivalent positions for the placement of core-particle-sized DNA. This in turn has two profound implications.

First, it implies that the "apparent" (i.e. measured) association constant for binding 146 bp-sized DNA to an intact histone core will be 20 times greater than the "actual" (i.e.

intrinsic) binding constant, because of a degeneracy contribution to the "apparent" constant. (The discrepancy between "apparent" and "intrinsic" binding constants would be even greater for shorter DNA or for DNA longer than about 185 bp, according to this "degeneracy" argument.) Thus the stability of the "bound state" between the DNA and the core in part derives from the existance of a multiplicity of energetically equivalent "microstates" (i.e. is "statistical" in nature).

The second implication is that the nucleosome may, under certain conditions, be able to shift between these energetically equivalent "microstates". Structurally speaking, this means that the precise positioning of the DNA on the core (i.e. its "register") may be subject to quantized "shifting". This shifting then would underlie the phenomenon of "sliding" of the histone core along the DNA (see section V A, 3).

V. The nucleosome as a changeable structure. 3. Specific dynamical processes which have been reported in the literature.

In this section, I will discuss the specific dynamical processes of nucleosomes which have been reported in the literature. I attempt to distinguish between processes that leave intact the basic structure of the nucleosome, and processes that greatly disrupt this basic structure. The former

include changes in hydration, small changes in the conformation of the histone core, and sliding of the core along the DNA. The latter include a global unfolding of the nucleosome (if in fact it occurs under physiological conditions), the release of DNA tails, and nucleosome dissociation.

A. Nucleosome dynamics leaving the histone/histone and DNA/histone bonding domains virtually intact

1. Changes in hydration

Quite plausibly, certain dynamical processes might be confined to the layer(s) of hydration surrounding a nucleosome, and might not greatly affect the bonding domains within the nucleosome itself.

Bradbury and coworkers have investigated nucleosome hydration using neutron scattering in $H_2O$ or $D_2O$, with or without added glycerol (Rattle et al., 1979). Also, Eisenberg and Felsenfeld (1981) have examined nucleosome hydration by equilibrium sedimentation of core particles in the presence of cosolutes of various molecular weights. Unfortunately, both studies provide no information on dynamical aspects of nucleosome hydration.

In princ'ple, it should be possible to repeat both the neutron-scattering and the sedimentation equilibrium studies at

various ionic strengths and temperatures, to learn how the nucleosome's different hydration layers are affected by these environmental factors. Such studies would be interesting in light of the proposal of Kopka et al. (1983), that a "spine" of water in the minor groove of (free) DNA is necessary for the stability of the "B" structure (see section I C, 4).

2. Small changes in the structure of the histone core

The effect of salt on the structure of the histone core within the nucleosome has been examined fairly extensively, by a number of techniques (see section IV A). Studies involving high-resolution 1H NMR, histone H3-thiol reactivities, histone-histone crosslinking, and histone tyrosine fluorescence anisotropy all point to the same conclusion: that there is no dramatic rearrangement of the histone core over 0.01 to 0.6 M bulk concentration of salt. (This conclusion, of course, holds only when the nucleosome concentration is high enough that no dissociation into free DNA and histones can occur; see section V B, 3.)

This is not to say, however, that salt is completely without effect on the histone core. There is, for core particles, a slight decrease in the steady-state anisotropy of histone tyrosine fluorescence, over the 0.01 to 0.75 M KCl range (Libertini and Small, 1982). This is interpreted to mean

a slightly enhanced "flexibility" of the core in elevated salt.

Bradbury and coworkers have begun to define more precisely the nature of the small dynamical change detected by the above technique. Using 1H NMR, and assigning resonances to particular histone regions on the basis of model studies, Cary et al. (1978) have determined that the salt effect involves increases in the mobilities of the N-terminal regions of histones H3 and H4, within the otherwise intact core particle. The mobilities of the hydrophobic central regions of all the histones appear to be unaffected by salt. Thus the "release" of the N-terminal regions, or "tails", of H3 and H4 apparently occurs without significant disruption of the overall structure of the histone core.

It seems probable that the release of the "tails" of H3 and H4 does not greatly affect the bonding domain between the histone core and the DNA. This assertion is based on the finding that proteolytic removal of these "tails" has no effect on core particles' DNAase I digestion patterns (Whitlock and Stein, 1978).

3. Small changes in DNA structure, and in the DNA/core bonding pattern

To talk rigorously about dynamical processes localized in either the DNA of nucleosomes, or in the bonding domain between

the DNA and the histone core, one must first review in some detail what is known about the structure of the DNA/core bonding domain.

a. The view, from electrostatics, of DNA/core bonding

The histone core has a charge of about +150, at pH 7 (from histone sequence information; see Lewin [1980]). As a consequence, there must be at least some electrostatic component to the attractive force between core and DNA, simply as a consequence of the Couloumbic attraction between oppositely-charged bodies. In principle, the magnitude of this electrostatic component could be calculated, given precise enough knowledge of the geometries of the core's (+) charges and the DNA's (-) charges, of the appropriate dielectric constant(s) to use, and of the disposition of small mobile counterions about the whole structure. However, knowledge of such detail is not available.

If the electrostatic contribution cannot be calculated, then can it instead be measured? The difficulty with this approach is that, in principle, any technique for measuring the free energy of interaction between the DNA and the histone core necessarily must measure the difference in G,H or S of two nucleosomal states, where each such quantity is a (nonseparable) sum of electrostatic and non-electrostatic

components. Therefore, to be successful, any attempt to resolve an observed free energy of DNA/core interaction into electrostatic and non-electrostatic components must incorporate ancillary data from model binding studies.

Such an attempt has been made by Yager et al. (part 3 of this thesis), who have studied the binding of the "tails", or termini, of the DNA to the histone core (see section V B, 2). These workers assumed that the purely electrostatic component of this binding interaction could be represented by oligolysine/DNA binding data (see Record et al. [1978]), and that the totality of the binding interaction could be represented by oligoarginine/DNA binding data. They then calculated, at various bulk concentrations of salt, the electostatic- and non-electrostatic components of the free energy change for "DNA tail-binding", from a theoretical expression for the equilibrium binding constant (see Record et al. [1978]). Note: there are also terms for DNA bending and for the repulsion between adjacent DNA coils, in the complete treatment of this problem (see part 3 of this thesis).

I note that, in certain cases, there may be a substantial non-electrostatic component to the bonding of the DNA to the core. This is suggested by the existance of DNA sequences upon which histone cores are "phased" (see Simpson and Stafford [1983] for a clear-cut recent example, and Zachau and Igo-Kemenes [1981] for a review of older literature). (It is,

of course, possible to imagine that phasing on a particular DNA sequence is due to some property of the DNA other than its ability to form non-electrostatic bonds with the core. Such a property might be an ability to "bend" or "kink" into a "locking" conformation [Mengeritsky and Trifonov, 1983].)

The above viewpoint attempts to resolve the energy of interaction between DNA and the histone core into electrostatic and non-electrostatic components. A complementary view focuses less on determining the electrostatic- or non-electrostatic character of the interaction, and more on the question of how "specific" or "localized" the regions of contact between the DNA and the core are.

b. The chemical nature of the bonds between the DNA and the histone core

McGhee and Felsenfeld (1979) have attempted to answer the question of whether, in a core particle, the histone core makes any specific contacts with the reactive ring nitrogens of the guanine bases of the DNA. They observed, for core particles containing random-sequence DNA, no specific pattern of protection of the DNA against reaction with dimethyl sulfate. They concluded that the DNA bases were not involved in bonding to the core. Another interpretation of their results is possible, however. It could be that bonding between the core

and DNA bases occurs, but is dynamic. The experiment of McGhee and Felsenfeld involved low levels of reaction. Thus, for their population of core particles, each position along the DNA was only incompletely and transiently "sampled" for the presence of a bond. This problem has not been examined further.

Attention has also been directed toward detecting interactions between the histone core and DNA phosphates. As suggested by the following studies, specific contacts between phosphates on the DNA and positive groups on the surface of the core (probably arginines, and possibly some lysines as well) play a major, if not nearly exclusive role in binding the DNA to the core.

McGhee and Felsenfeld (1980b) have estimated the number of specific ionic bonds that the two 25-30 bp DNA "tails", or termini, make with the histone core. These workers measured the dependence on ionic strength of the unbinding and denaturation of the DNA tails, in the low-salt thermal denaturation of core particles. The dependence which they observed is consistent with a model where approximately 15 +- 6 % of the DNA phosphates (i.e. 45 +- 20 phosphates) are bound to the histone core by specific bonds having a large electrostatic component. A very similar estimate (9-12% of the phosphates) was recently obtained by Yager et al. (see part 3 of this thesis), from measuring the salt-dependence of the unbinding of DNA "tails" over the 0.3-0.75 M NaCl range (see section V B, 3). It should

be noted that neither of these studies were able to examine the (putative) electrostatic bonds between the histone core and the central 90-100 bp of the DNA.

Yager et al. went on to show, with oligopeptide/DNA binding data, that the observed salt-dependence of the "tail-unbinding reaction" was more consistent with the assumption of phosphate/arginine bonds than with the assumption of phosphate/lysine bonds. The involvement of the former type of bonds is also suggested by the resonance raman study of Mansy et al. (1976), and by the protection to chemical modification which the DNA of a core particle apparently affords to core arginines, but not to core lysines (Ishimura et al., 1982).

For the case of phased nucleosomes, if indeed the phasing specificity derives from non-electrostatic bonds between the DNA and the core, then the most likely candidates are specific hydrogen bonds between charged groups on the histone core (lysines, arginines, histidines, glutamates, and aspartates), and the ring nitrogens, carbonyls and amines of the DNA bases (Seeman et al., 1976).

From all the above discussion, it seems that, to a reasonable first approximation, the bonding between the DNA and the histone core is restricted mainly to discrete points on the DNA (and especially to the phosphates), and has a large electrostatic component. Thus the fundamentally correct way to

analyse DNA/histone bonding, and changes thereof, is with a ligand-binding formalism which incorporates counterion condensation theory (Manning, 1978; Manning, 1979; Record et al., 1978; Record et al., 1981). The theory must be modified, however, to include the energetically unfavorable effects of bending the DNA about the core and bringing adjacent DNA coils into close apposition, and the favorable effect of degeneracy in the bonding domain between the DNA and the core.

c. The topographic arrangement of the bonds between the DNA and the histone core: the "cell" model

B-DNA may be represented as a long, 22 angstrom-diameter cylinder. In this model, the phosphate backbone of the DNA is wrapped in double-helical fashion about the perimeter of the cylinder. In a nucleosome, the long cylinder of the DNA would then be wrapped about the histone core, as thread about a spool. Clearly, only a few of the DNA's phosphates should lie in contact with the surface of the core (or "spool"). From the known periodicity of DNA on a nucleosome (1 turn/ 34 angstroms contour length, from x-ray diffraction), one in fact may estimate that, on each DNA strand, only about every tenth phosphate should contact the histone core. (If, instead, both strands are considered as a unitary entity, then there should be one contact every fifth phosphate.)

The above discussion leads naturally to the idea that, in a topographic map of DNA/core bonding, specific points of bonding between the DNA and the core should alternate with segments of "unconstrained" or "less-constrained" DNA, each 5-10 bp long. I turn now to an examination of the literature, for experimental evidence of such an alternating pattern of fixed DNA "cell boundaries" and less-constrained DNA "cells".

Consider first the "map" of DNA/core contact points, proposed by Mirzabekov and coworkers (see Mirzabekov et al. [1978] and Shick et al. [1980]). This map is schematized in Figure 1. Here, the helical ramp of the histone core in a nucleosome is represented as a horizontal line. Beneath this, 14 rectangles represent the 14 broad regions of "closest approach" the double helix of the DNA makes with this ramp. Open circles indicate single "contact points" made between the histone core and one of the DNA strands, while closed circles indicate "contact points" made with the other DNA strand. (Here, a "contact point" is defined operationally as a locus of crosslinking between a deoxyribose aldehyde in the DNA, generated by depurination, and an epsilon-amino group of a core lysine.)

Also in Figure 1, I have redrawn a DNA/histone "contact" as a vertical line (and several "contacts" close together as a broad vertical line); the DNA between adjacent "contacts" is then represented as a space between two vertical lines. This

Fig. I.1. The Pattern of Histone-DNA Contacts in the Nucleosome Core Particle (after Figure 5 in Mirzabekov, et al. [1978])

Mirzabekov and coworkers (Mirzabekov et al., 1978; Shick et al., 1980) have determined the pattern of crosslinking between deoxyribose 1'-aldehydes of depurinated DNA, and epsilon-amino groups of lysines in the histone core, for mouse Ehrlich ascites core particles. Their data (Figure 5 of Mirzabekov et al. [1978]) are reproduced here, in a form which imagines a (crosslinking-prone) DNA/histone "contact" to act as a "boundary" between adjacent "cells" of relatively less-constrained DNA. Additional details are given in the text.

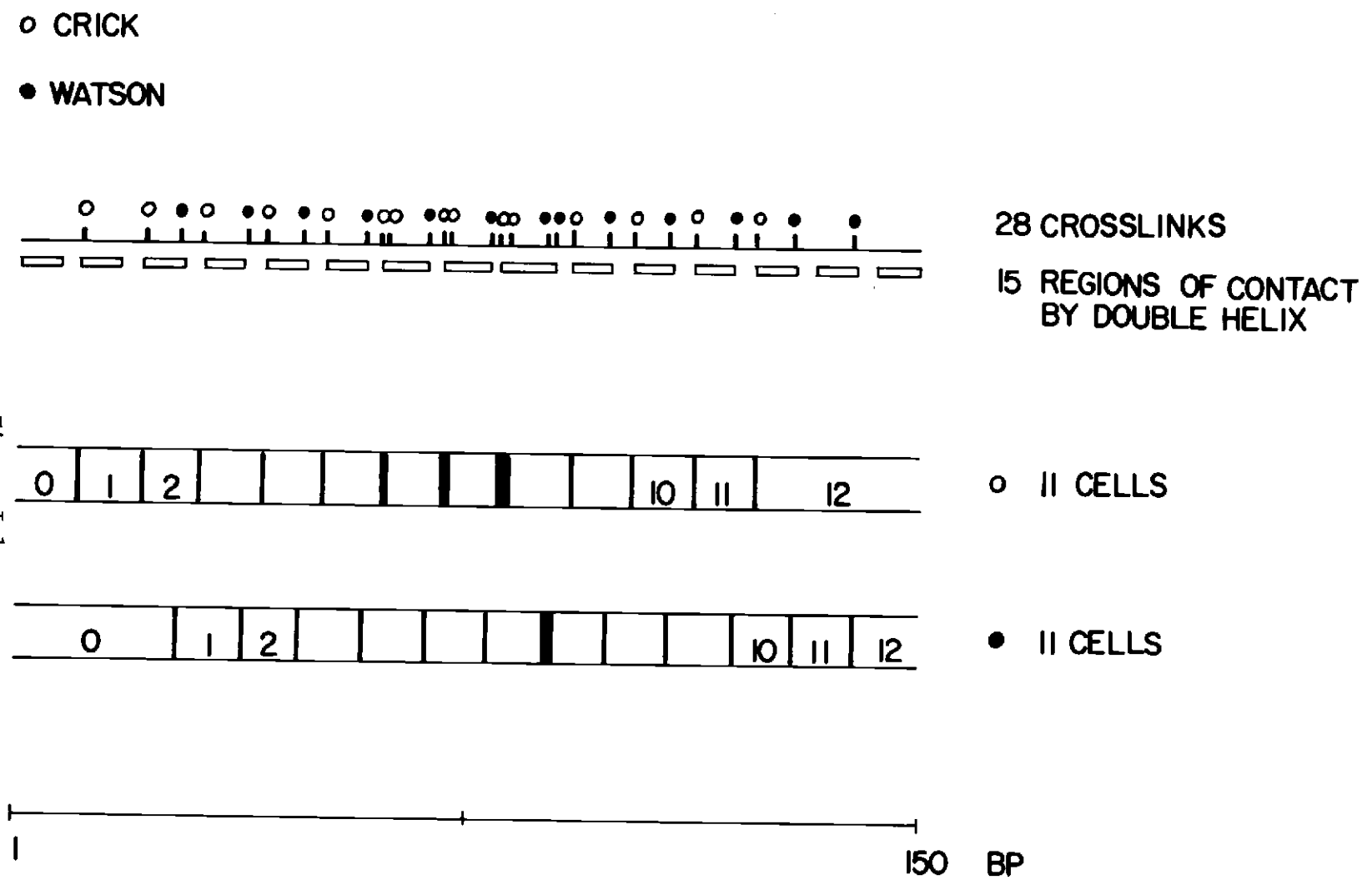
o CRICK
• WATSON
28 CROSSLINKS
15 REGIONS OF CONTACT BY DOUBLE HELIX
0 1 2 10 11 12
o 11 CELLS
0 1 2 10 11 12
• 11 CELLS
1
150 BP

Figure I.1

alternate representation makes clear the resemblance of the pattern of "contacts" to an alternating lattice of constrained and relatively unconstrained DNA segments ("cell boundaries" and "cells", respectively). The data of Mirzabekov and coworkers lead to an estimate of about 14 "cells" for each strand of the DNA in a core particle, or about 28 "cells" total. (I note that there is a difficulty in equating a region of contact between a deoxyribose aldehyde and a core lysine with a bona fide DNA/core bond. This point is discussed thoroughly in part 3 of this thesis.) The overall resemblance of the experimentally obtained map of "contacts" to the theoretically predicted "bonding map" is quite striking.

Are there any other lines of evidence for a "cell" model? Perhaps the most direct type of supporting evidence comes from the digestion of core particles with nucleases. When core particles are digested with DNAase I, DNAase II, MNase (Sollner-Webb et al., 1978), Exo III (Riley and Weintraub, 1978; Prunell, 1983), or Lambda exonuclease (Yager and van Holde [1983], unpublished observations), a ladder of sub-monomer DNA bands results, with a spacing of about 10 bp. Sollner-Webb et al. have presented a model which can explain the cutting patterns produced by the first three (endonucleolytic) enzymes above. Their model (critically reviewed by Lewin, 1980) postulates a series of "favored recognition sites" which are separated from each other by 10

bp. All three endonucleolytic enzymes recognize each site, but cleave slightly different distances away from its center. In the "cell model", these "recognition sites" would correspond approximately to the centers of the unconstrained DNA segments. Action by the last two (exonucleolytic) enzymes can be explained by postulating regions of DNA which block the procession of the enzyme (points of "contact" or "bonding" between DNA and core, or "cell boundaries"). These nuclease digestion studies lead to an estimate of about 14 "cells" for the DNA in a core particle. (In contrast to the view from the crosslinking studies of Mirzabekov et al., the DNA here is considered as a single lattice of cells, and not as two separate lattices (one for each strand).)

The data of McGhee and Felsenfeld (1980b), and of Yager et al. (part 3 of this thesis), on the unbinding of DNA "tails" from the core, are consistent with the "cell model". The salt-dependence of the unbinding of the two 25-30 bp DNA "tails", when assumed representative of all the DNA in the nucleosome, leads to an estimated total of 24-36 ionic bonds between the DNA and the histone core. I note, however, that these data say nothing about the distribution of these bonds between roughly 300 candidate phosphates, and therefore nothing about the fine structure of the lattice of "cells" and "cell boundaries".

A final, but weaker piece of evidence for the "cell" model

comes from a fluorescence anisotropy decay experiment of Genest et al. (1982). In this experiment, ethidium dye was bound to core particles at increasing dye/nucleosome ratios. At low ratios (less than 1 dye molecule/core particle), fluorescence anisotropy decay data could be fit by an equation containing terms for overall tumbling of the core particle, and for internal torsional motion of the DNA it contains. In this equation, the DNA was modelled as a string of short rigid rods each of length L ("cells"), coupled by Hooke's Law springs ("cell boundaries"). The length parameter L was adjusted to obtain best fit to the data; a value L=15 bp was found to be best. At intermediate dye/nucleosome ratios, the same fitting procedure was applied, leading to increased estimates of the correlation times t1 and t2 for the (biexponential) anisotropy decay, and a decreased estimate of the fundamental anisotropy Ao. The decrease in Ao was interpreted to mean that a second dye molecule binds within the same 15 bp DNA segment as the first, allowing fast excitation energy transfer between the two dye molecules. At yet higher dye/nucleosome ratios, when the same fitting procedure was applied, Ao remained the same, but now t1 and t2 decreased. This was interpreted to mean that a third dye molecule bound in an adjacent 15 bp stretch of DNA (far enough from the other two dye molecules to leave Ao unchanged), and then broke a DNA/histone bond between the two segments (causing decreases in t1,t2).

The work of Genest et al. therefore argues for the existence of about 10 "cells", each containing about 15 bp of double-helical DNA. It does not, however, provide a test of the "cell" model that is as unambiguous as the first two lines of evidence described above. One criticism of the work is that, in principle, it may not be accurate to represent two regions of relatively unconstrained DNA, connected by a DNA/histone bond, as two rigid rods separated by a Hooke's Law spring. A second criticism of the work is that no controls were done by an independent method to check for a dramatic alteration of nucleosome structure, such as unfolding or dissociation, upon binding the dye. (These respective transitions have been proposed by Wu et al. [1980] and McMurray and van Holde [manuscript in preparation, 1984]; see section V B, 1.)

d. Predictions of dynamical processes

The above discussion leads naturally to several predictions concerning the dynamics, in nucleosomes, of the DNA and of the DNA/core bonding domain. First, on the basis of counterion condensation theory, one may expect the "less-constrained segments" of DNA in a nucleosome ("cells", in the above model) to become more "flexible" in some sense, as the bulk salt concentration is raised (see section II C, 1). Second, there may be a considerable tendency, under all

conditions, for the "less-constrained segments" to undergo rapid internal motions, of the kind amply documented for free DNA (see section II A). Third, the exact amount of DNA (measured, for example, by the number of phosphates) in each of the "less-constrained segments" might fluctuate in time, due to breakage and reformation of DNA/core bonds, coupled with rapid DNA twisting motions.

What would be the broad effects of all these fluctuations? Recall, from section IV E, the "degeneracy principle". The principle states that there exist, for a nucleosome, a moderate to large number of energetically similar "microstates", defined with respect to the precise placement, or "register" of the DNA on the histone core. The above discussion predicts that an individual nucleosome may rapidly shift between these "microstates" in a fashion that involves, and perhaps requires, the transitory breakage and reformation of DNA/core bonds (see van Holde and Yager, 1985). The consequence of this would be a sliding of the histone core along the DNA (see below).

e. Observed dynamical processes

(i) rapid DNA motions

The problem of rapid DNA motions in nucleosomes and in chromatin has been approached through 31P NMR (Shindo and

McGhee, 1980), and through monitoring the motions of dye molecules (presumeably) intercalated into nucleosomal DNA, with fluorescence anisotropy decay (Wang et al., 1982; Ashikawa et al., 1983a, 1983b) and EPR (Hurley et al., 1982). Rapid (nanosecond) motions have been proposed for the phosphate- and sugar moieties of the DNA backbone, and for the DNA bases themselves. Such motions have generally been interpreted in terms of structural models which allow sugar puckering, and the twisting of the DNA base pairs in planes perpindicular to the long axis of the DNA.

I note that the above techniques are subject to all the difficulties discussed in the context of their application to DNA studies (see section II A, 1). Additional problems peculiar to the study of nucleosomes, such as dye-induced nucleosome unfolding or dissociation, are not unexpected (see sections V B 2, V B 4). Finally, in chromatin, the EPR study of Hurley et al. (1982) suggests that two domains of dye intercalation exist - core and linker DNA - with low and high affinities, respectively. The existance of multiple domains further complicates interpretation. Clearly, because of these problems, the techniques cannot provide as rigorous a test for DNA motion within nucleosomes as can x-ray crystallographic analysis (see section II A, 1). However, nucleosome diffraction patterns at 2 angstrom would be required for x-ray motional analysis.

It is not known what the effects of salt and temperature

are on the rapid motions of the "less-constrained" segments of DNA in the nucleosome.

(ii) Histone core sliding

The salt-induced sliding of histone cores along the DNA has been observed in many laboratories (reviewed in van Holde and Yager [1985]). The mechanism of sliding is unclear at present. Quite plausibly, this process may involve decreases in the average lifetime or stability of individual DNA/core bonds, coupled with rapid DNA motions (allowing the DNA to "slip" between degenerate positions on the core; see above).

A direct investigation of the DNA/histone bonds in the nucleosome could conceivable be made by some spectroscopic technique, such as N-P coupling in NMR. This, however, has not yet been attempted.

B. Nucleosome dynamics involving major changes in the histone/histone and histone/DNA bonding domains

1. The (putative) transition from "B-" to other forms, for DNA bound up in nucleosomes

It currently is debatable whether, by virtue of a

well-defined set of contact points between the DNA and the histone core, the DNA in a nucleosome is confined to a "B-type" form. This question apparently has been examined for the B-to-Z transition only.

Nickol et al. (1982) have reconstituted nucleosome-like "particles" with chicken erythrocyte core histones and the "B" form of poly(dG-$m^5$dC):poly(dG-$m^5$dC) (the polymer being heterogeneous in length above 160 bp). The "particles" showed micrococcal nuclease digestion stops at approximately 200, 180 and 160 bp. In a 0.1 M NaCl buffer, the "particles" sedimented at $s_{20,w}$ = 11.1 S. A DNAase I digestion pattern was obtained showing broad bands approximately every 10 bp.

An attempt was made to induce the B-to-Z transition in the DNA in micrococcal-nuclease-digested "particles", by changing the solvent conditions (initial conditions: 10 mM Tris [pH 8], 50 mM NaCl, 0.25 mM $CaCl_2$, 1 mM EGTA, 1 mM EDTA; final conditions: 75-200 uM $MgCl_2$, 200 uM Na Cacodylate, 5 mM EDTA; T=20 $^{o}$C, in both cases). As assayed by absorbtion spectroscopy, no conversion from B to Z form was observed. It was concluded that the contacts made to the "B" form DNA by the histone core prevented the B-to-Z transition.

It is worth noting that interpretation of this study is complicated by a tendency of material to aggregate (especially at higher temperatures), and also by the fact that the conditions favoring conversion to Z form also favor the

"low-salt-expanded" form of (B-DNA-containing) nucleosomes. Also, circular dichroism spectroscopy would be more discriminating that absorbtion spectroscopy, in detecting a B-to-Z transition.

2. Nucleosome "unfolding"

A recurrent idea in the literature is that, under certain conditions, the nucleosome may "unfold", to produce a highly extended structure, which still retains a full complement of histones.

Clearly, all unfolding events must involve changes in at least some of the DNA/histone and histone/histone bonding domains within the nucleosome. This may be where the commonality ends, though. It probably is misleading to believe that the "unfolding" produced by two different types of environmental perturbation will be the same, or even very similar. More realistically, each type of "unfolding" will be characterized by the replacement of the normal domains of bonding between the separate histones, and between the DNA and the histones, by another set of (altered) bonding domains.

a. Low-salt unfolding

It has been clearly documented that unfolding occurs

under conditions of very low ionic strength (see, for example, Uberbacher et al. [1983]). It seems plausible that the driving force for nucleosome unfolding in low salt involves both an increased repulsion between the two apposing coils of DNA in the nucleosome, and also an enhanced tendency for individual "segments" of the DNA to stiffen (see Manning [1978]). The driving force may also involve a decrease in relative stability, in low salt, of the histone-histone and DNA-histone bonding domains in the normal nucleosome, relative to the bonding domains of the "unfolded" state. Because this type of unfolding occurs under conditions that are not "physiological" (according to the definition adopted in section I), it will not be of further concern in this essay.

b. Transcriptional unfolding

It has been asserted that nucleosome unfolding occurs in transcriptionally active regions of the genome. The best evidence for this assertion comes from the literature on the production of "A particles" in the digestion, by micrococcal nuclease, of Physarum polycephalum rDNA chromatin (see Prior et al. [1983], and references therein). The "A particle" apparently contains the full complement of histones and 140-150 bp of DNA, but sediments at 5-6 S, instead of at the value of 10.7 S which is normal for core particles. In the case of the

"A particle", unfolding may be due to the binding of additional specific proteins (Prior et al., 1983; see section VI F).

c. Unfolding in the presence of "environmental perturbants"

It has been proposed that nucleosome unfolding can be caused by agents which solubilize the hydrophobic central regions of the histone core (e.g. urea) (Woodcock and Frado, 1977; Zama et al., 1977), and also by agents which intercalate into the DNA and cause it to stiffen (e.g. ethidium bromide) (Wu et al., 1980). I will not be concerned with such environmental "perturbants of structure", because they create environmental conditions falling outside the "physiological" category defined in section I.

d. Unfolding after trypsinization of the core histones

Evidence has been given that, after extensive trypsinization of the core histones, nucleosomes have a highly enhanced tendency to unfold (Lilley and Tatchell, 1977; Grigoryev and Krasheninnikov, 1982). Such a phenomenon will not be explored in this essay, because it falls outside the "physiological" category defined in section I.

e. High-salt unfolding

A fifth putative type of nucleosome unfolding is the chief concern of this section of the essay. It has been proposed that nucleosomes unfold as the bulk salt concentration is raised above about 0.2 M (Dieterich et al., 1977, 1979; Zama et al., 1977; Whitlock, 1979; Bode and Wagner, 1980; Russev et al., 1980a; Wilhelm and Wilhelm, 1980; Zayetz et al., 1981).

This proposal must be reexamined in light of current knowledge. It now seems that each of the studies cited above suffers from at least one of the following basic shortcomings:

(i) often, no account was taken of the (then poorly characterized) process of nucleosome dissociation;

(ii) techniques were often used which "averaged", instead of "resolved", the information coming from different subpopulations of "particles", or "entities" in a preparation. Thus, for example, when the CD of core particles in salt was monitored (see Wilhelm and Wilhelm [1980]), the signals from intact, dissociated, and (putatively) unfolded core particles were all blended together;

(iii) in preparation, nucleosomes were sometimes subjected to rather drastic modifications. For example, in the studies of Dieterich et al. (1977, 1979) and of Zama et al. (1979), bulky aromatic dyes were attached to the H3 cysteine sulfhydryl

groups, by transient exposure of the particles to 2-2.5 M salt. It is questionable whether, after passing through such a procedure, the resultant "particles" were any longer strictly comparable to native core particles;

(iv) little attempt was made to reconcile the interpretation of data with the strong evidence for an inherent stability of the $(H3.H4)_2$ tetramer, and for the finding that the tetramer can organize DNA into a supercoiled, DNase I-protected form (see sections III A, IV A).

From this critique, it seems wise to treat the claim of salt-induced nucleosome unfolding with skepticism, at least at this time. I do not wish to dismiss the possibility entirely, however: if the histones or the DNA of a core particle were extensively modified, the particle's dynamics might be substantially affected. It is to this possibility that I now turn.

### f. Unfolding because of histone acetylation

Bode et al. (1983) have examined the electrophoretic mobilities of acetylated- and non-acetylated core particles on "native"-type gels, under conditions of 10-100 mM ionic strength. They found acetylation to be correlated with a decrease in the particles' electrophoretic mobilities. These workers therefore proposed that the acetylation of histones H3

and H4 gives core particles a tendency to unfold under moderate ionic strength conditions.

(An earlier study by these workers asserted that acetylation of H3 and H4 gives nucleosomes a tendency to unfold when placed in 0.8-1.5 M NaCl solution (see Bode et al. [1980]). This study, however, has an alternate interpretation: acetylation may instead enhance the tendency for nucleosomes to dissociate;. see section V B, 3.)

3. Unbinding of DNA "tails"

It has been clearly shown that a very homogeneous preparation of core particles displays a biphasic melting profile in 1 mM ionic strength solution (Weischet et al., 1978). Both portions of the melting profile are characterized by an increase in optical absorbance at 260 nm and a change in heat capacity. For the first portion of the melt, the increase in 260 nm absorbance is of the magnitude expected for the denaturation of 40-55 bp of DNA in each core particle. Preceding the first melt is a "premelt" transition, which shows neither an increase in absorbance at 260 nm nor a change in heat capacity, but which does show an increase in circular dichroism at 273 nm. The joint interpretation of the "premelt" and first melting transitions is that, as the temperature is raised, the two termini of the DNA first become released from

the histone core (increasing the CD), and then denature (increasing the optical absorbance and causing a change in heat capacity). Note: since the study of Weischet et al. was done under conditions of 1 mM ionic strength, there is some question as to whether the core particle is in the "native" or the "low-salt unfolded" state (see section VB, 1).

The hypothesis of "DNA tail release" was elegantly tested by Simpson (1979). Core particles which had been reconstituted with double-end-labelled poly(dAT):poly(dAT) were placed under conditions where the two termini, or "tails" of the DNA were expected to be released and denatured. Under these conditions (I = 11 mM, T = 45 $^{o}$C.), the core particles' CD was enhanced by 75%, and their sedimentation coefficient (corrected to conditions of 20 $^{o}$C and water) was decreased by 15%. S1 nuclease was used to test for the presence of any single-stranded regions of the DNA. Upon exposure to the nuclease the DNA was digested to a 105 bp limit, and label at both ends of the DNA was lost. This indicated the presence of two 20 bp (denatured) DNA "tails". (I note that, in the CD and sedimentation experiments, the core particles, at I = 11 mM and at neutral pH, were undoubtedly in the "native" state. However, it is not entirely clear what state the core particles were in during S1 digestion, in a pH 5.1 buffer and in the presence of 0.1 mM $ZnSO_4$.)

The next paper to address the question of "DNA tail

release" was that of McGhee and Felsenfeld (1980b). These workers reexamined the ionic strength dependence of the "release" and melting of the DNA "tails" during the first stage of the thermal denaturation of core particles. To analyze the melting data, they employed the theory of DNA/protein interactions proposed by Record et al. (1978). They calculated that only 15+-6% of the available phosphates in the DNA tails were involved in specific ionic interactions with the histone core. (I note that, in their study, the ionic strength ranged from 0.4 to 3.5 mM. Thus, again, there is some doubt that their core particles were in the "native", and not the "low-salt unfolded" state.)

The above three studies were all done under conditions which, according to the operational definition given in section I, are not "physiological". It therefore was of interest to learn whether an analogous process of DNA "tail" release could occur at the higher salt concentrations and lower temperatures within this "physiological" range.

Harrington (1982) attempted to study the tail-release phenomenon under physiological conditions, by jumping core particles to various elevated concentrations of KCl at room temperature. He observed, after jumping to >0.35 M KCl, a large increase in the particles' intrinsic viscosity and intrinsic birefringence. The increase in intrinsic birefringence in 0.6 M KCl was analyzed in detail by a theoretical model which related

this parameter to the conformation of the DNA within the core particle. It was found to be consistent with the release and straightening of the two termini of the DNA to an extent of 20-30 bp each. Thus it seemed that a large increase in the concentration of monovalent neutral salt could induce the same structural change that occurred during the "premelt" transition in low salt.

There are two criticisms of Harrington's study. First, his core particles were prepared by sedimentation through sucrose gradients in 0.6 M KCl. Quite possibly, this procedure causes some nucleosome dissociation, and as a consequence contaminates the core particle preparation with free DNA (see Yager and van Holde [1984]). (At the high gradient loadings used by Harrington, even a 10% free DNA contaminant might not be resolved from the core particle peak shown in his Figure 1.) Second, there is a lag of about 1 hour between jumping the core particles to elevated salt concentration, and making the optico-hydrodynamic measurements. During this lag, some dissociation of the core particles may have occurred (see section V B, 3). Thus the salt-induced increases in intrinsic viscosity and intrinsic birefringence which Harrington observed may have had contributions from the appearance of completely free DNA.

The possibility of DNA "tail" release in physiological salt was then reexamined by Yager et al. (part 3 of this thesis).

Using the techniques of analytical velocity centrifugation and circular dichroism, these workers observed both a fast and a slow transition in response to a sudden increase in salt concentration. The slow transition appeared to involve a dissociation of the core particles to produce free DNA (see section VB, 3). The fast transition, occurring over the 0.35 to 0.75 M NaCl range, involved a 15% decrease in sedimentation coefficient (corrected to conditions of 20 °C and water), and an increase in the CD at 282.5 nm corresponding to the apparent straightening of about 55 bp of DNA. As determined by the CD assay, the fast transition was reversible and time-independent. The Kirkwood theory (Kirkwood, 1954; Bloomfield et al., 1967; Bloomfield et al., 1974) was used to show that the magnitude of the decrease in sedimentation coefficient was consistent with the release of two 35 bp DNA "tails" from the surface of the histone core.

In the work of Yager et al., the salt-dependence of the changes in CD and sedimentation coefficient was interpreted in terms of a two-state model, involving an equilibrium between core particles with DNA tails "released" and core particles with DNA tails "bound". An equilibrium association constant was defined for the "tail-binding reaction", and its salt dependence analyzed with the theory of Record et al. (1978), after the theory had been modified to include the effect of bending the DNA about the core. This thermodynamic approach

allowed several inferences to be made regarding the nature of the bonding between the DNA "tails" and the histone core. Thus the release of the two DNA "tails" appeared to involve the breakage of 10-14 electrostatic bonds. The salt-dependence of the "tail" release process was compared with that of the release of DNA from association with model oligopeptides. From this comparison, it appeared that the bonds between the histone core and the DNA "tails" were energetically much more similar to arginine/DNA bonds than they were to lysine/DNA bonds. It was concluded that these bonds probably had considerable non-electrostatic character.

Is the bonding between the DNA "tails" and the histone core affected by histone or DNA modification? A study of Simpson (1978a) suggests that acetylation of the histones may decrease the stability of this bonding. Simpson compared the physical properties of core particles from normal and butyrate-treated HeLa cells. He found that the latter core particles, which carried high (but not unphysiological) levels of acetylation on histones H3 and H4, had an enhanced CD signal at 280 nm, and a several-fold enhanced rate of removal of 5' end-label by micrococcal nuclease. Unfortunately, there do not exist more definitive studies of the effect of histone- or DNA modification on the DNA "tail" release reaction.

## 4. Nucleosome dissociation

### a. Documentation of the phenomenon; potential problems of study

Between 1979 and 1982, several workers observed that, when nucleosomes at high dilutions ($A_{260}$ <1) were jumped to moderate NaCl concentrations (>0.2 M), free DNA apparently was generated (see Yager and van Holde [1985] for references to these studies).

The early studies of nucleosome dissociation each suffered from at least a few of six basic methodological problems:

(i) In nucleosome preparations, the particles' DNA lengths may have spanned 146 bp. Since it has been suggested that nucleosomes with DNA shorter than 146 bp are relatively unstable (Erard et al., 1981), the early studies may have been dealing with a mixture of two nucleosome populations, of differing stabilities;

(ii) there may have been, in the early nucleosome preparations, heterogeneity with respect to the presence of contaminating proteins, and also with respect to histone- and DNA modifications. This in turn may have led to the coexistance of differentially stable nucleosome subpopulations, in the material being studied;

(iii) there was no rigorous demonstration that the "free DNA" which was generated actually was completely free of histones;

(iv) It was not adequately determined whether, in elevated concentrations of salt, the nucleosomes which remained undissociated had kept their full complement of histones or their native conformation;

(v) it was not adequately tested whether the dissociation process was reversible;

(vi) the multiple equilibria between various released histones, and between the released histones and the DNA, were ignored.

Three recent studies (Ausio et al., 1984; Yager and van Holde, 1984; part 3 of this thesis), when considered jointly, probably deal adequately with problems (i), (iii), (iv) and (v), and, somewhat less completely, also with problem (ii). Work in progress in the laboratory of van Holde (1984, unpublished) is addressing the complication of problem (vi). These recent studies clearly document that elevated NaCl causes the reversible generation of free DNA, from nucleosomes which are free of non-core proteins. No qualitative differences were found for nucleosomes containing different lengths of DNA (between 145 and 280 bp).

Besides the dissociation, and perhaps independently of it, a small decrease in the sedimentation coefficient and a small

increase in the CD around 280 nm were observed, for the fraction of nucleosomes remaining intact in the elevated salt (Ausio, et al., 1984; Yager and van Holde, 1984; H. Eisenberg and coworkers, unpublished observations, 1984; part 3 of this thesis). These smaller effects were ascribed to conformational changes of the types discussed in section V A - in particular, to the unbinding of DNA "tails" and to the unbinding of the N-terminal regions of histones H3 and H4.

b. The thermodynamics of dissociation

It is somewhat unclear what the driving forces for nucleosome dissociation are. The reductionist slant of this essay suggests a division into four thermodynamic components: (i) the mechanical straightening of the DNA; (ii) the separation of adjacent DNA coils (which are close together in an intact nucleosome); (iii) the effects of various histone/histone equilibria which arise upon nucleosome dissociation; and (iv) changes in the bonding interactions between DNA, histones, counterions, and water.

Can one make an educated guess about the relative contributions of these four terms?

(i) A variety of theoretical calculations (reviewed in part 3 of this thesis) suggest that the complete straightening of the core particle's DNA should produce a standard free energy

decrease of roughly 20-100 Kcal/mol. The entropic and enthalpic portions of this free energy change are uncertain, although a paper by Harrington (1977) suggests that the major component is enthalpic.

(ii) No experimental estimates exist of the repulsive energy between adjacent DNA coils in a nucleosome. This term, though, may make a significant contribution. (For an idea of its potential significance, see the hypothesis that "coil-coil repulsion" underlies the "plateau effect" observed in the release of DNA "tails" from core particles [section V B, 2 and part 3 of this thesis].)

(iii) From the data and discussion presented in sections III C and IV A, it seems that a further dissociation of the released histone core will be favored over the 0.1 to 0.75 M NaCl range, to produce $(H3.H4)_2$:(H2A.H2B) hexamers, $(H3.H4)_2$ tetramers, and (H2A.H2B) dimers. Without more extensive data on the salt-dependencies of the equilibria between these species, however, one cannot state what the standard free energy change will be, in this salt range, for dissociation of the histone core. The work of Benedict et al. (1984) indicates that core dissociation has a large enthalpic component, at least in 2 M NaCl.

(iv) Effects (i), (ii) and (iii) above all contribute unfavorably to the stability of the nucleosome. For the nucleosome to be a stable entity, therefore, the (favorable)

free energy of binding the DNA to the histone core must overcome these effects. Presumeably, to be theoretically rigorous, a treatment of DNA/core binding must be phrased in terms of counterion condensation theory (see Record et al. [1978]).

c. The Mechanism of Dissociation

It seems likely that the mechanism of nucleosome dissociation is not simple. There may even be several different mechanisms, each contributing to an extent which varies with environmental conditions.

What are the experimental facts that a proposed mechanism must explain?

(i) For any proposed mechanism, the principle of microscopic reversibility must hold: at equilibrium, any reaction and its exact reverse must be proceeding at equal rates (see Moore [1972]). Thus any proposed mechanism must involve steps which, at the microscopic level, are completely reversible.

(ii) The rate of nucleosome dissociation displays fairly sharp depencencies on temperature and salt concentration, increasing as either of these parameters is raised (Ausio et al., 1984; Yager and van Holde [1984], and unpublished observations).

(ii) The sliding of the histone core along the DNA has been

observed to occur under the same conditions that allow dissociation (Beard, 1978; other pertinent literature reviewed in van Holde and Yager [1985]). Therefore, at least for nucleosomes with longer DNA, sliding of the histone core must be taken into account, either as a competing reaction, or as an integral part of a dissociation pathway.

(iv) From the work of Germond et al. (1976), it appears that transfer (by some unknown mechanism) of histone cores from supercoiled SV-40 minichromosomes to supercoiled SV-40 DNA cannot occur below 0.8 M NaCl. However, it is also known that transfer of histone cores from core particles to linear DNA occurs at 0.7 M NaCl (R.T. Simpson, personal communication [1983]; T. Yager, unpublished observations [1984]). Thus a dissociation mechanism must account for nucleosome stability differences on circular and linear DNA.

What are the various models for nucleosome dissociation which have been proposed?

(i) Stein (1979) has proposed a mechanism in which two nucleosomes transiently come into contact, effecting the transfer of a histone octamer from one of them to the other. This would produce free DNA and a second entity consisting of two histone octamers and one molecule of DNA. One of the histone octamers would then dissociate from the latter complex, producing a free octamer and an intact nucleosome. After each "turn" of this "reaction cycle", two nucleosomes would have

been converted into one nucleosome, a histone "octamer" (probably itself unstable), and a piece of DNA.

There are three strong arguments against this model. The first relates to the demonstration that, when an equimolar mixture of the inner histones is added to a solution of core particles, the core particles actually do bind extra histones, to form a "complex" (of somewhat unknown stoichiometry, and of completely unknown internal structure) (Voordouw and Eisenberg, 1978; see section VI A). The point to be noted here is that, as the ratio of extra histones to core particles approaches zero (which is the situation existing in true nucleosome dissociation), this "complex" is not observed.

The second argument against Stein's model is that it requires the transitory coupling of two highly negatively charged entities (two intact nucleosomes). This seems, on the basis of transition state theory, unlikely to occur (see Moore [1972]). In fact, the association of nucleosomes has never been observed to occur, under relevant conditions.

The third argument is the following. The model was proposed initially by Stein to explain a "non-equilibrating DNA fraction" in an experiment in which core particles were dissociated in 2.5 M NaCl, and were then reassociated by (simultaneously) jumping to 0.6 M NaCl and diluting. There was, however, a 10-20% contaminant of extra DNA in Stein's preparation of core particles (probably due to sedimentation of

the particles through sucrose gradients containing 0.6 M NaCl; see his figure 1). Therefore all his reassociation data must be viewed with reservations.

(ii) It has been proposed by van Holde and Yager [1984] that dissociation may proceed via a sliding of the histone core. According to this mechanism, the core would slide until a critical displacement along the DNA had been reached; at this point, a second process (loss of (H2A.H2B) dimers, and straightening of the DNA?) would take place (resulting in the production of DNA bound to an $(H3.H4)_2$ tetramer?). This would finally give rise to the fully dissociated state.

There are several testable features of the model of van Holde and Yager. First, it predicts no dissociation of cores from circular DNA (possibly consistent with the SV40 data of Germond et al. (1976), cited above). Second, it predicts a sigmoidal dissociation curve having an initial lag phase. This lag phase would arise because the cores would have to slide to a "critical excursion distance" before dissociation commenced. This lag time is predicted to increase in proportion to the length of DNA in the nucleosomes.

(iii) A third mechanism has been proposed by Stacks and Schumaker (1979). In this mechanism, dissociation is mediated by a transitory complex formed between an intact nucleosome and a piece of free DNA. This model also predicts sigmoidal dissociation kinetics, but no dependence of the apparent

initial "lag" on the length of the DNA.

It seems that a weak point of the model of Stacks and Schumaker is the assumption of a complex between a nucleosome and a piece of DNA. As for the case of the transient "double nucleosome" proposed by Stein (see above), such a complex seems quite unlikely, because both species are highly negatively charged. Furthermore, one might predict that, were such a complex possible, then the histone core would bind >160 bp of DNA (in the sense of conferring DNAase I protection), which it does not.

(iv) A fourth model for nucleosome dissociation has been proposed by Ellison and Pulleyblank (1983a, 1983b, 1983c). These workers have isolated what appears to be a complex ("P2") containing one molecule of DNA, one molecule each of H3 and H4, and two molecules each of H2A and H2B. They find that this complex can be converted, by the addition of H3 and H4, to another complex ("P3"), which appears in many ways to resemble a nucleosome.

Their method of producing "P2" involves mixing stoichiometric amounts of the inner histones with sonically sheared DNA in 0.15 M NaCl, sedimenting out roughly 80% of the material as a precipitate, performing a micrococcal nuclease digestion on the remaining soluble material, and finally isolating the "particles" so produced. On this basis they propose a dissociation mechanism in which (H3.H4) dimers and

(H2A.H2B) dimers dissociate alternatingly from the nucleosome.

Criticisms of this study are as follows. First, a high proportion of the reconstituted material is insoluble, and is removed before nuclease digestion. Thus the model is based on information obtained from only 20% of the resonstitution product. Second, the nuclease digestion - an integral part of the detection assay - may be influcencing fundamentally which species ultimately are observed. Third, acid-extracted histones are used exclusively. Core particles reconstituted with these histones have been observed to have a different stability, with respect to dissociation in salt, than core particles reconstituted with salt-extracted histones (J. Ausio and H. Eisenberg, personal communication [1984]). Fourth, the data are difficult to reconcile with the strong evidence for a high inherent stability of the $(H3.H4)_2$ tetramer, even in the presence of DNA (see sections III C, IV A), and with evidence that only H2A and H2B are lost from chromatin fragments below 1 M NaCl (Burton et al., 1978, 1979).

Because of the above difficulties, I find it most plausible to consider the "P2" particle a minor- or side-product of the dissociation reaction. However, further study of the conditions of its stability is necessary.

VI. The nucleosome as a changeable structure. 4. An approach to a broader context: the binding of additional

proteins to nucleosomes

For philosophical satisfaction, one should attempt to understand the dynamical processes of nucleosomes in a broader context than has been given above. One such context is that of the physiological processes of DNA replication, repair, recombination, and transcription. There have been many investigations of these phenomena in eukaryotic (i.e. chromatin-based) systems (for reviews, see Kornberg [1980], Lewin [1980], Cartwright et al. [1981]).

On the chromosome, are such physiological processes carried out on regions of free DNA that are structurally separated from chromatin domains? An alternative hypothesis is that they occur within the chromatin domains themselves, and in close proximity to nucleosomes. There is, in fact, evidence for the latter view (see Lewin [1980], Cartwright [1981]). If this view turns out to be generally correct, then it will be very important to understand how the physiological machinery for manipulating DNA (i.e. the collection of DNA enzymes in the cell nucleus) interacts directly with nucleosomes.

I will touch upon this broad problem by briefly reviewing what is known about the specific interactions of nucleosomes with other proteins in the cell nucleus. There are to date seven types of interaction for which some information has been obtained. These involve the possible binding of nucleosomes to:

(A) additional core histones; (B) histone H1; (C) some of the "high mobility group" ("HMG") proteins; (D) topoisomerases; (E) DNA polymerase a and b; (F) nuclear lipoproteins; and (G) RNA polymerase II. In addition, both the inner histones and DNA transiently bind to nucleoplasmin.

A. The binding of additional inner histones to nucleosomes

If an equimolar mixture of the inner histones is added to a solution of core particles, then as a 2:1 molar ratio is approached, an apparently discrete complex is formed, which sediments at 13 S (Voordouw and Eisenberg [1978]). Presumeably, this complex was produced by an equilibrium binding reaction (and not an irreversible aggregation). The concentration-, salt- and temperature-dependencies of the binding reaction were not determined.

It was proposed that the complex contained one molecule of DNA and two molecules of each of the inner histones. It was further proposed that the extra histones were arranged as a core octamer, bound to the outside of the (otherwise unperturbed) core particle. However, the histone stoichiometries, the exact topographic relationship of the histones to each other, and the topographic relationship of the histones to the DNA were not determined.

Because of the existance of a cytoplasmic (and so, perhaps, a nuclear) pool of free histones (Lewin, 1980), this binding reaction may be of importance in vivo.

B. The Binding of H1 to Nucleosomes

H1 has been implicated as being necessary for the transition to higher-order structure which oligo- and polynucleosomes undergo at elevated ionic strength (see, for example, Suau et al. [1979]; Thoma et al. [1979]; Allan et al. [1982]). In an attempt to understand the structural basis for this transition, the interaction of H1 with individual nucleosomes has been studied considerably. Much of this work is rendered somewhat ambiguous, however, by heterogeneity in sample preparations.

A very significant early study was that of Simpson (1978b). From a micrococcal nuclease digestion of chicken erythrocyte chromatin, Simpson isolated a mononucleosomal particle containing 160-170 bp of DNA, two copies of each of the inner histones, and in addition, some amount of the histone(s) H1a, H1b, and/or H5. From comparing the protein:DNA stoichiometry of this particle to that of the core particle, he inferred, reasonably, that the particle was a long-DNA-containing nucleosome to which one copy of either H1a, H1b or H5 was bound. He termed such a particle a "chromatosome".

In the chromatosome, the DNA has been digested by micrococcal nuclease to a fairly sharp 160-170 bp limit. This suggests that an H1 or H5 molecule binds to a core particle (in chromatin) in such a way that an additional 15-20 bp of DNA is physically shielded from contact with the nuclease. Significantly, from the model of Klug et al. (1980), this additional 15-20 bp would be just enough to force the DNA in the core particle to make two complete turns about the histone core.

Simpson showed that chromatosomes containing H1 or H5 have $s_{20,w}$ = 11.7 S (relative to core particles' 10.7 S), a (circular dichroic) ellipticity near 280 nm which is 40% greater than that of core particles, and an increased Tm of both the first and second components of thermal denaturation (relative to chromatosomes lacking H1/H5). The first of these findings indicates that the chromatosome is a compact particle. The second finding suggests that the termini of the DNA in the chromatosome are in a somewhat more "extended" conformation than is the rest of the DNA (but not in a completely extended conformation). The third finding suggests that H1 or H5 bind both to the DNA termini (raising the Tm of the first melt), and also to the main body of the nucleosome (in such a way as to stabilize the entire structure against catastrophic denaturation in the second melt).

Simpson compared the DNAase-I digestion patterns of

end-labelled chromatosomes lacking H1 or H5 with the digestion patterns of end-labelled core particles. His data can be explained most simply by a model in which the DNA lies symmetrically upon the histone core, with two 7-10 bp "tails", at either end of the DNA, completing the second full turn about the core.

From Simpson's work, it seems reasonable to conclude that, in a chromatosome, histone H1 makes physical contacts with at least the two 7-10 bp lengths of DNA on either side of a central 146 bp region.

Bonner and Stedman (1979) and Boulikas et al. (1980) have examined the contacts made by H1 to the core histone octamer in nuclei, in long chromatin fragments, and in mononucleosomes. Both groups made use of the "zero-length" crosslinker EDAC. On the basis of crosslinking and identification of proteolytic fragments, a model was proposed in which a portion of the central globular region of H1 (positions 74-106 in the amino acid sequence) lies in close contact with the (partially globular) central- and C-terminal regions of H2A (positions 58-129). Similar crosslinking patterns were observed for preparations in which ubiquinated H2A had partially replaced H2A.

Although the above studies provide a good starting point, much remains to be learned about the binding of H1 and H5 to the nucleosomes. For example, even such a basic point as the

stoichiometry of binding is still not completely resolved: it has been proposed that the nucleosome may actually be able to bind two molecules of H1 or H5 (reviewed in Bates and Thomas [1981]). Also, no estimates of equilibrium binding constants have been obtained. Finally, there is evidence that H1 or H5 can interact also specifically with other chromatin-binding proteins, such as HMG 14 (Espel et al., 1983). Clearly, more work is required for a rigorous and complete understanding of the interaction of H1 with nucleosomes.

C. The binding of "high-mobility group" ("HMG") proteins to nucleosomes

1. The binding of HMGs 14 and 17

Eukaryotic chromatin contains a prominent group of non-histone proteins, distinguished in part by their high mobilities on gels (and therefore called the "high-mobility group", or "HMG", proteins). The four main types have been called HMG 1,2,14 and 17. HMGs 14 and 17, at least, have been implicated as being present in transcriptionally active chromatin (for a review, see the volume edited by Johns [1982]).

A number of fairly detailed physical studies have been done on the binding of HMGs 14 and 17 to nucleosomes. Mardian et al.

(1980) have shown that, when core particles are mixed with HMG 14, HMG 17, or a mixture of the two proteins, two additional, discrete, more slowly migrating bands are observed on a particle gel (in a 25-50 mM ionic strength buffer). When the molar ratio of HMG 14/17 to core particles is increased from 0 to 2.6, the band of intermediate mobility is generated first; it is then replaced by the slowest band. This is interpreted in terms of a model in which: (i) there are two discrete binding sites per core particle for either HMG 14 or 17; (ii) binding at these sites is non-cooperative (at least at low ionic strength); and (iii) the two HMG proteins bind interchangeably. Sandeen et al. (1980) have confirmed these observations. In addition, these workers give evidence that the binding reaction is reversible, and that it becomes cooperative at elevated ionic strength (so that only the slowest-moving band is seen on particle gels). In a very careful study, Paton et al. (1983) have determined that the cooperativity of the double-binding event is not eliminated by crosslinking the histones and the DNA in the core particle together. Therefore the cooperativity probably is not mediated by a conformational change in the core particle.

Some information concerning the structure of the complex between the core particle and two molecules of HMG 14 comes from neutron scattering in solvents of different densities ($H_2O/D_2O$ ratios). Uberbacher et al. (1982) observe a 5-6%

increase in the DNA radius of gyration, and a 2-3% increase in the protein radius of gyration, upon complex formation. The relatively small nature of these increases clearly is not consistent with structural models in which either the DNA or the protein are in a highly extended conformation. Harrington et al. (1982), reasoning from flow birefringence data, reach similar conclusions.

DNAase I digestion studies provide additional evidence arguing against a dramatic rearrangement of structure upon binding HMGs 14 and/or 17. Although binding seems to enhance the rate of digestion (Stein and Townsend, 1983), it does not greatly alter the nature of the digestion pattern (Mardian et al., 1980; Sandeen et al., 1980).

Some inferences have been made, from thermal denaturation studies, about the structure of the bonding domain between core particles and HMG 14 or 17. Sandeen et al. (1980) demonstrated that core particles acquire an enhanced stability toward thermal denaturation upon binding HMG 14 or 17. Paton et al. (1983) then showed that this was due to two separate effects: an upshift of the second melting transition, and a partial elimination of the first transition (see section V B, 2). Only half the effect on the first transition was seen when only one HMG 14 or 17 molecule was bound. The partial elimination of Tm1 suggests that the ends of the DNA in the core particle are stabilized by the binding of HMG 14 or 17. The upward shift of

Tm2 suggests that, in addition, the stability of the core particle as a whole is enhanced.

Swerdlow and Varshavsky (1983) have discovered a selectivity in the binding of HMG 17 to different members of a heterogeneous population of mononucleosomes and dinucleosomes. Their investigative technique involved running the mixture of bound complexes on a particle gel, and then sizing the DNA contained in the complexes via a second dimension of electrophoresis. In their heterogeneous mixture, the mononucleosomes (80% of the total) had DNA lengths ranging from about 140 bp to about 300 bp. (Note: it is difficult to estimate the size distribution of the mononucleosomal DNA precisely, because the only two reference points available are the micrococcal nuclease digestion stops of 140-150 bp and roughly 350 bp, for the DNA extracted from mono- and dinucleosomes, respectively; see their Figure 1C.) Within this mixture they observe that HMG 17 binds preferentially to those mononucleosomes with DNA considerably longer than the 140-150 bp minimum. This preference is especially strong at low HMG 17/ mononucleosome ratios (cf. their Figures 2G,2C,2D). Stein and Townsend (1983), using a roughly equimolar mixture of HMG 14 and HMG 17, also report a preferential binding to mononucleosomes containing long (160-200 bp) DNA, relative to those containing short (140-160 bp) DNA.

The thermal denaturation data of Paton et al. (1983), and

the competitive binding studies of Swerdlow and Varshavsky (1983) and Stein and Townsend (1983) both suggest that HMGs 14 and 17 bind to the region of the nucleosome where the termini of the DNA are found. This, of course, is the region where H1 also is thought to bind (see section VI B). Therefore the question is raised of whether the binding of HMGs 14/17 is interactive with the binding of histone H1.

The simultaneous binding of H1 and HMG 17 to nucleosomes has been investigated by Albright et al. (1980). These workers prepared a mixture of "stripped" chromatin fragments (containing mononucleosomes with DNA lengths in the 140-200 bp range). They mixed these chromatin fragments with H1 and HMG 17 at a NaCl concentration greater than 0.6 M, and then lowered the NaCl concentration by step dialysis. From previous studies on the salt-dependencies of the removal of H1 and HMG 17 from chromatin (referenced in their paper), H1 was expected to bind first, followed by HMG 17 (if, in fact, HMG 17 was able to bind in the presence of H1). These workers observed the generation of a mononucleosomal particle ("MV") which, when excised from a preparative gel and analyzed for protein composition, was found to contain, per nucleosome equivalent, roughly 1 equivalent of H1 and 2 equivalents of HMG 17 (see their Figure 7). Thus the binding to a nucleosome of 1 molecule of H1 and 2 molecules of HMG 17 are not mutually exclusive. Further study will be necessary to see if this conclusion extends to the joint

binding of HMG 14 and H1, or if there is any dependence of joint binding on the length of DNA in the nucleosome.

2. The binding of HMGs 1 and 2

Early attempts to bind HMG 1 and/or HMG 2 to mononucleosomes containing 140-200 bp DNA (Albright et al., 1980), or to core particles containing 140-150 bp DNA (Mardian et al., 1980), were unsuccessful (as assayed by the absence of discrete bands on a particle gel). Schroter and Bode (1982) have been successful, however, after approaching the problem in a different way. They mixed HMG 1 and HMG 2 with nucleosomes containing either 140 bp DNA or 180 bp DNA, in a 2:1 molar ratio. They then resolved each mixture on salt-free sucrose gradients. From the centrifugation involving 180 bp-nucleosomes, a band was isolated from the gradient which contained approximately 1 equivalent each of HMG 1 and HMG 2 per nucleosome equivalent. No such band could be obtained from the centrifugation involving 140 bp-nucleosomes. These workers therefore concluded that HMGs 1 and 2 bind to the linker region of the DNA in nucleosomes which contain long DNA. In substantiation of this thought, these workers observed that HMGs 1 and 2 had a greater affinity for binding to 180 bp DNA than they had for binding to 180 bp-nucleosomes.

Bernues et al. (1983) have reported that HMG 1 can be

crosslinked stoichiometrically to either the (H2A.H2B) dimer, or to the $(H3.H4)_2$ tetramer. Their reactions used highly purified proteins (with no DNA present), and the "short" crosslinkers EDAC and dimethylsuberimidate.

From the above two studies, I conclude that HMG 1 and HMG 2 may be able to form stoichiometric complexes with long DNA-containing nucleosomes. In such complexes, HMG 1 or HMG 2 may make specific contacts with linker DNA, and also with the (H2A.H2B) dimer and the $(H3.H4)_2$ tetramer.

D. The binding of topoisomerase to nucleosomes

The first indications of an interaction between eukaryotic topoisomerase I and nucleosomes came from affinity chromatography (see, for example, Weisbrod and Weintraub [1981], and Weisbrod [1982]).

Recently, Javaherian and Liu (1983) examined the possibility of a specific interaction more directly. These workers isolated mononucleosomes from a micrococcal nuclease digestion of HeLa nuclei, using sucrose gradients in 350 mM NaCl. The mononucleosomes isolated in this fashion were not characterized very well. There may have been some free DNA in the preparation, due to nucleosome dissociation in the high-salt sucrose gradients (see section V B, 3). The DNA in the nucleosomes ranged from 140 bp to 200 bp in length. Very

likely, some H1 and non-histone proteins were present (see Yager and van Holde [1984]. After purification in this manner, no topoisomerase activity was associated with the nucleosomes (cf. their Figure 1).

The nucleosomes were mixed with HeLa topoisomerase I in a 1:1 weight ratio, and the mixture resolved on an I=0.11 M sucrose gradient. Two peaks of topoisomerase activity were observed, sedimenting at 4.5 S and 12.3 S. It was asserted (but not shown rigorously) that the slow peak corresponded to free topoisomerase, and that the fast peak corresponded to a topoisomerase I/nucleosome complex.

If the above result is to be believed, it appears that a "complex" can form between topoisomerase I and nucleosomes. From the sucrose gradient loadings, the association constant for this complex, in 0.1 M NaCl, was estimated to be at least $10^8$. Since no complex was observed at 0.35 M NaCl, the association seems to be highly salt-dependent.

Interestingly, Javaherian and Liu observe that HeLa HMGs 1,2,17 and histone H1 can each stimulate the activity of the HeLa topoisomerase I. Calf thymus HMG 17 gives heterologous stimulation of HeLa and human placental topoisomerase I. Thus, in addition to perhaps binding to nucleosomes, topoisomerase I may also bind to proteins in the cell nucleus which themselves bind to nucleosomes. This suggests the possibility of a complicated set of coupled equilibria between nucleosomes and

their binding proteins.

E. The binding of DNA polymerase to nucleosomes

One report has appeared suggesting the specific association of eukaryotic DNA polymerase a and b with nucleosomes. Schlaeger et al. (1978) performed a micrococcal nuclease digestion of mouse ascites cell nuclei, and isolated the resultant chromatin fragments on a sucrose gradient. (Their nucleosomes were not characterized well in physical terms. Most probably, they contained DNA ranging from 140 bp to 280 bp in length, and also extensive amounts of non-core proteins [see Yager and van Holde, 1984].) These workers found that DNA polymerase activity co-sedimented with the "mononucleosome" fraction of the gradient (as indicated by the ability of this fraction to catalyze nick translation; see their Figure 1).

The following experiments were done, to try to determine whether the observed cosedimentation of DNA polymerase activity and nucleosomes was just coincidental, or was due to complex formation. (i) The mononucleosome peak was precipitated with 20 mM MgSO4. (Precipitation occurs because of the presence of H1 (Honda et al., 1975; T. Yager, unpublished observations [1984].) About 97% of the "endogenous" DNA polymerase activity precipitated along with the mononucleosomes. Next, purified DNA polymerase a or b was added exogenously to the mononucleosomes,

and the precipitation with 20 mM $MgSO_4$ was repeated. Roughly 25-40% of the polymerase activity precipitated along with the nucleosomes. Finally, as a control, purified DNA polymerase a or b alone was placed in a solution of 20 mM $MgSO_4$; no precipitation of polymerase activity could be observed. Thus DNA polymerase a or b, although quite soluble in 20 mM $Mg^{2+}$ when present alone, is rendered insoluble in the presence of (H1-containing) nucleosomes. (ii) The 11-12 S mononucleosome peak (containing "endogenous" DNA polymerase activity) was recentrifuged through a 0.4 M NaCl sucrose gradient, and the gradient fractions reassayed for DNA polymerase activity. Activity was observed to sediment only at 4-5 S.

The above results are suggestive of a complex between DNA polymerase and nucleosomes. However, considerably more work must be done before this can be considered to be rigorously shown.

F. The (possible) binding of specific proteins to nucleosomes, in transcriptionally active chromatin

Particles bearing some resemblence to nucleosomes have been isolated from the transcriptionally active rRNA-encoding region of the Physarum genome (Prior et al., 1983). The isolation of these particles depended on the fact that they sediment at 5 S in sucrose gradients (instead of the normal nucleosomal 10.7

S). These so-called "A particles" show an enhanced reactivity to H3-SH modification, relative to nucleosomes from transcriptionally inactive Physarum chromatin. Also, their DNA is more sensitive to reaction with psoralin, and to endonucleolytic cleavage by MNase, than is the DNA from "inactive" nucleosomes. These observations suggest that the "A particle" is an unfolded, or highly extended structure.

When the proteins from "A particles" and from (presumeably) transcriptionally inactive Physarum nucleosomes are analyzed on an SDS gel, one observes several intense bands in the former sample which do not appear in the latter (see, for example, Figure 4A of Prior et al. [1983]). (Unfortunately, both the "A particle" and the "nucleosomal" preparations are highly contaminated by many proteins, as is evident in silver-staining, so this observation is not entirely unambiguous.) Prior et al. speculated that certain additional, non-histone proteins may selectively bind to Physarum nucleosomes to induce (and stabilize) a "transcriptionally active unfolded state".

As should be obvious from above, nothing may be said with high precision concerning the structure of these "A particles". To determine without ambiguity even whether additional non-histone proteins really are present, a better purification scheme will have to be developed, which yields "A particles" and nucleosomes in the absence of contaminants. Once this is

achieved, then reconstitution experiments can be done to determine whether binding of additional proteins in fact does occur.

G. The binding of RNA polymerases to nucleosomes

1. E. coli RNA polymerase

Two early works, by Bustin (1978) and Shaw et al. (1978), studied the apparent "transcription", by E. coli RNA polymerase, of mononucleosomes containing random-sequence DNA. Aside from the problem that prokaryotic, and not eukaryotic RNA polymerase was used, there were at least four other problems with these studies. First, the length of the DNA in the mononucleosomes was quite heterogeneous, ranging from 140 bp to 250 bp in the study of Shaw et al., and from 140 bp to 180 bp in the study of Bustin. Second, there almost certainly was contamination by H1, and by non-histone chromosomal proteins. Third, there was 5-10% contamination by dinucleosomes. Fourth, no rigorous controls were done to test for nucleosome dissociation during transcription. (In the study of Shaw et al., dissociation may have been a serious problem, because the ionic strength was about 240 mM; Bustin, however, used a low ionic strength transcription buffer.) The potential problem of nucleosome dissociation is critical because, in a transcription

assay, a small amount of free DNA could actually direct the majority of the transcription. Because of these difficulties, I feel that no unambiguous conclusions can be drawn from these studies concerning the specific binding of (E. coli) RNA polymerase to nucleosomes.

2. Eukaryotic RNA polymerase II

The next study of nucleosome transcription, that of Lilley et al. (1979), used a eukaryotic RNA polymerase. These workers prepared fairly homogeneous (143-148 bp) core particles from chicken erythrocytes. From the same source, they also prepared "long-DNA nucleosomes", containing 150-190 bp DNA. In either preparation, there was 5-10% contamination by particles containing DNA that was shorter than desired. Staining with Coomassie blue showed only traces of H1 and H5 remaining in either preparation. No more sensitive staining method (e.g. silver) was used, to attempt to detect trace contaminants of other proteins. Both types of nucleosome were 5'-end-labelled with 32P, using polynucleotide kinase. Wheat germ RNA polymerase II was obtained commercially. It was not characterized, except for showing the presence of some contamination by nuclease(s).

To determine whether nucleosome dissociation could occur under transcription conditions, these workers incubated both

types of nucleosomes at 2 ug/ml ($A_{260}$ = 0.02) in a buffer containing 40 mM Tris (pH 7.9), 1 mM $MgCl_2$, 20-150 mM $NH_4SO_4$. A significant amount (5-20%) of nucleosome dissociation was seen. The addition of BSA or ovalbumin decreased the extent of this dissociation; significantly, addition of the RNA polymerase II inhibitor rifampicin had the opposite effect.

Under transcription conditions, RNA fragments approximately 150 nt in length were generated. Lilley et al. proposed that these could be accounted for simply by the action of the RNA polymerase on DNA that was released by nucleosome dissociation.

These workers also incubated polymerase and long-DNA nucleosomes in the "transcription buffer", and then resolved the mixture on sucrose gradients which were made up in this buffer. They observed two peaks of radioactivity, sedimenting at about 11 S and 15-16 S. The former probably corresponded to intact nucleosomes. It is not entirely clear what the identity of the latter peak was, just on the basis of the sucrose gradient results. Purified RNA polymerase is observed to sediment at about 17 S (Baer and Rhodes, 1983); thus a complex between RNA polymerase and a nucleosome would be expected to sediment considerably faster than 15-16 S. The protein composition of the 15-16 S peak was not determined. Because of the limited quality of the data, I feel that little can be said with certainty concerning either the identity or the homogeneity of material in the 15-16 S peak.

Upon DNAase I digestion of the 15-16 S peak, a "10 bp ladder" was generated, which bore fair resemblance to that obtained from the long-DNA nucleosomes alone. Thus the material in the 15-16 S peak may have had at least some nucleosomal character (assuming no "DNAase I-like ladder" can be generated from a complex between RNA polymerase and free DNA).

I now turn to a more recent studies of the interaction between RNA polymerase II and nucleosomes. Baer and Rhodes (1983) prepared RNA polymerase II from calf thymus. They did not characterize it, other than showing that it sedimented in a sucrose gradient at about 17 S. These workers also purified "core particles" from cultured mouse myeloma cells. The size distribution of the DNA in the core particles was not given. The inner histones were present in approximately equimolar ratios. No H1 could be observed, in staining with Coomassie blue. No check, however, was made with silver staining for the presence of residual H1 (or for the presence of other contaminating proteins).

Polymerase and 5' end-labelled core particles were mixed in an I=0.2 M buffer in a 10:1 molar ratio, with the core particles at a concentration of 2 ug/ml ( $A_{260}$= 0.02). After an incubation step, the mixture was then examined on a low-salt (I=10 mM) sucrose gradient. Three peaks of radioactivity were observed, corresponding apparently to free DNA (from core particle dissociation under these conditions), intact core

particles, and a putative "polymerase II/ core particle complex" (sedimenting at 5-6 S, 10-12 S and 18 S, respectively). The peaks were present in approximately a 1:80:10 ratio. In an analogous experiment in which the histones of the core particle sample had previously been labelled in vivo with $^{14}$C-arginine, analysis of the histones in the 18 S peak revealed an H2A:H2B:H3:H4 stoichiometry of 0.5:0.6:1.0:1.0. Thus the conclusion was drawn that an (H2A.H2B) dimer was lost from nucleosomes upon polymerase binding.

There are three criticisms of the above experiment. First, the ratios of the histones to the various polymerase II proteins, and of the histones and polymerase II proteins to the DNA were not determined, for the material in the 18 S peak. It seems that a complex between a complete 11 S nucleosome and a complete 17 S RNA polymerase should sediment considerably faster than 18 S. Second, no attempt was made to determine the homogeneity of the 18 S peak. Complexes lacking some or all the histones or RNA polymerase proteins might not be resolvable in a sucrose gradient from an authentic "RNA polymerase/nucleosome complex". Third, the generation of free DNA (which the polymerase could complex with) seems plausible, because the above experiment was done at core particle- and salt concentrations favoring nucleosome dissociation (Lilley et al, 1979; Yager and van Holde, 1984).

The above criticisms notwithstanding, it is probable that at least some portion of the 18 S peak was due to a complex between (some or all of) the polymerase molecule and a (possibly H2A,H2B-depleted) nucleosome. Furthermore, the complex must have retained considerable nucleosome-like structure. These assertions are supported by the gel analysis of the histones in the 18 S peak, mentioned above. They also are supported by experiments in which both the 18 S peak and the core particle peak from the sucrose gradient were digested with DNAase I: in autoradiography of denaturing gels, a "10 bp ladder" was observed for the 18 S peak. (Significant deviations of the intensities of individual digestion bands were observed, however, relative to what was expected for core particles. No control was done in which a polymerase II/ DNA complex was digested and analyzed.)

A mixing experiment was done, in which the ratio of polymerase II to (5' end-labelled) core particles was varied from 0.01 to 10. At a ratio of 10, only 15% of the radiolabel had been driven into the 18S peak. This suggests that the polymerase was able to interact with only a 15% subpopulation of the core particles.

A cDNA copy of the poly(A)-mRNA population from mouse myeloma cytoplasm was made, and was used to probe for transcribed sequences, both within the 18S peak, and within the core particle peak. The DNA in the 18 S peak was enriched about

5-10 X in complementary sequences, relative to the DNA in the core particle peak. Thus it was suggested that the polymerase bound preferentially to "active genes".

A recent paper by Sakuma et al. (1984) studied the "complex" formed between wheat germ polymerase II and mononucleosomes prepared from mouse hepatoma cells. This study, as the previous one, is deficient in characterization of the polymerase and the nucleosomes. From a "native" gel of the DNA purified from the nucleosomes, one sees that this DNA spans the 140-190 bp range (cf. their Figure 4C). From an acid-urea gel, one sees that H1 is present in at least some of the nucleosomes.

These workers mixed the polymerase II and the nucleosomes in a 0.8:1 molar ratio, at a core particle concentration of 40 ug/ml (A260 = 0.4), in an I=140 mM buffer. (Less than 5% nucleosome dissociation is expected at these nucleosome- and salt concentrations; see section VI C.) The mixture was then resolved on an I=60 mM sucrose gradient; two peaks were observed. The slow peak corresponded to nucleosomes, and the fast peak corresponded, presumeably, to the 18 S peak of Baer and Rhodes' study. The peaks were recovered, and their DNA and protein analyzed. In the fast peak, the DNA was 160-190 bp in length, while in the slow peak, it was almost exclusively 140-160 bp in length. Also, virtually all the H1 was distributed in the fast peak. From these results, it was

concluded that, in the "complex" formed between polymerase II and the nucleosome, the polymerase has an affinty for linker DNA and/or H1. The acid-urea gels were not scanned and quantitated, so it could not be determined whether, as in the study of Baer and Rhodes, H2A and H2B were depleted in the fast peak.

DNAase I digestions were performed on the fast and slow peaks of the sucrose gradient, and also on the original nucleosomes. In these experiments, the DNA was uniformly labelled with $^{3}$H-thymidine, and autoradiographs were made of the electrophoretically-separated digestion products. There appeared to be a uniformly enhanced susceptibility to digestion, for the material of the fast sucrose gradient peak. Because of the uniform labelling of the DNA and the low resolution of the particular gel system used on this study, however, no conclusion could be drawn concerning slight shifts in cutting frequencies within the pattern.

The above mixing reaction was also carried out in the presence of ATP, GTP and [$\alpha$32P]-UTP (but no CTP), to allow initiation of RNA synthesis. In consequence, the fast sucrose gradient peak was observed to acquire $^{32}$P-radioactivity. This suggests that initiation, and, possibly, a limited amount of transcription occurred, to form a stable "ternary" complex of polymerase II, "nucleosome", and RNA. The structure of this complex was not investigated.

As can readily be seen, the criticisms given for the work of Baer and Rhodes apply also to this work. Thus each suffers from some serious unresolved issues. Nonetheless, together the two papers give reasonable evidence that a specific complex between polymerase and nucleosomes can form. Further characterization of this complex is desireable.

3. Eukaryotic polymerase III

There is some evidence, albeit rather indirect, for the specific binding of RNA polymerase III to nucleosomes. Wittig and Witting (1982) worked with nucleosomes which had been reconstituted on a chick embryonic tRNA gene flanked by long portions of pBR322. Nucleosome reconstitution depended upon the use of a "nucleoprotein fraction" from chick embryo nuclei, and apparently was coupled to the synthesis of the complementary strand of their exogenously added (single-stranded) DNA template. Reconstitution upon the double-stranded version of the template was deemed successful by the criteria that, in subsequent digestions, MNase generated a 160-220 bp protection fragment, and Exo III generated 140-150 bp protection fragment.

From an analysis of the restriction sites remaining in the nuclease-protected fragments of the template, it was determined that the reconstituted nucleosomes were phased in a number of

different (but still well-defined) positions. As a "control" for phasing, reconstitution was also carried out on pBR322 which lacked the tRNA gene insert; it was stated that nucleosome placement was random in this control sequence.

The structure and stability of this reconstituted "chromatin" - i.e. the number of nucleosomes per DNA template molecule, the possible existance of single-stranded regions and nicks, the tendency for nucleosome dissociation, etc. - was not investigated.

The reconstituted "chromatin" was transcribed using an endogenous RNA polymerase (presumeably type III) within the same "nucleoprotein fraction" used for reconstitution. The sequences of the RNA transcripts were determined by hybridization with various defined subfragments of the 5S tRNA gene, followed by S1 mapping.

It was asserted that, for the tRNA gene in the "chromatin" to be highly transcribed, the sequence TTCGA within the gene's promoter had to be located at the center of a length of DNA associated with a histone core. Presumeably, this sequence was also in the locus of interaction with the polymerase.

These results, although highly suggestive, cannot be considered unambiguous. Further progress will depend upon the physical characterization of the putative RNA polymerase III/nucleosome complex.

H. The (putative) binding of nucleoplasmin to "octamers" of the inner histones, and (transiently) to nucleosome-like structures

Laskey and coworkers (Laskey et al., 1977) observed that an extract from unfertilized X. laevis eggs could assemble chromatin upon exogenous DNA, under physiological conditions (0.1 M monovalent neutral salt). Upon partially characterizing the "assembly extract", these workers found it to contain, as essential components, X. laevis histones, a "nicking-closing" activity, and a third unidentified factor (or set of factors).

Later work (Mills et al., 1980; Earnshaw et al., 1980) determined that this factor was an acidic protein of protomer MW = 29,000; it was found to be the most abundant protein in the X. laevis cell nucleus, constituting 7-10% of the total protein mass. This protein was named "nucleoplasmin".

From dimethylsuberimidate crosslinking studies, the functional form of nucleoplasmin appeared to be a pentamer. Crosslinked nucleoplasmin functioned in a chromatin-assembly assay with 70% of the activity of native nucleoplasmin.

In mixing experiments on sucrose gradients, or upon chromatography through DNA-cellulose, nucleoplasmin did not show any affinity for either free DNA or for assembled chromatin. This protein was, however, able to prevent the binding of histones to (negatively charged) carboxymethyl

cellulose. Also, it was able to enhance the binding of histones to positively-charged DEAE. Thus nucleoplasmin appeared to have a definite affinity for histones. In the latter study, equimolar H2A/H2B competed with equimolar H3/H4 for nucleoplasmin-mediated enhancement of binding to DEAE. This suggested that H2A/H2B and H3/H4 did not have independent binding sites on the nucleoplasmin molecule.

A model was proposed in which: (i) one (pentameric) molecule of nucleoplasmin bound one octamer-equivalent of the inner histones; (ii) the histones were then transferred from the nucleoplasmin to a piece of DNA, thus forming a nucleosome. This model of necessity postulates the transient existance of a ternary complex of DNA, histones, and nucleoplasmin.

Concerning the first part of the proposed model, no work has yet been done to directly demonstrate the reversibility and stoichiometry of a nucleoplasmin/histone binding interaction. Also, the internal structure of the nucleoplasmin/histone complex has not been studied. Thus if an "octamer" of bound histones in fact exists as a stable entity, it may not have the same pattern of histone-histone contacts as does an intact histone octamer.

The second portion of the model has not been critically examined, either. Thus nothing can be said with certainty of the mechanism of transfer of histones from nucleoplasmin to DNA (if in fact such direct transfer occurs).

Interestingly, Stein et al. (1979) have discovered that poly(L-glutamic acid) can act as a nucleosome assembly factor at physiological ionic strength. Also, Earnshaw et al. (1980) have determined that calf brain calmodulin (a very anionic protein: pI = 4.3) does not have such an activity. Thus a lack of well-defined secondary and tertiary structure may be an essential characteristic of a nucleosome assembly factor.

## VII. Summary

This essay has presented a highly reductionist view of nucleosome dynamics.

Even within its restricted scope, however, many problems of a fundamental nature remain unsolved. These include: (i) rigorous determination of the extent to which counterion condensation theory applies to DNA bound up in chromatin; (ii) elucidation of experimental methods for studying the stabilities and lifetimes of individual bonds between the DNA and the histone core in a nucleosome; (iii) specification of the various modes of motion of the DNA within a nucleosome (for example, by an analysis of high resolution x-ray diffraction patterns); (iv) specification of a complete set of equilibrium association reactions between the various components of the nucleosome, and of the magnitudes and salt-dependencies of the various equilibrium constants; (v) specification of the effects of

histone modifications on all the presently well-documented nucleosome instabilities (DNA "tail release", nucleosome dissociation, histone core sliding, etc.).

Although these problems (and others) are yet unsolved, the experimental and theoretical tools exist to determine rigorously their answers. Therefore it seems justified to believe that, at this time, the field of "nucleosome dynamics" stands on firm experimental and theoretical ground.

It follows that time is right to consider the final - and most difficult - task in chromatin research. This task will be to explain the biological functions of chromatin in terms of the structures and instabilities of its constituent nucleosomes.

# Dynamics and Equilibria of Nucleosomes at Elevated Ionic Strength

Thomas D. Yager and K.E. van Holde[†]

Department of Biochemistry and Biophysics
Oregon State University
Corvallis, Oregon 97331

[†]To whom correspondence should be addressed.

Running title: Dynamics and Equilibria of Nucleosomes

## I. Abstract

We have prepared chicken erythrocyte nucleosomes lacking proteins other than the inner histones, and containing long DNA. Our nucleosomes' DNA has mean length ± S.D. = 190 ± 15 base pairs (bp). No DNA < 155 bp is present.

Nucleosome stability in salt was examined by boundary and band sedimentation, and by particle gel electrophoresis. We find: (i) A second species is slowly generated by treatment with salt. This species sediments with $s_{20,w}$ = 5.5 S (as does purified nucleosomal DNA), is not associated with histones, and electrophoretically migrates as mononucleosomal DNA. We conclude it is free DNA. Thus salt causes nucleosomes to dissociate, independently of either non-core proteins, or of any nucleosome population with DNA < 146 bp. (ii) Dissociation is reversible, and is enhanced by nucleosome dilution. Thus it appears to follow the law of mass action. (iii) The equilibrium extent of dissociation increases with salt.

A second effect of salt is a fast, reversible 10% decrease in $s_{20,w}$ of the nucleosomes left intact. From hydrodynamic calculations, this is consistent with either a slight unfolding of the entire nucleosome, or an unbinding of the terminal DNA regions from the histone core.

## II. Introduction

There has been considerable controversy concerning the effects of moderate to high salt concentrations on nucleosome structure. for example, some recent papers have suggested that an increase in salt

concentration above ~0.2 M may promote dissociation of nucleosomes into free DNA and histones (Burton et al., 1978; Stein, 1979; Lilley et al., 1979; Stacks and Schumaker, 1979; Russev et al., 1980; Bode and Wagner, 1980; Bode et al., 1980; Cotton and Hamkalo, 1981; Eisenberg and Felsenfeld, 1981; Vassilev et al., 1981; Erard et al., 1981). On the other hand, there also are a number of papers which assert that unfolding of the nucleosome is the principal effect of salt (Bode and Wagner, 1980; Bode et al., 1980; Zama et al., 1977; Dieterich et al., 1977; Dieterich et al., 1979; Whitlock, 1979; Wilhelm and Wilhelm, 1980; Zayetz et al., 1981). In this view, the DNA remains bound to the histones, but the nucleosome adopts a much more extended conformation.

Many previous attempts to study this problem may have been rendered ambiguous because of certain features of the nucleosome preparations. There are at least four potential sources of ambiguity in such experiments:

(i) If the preparation of core particles is attempted, some nucleosomes will have DNA with length $\geq$ 146 bp , while others may have lengths less than this limit. It has been suggested that, in an individual nucleosome, the DNA may be 'anchored' to the histone core by strong bonds near its termini (Erard et al., 1981; McGhee et al., 1980). Were this true, a subpopulation with DNA length < 146 bp might be preferentially destabilized by an increase in salt. Such a 'critical length' effect has in fact been reported (Erard et al., 1981).

(ii) Different nucleosomes may contain different combinations of

H1, H5 and non-histone chromosomal proteins. For example, it has been reported (Sandeen et al., 1980) that, under certain conditions, HMGs 14 and 17 bind preferentially to nucleosomes containing β-globin gene sequences. The problem of hereogeneity of associated proteins probably would be lessened if redistribution were extremely fast, for then all nucleosomes would have the same average composition. (In this connection, there is evidence that H1 (Caron and Thomas, 1981) and HMG 17 (Albright et al., 1980), at least, can exchange quickly between nucleosomes at low to moderate ionic strengths). Nonetheless, on a short enough time scale, nucleosome heterogeneity with respect to these associated proteins will exist. Also, their redistribution during an unfolding or dissociation process could severely complicate interpretation.

(iii) Different nucleosomes may contain different genetic variants of the histones (Urban et al., 1979). In addition, histones of identical amino acid sequence may carry different degrees of post-translational modification, such as acetylation, phosphorylation and methylation (Isenberg, 1979).

(iv) There are reports that nucleosomes may be associated with DNA in a sequence - specific manner (Zachau and Igo-Kemenes, 1981); thus functionally different subclasses of nucleosomes may exist by virtue of containing different particular DNA sequences. Even if no discrete subclasses exist on the basis of sequence, a microheterogeneity may be expected because different nucleosomes will contain, at random, different DNA sequences. Also, the DNA in certain

nucleosomes may contain modified bases (Ehrlich and Wang, 1981; Pech *et al.*, 1979; Igo-Kemenes *et al.*, 1980).

By taking particular care in the preparation of nucleosomes, one may try to eliminate some of the above complications. Thus, by design, our preparative procedure removes all non-core proteins from a population of nucleosomes, and also removes those members of the population with DNA lengths less than 146 bp. Our nucleosomes are still heterogeneous with respect to DNA length, sequence and modifications, and also with respect to chemically modified and genetically variant forms of the histones. However, we feel these factors are of relatively minor consequence; the main sources of potential abiguity - proteins other than the inner histones, and nucleosomes with DNA lengths less than core size - have been eliminated.

We have studied the response of such nucleosomes to an increase in salt concentration, both before and after crosslinking of the core histones. The major change which we observe is largely reversible. It seems to involve a dissociation in which DNA is released from the histone core, following the law of mass action. The dissociation is accompanied by a much faster, minor structural change in the remaining undissociated nucleosomes. The latter change, which also is reversible, may be a relatively small unfolding event, or a partial unbinding of core DNA from the histone octamer.

## III. Materials and Methods

### A. Initial preparation of chromatin

Chicken erythrocyte chromatin was prepared following Shaw *et al*. (1976), but with a number of modifications. In each preparation, blood was pooled from about five white leghorn chickens; the erythrocytes were washed twice by a 500 x g, 5 min centrifugation through 1L of 150 mM NaCl, 15 mM Na Citrate, pH 7.2 (buffer A). After the second wash, the packed erythrocytes were apportioned into about fifty 5 ml aliquots, frozen in liquid $N_2$, and stored at $^{-}60°C$.

For each experiment, 5 ml of erythrocytes were lysed by thawing. All subsequent operations, except the nuclease digestions, were done at 0-4°C. A volume of 60 ml of buffer A containing 1 mM phenylmethylsulfonyl fluoride (PMSF) was added to the 5 ml of ruptured cells. The nuclei were then isolated by centrifugation at 500 x g for 5 min, and subsequently were washed once or twice by a 5 min, 500 x g centrifugation through 60 ml buffer A.

The nuclei were then resuspended in 10 ml of buffer A, and 10 ml of buffer A containing 0.25% Nonidet P-40 was added stepwise with gentle agitation, over a period of 1 min. After an additional 30 sec of gentle agitation, 50 ml of buffer A containing 1 mM PMSF was added. This last addition is neccessary to dilute the detergent, so that the nuclei will not lyse upon centrifugation. The nuclei were then centrifuged at 500 x g for 5 min and the supernatant removed.

The nuclei were resuspended in 10 ml of 0.3 M sucrose, 0.75 mM $CaCl_2$, 10 mM Tris, pH 7.2, by adding the sucrose solution dropwise and gently agitating the resultant suspension. After the addition, the nuclei were at a concentration of $\sim 10^8$/ml, and appeared intact but somewhat clumped together under 1000x magnification. The suspension was warmed to 37°C, and Staphylococcal aureus (Foggi) nucelase (Sigma; MNase) was added to 50 U/ml. Digestion proceeded 10-15 min. Then the solution was cooled, digestion was stopped and the nuclei were lysed by 1 min of medium Virtis homogenization on ice. At this step, we have chosen to homogenize the suspension, instead of pelleting the nuclei and discarding the supernatant. This choice reflects our observation that, in the digestion buffer, some mono- and oligonucleosomes are released from the nuceli (not shown; see also Sanders, 1978 and Davie and Saunders, 1981); thus, were the nuclei pelleted, a selective loss of subpopulation of nucleosomes into the supernatant might occur (Sanders, 1978 and Davie and Saunders, 1981).

The homogenized suspension was centrifuged at 1500 x g for 5 min to remove debris, in preparation for a second nuclease digestion. During the course of our work we found that the concentration of $Ca^{2+}$ critically affects the redigestion. In 0.75 mM $Ca^{2+}$, core particles are quickly produced (cf. Figure 5D); in long digestions, they will come to predominate over mononucleosomes with longer DNA. In contrast, when redigestion is done in 10 mM $Ca^{2+}$, the latter species predominates (not shown). As assayed by particle gels (see

below), increasing the concentration of $Ca^{2+}$ from 0.75 mM to 10 mM in the redigestion step does not cause any dissociation of nucleosomes into histones and free DNA (not shown). For redigestions in 0.75 mM $Ca^{2+}$, the chromatin solution was warmed to 37°C, and nuclease was added to 30-100 U/ml. For redigestions in 10 mM $Ca^{2+}$, $CaCl_2$ was added from a 1 M stock, slowly and with stirring, to 10 mM. The solution, which immediately became turbid, was then warmed to 37°C, and nuclease was added to 30-100 U/ml. In both cases digestion proceeded 5-20 min, and was then stopped by chilling to 0°C and adding EDTA to a 2-5 mM excess. For the digestions in 10 mM $Ca^{2+}$, the precipitated chromatin was next brought back into solution by dialysis against 10 mM Tris, 5 mM EDTA, pH 7.5 at 4°C for ~15 h, and then cleared of a slight residue by 2 min centrifugation at 8800 x g.

We next eliminated all mononucleosomes lacking H1/5 [a class which includes all particles having DNA lengths less than ~160 bp (Simpson, 1978)], by precipitating the H1/5-containing chromatin with 100 mM KCl, and discarding the supernatant (Simpson, 1978). After 30 min, the precipitate was gathered into a pellet by centrifugation at 1500 x g for 10 min. The supernatant was discarded, and the pellet was resuspended in 2.5 ml of 10 mM Tris, 0.75 mM EDTA, pH 7.5 (buffer B). At this stage, we had discarded into the supernatant about 90% of those mononucleosomes with DNA lengths less than ~160 bp. The KCl-precipitation was repeated, so that less than 1% of the mononucleosomes with DNA lengths $\leq$160 bp ultimately were retained in the pellet. The second pellet was resuspended in 2 ml of buffer B. We found that this precedure failed to remove mononucleosomes with DNA

lengths $\leq$ 160 bp when redigestion was done in 0.75 mM $Ca^{2+}$ and was extensive (cf. Figure 5D). In such cases, we deemed the material acceptable for use on particle gels, but not for use in physical studies.

Next H1 and H5 were selectively removed (Libertini and Small, 1980) from the material in the resuspended pellet. 1 M NaCl was added, slowly and with stirring, to a final concentration of 50 mM. Then, again slowly and with stirring, Carboxylmethyl Sephadex (Pharmacia) was added to 30 mg/ml. The resultant suspension was stirred for 1 hour. The cation exchange resin was removed, either by 10 s centrifugation at 8700 x g, or by passing the suspension through a Pasteur pipette that had been plugged with glass wool. In either case, the resin was then washed twice with 1 ml of buffer B, and the washes were combined with the first supernatant or eluent. The final solution was clarified by centrifugation at 8800 x g for 15 min. We noticed that, if the redigestion had been done in 10 mM $Ca^{2+}$, this procedure failed to remove all the H1/5 from the chromatin. However, when the chromatin was subsequently resolved into different size classes on a sucrose gradient (see below), we found none of the remaining H1/5 within the mononucleosome fraction (not shown).

A typical yield, for 5 ml packed erythrocytes, was 4 ml of H1/5-depleted mono-, oligo- and polynucleosomes, showing an absorbance of 50 at $\lambda$ = 260 nm. About 10% of this (i.e. 1 mg, or 4 nmol) was mononucleosomes.

To calculate nucleosome concentrations, we assumed (i) that an $A_{260}$ = 1.0 solution contains 50 µg/ml DNA (Stein, 1979; Bloomfield et

al., 1974; Harrington, 1977; Klevan et al., 1978) ; (ii) that absorbance of light by DNA is unaffected by histones (Stein, 1979; Harrington, 1977; Klevan et al., 1978); (iii) that, in our nucleosomes, there are equivalent amounts of only the four core histones, and 190 bp DNA (see below). Assuming M = 108,000 for the histones and M = 650/bp for the DNA, we then calculated that $A_{260}$ = 1.0 corresponds to a nucleosome concentration of 430 nM.

B. Purification of mononucleosomes

The solution was dialyzed, in Spectrapor tubing (cutoff $\leq$ 8,000 daltons), against either of two buffers. Buffer C was 5 mM Tris, 1 mM EDTA, 50 mM NaCl, pH 7.5, while buffer D was 10 mM Tris, 0.25 mM EDTA , pH 7.4. After dialysis, the solution was clarified by centrifugation for 15 min at 8800 x g. The mono- and oligonucleosomes were then resolved on isokinetic gradients (McCarty et al., 1974), which were made 5% to 26% sucrose in either buffer C or D. Buffer C was chosen initially because, in sucrose gradients, the separation of mono- from oligonucleosomes appears to depend on salt concentration, being optimized at 50 mM (Strätling, 1979). However, we came to suspect that 50 mM salt caused some dissociation at the nucleosome concentrations used (see below). Therefore buffer D was used instead in later experiments.

In a preparation from 5 ml packed erythrocytes, typically we loaded 200-1000 μl x $A_{260}$ = 50 of solution upon each of six 33 ml gradients. The gradients were centrifuged in an AH-627 or SW-28 rotor at 25,000 rpm for 20-24 hours, and were then pulled from the bottom through a flow monitor set at λ = 254 nm. The mononucleosome

peak was collected and stored on ice. In some experiments the mononucleosome peak was concentrated at this point by ultrafiltration (Amicon YM 30). The sucrose was left in solution until just before the nucleosomes were used, to stabilize against protein denaturation (Lee and Timasheff, 1981).

We required that there be no more than 5% contamination by dinucleosomes, and no contamination by larger oligonucleosomes. If the mononucleosome peak was initially of this purity, it was put directly into buffer D by filtration of 1 ml aliquots through a 1.1 x 30 cm Bio-Gel P-150 column. The nucleosomes eluted at the void volume, well ahead of the sucrose gradient buffer [as shown by conductivity and a chemical assay for sucrose (Yemm and Willis, 1954)]. If there was more than 5% of such contamination, 1 ml aliquots were filtered instead through a 0.8 x 27 cm Bio-Gel A-50m column in buffer D. We retained the trailing two-thirds of the eluent peak, which was depleted in the di- and oligonucleosomal contaminants (not shown). The mononucleosomes were then concentrated and the buffer changed to pure 'D' by ultrafiltration (Amicon PM 10).

In subsequent experiments, a sudden elevation of salt was accomplished in either of two ways. By one method, NaCl was added from a 3 or 5 M stock in buffer D, with stirring. The rate of addition was about 1/300 volume/second. As an alternate method, concentrated mononucleosomes were diluted into buffer D which already contained NaCl at slightly greater than the desired final concentration. In either case, as a precaution, a brief centrifugation then followed, to remove any aggregated material.

C. Crosslinking of the histone core

Nucleosomes were crosslinked with dimethyl suberimidate (DMS; Thomas and Kornberg, 1975; Stein et al., 1977). Solid DMS·2HCl (98% grade, Tridom-Fluka) was stored at 0-6°C, desiccated and under He or Ar. A stock DMS solution of 100 mg/ml in 100 mM Na Borate (final pH ≈7) was prepared. We have found this stock cannot be deoxygenated with He and frozen in liquid $N_2$ for later use; crosslinking will then be unsuccessful. Therefore the stock was always prepared fresh and used immediately. Slowly and with stirring, 1/9 volume of the stock was added to a 220-640 nM ($A_{260}$ = 0.5 - 1.5) solution of nucleosomes, which had been dialyzed from the sucrose gradient buffer into buffer B or D. 1 M NaOH was then added slowly and with stirring, until the pH was raised to ~9.5. The solution was incubated ≤ 2 hours at 22 ± 2°C. Care was taken to keep the nucleosome concentration ≤ 640 nM during the reaction; at higher concentrations, there was extensive crosslinking of nucleosomes to each other. After incubation, the pH was brought down to ~7 by adding 1 M HOAc slowly and with stirring. The crosslinked nucleosomes were then dialyzed into buffer D, and concentrated by ultrafiltration (Amicon PM 10). After clarification at 8800 x g for 15 min, the nucleosomes were then purified away from crosslinked oligomers by filtration on a 46 x 1.1 cm Bio-Gel A-50m column in buffer D. The lagging half of the eluent peak, which was depleted in oligomeric products, was concentrated by ultrafiltration (Amicon YM 30), and was then dialyzed against buffer D.

D. Gel electrophoresis

Nucleosomes were examined during preparation and experiments by three types of electrophoresis. For an analysis of proteins, samples were precipitated with trichloroacetic acid [in the presence of deoxycholate, when very dilute (Bensadoon and Weinstein, 1976)], washed with diethyl ether/ethanol, and then heated 2 min at 90°C in a buffer containing SDS and β-mercaptoethanol (Laemmli, 1970). The denatured proteins were resolved on 0.3 mm thick polyacrylamide minislab gels (Idea Scientific, Corvallis, OR), according to Laemmli (1970). The stacking portions of the gels were either 3% or 6% acrylamide, and the resolving portions were either 6%, 12%, 13.5%, or 15% acrylamide. The bis- to acrylamide ratio was always 1 to 37.5. Molecular weight markers included calf thymus histones (Worthington), BSA (Sigma), phosphorylase b (obtained from Dr. S. Anderson), and *Octopus dofleini* hemocyanin (obtained from Dr. K. Miller). The gels were run at 20-30 V/cm, for 1-3 h at 4°C. Staining was by either Coomassie Blue (Weber and Osborn, 1961) or silver (Wray *et al*., 1981).

DNA was extracted (Britten *et al*., 1974) from chromatin, and was characterized by electrophoresis on 0.8 mm thick polyacrylamide minislab gels. The gels were 3.5% or 5% acrylamide, with a bis- to acrylamide ratio of 1 to 20, in 40 mM Tris, 20 mM NaOAc, 1 mM EDTA, pH 7.2. In these gels, the DNA runs in double-stranded form (Kovacic and van Holde, 1977; Kovacic, 1976). For size markers we used Cfo I- and Hpa II - generated fragments from pBR322 (Sutcliffe, 1979), and Hae III - generated fragments from ΦX174 (Sanger *et al*., 1977). The

gels were run at 10-30 V/cm, for 0.5 - 2 h at 4°C. Staining was by ethidium bromide (Lohr et al., 1977).

One may determine precisely the distribution of DNA lengths in a gel band in the following manner. The gel is photographed and the negative scanned. From the scan of the marker lane, one obtains a curve of response vs. fragment size for the entire detection system (stain, camera, film, and scanner). This is based on the fact that the different marker fragments, deriving from plasmid restriction, are present in equal molar amounts.

Markers are also included in one of two "sample" lanes, to provide a distance vs. ln(M) calibration. The scan of the lane containing sample only is then adjusted for non-linearities in the detection system (using the first calibration curve), and is mapped onto distance vs. ln(M) axes (using the second calibration curve). Ultimately, a plot of relative molar amount versus fragment size is obtained.

A fundamental limitation in this technique arises in attempting to trace the baseline underneath the mononucleosomal DNA peak. The baseline may be biased upward in the high molecular weight region, due to the presence of a slight dinucleosomal DNA contaminant. This will result in an underestimate of the relative amounts of the larger mononucleosomal DNAs. It will not, however, change one's conclusion as to where, on the low end, the distribution stops.

Intact and dissociating nucleosomes were examined on six types of particle gels, following Todd and Garrard (1977), or Levinger and Varshavsky (1980). Five percent acrylamide, 1.2 mm thick minislabs

were used. In gels of types I, II or III (Todd and Garrard, 1977), the buffer was 6.7 mM Tris, 3.3 mM NaOAc, 0.3 mM EDTA, pH 7.2, and the bis- to acrylamide ratios were, respectively, either 1 to 20, 1 to 27, or 1 to 40. In gels of types IV, V, or VI (Levinger and Varshavsky, 1980), the bis- to acrylamide ratios were respectively as above, but the buffer was 10 mM HEPES, 0.5 mM EGTA, 0.5 mM EDTA, pH 7.5. Calibrants were as for the DNA gels, above. The gels were run at 10-30 V/cm, for 1-4 h at 4°C. Staining was by ethidium bromide.

For photographing Coomassie Blue- and silver-stained gels, a fluorescent light box gave back-illumination; for photographing ethidium bromide-stained gels, a long wave UV transilluminator served this purpose. Polaroid types 55 P/N or 108 film were used, always with a red filter. Negatives from the type 55 film were scanned on a Gilford 2520-Beckman DU densitomerer at $\lambda$ = 580 nm; relative band areas were obtained by cutting out and weighing paper traces.

E. Analytical centrifugation

Boundary sedimentation was done in a Beckman Model E analytical ultracentrifuge. Either 12 mm or 30 mm double sector cells were used, with nucleosome concentrations adjusted to give an absorbance at $\lambda$ = 265-286 nm of 0.2 - 1 in the scanner optical system. Centrifugation was at either 40,000 or 44,000 rpm. Runs were done at approximately room temperature; within each, the temperature varied by $<$ 0.1°C. Occasionally after a run, a sample was recovered and checked for degradation on one of the gel systems, above.

F. Data analysis

In analytical centrifugation, when slow and fast boundaries were

resolved in a run, we often calculated their relative proportions; in such calculations, we first corrected for their unequal radial dilutions (Svedberg and Pederson, 1940). To determine sedimentation coefficients we routinely did an integral distribution of S calculation (van Holde and Weischet, 1978), either by hand or with a Hewlett-Packard 9864A digitizer/9821A computer.

To correct centrifugation data to 20°C and water, standard density and viscosity tables were used (Svedberg and Pederson, 1940; Wishborn, 1928). For DNA in buffer D + 0, 0.5 or 0.75 M NaCl, respectively, we have used $\bar{v}$ = 0.499, 0.512, or 0.521 $cm^3/g$, obtained by interpolation from the data of Cohen and Eisenberg (1968). For nucleosomes in buffer D + NaCl concentrations up to 1 M we have used the empirical value $\bar{v}$ = 0.66 $cm^3/g$ (J. Ausio, D. Seyer and H. Eisenberg, personal communication; see also Eisenberg and Felsenfeld, 1981 and Olins _et al_., 1976).

Nonlinear data and linear data of respectively low scatter were fit to equations by least-squares methods. Linear data of high scatter (i.e. with relative standard deviations of > 5%) were fit by robust methods (see Launer and Wilkinson, 1979 for a general discussion of such methods); the fitting was done on a PDP-11 computer.

A note on our choice of techniques: we have used analytical centrifugation and particle gels to study dissociation because these techniques 'resolve' rather the 'average' information from different species in a mixture. With a 'resolving' technique, a sample having

a minor contaminent (such as mononucleosomes with a little free DNA, or with some dinucleosomes) will yield two separate, distinguishable signals. In contrast, with an 'averaging' technique (such as viscometry or some type of spectroscopy) the same sample will yield a single signal that is a weighted average from both the species of interest and the contaminent. The use of 'resolving' techniques allows us to subtract out the contaminent signals, during analysis. Thus we have been able to tolerate a contamination of our mononucleosomes by up to 5% dinucleomoes or 10% free DNA.

# IV. Results and Discussion

## A. Characterization of the nucleosomes

### 1. Distribution of DNA lengths

As described in the preceeding sections, our preparative method was designed to exclude specifically nucleosomes with DNA lengths less than 146 bp. Gel electrophoresis of the DNA from a typical preparation is shown in Figure 1A. In this example, the DNA ranges in size approximately from 160 to 230 bp. A more extensive nuclease digestion produces a downward shift of the size distribution; our strongest digestion gave a distribution ranging approximately from 160 to 200 bp, with a faint shoulder between 145 and 160 bp (not shown).

Figure 1B shows the exact distribution of DNA lengths for a sample from the same preparation as Figure 1A is from (cf. Materials and Methods). Note the complete absence of DNA smaller than 155 bp. Note also that the observed distribution is skewed toward larger DNA sizes, as might be expected for a mild nuclease digestion (Lohr et al., 1977). These general features are preserved with increasing extents of nucelase digestion, although the mean is shifted downward, and the standard deviation and high-end skew are decreased.

### 2. Absence of proteins other than core histones

After precipitation with KCl but before fractionation on sucrose gradients, the mono-, oligo- and polynucleosomes were exposed to 50 mM NaCl + 30 mg/ml Carboxymethyl Sephadex, to remove weakly bound cationic proteins. Figure 2A shows the proteins associated with this chromatin, before and after such a stripping step. Clearly this

Fig. II.1A. Gel electrophoresis of mononucleosomal DNA

DNA from mononucleosomes was run on a 3.5% acrylamide gel, stained with ethidium bromide and photographed, as in Materials and Methods. Lane 1: ~500 ng CfoI-cut pBR322, as marker. Fragment sizes: 393, 348, 337 + 332, 270, 259, 206, 190, 174, 153 + 152 + 151, 141, 132 + 131 bp. The 206 and 270 bp fragments run anomalously slowly on this gel, and on other gels of the same composition. Lane 2: ~500 ng mononucleosomal DNA. Lane 3: mixture of marker and mononucleosomal DNA. A different gel, showing lower background, was used for determining the distribution of DNA lengths.

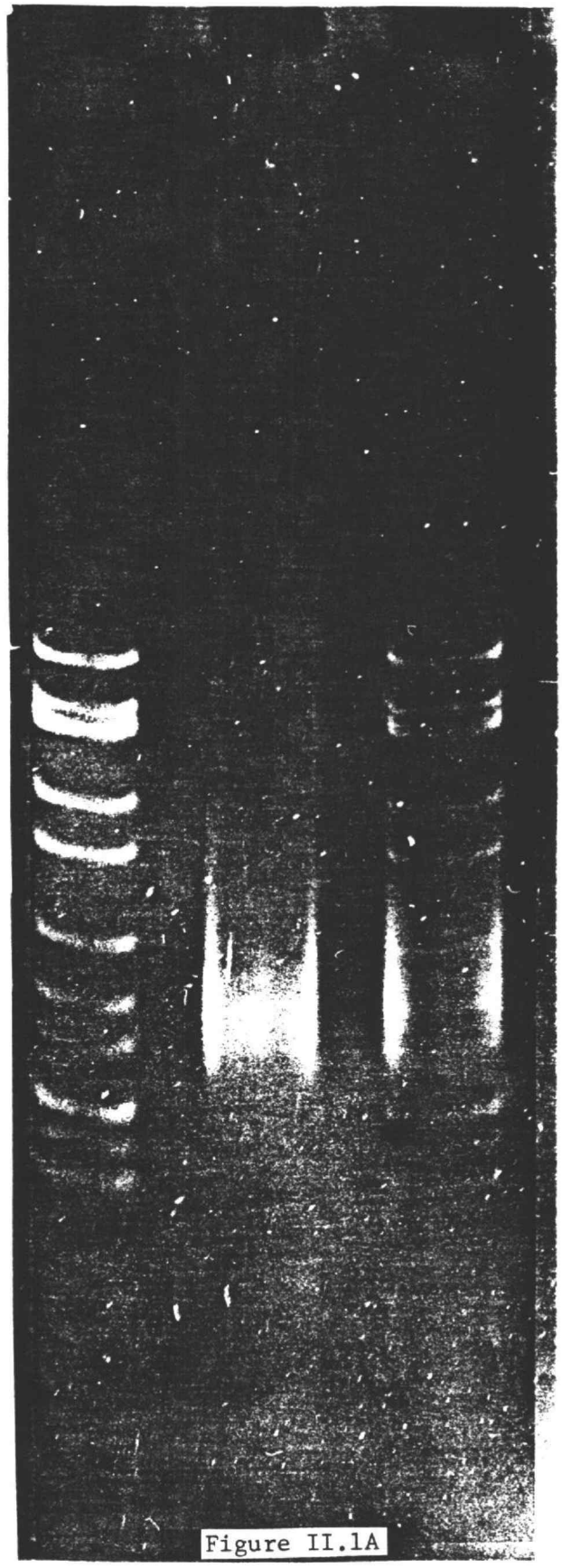

Figure II.1A

Fig. II.1B. Distribution of mononucleosomal DNA lengths

A negative of suitably low exposure and background was obtained from a gel similar to that of Figure 1A. The negative was then analyzed as in Materials and Methods; both sigmoidal ( o ) and linear ( ● ) response curves were used in the calibration of the detection system with restriction markers. Solid line: relative mole % versus fragment size. Dashed line: Gaussian curve, with $\bar{x}$ = 192 bp, $\sigma$ = 15 bp ($\Delta$ indicates 0.5 $\sigma$ deviations). The observed distribution is not Gaussian, for it begins abruptly at 155 bp, and is skewed high.

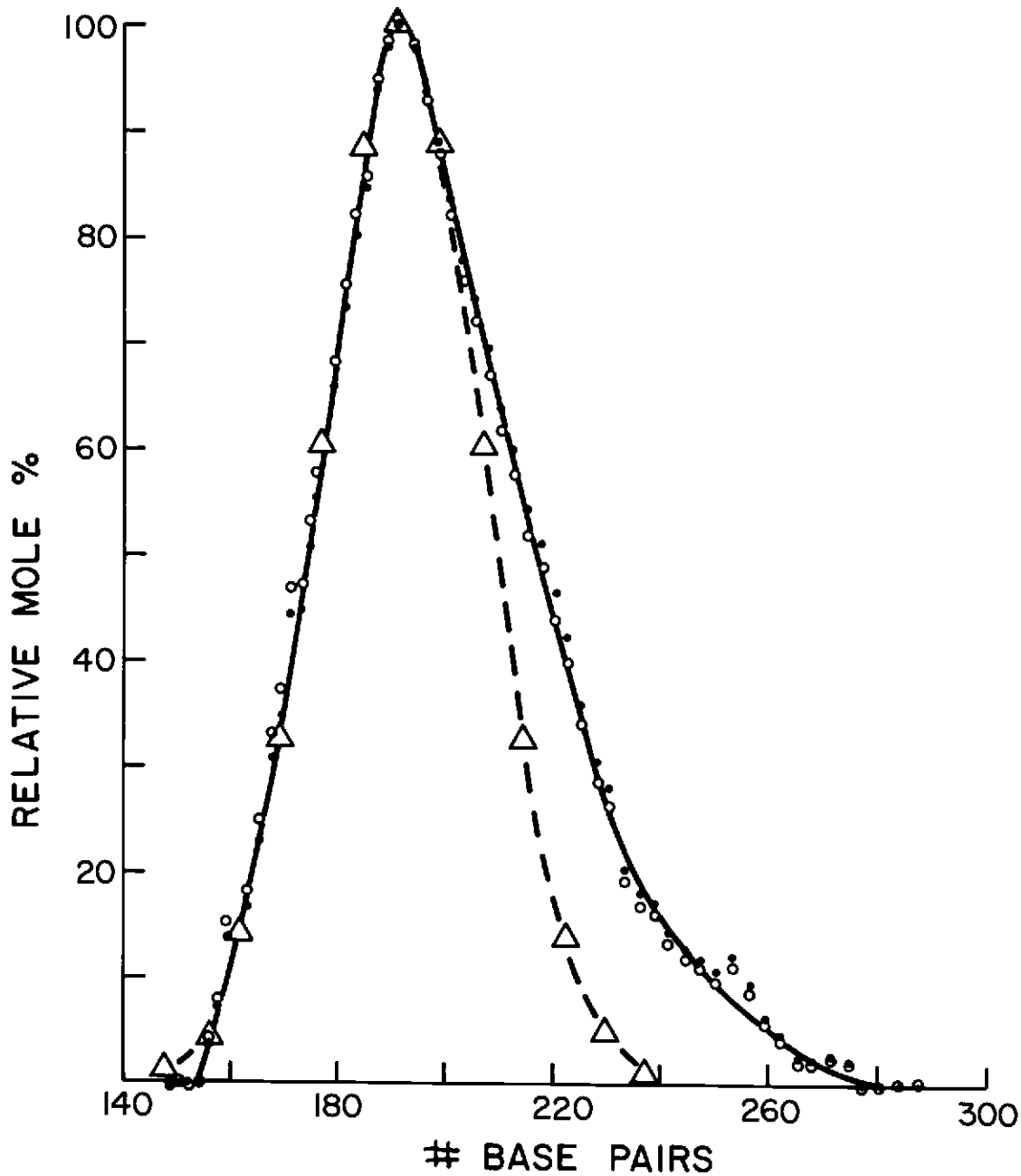


Figure II.1B

Fig. II.2A. Gel electrophoresis of chromatin proteins, with staining by coomassie blue

Chicken erythrocyte chromatin was prepared as in Materials and Methods, with the second nuclease digestion performed in 0.75 mM $Ca^{2+}$. After twice precipitating the chromatin with KCl, total protein from the pellet was prepared for SDS polyacrylamide gel electrophoresis as in Materials and Methods. Lanes 2, 3: ~1 μg total protein from chicken erythrocyte chromatin, before and after treatment with Carboxymethyl Sephadex/salt, respectively. Lane 1: ~2 μg histones from calf thymus chromatin, as a standard.

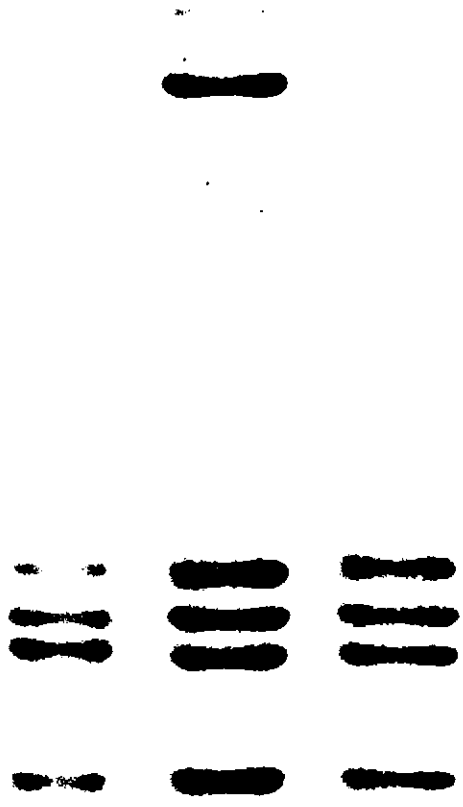

Figure II.2A

treatment removes virtually all the H1 and H5.

In order to detect any remaining traces of these and other unwanted proteins, the same gel was restained with a more sensitive silver-based stain. Figure 2B shows that, in addition to H1 and H5, other non-core proteins were present before stripping; after such treatment, virtually only the core histones remain.

We have eluted the resin-bound proteins with 2 M NaCl, and examined them by gel electrophoresis (not shown). Besides H1, H5 and various non-histone proteins (including about thirty at levels too low to see in Figure 2), we found trace amounts of the core histones. From comparing the amount of core histone bound by the resin to the total amount passed into it in the form of chromatin, we estimate that < 1% of our nucleosomes are disrupted in the stripping step. To corroborate this, we examined on a particle gel the eluent from the resin (not shown). We found that < 1% of all the mononucleosome-sized DNA ran free, while the remaining > 99% was bound up in mononucleosomes. We conclude that Carboxymethyl Sephadex causes only a slight loss of core histones, while removing all non-core proteins to barely detectable levels.

3. Nucleosomes with crosslinked histone cores

For some experiments the histone core of our nucleosomes was crosslinked with DMS. We have examined the extent and homogeneity of crosslinking by electrophoresis of the crosslinked histone octamer on 6% gels. Figure 3 shows a plot of log (M) versus relative mobility for intermediates in the crosslinking reaction, and also for the external calibrants BSA (M = 64,000), phosphorylase b (M = 92,500),

Fig. II.2B. Gel electrophoresis of chromatin proteins, with staining by silver

The gel of Figure 2A was restained with silver to detect trace proteins (Wray *et al.*, 1981). The lanes are defined as in the legend of Figure 2A. When loadings are increased to about 5 μg/lane, we begin to see H1, H5 and other contaminants in the 'stripped' lane (not shown).

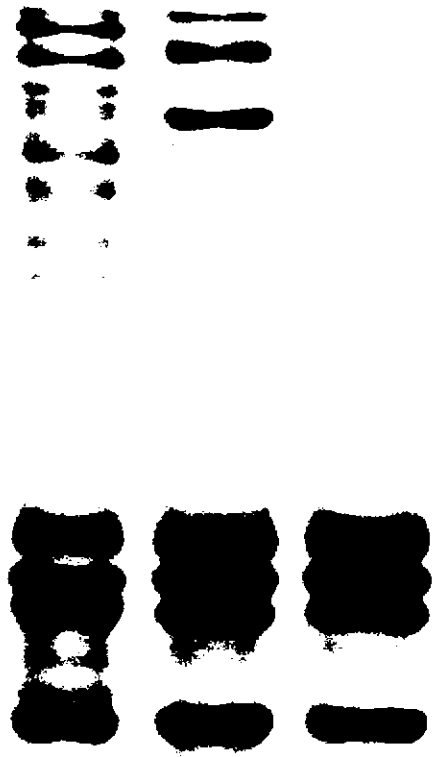

Figure II.2B

Fig. II.3. SDS gel electrophoresis of the crosslinked histone core

Mononucleosomes were crosslinked with DMS, and ~10 μg core protein prepared and run on a 6% acrylamide gel, along with the standards BSA, phosphorylase b and O. dofleini hemocyanin. Staining was with Coomassie blue. Relative migration distance versus ln(M) was measured, and fit to a line by least-squares analysis. Open circles: intermediates in the crosslinking reaction (4-8 mers). Closed circles: molecular weight standards.

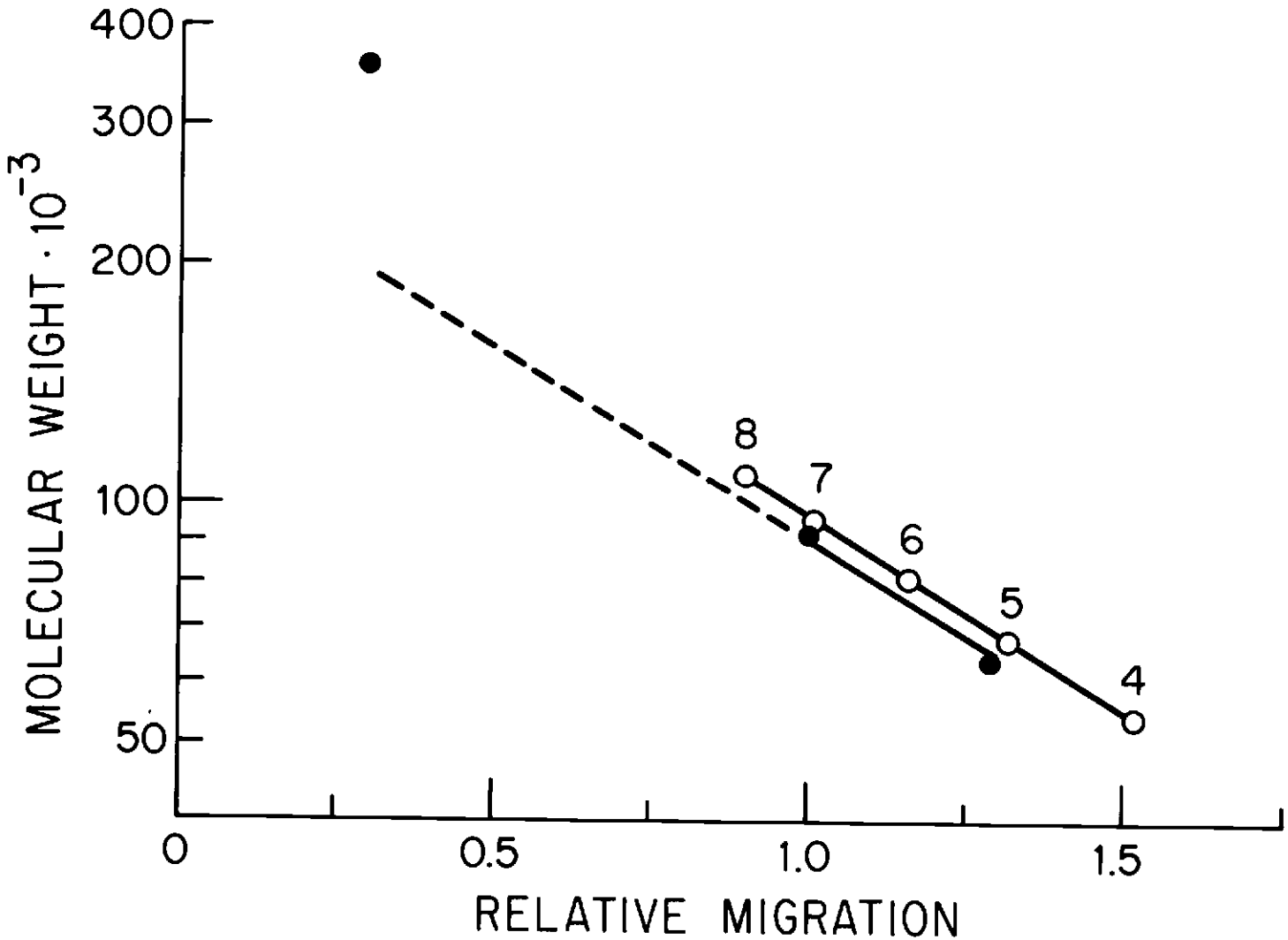
400
300
200
100
50
MOLECULAR WEIGHT · $10^{-3}$
8
7
6
5
4
0
0.5
1.0
1.5
RELATIVE MIGRATION

Figure II.3

and Octopus dofleini hemocyanin [M = 359,000 (Miller and van Holde, 1982)]. BSA and phosphorylase b have been observed to fall on a straight line, together with the proteins β-galactosidase (M = 116,000) and RNA polymerase (β + β' subunits; M = 160,000), for a gel of this buffer composition, acrylamide percentage, and bis- to acrylamide ratio (Miles Laboratories, 1980). The straight line for the intermediates is parallel to but offset from that through the external calibrants, reflecting the former's anomalous mobility on this type of gel. Even after the crosslinking reaction has proceeded to completion, the octameric band remains considerably broader than diffusion alone can account for (not shown). We interpret this to mean that the reaction has produced a population of octamers heterogeneous with respect to crosslinking sites.

In all studies involving crosslinked nucleosomes, we used only those samples which showed < 5% silver-staining material migrating below the octamer band in 6% and 12% gels.

B. Dissociation of nucleosomes in salt

1. Moderate salt leads to the reversible generation of a slowly sedimenting species

We have jumped the nucleosomes described above to concentrations of salt between 0.2 and 1 M. In the analytical ultracentrifuge we see a new, second boundary, moving considerably more slowly than the 10.5 S observed for structurally unaltered nucleosomes. After the jump, the amount of slowly sedimenting material increases with time, until finally it reaches a stable maximum. The process of increase takes less than 90 min in 1 M salt, but about 25 hours in 0.5 M or 0.75 M salt (cf. Figure 4B).

Figure 4A shows scans at $\lambda$ = 265 nm for nucleosomes either left in 0 M salt or jumped to 0.5 or 1 M salt. These scans were all made after the slow boundary had ceased to increase. In preparations originating from sucrose gradients run in 50 mM salt, we observed a small amount of the slow component in 0 M salt. This finding correlates with past observations (Lilley et al., 1979; Wilhelm and Wilhelm, 1980; Lee et al., 1982; Harrington, 1982) of apparent free DNA in low-salt ($I \leq 60$ mM) preparations of core particles. We discuss this further below.

In order to learn whether this destabilization of nucleosomes by salt could be reversed, we conducted the following experiment. Nucleosomes in buffer D were either left in 0 M salt or were jumped to 0.75 M salt and were incubated 32 h at 20 ± 3°C. (This length of time was necessary to insure that dissociation had ceased). In the two samples, the nucleosome concentrations were identical. Both samples were then brought to 0.5 M salt and lower (identical) nucleosome concentrations, by adding buffer D with or without salt.

Figure 4B shows how the percentage of slow boundary in the two samples changes with time. After the second jump (to 0.5 M salt), the two samples approach the same extent of dissociation; we consider this to be evidence that the generation of the slow boundary is a reversible process. At the end of the experiment, the two samples remain different in extent of dissociation by about half the amount that either of them has changed following the jump to 0.5 M salt. We believe the samples did not ultimately reach exactly the same state because of some competing process - very likely histone aggregation

Fig. II.4A. Sedimentation of mononucleosomes in moderate salt

The analytical ultracentrifuge was used to examine mononucleosomes in buffer D (top), buffer D + 0.5 M salt (middle), or buffer D + 1 M salt (bottom). These scans were taken ~1.5 h after 44,000 rpm rotor speed was attained.

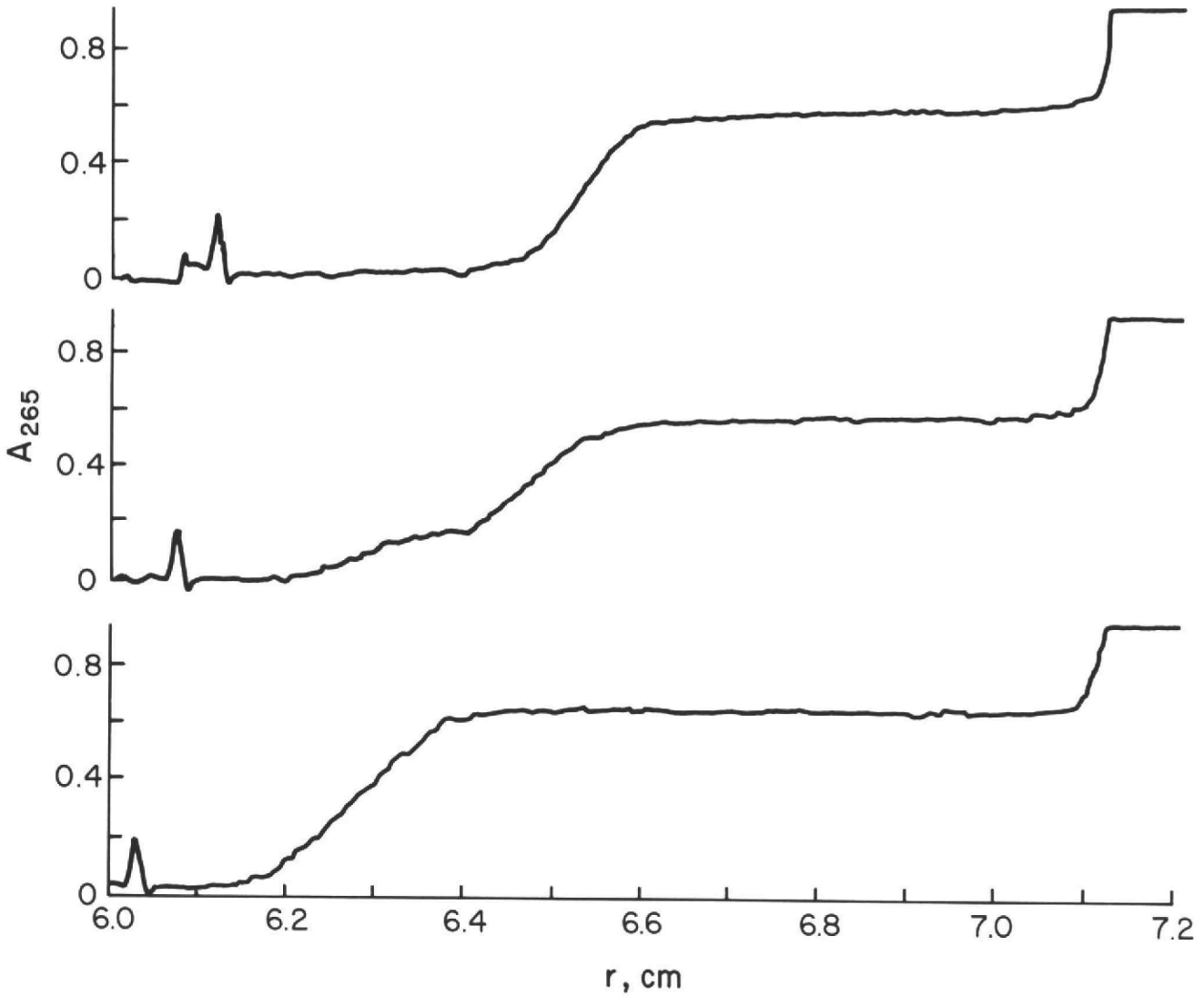


Figure II.4A

Fig. II.4B. Nucleosomes approach the same state, if jumped to the same salt concentration from different directions

Mononucleosomes in buffer D were either left at 0 M salt or were jumped to 0.75 M salt, by adding buffer D ± 5 M salt with stirring. The two samples were at identical nucleosome concentrations. After a brief centrifugation to remove any aggregated material, they were placed into incubation at 20 ± 3°C (time 'I' on figure). Incubation continued for 32 h. Aliquots were then examined in the analytical ultracentrifuge, and the percent of slow boundary determined for each. The samples were then both shifted to 0.5 M salt, by adding D ± 1.5 M salt with stirring. They again were at identical nucleosome concentrations, although more dilute than before. After another brief centrifugation to remove any aggregated material, the samples were incubate at 20 ± 3°C (time 'II' of figure). Periodically, aliquots were removed and examined in the analytical ultracentrifuge, and the percent of slow boundary determined for each.

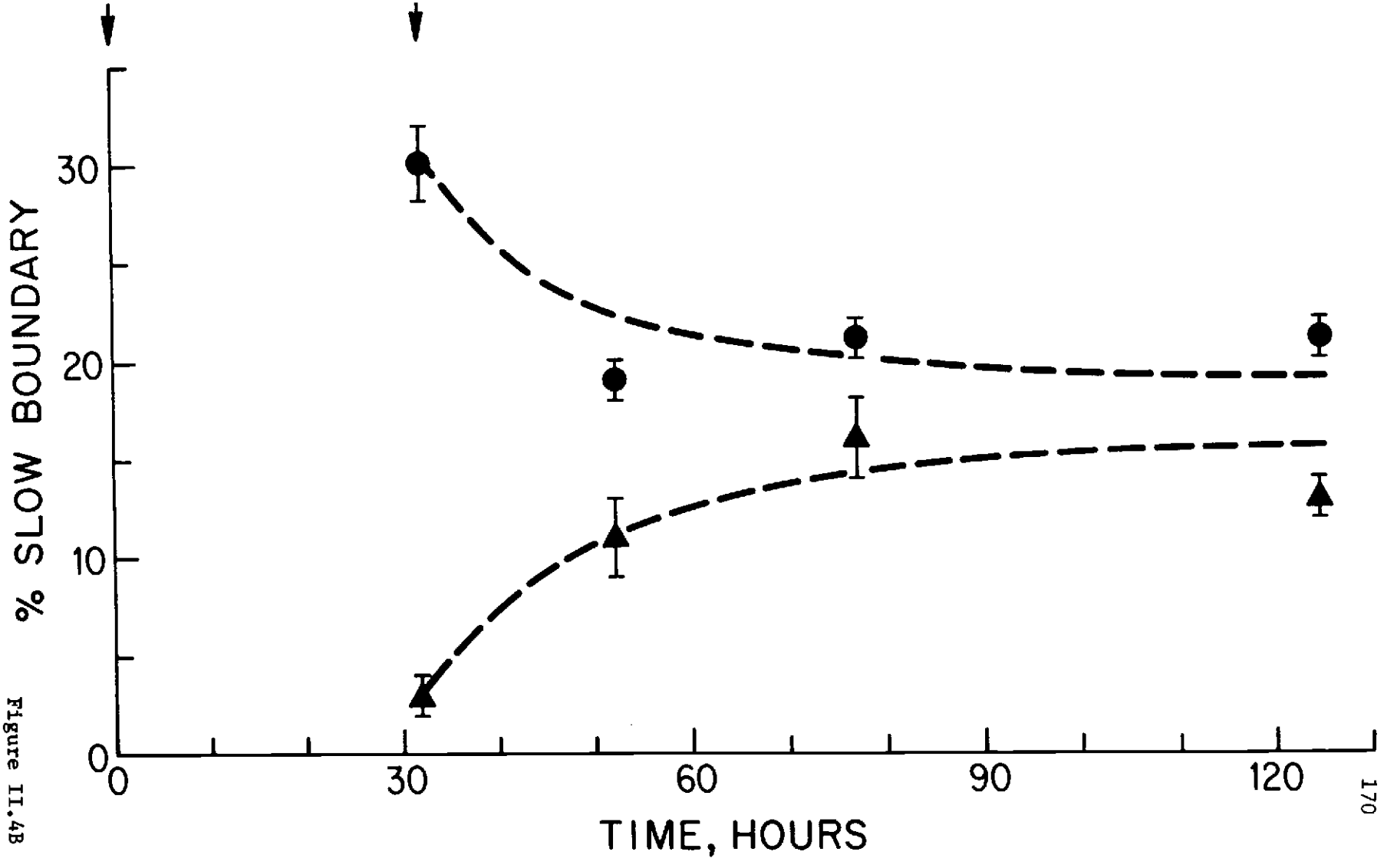


Figure II.4B

in high salt (Harrington, 1982; Tatchell and van Holde, 1977; Tatchell and van Holde, 1979).

2. In moderate salt, nucleosomes dissociate to yield free DNA

If we can show without ambiguity that the slow boundary in the analytical centrifuge is free DNA, rather than some unfolded form of nucleosome, then we may conclude that salt causes nucleosomes to dissociate. There are five pieces of evidence for this.

First, when non-crosslinked nucleosomes are jumped to 0.6 M NaCl and centrifuged through a sucrose gradient containing 0.6 M NaCl, a fast and a slow band are generated. When we isolate and examine the slow band, we find DNA in appreciable quantity, but histones in only trace amounts, and then not in the correct ratios for an intact nucleosome (not shown).

Second, when a non-crosslinked sample is jumped to 0.6 M NaCl in buffer D, incubated for ~24 hours at room temperature and then analyzed on a particle gel we see, in addition to the upper nucleosome band, a lower band which moves at the correct rate for free DNA (Figure 5A).

To obtain the third piece of evidence that the slow boundary in analytical centrifugation is free DNA, we have calculated the integral distribution of $s_{20,w}$ (van Holde and Weischet, 1978) of scans such as those shown in Figure 4A. Figure 5B shows the results of our analysis for non-crosslinked nucleosomes at 0, 0.5, and 0.75 and 1 M NaCl, and also for free DNA purified from our nucleosomes and examined under these conditions. As usual, we discount the upper and lower

Fig. II.5A. Particle gel analysis of mononucleosomes in 0.6 M salt

Mononucleosomes in buffer D were jumped to 0.6 M salt and incubated ~24 hours at room temperature. They were then analyzed on a particle gel. Staining was with ethidium bromide. Lane 1: mononucleosomes, plus free DNA due to dissociation. Note a bit of dinucleosome contamination. Lane 2: DNA purified from mononucleosomes, and jumped to 0.6 M salt. Note contamination by dinucleosomal DNA. Lane 3: same as lane 1, but mixed with CfoI-cut pBR322. Lane 4: CfoI-cut pBR322.

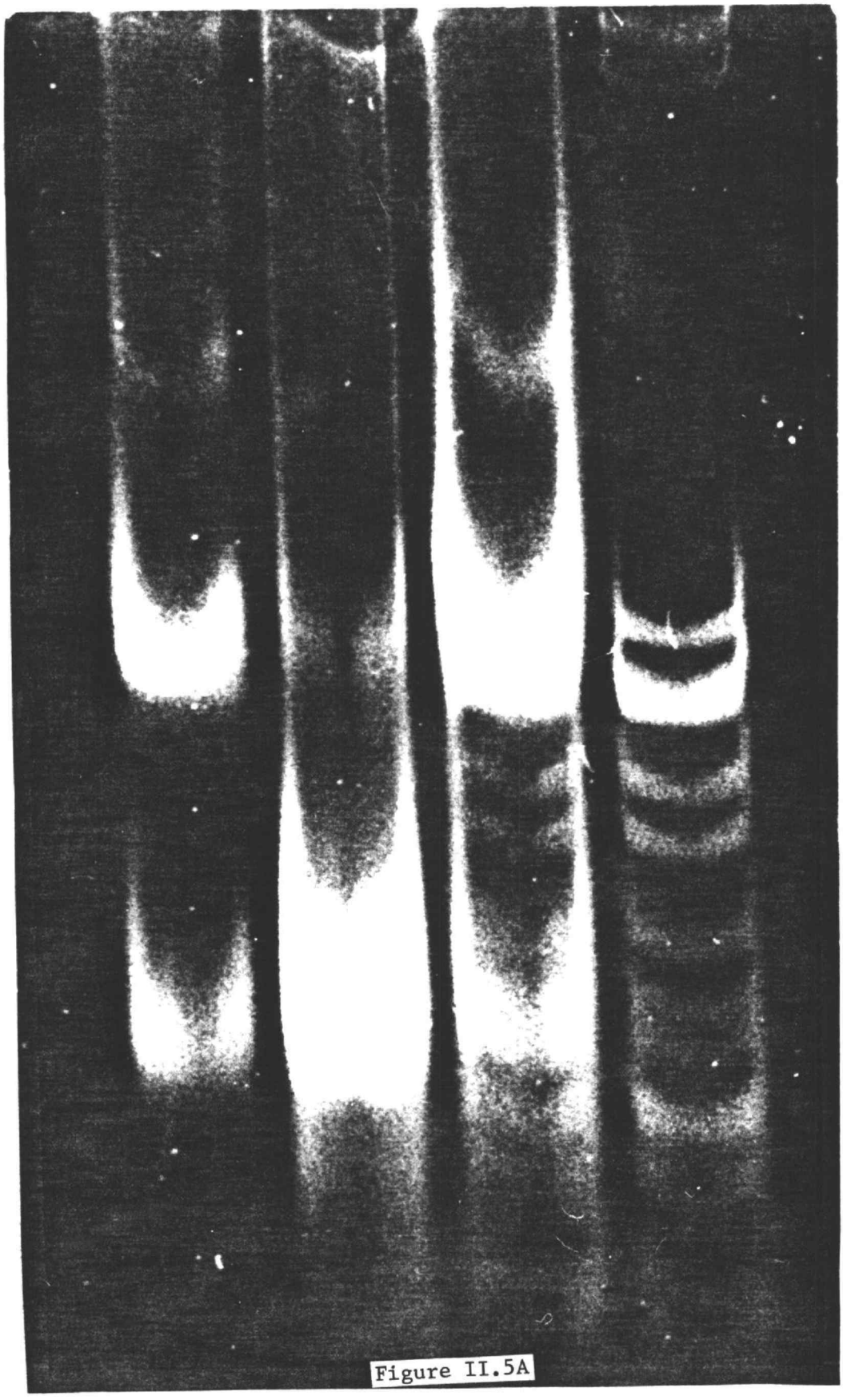

Figure II.5A

Fig. II.5B. Integral distribution of S, for nucleosomes or DNA in salt

Mononucleosomes or DNA, in either buffer D, or buffer D plus salt, were incubated at 20 ± 3°C until an equilibrium amount of slow boundary material was generated. The samples were then examined in the analytical ultracentrifuge. For each, the integral distribution of $s_{20,w}$ was calculated from a series of scanner traces, as described in Materials and Methods. ○ ,-----: nucleosomes in 0 M salt; □ : nucleosomes in 0.5 M salt; Δ: nucleosomes in 0.75 M salt. Not shown: nucleosomes in 1 M salt; the distribution is heterogeneous, ranging from 5.5 to 8.5 S. ● : DNA in 1 M salt. Not shown: DNA in 0.5 or 0.75 M salt; the former's distribution is identical to that of DNA in 1 M salt, while the latter's, still homogeneous, falls 0 - 0.5 Svedberg higher.

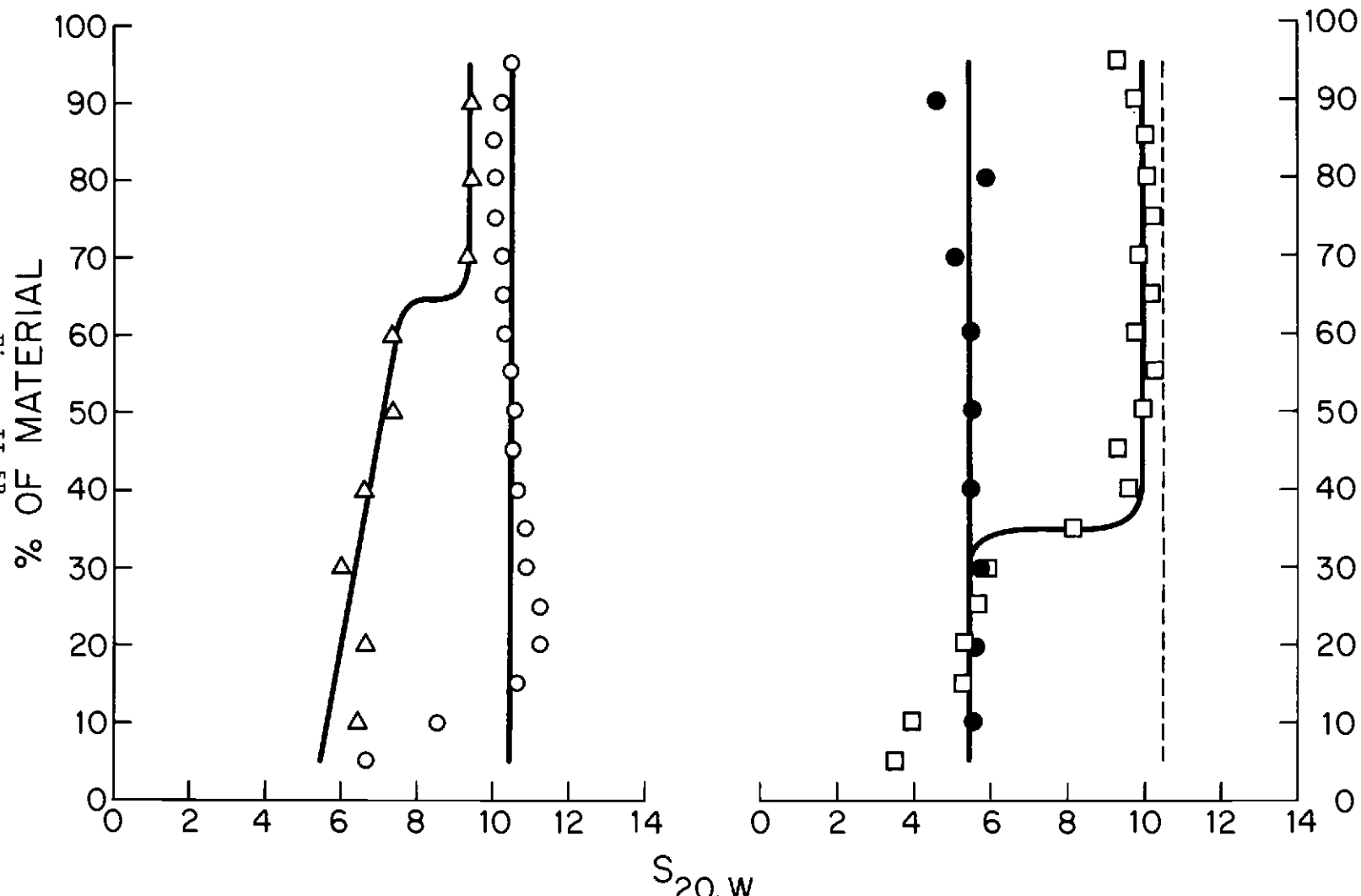


Figure II.5B

10th percentiles of the integral distribution, since these regions of the graph contain large errors. We find that in 0.5 M NaCl, the slow boundary sediments homogeneously, and at the same rate as purified DNA. Note, however, that as the salt is raised to and above 0.75 M, the slow boundary begins to sediment faster than free DNA, and homogeneity is lost. We believe that this reflects, at these higher concentrations of salt, a nonspecific association of histones with the DNA released in dissociation.

As a fourth argument that the slowly sedimenting boundary is due to dissociation (as opposed to unfolding), it seems reasonable to suppose that unfolding requires a large conformational change in the histone core. Thus it should not occur when the core is crosslinked. However, we observe both the slow centrifuge boundary and the rapidly migrating band on a particle gel even when the core is crosslinked (not shown).

Our fifth and final argument for free DNA comes from kinetics. Both folding and unfolding processes should be unimolecular; thus, the degree of unfolding should not depend on nucleosome concentration. In contrast, we expect nucleosome dissociation to be unimolecular, but reassociation to be at least a bimolecular reaction; thus, if a reversible dissociation occurs, it should be enhanced by nucleosome dilution. From this reasoning, if the slow boundary in analytical centrifugation is due to unfolded nucleosomes, we expect no dilution effect; however, if it is due to free DNA, we expect it to increase with nucleosome dilution.

Figure 5C shows the joint effect of salt and nucleosome concentration on the generation of the slow boundary material, for non-crosslinked nucleosomes. Each bar on this graph is the average of 4-7 scans from a single centrifuge run. Each run was made long enough after salt addition that the proportion of material in the slow boundary had ceased to increase. Some uncertainty in the data remains even after subtracting contributions to the scans by a slight dinucleosome contaminant (see Materials and Methods). This uncertainty arises because we are not always able to clearly resolve slow and fast boundaries. There are several causes for this inability. (i) In 0.5 and, to a larger extent, in 0.75 M salt, there is a decrease in the sedimentation coefficient of the fast boundary (cf. Figure 5B, and discussion below). (ii) In 0.75 M salt, the slow boundary is not homogeneous, but spans 5.5 - 9.5 S (cf. Figure 5B). (iii) At the highest salt concentrations, where dissociation is probably more rapid, there may be some interconversion between species. This uncertainty, however, does not obscure the main conclusion: A dilution effect, 2-3 times larger than experimental error, occurs in both 0.5 and 0.75 M NaCl. We have not attempted to calculate "equilibrium constants" for the dissociation process, since we do not know the aggregation states of the histones which have dissociated (see below).

From the five experiments described above, we are convinced that the slow boundary observed in analytical centrifugation at salt concentrations of 0.5 M and below is free DNA, and thus that moderate salt concentrations cause nucleosomes to dissociate. At > 0.75 M

Fig. II.5C. Dissociation of nucleosomes is enhanced by their dilution

Mononucleosomes in buffer D were diluted into buffer D ± salt, to give final nucleosome concentrations of 430, 215 or 66 nM ($A_{260}$ = 1, 0.5 or 0.15 respectively), and final salt concentrations of 0, 0.5 or 0.75 M (nine combinations). After a brief centrifugation to remove any aggregated material, the samples were incubated at 20 ± 3°C for 30-31 h, and were then examined in the analytical ultracentrifuge. Always, the three samples at a particular salt concentration were run together in the same rotor. To the most dilute sample in 0 M salt, 0.5% sucrose by weight (~15 mM) was added immediately before the run, to stabilize the sedimenting boundary against turbulence. 30 mm cells were used. Scans were made at λ = 265 - 286 nm, with the wavelength adjusted to give a total absorbance of 0.3 - 1. For each sample, a set of 4-7 values for the percent of slow boundary was obtained from a series of scanner traces. The values were corrected for radial dilution, and then averaged.

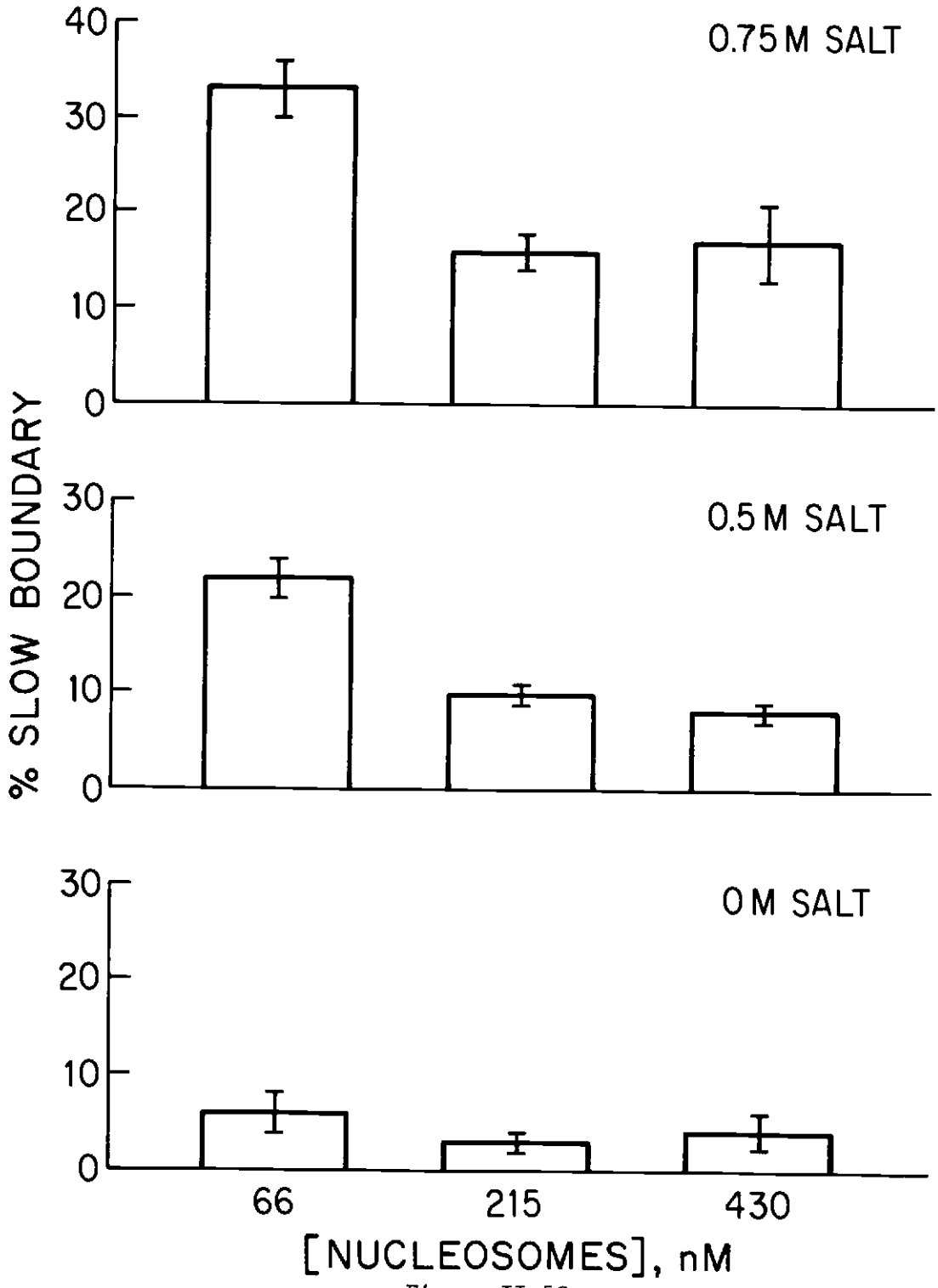
0.75 M SALT
0.5 M SALT
0 M SALT
% SLOW BOUNDARY
40
30
20
10
0
66
215
430
[NUCLEOSOMES], nM

Figure II.5C

salt, the DNA from dissociation seems to bind the released histones nonspecifically.

Our nucleosomes are still heterogenous in several ways [most obviously in DNA length (cf. Figure 1)]. Thus, conceivably, the dissociation we observe in moderate salt could be occurring in just a nucleosome subpopulation. In order to see if nucleosome stability varied with DNA length, we incubated nucleosomes in buffer D + 0.6 M salt for ~24 hours at room temperature, and then ran them on a particle gel, along with whole DNA purified from intact nucleosomes. We then compared the distribution of lengths of the free DNA from the particles with the distribution of the whole DNA. No difference was evident (Figure 5A and less heavily loaded gels, not shown). Thus we believe that mononucleosome dissociation is not strongly biased toward any particular DNA length in our sample.

3. Dissociation in low salt

It is striking that our nucleosome preparations sometimes contained up to 10% free DNA (not shown). The existence of this free DNA seemed to be correlated with the presence of 50 mM NaCl in our sucrose gradient purification step. Such free DNA has also been observed by others, in low-salt preparations of core particles (Lilley et al., 1979; Wilhelm and Wilhelm, 1980; Lee et al., 1982; Harrington, 1982).

In a sample of nucleosomes which had been removed from a 50 mM NaCl sucrose gradient, the amount of free DNA did not change as the nucleosome concentration was subsequently varied between 40 and

200 nm (in buffer D + 0 mM salt). Thus we do not believe this DNA to have resulted from a reversible dissociation of the type observed at higher salt concentrations. We believe instead that the DNA was generated from nucleosomes by some irreversible process, which occurred in our preparative procedure at one or more of the following stages: (i) before purification on sucrose gradients; (ii) during the sucrose gradient purification step; (iii) in subsequent storage in the sucrose gradient buffer; (iv) during electrophoresis or analytical ultracentrifugation.

In later experiments, we have taken samples of nucleosomes from a 0 mM NaCl sucrose gradient and examined them immediately, by both particle gel electrophoresis and analytical ultracentrifugation. In such cases, we see neither the slow centrifuge boundary, nor the DNA band on the particle gel (cf. Figures 4A, 5C, 5D). We conclude: (i) that if a nucleosome sample is intact to begin with, low salt electrophoresis or analytical ultracentrifugation alone is not enough to generate the free DNA; and (ii) that the free DNA which we have on occasion observed must arise during dilution into and centrifugation through sucrose gradients in 50 mM salt.

Given that stage (ii) of our protocol generates free DNA as an artifact, we next attempted to learn whether free DNA is generated also in stage (iii). Thus we have transferred nucleosomes from sucrose gradients in 0 M salt to buffer D + 0, 10, 25, 50, 75 or 100 mM salt, incubated them at 6°C at a nucleosome concentration of 260 nM, and then periodically examined them on particle gels.

We observe a small increase in free DNA with time, at a salt concentration as low as 25 mM, and possibly even as low as 10 mM (Figure 5D Thus free DNA probably always is generated during storage in low concentrations of salt, if sufficient time elapses. This finding has been reported previously for core particles at somewhat higher ionic strength (Burton et al., 1978). The striking observation of free DNA in salt as low as 10 mM argues that storage of nucleosomes in buffers containing any salt should be avoided. We note that, in this experiment, the mononucleosome population consisted roughly of 80-90% nucleosomes with long DNA, and 10-20% core particles. We observe in Figure 5D no significant difference in stability between the two types of particles. This finding does not agree with what has been reported previously (Lilley et al., 1979), for unknown reasons.

We now inquire into the nature of the irreversible process generating the free DNA in stages (ii) and (iii) of our protocol. We favor the following hypothesis: when diluted into gradients in 50 mM salt, a small fraction of the nucleosomes dissociate into free DNA and histones. The histones then either remain separate from each other very near the top of the gradient, or aggregate and sediment to the bottom. At the same time, the free DNA moves some distance into the gradient (at least partially into the mononucleosome peak), thus becoming separated from the histones. The mononucleosomes from the gradient thus become contaminated with excess free DNA, but not with

Fig. II.5D. Free DNA from Nucleosomes, in Low Salt: Particle gel

Nucleosomes in buffer D were either left at 0 M salt or were jumped to 10, 25, 50, 75 or 100 mM salt, by adding buffer D +- 1.6 M salt with stirring. All samples were at the same nucleosome concentration. After a brief centrifugation to remove any aggregated material, they were incubated at 6 C. Periodically, equal aliquits were removed and run of a particle gel of Type I. The gel was stained with ethidium bromide and photographed.

Lanes 1-6: material incubated for 6 days, in buffer D + 0, 10, 25, 50, 75 or 100 mM salt, respectively. Lane 7: CfoI-cut pBR322. Lane 8: purified mononucleosomal DNA. The film has been overexposed to bring out the free DNA bands.

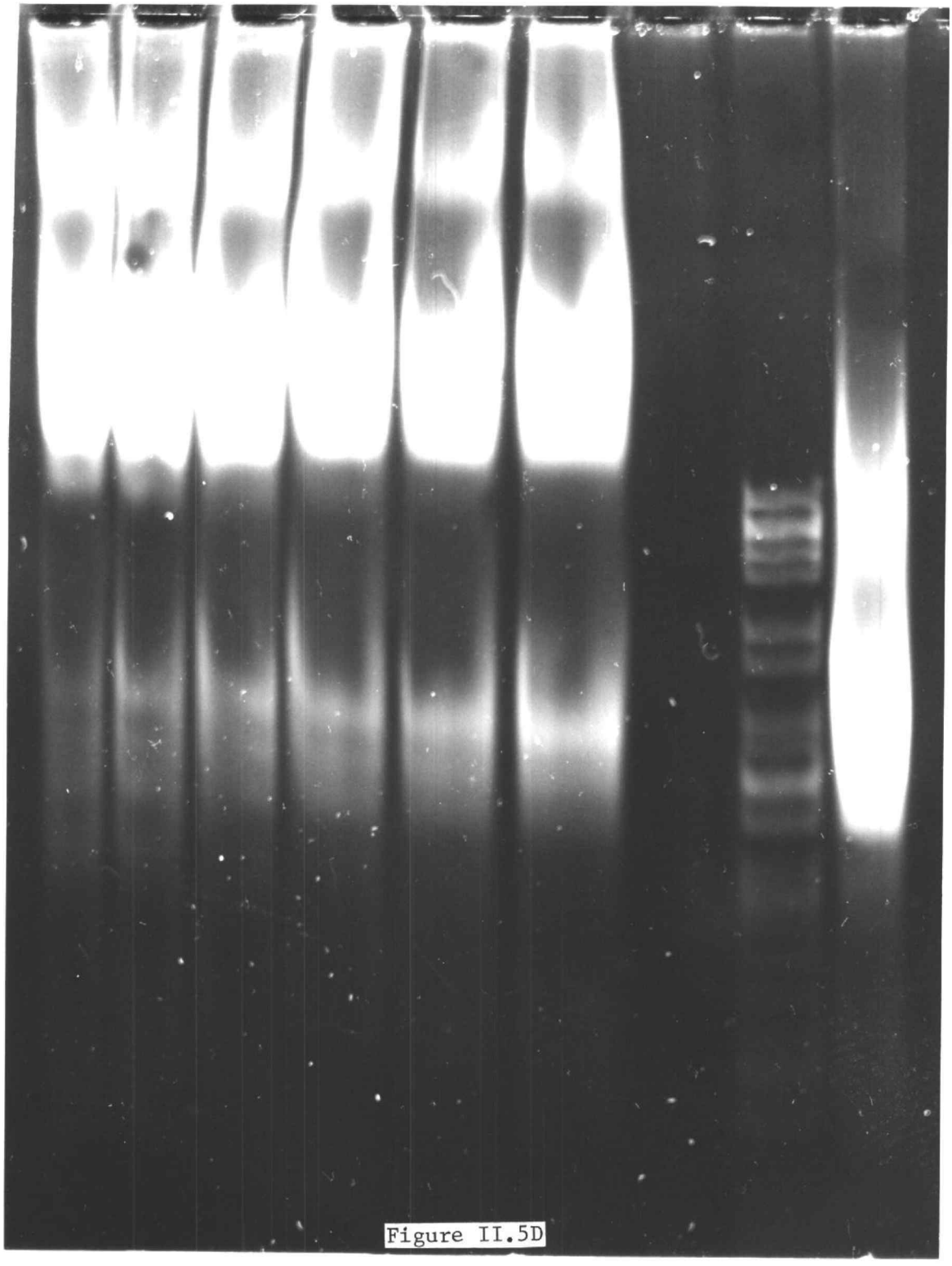

Figure II.5D

Fig. II.5E. Free DNA from Nucleosomes, in Low Salt: Scan of Particle Gel

The film negative from Figure 5D was scanned. Since the film negative has been overexposed, the scans are non quantitative.

(I) top of gel; (II) dinucleosomes; (III) mononucleosomes; (IV) core particles; (V) DNA from mononucleosomes; (VI) DNA from core particles. The spike near peak VI in 25 mM salt is due to a defect in the film negative.

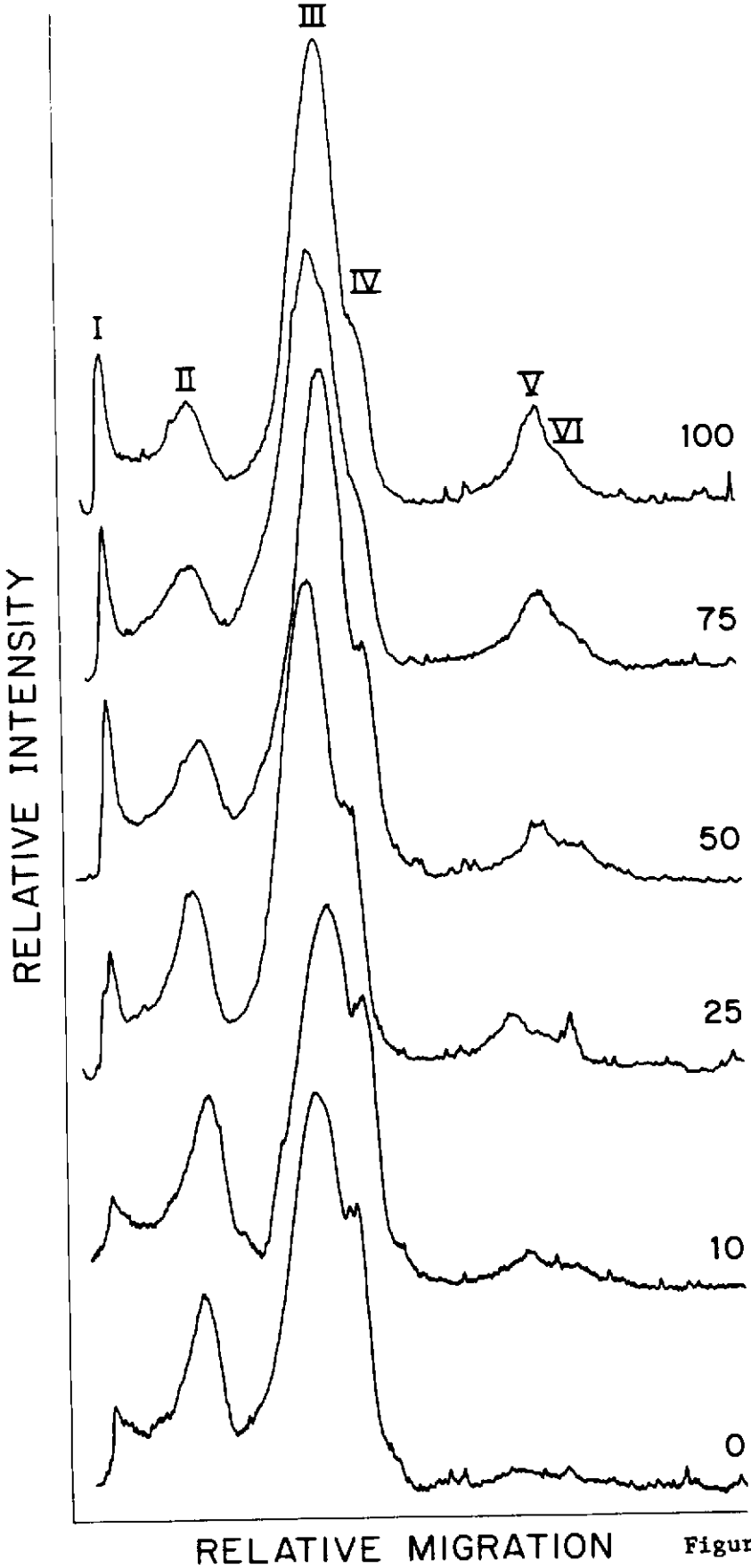
III
IV
I
II
V
VI
100
75
50
25
10
0
RELATIVE INTENSITY
RELATIVE MIGRATION

Figure II.5E

excess histones. Since the excess DNA in the mononucleosomal fraction has no histones to bind to, its continued presence is independent of subsequent dilution or concentration of the sample. More nucleosome dissociation then ocurs during storage. This secondary dissociation might be reversible; it might instead be irreversible, driven by aggregation or adsorption of the released histones to the container walls.

One might attempt to explain the presence of free DNA in nucleosome samples with an alternate hypothesis; that pairs of nucleosomes can interact in the presence of salt, each pair producing one free DNA molecule and a nucleosome bound to the second histone octamer (Stein, 1979).

If this occurred as an equilibrium process in the sucrose gradient, we would expect the free DNA, nucleosome, and nucleosome/octamer peaks to be smeared together (due to rapid interconversion of the species). In the mononucleosomal fractions from the gradient, free DNA and nucleosome/octamer complexes would thus be present in roughly equimolar amounts. Their stoichiometries being equal, we would expect to see the percentage of free DNA decrease back to zero as the salt is subsequently lowered from 50 mM to 0 mM. This, however, is never seen, even after incubation in 0 mM salt for as long as several weeks (not shown).

If the free DNA arose instead through an irreversible binding of a histone octamer to a nucleosome, we would expect to always see, in proportion to the amount of free DNA present, (i) a discrete boundary sedimenting faster than 10.5 S, in the analytical centrifuge; and

(ii) in addition to the nucleosome band in a particle gel, another, more slowly migrating nucleoprotein band. However, with samples of sufficient purity (i.e. completely free of contamination by di- and oligonucleosomes), we see neither (i) (Figure 5B), nor (ii) (not shown). We therefore do not believe nucleosome/histone octamer binding to be the source of the free DNA.

4. Crosslinking of the histone core with dimethyl suberimidate changes the salt-dependence of nucleosome dissociation

As the salt is raised and the nucleosome dissociates, a number of histone-histone equilibria also become involved. Therefore it would be simplistic to assume an equilibrium between DNA and only a single histone species (e.g. the core octamer). Crosslinking the histone core should eliminate virtually all histone-histone equilibria; thus equilibrium constants obtained with crosslinked nucleosomes would have an unambiguous structural meaning.

A fundamental assumption of the crosslinking approach is that, in dissociation from the DNA, the native and crosslinked cores behave exactly alike. That is, the precise pattern of electrostatic bonding between the DNA and the histone core is assumed to be unaffected by crosslinking. This assumption immediately becomes suspect when one recalls that crosslinking modifies up to 80% of the core histone lysines (Stein et al; 1977), quite possibly including some involved in binding DNA.

We observe, in fact, two pronounced differences between the behavior of native and DMS-crosslinked nucleosomes. (i) Whereas at salt concentrations in the range 50-100 mM, $<$ 10% of a native

nucleosome preparation is dissociated, about 30% of an equally concentrated crosslinked preparation is dissociated (not shown). (ii) At salt concentrations above 100 mM, the dissociation of the crosslinked particles is much less sensitive to a further increase in salt (not shown). Both observations are consistent with the hypothesis that crosslinking with DMS destabilizes the nucleosome by decreasing the number of electrostatic bonds between the DNA and the histone core. Similar observations have been reported for core particles in lithium chloride, by Vassilev et al. (1981). Thus, the hope of simplifying the analysis of DNA-core interactions by crosslinking the histones with DMS must remain unrealized.

C. Nucleosome unfolding: does it occur?

From all the above data and arguments, we conclude that salt causes nucleosomes to dissociate. We turn now to the possibility that, in salt, unfolding occurs as well.

If a nucleosome were to unfold, it could either retain all its histones during the process, or could selectively lose a certain subset of them. To determine which of these two possibilities actually occurs, we have centrifuged nucleosomes through a sucrose gradient in 0.6 M NaCl, obtaining a fast and slow band. As mentioned above, the slow band contains only DNA. We assume that 0.6 M is a high enough concentration of salt to push a putative unfolding process virtually to completion (Bode and Wagner, 1980; Bode et al., 1980; Zama et al., 1977; Dietrich et al., 1977; Dietrich et al., 1979; Whitlock, 1979; Wilhelm and Wilhelm, 1980; Zayetz et al., 1981) thus nearly all the nucleosomes in the fast gradient band should be unfolded, with very

few still in the native state. We find that the fast band contains DNA, and also the four inner histones in the correct ratios for an intact nucleosome (not shown). That is, none of the histone bands on our gels are reduced to half their expected intensity (which would indicate loss of one copy of the particular histone, per nucleosome), or to zero intensity (indicating loss of both copies). We are thus led to conclude from our data that if a nucleosome unfolds, it cannot suffer stoichimetrically unequal losses of the four histones. This is consistent with the same sucrose gradient experiment done on core particles (Wilhelm and Wilhelm, 1980), and also with the observation that core particles, after being incubated in 0.6 M salt and then run on a particle gel, retain the four histones in equal ratios (Zayetz et al., 1981). We note that neither our experiment nor those of Wilhelm and Wilhelm (1980) or Zayetz et al. (1981) could detect the loss, per nucleosome, of exactly one copy of each of the histones. However, if such massive loss ocurred we would expect a large decrease in $s_{20,w}$ of the fast boundary in the analytical ultracentrifuge, which we do not see. Thus it is reasonable to conclude that unfolding, if it occurs, does not involve any histone loss.

Reports concerning the unfolding of nucleosomes in high salt have been somewhat contradictory. Nucleosomes with long DNA and associated proteins have been reported to change only very little in sedimentation coefficient ($\sim$5%) between 0 and 0.7 M (Russev et al., 1980), whereas comparable studies with core particles have claimed between 12 and 17% decrease in $s_{20,w}$ over the range (Eisenberg and Felsenfeld, 1981; Erard et al., 1981; Wilhelm and Wilhelm, 1980;

McGhee et al., 1980). We note that all of the above determinations utilized either sucrose gradients, or calculations based on the midpoint of the fast boundary observed in the analytical ultracentrifuge. In our experience, the appropriate midpoint is difficult to determine with accuracy when boundaries are poorly resolved, as is the case here. Therefore, we have turned to an analysis of the entire boundary, using a method which calculates the integral distribution of the sedimentation coefficient (van Holde and Weischet, 1978). By correcting for the effect of diffusion, this allows the resolution of overlapping boundaries.

Figure 5B (open circles) shows the integral distribution of $s_{20,w}$ of our nucleosomes in low salt (I < 15 mM). We obtain $s_{20,w}$ = 10.5 ± 0.4 S, which is slightly less than the value of 10.8 ± 0.3 S obtained for core particles in our laboratory (Tatchell and van Holde, 1977; Tatchell and van Holde, 1979; Weischet et al., 1978). Supposing (from Figures 1A, 1B) our nucleosomes to contain an additional ~44 bp of DNA, and ignoring trace amounts of associated proteins, we calculate that our nucleosomes are the more massive by about 14%. Therefore, on the basis of mass alone, from the relation

$s = \frac{M(1-\bar{v}\rho)}{N_o f}$, we would expect our nucleosomes to have $s_{20,w} \approx 12.3$ S. We conclude that, in low salt, our nucleosomes' frictional coefficient f is increased over that of core particles by about 15%, most likely due to the extra DNA they contain. This DNA probably is an extended conformation (Simpson, 1978; Houssier et al., 1981; Tsaneva, 1980), as would be consistent with the model of Klug et al.

(1980), in which the histone core is not able to accomodate much more than 146-166 bp of DNA.

In 0.5 M salt (Figure 5B, open squares), the fast boundary sediments homogeneously at $s_{20,w}$ = 10.0 ± 0.3 S. In 0.75 M salt (closed triangles), it is still homogeneous, and moves at $s_{20,w}$ = 9.4 ± 0.1 S. Thus as the salt is raised from 0 to 0.5 M, we see a 5% decrease in $s_{20,w}$; upon raising the salt further to 0.75 M, there is an additional 5% decrease.

This relatively small decrease in $s_{20,w}$ with salt could be due to a partial unfolding of the whole nucleosome. Alternatively, it could be due to a less radical change, most plausibly a further unbinding of the ends of the DNA from the core.

We have carried out hydrodynamic calculations, using the Kirkwood theory (Bloomfield et al., 1967), to predict the change in $s_{20,w}$ expected either from global unfolding or DNA unwrapping. The details of these calculations will not be presented here, for they are relatively non-discriminating. They confirm, however, that the small decreases in $s_{20,w}$ observed could arise from either a slight global unfolding or an unwrapping of some portion of the DNA. Gross conformational changes are excluded.

V. Summary

This study has utilized nucleosomes containing DNA longer than the core size, yet wholly stripped of proteins other than the core histones. We present evidence that two processes occur when the nucleosomes are exposed to concentrations of salt 0.5 M and greater.

(i) There is a partial dissociation to yield free DNA. This process seems to be reversible (or nearly so), and behaves qualitatively as expected from the law of mass action; with our nucleosomes, it is slow. (ii) The remaining, undissociated nucleosomes have undergone a small conformational change in high salt; the observed change in $s_{20,w}$ is consistent with either a slight unfolding of the entire nucleosome, or a partial unwrapping of the DNA from the histone core.

We have found that nucleosomes prepared at very low ionic strength are stable to dissociation for long periods, if maintained at high concentrations or very low ionic strength. However, some irreversible dissociation is observed if the nucleosomes are either exposed to 50 mM salt during preparative sucrose gradient centrifugation, or are stored at low concentration even in quite moderate salt concentrations. The simplest explanation for these results is that histones have been irreversibly lost, by aggregation or adsorption to container walls. Our data are not supportive of a model (Stein, 1979) which suggests that the appearance of free DNA is a consequence of a disproportionation reaction between nucleosomes.

We do not find any evidence to support the major conformational change at high salt that has been proposed by some workers (Dieterich _et al_., 1977; Dieterich _et al_., 1979). It is noteworthy that those studies have utilized nucleosomes modified by the attachment of bulky adducts to histone H3.

Finally, we observe that crosslinking of nucleosome cores with dimethyl suberimidate greatly destabilizes histone-DNA interaction.

In work currently in progress, we have extended these studies to core particles, seeking to understand the mechanisms of the dissociation and conformational change, and the relationship between them.

VI. Acknowledgements

The major portion of this work was supported by research grants from the American Cancer Society (NP355A) and the Public Health Service (GM22916). Support also came from President's and Tartar Fellowships to T.D.Y. from Oregon State University. One of us (K.v.H.) wishes to express appreciation for an American Cancer Society Research Professorship.

Within our research group, we would like to thank J. Davie, A. Paton and F. Ziemer for criticism and advise, and G. Riedel for technical help with particle gels and silver staining. We would also like to thank I. Isenberg and T. Tibbitts for robust fitting programs, W. Weischet and M. Zehfus for intergral distribution-of-$s_{20,w}$ programs, P. Meagher for help in implementing our hydrodynamic models on the computer, and H. Eisenberg for a critical reading of the manuscript. Finally, we would like to thank P. Duckworth for her patience in typing the many drafts of this manuscript.

## VII. List of Abbreviations

Abbreviations used are: BSA, bovine serum albumin; DMS, dimethyl suberimidate; EGTA, ethylene glycol bis (β-aminoethyl ether)-N,N,N',N'-tetraacetic acid; EthBr, ethidium bromide; H1/5, histones H1 and H5, considered together; MNase, Staphylococcal aureus (Foggi) nuclease; NaOAc, sodium acetate; PMSF, phenylmethylsulfonyl fluoride; SDS, sodium dodecyl sulfate; $A_{260}$, absorbance at $\lambda$ = 260 nm; (#) bp, (number of) base pairs of DNA; rpm, revolutions per minute.

# The release of DNA from nucleosome core particles at elevated ionic strength

Thomas D. Yager, Cynthia T. McMurray, and K. E. van Holde[†]

Department of Biochemistry and Biophysics

Oregon State University

Corvallis, Oregon, 97331

[†]To whom correspondence and reprint requests should be addressed.

running title: Release of DNA Tails from Core Particles, in NaCl

I. Abstract

In this paper, we report on the nature of the fast conformational change induced in nucleosome core particles by NaCl. The fast change involves an increase in circular dichroism, which we believe is due to a conversion of ~55 bp[1] of DNA from a "nucleosomal" form to one more closely resembling the "solution B" form. This change can be first detected at 0.35 M NaCl, and increases in extent up to 0.75 M NaCl. It is reversible and independent of nucleosome concentration over this entire range of salt concentration. The increase in circular dichroism parallels a decrease in sedimentation coefficient with increasing NaCl, the magnitude of which is predicted by theoretical calculations of the effect of unbinding two 35 bp DNA "tails" from the core.

Assuming a two-state model for the core particle (with tails "in" or "out"), an equilibrium constant may be defined, and its salt-dependence analyzed. We find the fast change to be entropy-driven, and to involve rupture of ~10-14 electrostatic bonds. We conclude that ~9-12% of the DNA tails' phosphates are involved in electrostatic bonding with the histone core. The free energy change of the process may be resolved into two primary components, one involving a mechanical unbending of 55 bp of DNA, and the other involving the rupture of electrostatic bonds between the DNA and the core, coupled to the uptake of counterions. Calculations indicate that the bonds are much too strong to be of the canonical "lysine/phosphate" type. We suggest that they may instead be very strong examples of the "arginine/phosphate" type-a conclusion consistent

with the known inaccessibility of most core arginines to chemical modification and protease attack.

## II. Introduction

In a recent publication, we have described the effects of elevated concentrations of salt on nucleosomes depleted of histone H1 and containing long (> 155 bp) DNA (Yager and van Holde, 1984). These experiments suggested that at least two processes – a rapid conformational change and a slow dissociation into free DNA and histone – were ocurring. In order to examine these phenomena in more detail, and to attempt to relate them to other studies, we have now carried out parallel experiments on core particles. In these new experiments, we have utilized not only sedimentation measurements, but circular dichroism as well. By this combination of techniques, we have been able to describe these processes much more exactly and unambiguously than before. In this paper, we focus on the fast conformational change.

## III. Materials and Methods

### A. Preparation of core particles

Chicken erythrocyte core particles were prepared by either of two methods. These methods were found to give core particles of almost identical quality. Method I, basically a modification of that of Lutter (1978), has been described by Paton et al. (1983). We note

that this method involves a light nuclease digestion of chromatin in nuclei, pelleting of the nuclei by centrifugation, resuspension and lysis of the nuclei in EDTA, and removal of debris by centrifugation. We have no information as to whether a selective loss of a chromatin subpopulation occurs during the centrifugation steps. The yield of core particles from the 50 ml blood of one chicken was 1-1.5 ml x 100 $A_{260}$ (50-75 nmol). Core particles prepared by this method were stored at a concentration of 10 mg/ml and a temperature of 6°C, until use. No preparations over one month old were used.

Method II is a more radical modification of Lutter's method, which gives an increased yield of core particles. Chicken blood was collected and immediately mixed with 1/75 volume of 1000 U/ml heparin, to prevent clotting. It was next filtered through four layers of cheesecloth and centrifuged 4 min at 1000 x g, and the supernatant (plasma and erythrocyte buffy coats) was discarded. All subsequent operations except for nuclease digestions were done at 0-4°C. With a glass rod, the pellet was resuspended in 20-30 volumes of 0.34 M sucrose, 15 mM Tris, 60 mM KCl, 15 mM NaCl, 0.5 mM spermidine, 0.15 mM spermine, 2 mM EDTA, 2 mM EGTA, 15 mM β-mercaptoethanol, pH 7.5 (buffer "A") + 0.1 mM PMSF, and was repelleted by 4 min centrifugation at 1000 x g. The erythrocytes were washed twice more by resuspension and pelleting in 20-30 volumes buffer A + 0.1 mM PMSF, as above. Next, the pelleted erythrocytes were lysed by resuspending them with a tissue homogenizer in 20-30 volumes of Buffer A + 0.1 mM PMSF + 0.5% Nonidet P-40. The nuclei were then pelleted by 5 min

centrifugation at 1000 x g. The nuclei were washed twice more, by resuspension and pelleting in 40-60 volumes of Buffer A + 0.1 mM PMSF + 0.5% Nonidet P-40, as above (each time using a tissue homogenizer to resuspend the pellet).

Next, in preparation for a first nuclease digestion, the EDTA and EGTA were removed by resuspending the nuclei with a glass rod in 40-60 volumes of 0.34 sucrose, 15 mM Tris, 60 mM KCl, 15 mM NaCl, 0.5 mM spermidine, 0.15 mM spermine, 15 mM β-mercaptoethanol, pH 7.5 (Buffer "B") + 0.1 mM PMSF, and centrifuging for 4 min at 1000 x g. The nuclei were washed twice more by resuspension and pelleting in 40-60 volumes Buffer B + 0.1 mM PMSF, as above. The nuclei next were resuspended in 5-10 volumes Buffer B, and the absolute concentration of DNA determined by measuring the absorbance at $\lambda$ = 260 nm of a 100-fold diluted lysate in 0.1 N NaOH, against a blank of 1/100 Buffer B in 0.1 N NaOH. Buffer B was added to the suspension of nuclei until the differential absorbance at $\lambda$ = 260 nm of the 1/100 lysate was 0.65; usually this required adding another ~10 volumes of Buffer B.

The suspension was warmed to 37°C, and $CaCl_2$ was added to 1 mM from a 100 mM stock, slowly and with stirring. Staphylococcus aureus (Foggi) nuclease (Sigma) was added to 45 U/ml, and the digestion allowed to proceed for 5 min. It was then stopped by adding EDTA to a free concentration of 1.5 mM from a pH 7.5 stock, and cooling the suspension in ice. The nuclei were then pelleted by centrifuging 5 min at 8000 x g. The above digestion generates very long fragments

of chromatin, which remain within the nuclei during the centrifugation step.

The nuclei were lysed by resuspension in 5-10 volumes of 0.25 mM EDTA, pH 7.5, followed by gentle stirring for 1 hr. Debris was eliminated by centrifuging for 20 min at 8000 x g, and discarding the pellet. At this point, approximately 50-75% of the chromatin remained in the supernatant, and the other 25-50% was discarded. We have no information on whether a fractionation according to some physical property occurred at this step. The soluble chromatin was diluted to $A_{260}$ = 50 with 0.25 mM EDTA, pH 7.5; 1/100 vol. of 1 M Tris, pH 8.0, was then added. The final solution was ~0.25 mM EDTA, 10 mM Tris, pH 8.0.

H1, H5 and non-histone proteins were next removed by a modification of the method of Libertini and Small (1980). NaCl was added to 0.35 M, slowly and with stirring, from a 4 M stock. Carboxymethyl Sephadex (Pharmacia or Sigma) was next added, slowly and with stirring, to 30 mg/ml. The resultant suspension was stirred gently for 3 hr. The cation-exchange resin was then removed by centrifugation for 20-30 min at 8000 x g, followed by careful aspiration of the supernatant with a pasteur pipette.

In preparation for a second nuclease digestion, the chromatin was dialyzed into Buffer B, and then diluted to a concentration of $A_{260}$ = 25. The temperature was raised to 37°C, and $CaCl_2$ was added to 1 mM slowly and with stirring, from a 100 mM stock. Nuclease was added to 50 U/ml, and the digestion was allowed to proceed 10 min. It was then stopped by cooling on ice and adding 0.25 M EDTA, pH 8.0,

to a free concentration of 1.5 mM. This second nuclease digestion generates about 50% mononucleosomes and about 50% higher nucleosome oligomers; a large fraction of the mononucleosomes contain DNA considerably longer than 146 bp.

To isolate the mononucleosomes produced above, the redigested chromatin was concentrated to $A_{260}$ = 100 by ultrafiltration (Amicon PM 30), and then loaded in $\leq$ 25 ml batches onto a 175-200 cm x 20 $cm^2$ Sephacryl S-300 or S-400 gel filtration column (Pharmacia). The column buffer was 20 mM NaCl, 5 mM Tris, 0.2 mM EDTA, 2 mM β-mercaptoethanol, pH 7.5 (Buffer "C"). At a flow rate of 1-2 ml/min, the mononucleosome peak eluted at ~1500 ml. Mononucleosome fractions were examined by gel electrophoresis (see below); those showing DNA lengths less than about 160 bp were discarded, while those showing DNA lengths greater than this limit were all pooled.

In preparation for a third nuclease digestion, 0.1 M $CaCl_2$ was added, slowly and with stirring, to the pooled mononucleosomes in Buffer C, to give a free concentration of 0.8 mM. At this point, a series of test digestions must be done on aliquots of the mononucleosome pool, to determine the digestion conditions which maximize the yield of core particles (containing ~146 bp of DNA), while holding the production of subnucleosomal particles (containing < 146 bp of DNA) to an acceptable minimum. (For mononucleosomes at a concentration of $A_{260}$ ≈10 and nuclease at 10 U/ml, an optimal digestion requires 2-15 min at 37°C.) The remainder of the mononucleosome pool was then heated to 37°C, and nuclease was added to 10 U/ml; the digestion was stopped after the appropriate time (in accordance with

the above test digestion), by cooling and adding EDTA to a free concentration of 1.7 mM.

The above digestion produced "trimmed" mononucleosomes, which were concentrated to $A_{260} \approx 100$ by ultrafiltration (Amicon PM 50) and loaded on the Sephacryl column, as above. Fractions were examined by gel electrophoresis (see below), and those containing homogeneous core particles were pooled. The pooled core particles were concentrated by ultrafiltration to $A_{260} \approx 10$ (Amicon PM 50), dialyzed into 10 mM Tris, 0.25 mM EDTA, pH 7.5, and stored on ice. The typical yield from 50 ml blood was ~100 ml of solution with an absorbance of 10 at $\lambda$ = 260 nm (~500 nmol core particles). This corresponds to about 20% of the starting material (core particles in chromatin), and is about 7-10 X the yield of method I. No preparations were used that were over one month old.

B. Electrophoresis

The integrity of our core particles was checked by four different types of electrophoresis. Histones were prepared and run on SDS gels, following the method of Laemmli (1971). Gels were stained both by Coomassie blue and silver. Details of histone preparation, gel running and staining, and photography are given in a previous publication (Yager and van Holde, 1984).

Intact core particles were examined for the presence of minor contaminating species of different electrophoretic mobilities and for free DNA, on nucleoprotein particle gels. Staining was by ethidium bromide. Details are as given by Yager and van Holde (1984), except that the gels used were of the "native" type (see below).

The DNA in our core particles was purified and examined both in native, and in single-stranded form. "Native" gels were prepared and run by the method of Kovacic (1976) [also see Kovacic and van Holde (1977)], stained with ethidium bromide, and photographed.

"Single-stranded DNA" gels were prepared by the method of Maniatis et al. (1975), except that no SDS was used, either in the gels or in the running buffer. "Minislab" gels, 0.8 mm thick, were used (Idea Scientific, Corvallis, OR). Purified core particle DNA in 10 mM Tris, 0.25 mM EDTA, pH 7.5 was either mixed with restriction markers in this buffer, or with the buffer alone, and then was made 30% in analytical grade DMSO, 5% in glycerol, and 0.025% in each of bromophenol blue and xylene cyanol. The samples were heated to 100°C for 5 min, cooled on ice, loaded onto gels and run immediately. The voltage gradient was ~4 V/cm initially, and was increased to ~25 V/cm as soon as the samples entered the gel. Running temperature was 4°C. Gels were simultaneously washed free of urea and stained in 0.5 μg/ml ethidium bromide, by shaking at 4°C. They were then photographed on a near-UV transilluminator.

C. Sedimentation velocity measurements

A Beckman model E ultracentrifuge with photoelectric scanner was employed. Experiments utilized both 12 mm and 30 mm cells, with solutions ranging from 0.2 to 0.8 in optical density, at 265 nm. All experiments were at 20.5 ± 1.5°C, controlled within a run to within 0.1°C. All studies utilized a 10 mM Tris, 0.25 mM EDTA buffer to which varying concentrations of NaCl were added [final pH = 7.50 ±

0.05 (22°C)]. For very dilute solutions, in the absence of added salts, 0.5% sucrose was added to stabilize the boundary.

When boundaries were analyzed directly for the fraction of dissociated material, several scans were measured, individually corrected for radial dilution, and the results averaged. Some experiments were analyzed by the method of van Holde and Weischet (1978) to determine the integral distribution of the sedimentation coefficient. Between five and eight scans were measured in such cases. All sedimentation coefficients were corrected to $s_{20,w}$ using standard corrections for buffer density and viscosity. In accord with the results of Olins et al. (1976) and Eisenberg and Felsenfeld (1981), we have assumed the partial specific volume $\bar{v}$ = 0.66 $cm^3/g$, independent of NaCl concentration over the range employed.

D. Circular dichroism measurements

All circular dichroism measurements were performed on a Jasco J41A spectropolarimeter. Most experiments were conducted at a fixed wavelength (282.5 nm), at a scale expansion of 0.5 millidegree/cm, with a time constant of 4 or 16 seconds and with a slitwidth of $\sim$2 μm. The instrument was allowed to stabilize with the lamp and photomultiplier circuit turned on for 3-6 hrs before beginning a set of measurements; this reduced baseline drift, at the above instrument settings, to less than 0.2 millidegree per hr. As all measurements took $\leq$ 45 min each and involved increases above baseline of at least 1.5 millidegrees, we calculate the maximum amount of baseline drift during a measurement to be 10%. Nonetheless, the baseline was

determined before and after each measurement, and correction for drift was made across the duration of the measurement.

Thermostatted 1 cm or 10 cm cuvettes were used, and the temperature in the cuvettes checked with a calibrated thermistor probe. Temperatures within the cuvettes were held constant to about ± 0.1°C, and were judged accurate to within ± 0.25°C. Solution concentrations were adjusted to give absorbances at 260 nm of 0.7-0.9 in either cuvette. As in the centrifugation experiments, all studies were done in a 10 mM Tris, 0.25 mM EDTA buffer, to which varying concentrations of NaCl were added (final pH = 7.50 ± 0.05, at 22°C).

The CD data of this study are subject to three types of distortion, and corrections to the data must be considered (see Fasman, 1979). First, the data will be affected by the sensitivity of DNA winding to changes in salt concentration. The way in which we correct for variation in salt concentration is described in the Results and Discussion sections. Second, the data will be affected by the sensitivity of DNA winding to to changes in temperature. As shown in the Appendix, the corrections for temperature variation will exactly cancel out of all formulae we employ. Third, the data could be subject to light-scattering artifacts, if any aggregation occurred. From the sedimentation velocity studies, we note that the addition of salt to 0.75 M does not cause aggregation. Also, no turbidity was apparent after the salt concentration was raised to ~2.6 M. Thus no correction for light-scattering is deemed necessary.

## IV. Results

### A. Characterization of the core particles

We have paid particular attention to the quality of our core particles, making sure that all experiments were done on highly homogeneous preparations. The core particles were analyzed by four types of electrophoresis, and also by sedimentation velocity in the analytical centrifuge. Virtually identical results were seen for core particles prepared by Method I and Method II.

Figure 1A (lanes 8-12) shows successively higher loadings of DNA purified from core particles prepared by Method II, and run on a "native" gel. On this type of gel, the DNA runs in double-stranded form (Kovacic, 1976; Kovacic and van Holde, 1977). Lanes 1, 7, and 13 show CfoI-cut pBR322, for calibration. Note markers at 131 + 132, 141, and 151 + 152 + 153 bp: the use of multiple markers near 146 bp allows the precise sizing of core particle DNA. Both Method I and Method II yield core particles with highly homogeneous DNA. The center of the DNA size distribution always lies at 144 ± 3 bp, and the half-width of the distribution is always about 3 bp.

Figure 1A also shows intact core particles prepared by Method I, and run on this gel at successively lower loadings (lanes 2-6). Note the virtual absence of nucleoprotein bands other than the main core particle band (at high loadings), and the narrowness of the core particle band at low loadings. These two features indicate high homogeneity in the population of core particles. Even at very high loadings, there is no trace of free DNA in the core particle lanes on this gel.

Fig. III.1A. Characterization of Nucleosome Core Particles and Core Particle DNA, by Gel Electrophoresis

Core particles in 10 mM Tris, 0.25 mM EDTA, pH 7.5 were mixed, with stirring, with an equal volume of 10 mM Tris, 0.25 mM EDTA, 20% glycerol, pH 7.5. The resultant core particle concentration was 470 ng/μl ($A_{260}$ = 4.7). Amounts of 940, 470, 240, 90 or 50 ng, respectively, were loaded in wells 2-6 of a "native" gel. Purified core particle DNA, 235 ng/μl in 10 mM Tris, 0.25 mM EDTA, 0.00125% bromophenol blue/xylene cyanol, was loaded in amounts of 25, 50, 120, 240 or 470 ng, respectively, in wells 8-12 of the gel. Markers in lanes 1, 7, 13 are CfoI-cut pBR322, in the same buffer as is the core particle DNA. From the top, the marker sizes are 393, 348 + 337 + 332, 270, 259, 206, 190, 174, 153 + 152 + 151, 141, 132 + 131, 109, 103, 100, 93, 83, 75 + 67 + 62 + 60; also, below these bands, there is an unresolved smear of smaller RNA fragments. This 0.8 mm thick "native" gel was 3.5% polyacrylamide (bisacrylamide:acrylamide = 1:20), with gel- and running buffers of 40 mM Tris, 20 mM NaOAc, 1 mM EDTA, pH 7.2. Electrophoresis (at 4°C) was at ~3 V/cm for ~5 min, then at ~15 V/cm for ~60 min. Staining was with 0.5-1 μg/ml ethidium bromide.

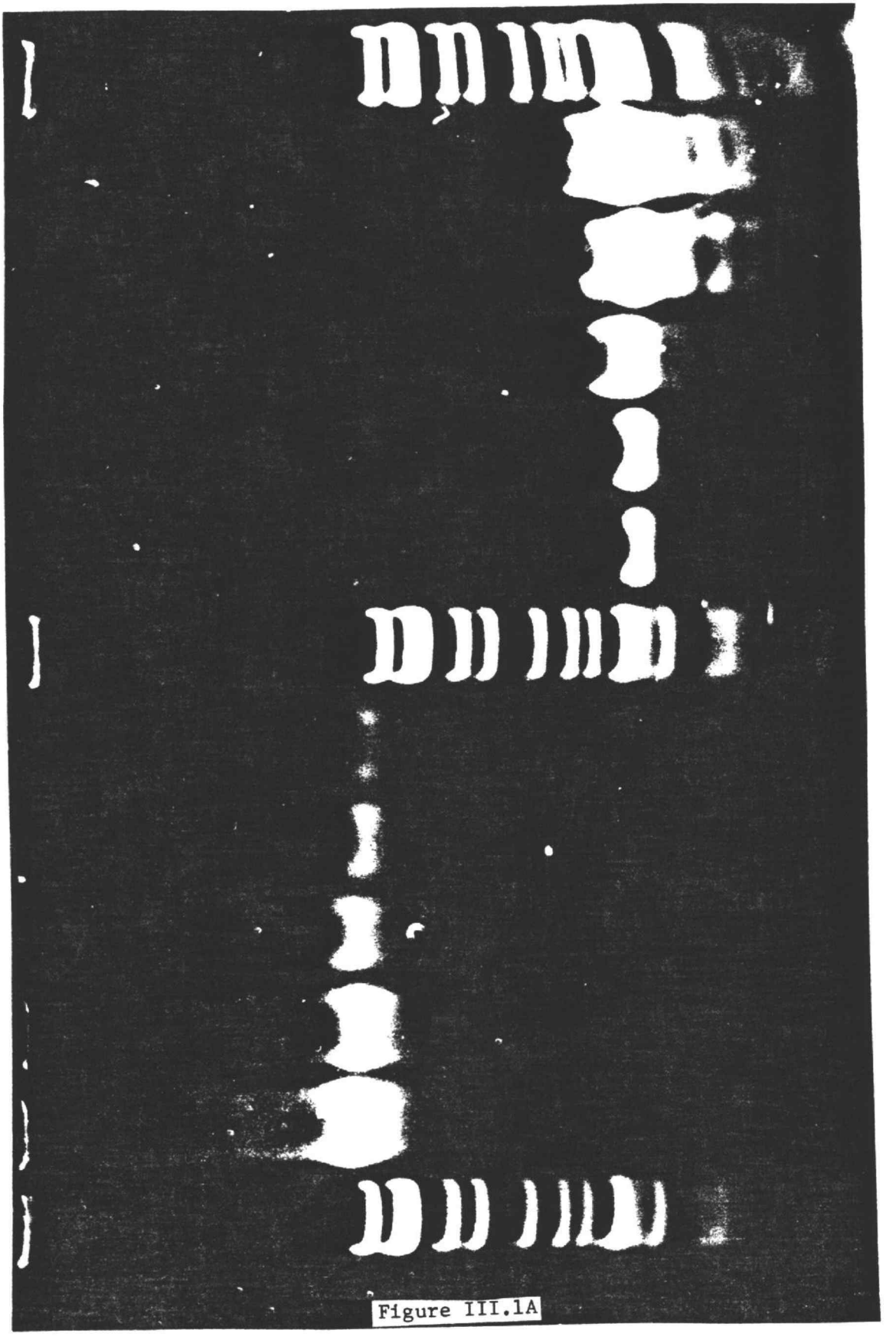

Figure III.1A

In some preparations of core particles, we have seen a slight trace of free DNA on this type of gel. By comparing the relative intensities of the DNA- and core particle bands for such samples [taking account of the fact that, in this type of gel, free DNA gives 2.9X the fluorescence of an equivalent amount of DNA in core particles (not shown)], we calculate that $\leq$ 1% of the DNA in <u>any</u> of our core particle preparations is in the free, uncomplexed form. In fact, even this may be an overestimate, for we have found that an electric field and the presence of bromophenol blue in the sample buffer for these gels can independently promote some nucleosome dissociation (data of E. Gillman, not shown).

These conclusions about particle homogeneity and the lack of free DNA are supported by an analysis in the analytical centrifuge, using core particles prepared by Method I. When a sedimentation velocity run in 10 mM Tris, 0.25 mM EDTA, 0.5% sucrose, pH 7.5 was analyzed by the method of van Holde and Weischet (1978), we found virtually all material in a single, homogeneous boundary with sedimentation coefficient $s_{20,w}$ = 10.7 ± 0.15 S (see Figures 4 and 5). It is difficult to estimate precisely the percentage of free DNA (sedimenting with $s_{20,w}$ ≈ 5.7 S; see Figure 5), for we have noticed (i) that even in low ionic strength buffers, core particles will exhibit some dissociation if made sufficiently dilute (as in the experiment of Figure 3), (ii) that the high pressures attained in the ultracentrifuge cause an additional small amount of dissociation, in

10 mM Tris, 0.25 mM EDTA, pH 7.5, and (iii) that as the sucrose concentration is increased to 2%, the percentage of slow boundary decreases, indicating that some component of it may be an artifact of turbulence, at least at very low core particle concentrations. (See below for more discussion of these effects.) By extrapolating the observed percentage of free DNA to zero sedimentation time (i.e. to minimal pressure), we estimate from the analytical centrifugation assay that there is < 3% free DNA in the sample (see Figure 3).

We have also examined purified DNA from core particles (prepared by Method II) on a "single-stranded DNA" gel (not shown). This gel was run to test for regular nicking within the DNA in our core particles. We find that ~96% of the DNA runs homogeneously between 130 and 150 nt. At high loadings, we see ~4% of the DNA distributed in bands at ~120-130, ~110-120 and ~80-90 nt; presumably, these bands arise from nuclease action. Slightly less of this regular nicking was seen for the DNA of core particles prepared by Method I. We note that this gel is insensitive to small amounts of random nicking, which would produce a low-intensity smear below the main band.

Figures 1B and 1C examine the histone profiles of core particles prepared by Method II. In Figure 1B, total protein from core particles was prepared and run on a 15% Laemmli-type gel, and the gel was stained with Coomassie blue. Lanes 2-5 show successively higher loadings of sample, while lanes 1 and 6 show a standard of calf thymus histones. We see that the staining intensities of the four core histones from the core particle sample are about equal, indicating their molar ratios are approximately equal. At the highest

Fig. III.1B. Characterization of Nucleosome Core Particle Histones, by Gel Electrophoresis. Coomassie Blue Stain.

Purified core particle histones, at 3.8 μg/μl in 60 mM Tris (pH 9), 2% SDS, 5% β-mercaptoethanol, 10% glycerol, 0.001% bromophenol blue, were heated to 100°C for ~5 min, then placed on ice. Amounts of 2, 4, 8 and 16 μg, respectively, were loaded in wells 2-5 of a Laemmli-type protein gel. For a marker, calf thymus histones (Worthington) were prepared similarly, and were loaded in 20 μg amounts in wells 1, 6. The stacking and running portions of this 0.5 mm thick gel were 6% and 15% polyacrylamide, respectively (each with bisacrylamide:acrylamide = 1:37.5). Details of buffer composition are given in Laemmli, 1971. Electrophoresis (at 4°C) was done at ~25 V/cm for ~90 min. Staining was with Coomassie blue.

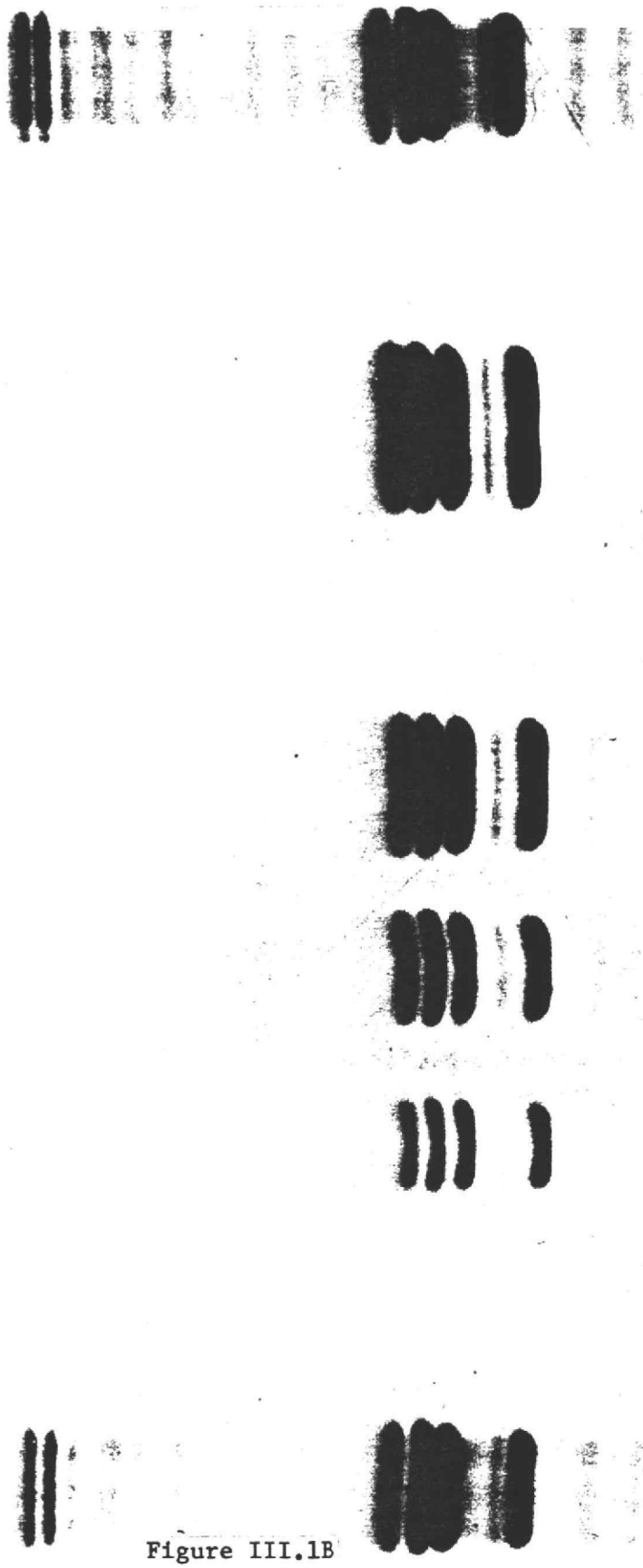

Figure III.1B

Fig. III.1C. Characterization of Nucleosome Core Particle Histones, by Gel Electrophoresis. Silver Stain.

The gel from (B) was restained with silver, according to the method of Wray et al. (1981). To bring out any contaminant bands which may have been present in extremely small amounts, the staining reaction was allowed to proceed for a long time (resulting in blackening together of the histone bands, and some rise in background).

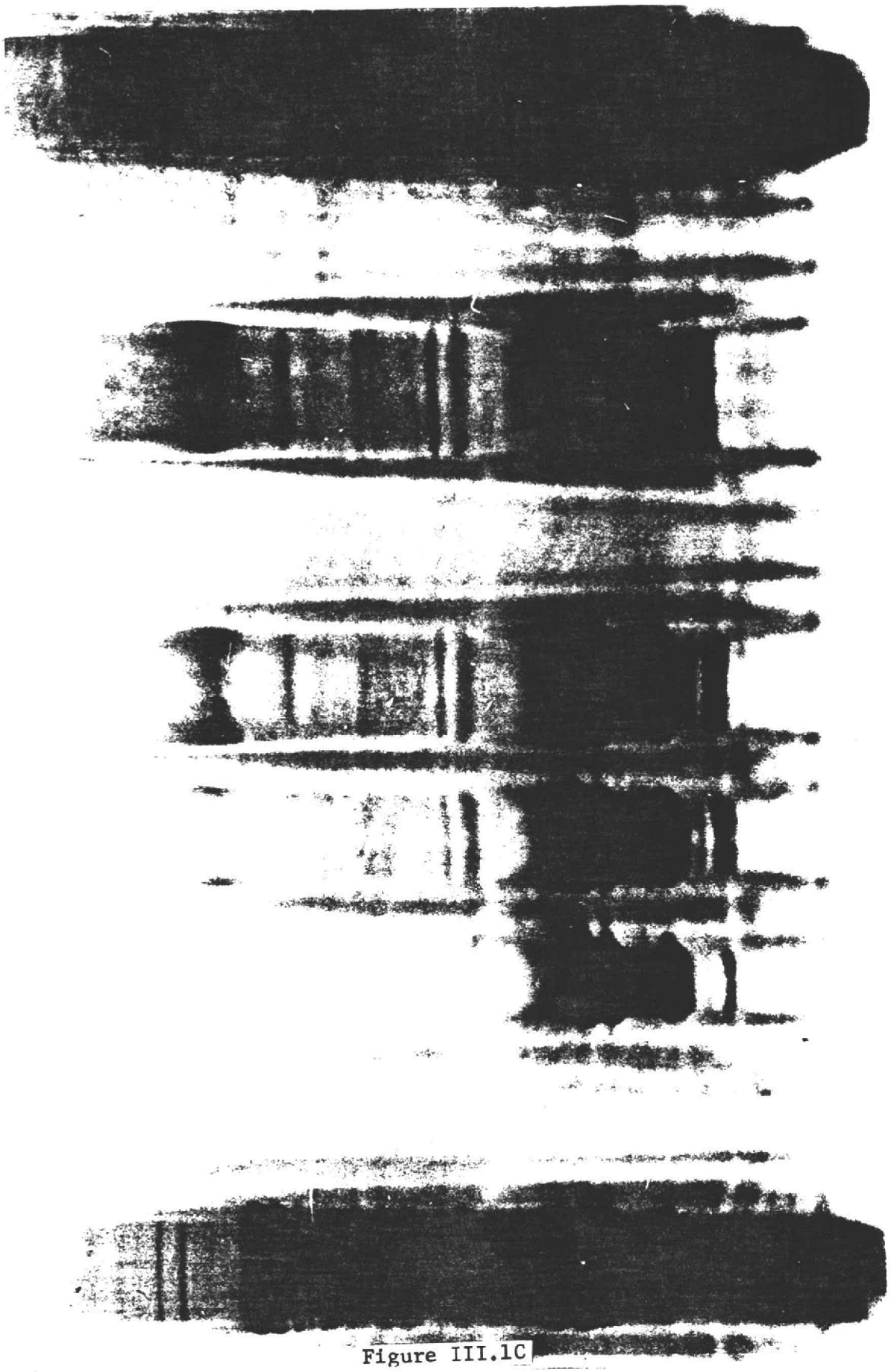

Figure III.1C

loading (16 μg), we see no contamination by H1/5, and very little by non-histone proteins or histone variants.

We have determined the maximum amount of contamination by H1/5 in our core particles through reference to a standard of chicken chromatin that has not been treated with the cation-exchange resin. For such a "non-stripped" standard, the ratio of staining intensities of the set of H1/5 bands and the set of core histone bands is 0.7-0.9 (data not shown). In a densitometric scan of the Coomassie blue-stained gel of Figure 1B, the limit of detection for any single band is about 0.2% of the staining intensity of the set of core histone bands in lane 5 (data not shown). Assuming the three H1/5 species to be present in equal amounts and to stain equally well, we calculate that < 1% of any one of them can still remain in our core particles after the stripping step.

One should not, however, take the above analysis to prove the complete absence of contaminant proteins. When the gel of Figure 1B is restained with silver, we are able to see some H1/5, and also ~12 other, minor bands (Figure 1C). (The broad smear which runs slightly above the position of H1/5 is DNA from the core particles.) The fact that these bands cannot be seen in staining with Coomassie blue indicates that each one is present at less than 0.2% of the amount of the set of the core histones. We note that both Method I and Method II seem to give core particles slightly more contaminated with H1/5 and non-histone proteins than the nucleosomes we have obtained previously, after a similar stripping step (Yager and van Holde, 1984). We believe this is due to the stripping in Methods I

and II being done on larger, hence more highly "structured" chromatin fragments than in our previous study. This conclusion is supported by the observation that, in the previous paper, stripping required only a 1 hour treatment with 50 mM NaCl, while here it requires a 3 hour treatment with 350 mM NaCl.

We note, finally, that the cation-exchange resin is known to remove trace amounts (< 1%) of the core histones from chromatin (Yager and van Holde, 1984).

After storage for 6 weeks at 0°C, we reexamined the integrity of our core particles (prepared by Method II), by three types of electrophoresis. We observed no trace of histone degradation on Laemmli-type protein gels, highly overloaded and stained with Coomassie blue. Core particles migrated as a single, narrow band on "native" gels. When DNA was purified from the core particles and examined on a "native" gel, we observed ~94% of the DNA migrating at 144 ± 3 bp, and the remaining ~6% distributed in discrete bands at ~100, ~85, and ~40-50 bp. We conclude that after 6 weeks' storage at 0°C, there has been no histone degradation, and only a slight degradation of the DNA in our core particles. Since no preparations over one month old were used, we do not consider this slight degradation to be a serious problem.

B. Sedimentation studies of the effects of ionic strength on core particle structure

Previous studies of nucleosome dissociation is salt solutions have suggested that this process may be time-dependent (Yager and van Holde, 1984). To determine more precisely the time-course of

dissociation of core particles, in order to resolve this process kinetically from a second, much faster salt-induced change (see below), we conducted the following experiments.

A stock of core particles in 10 mM Tris, 0.25 mM EDTA, pH 7.5 was split into several portions, and the portions mixed with the same Tris/EDTA buffer containing different concentrations of NaCl. At various times, aliquots of each of the resultant solutions were examined in the analytical centrifuge. The solutions were maintained at 20.5 ± 1.5°C between runs. With the most rapid handling, an aliquot of a solution could be placed in an ultracentrifuge cell and brought to speed in about 40 min. Figure 2 clearly demonstrates the time-dependence of the dissociation process. Figure 3 depicts the fraction of the slow boundary (free DNA) as a function of time, at a number of salt concentrations. At each concentration, a plateau value is reached between 40 and 400 minutes after mixing (at 20.5 ± 1.5°C). We note that, if the kinetics are to be determined any more precisely than this, a different investigative technique is necessary.

In the analytical centrifuge, there is a little ($\leq$ 3%) dissociation in "zero" salt (10 mM Tris, 0.25 mM EDTA, 0.5% sucrose, pH 7.5). This is probably a consequence of three separate effects. First, to obtain the "zero" salt scans, we diluted core particles from $A_{260}$ = 10-100 (5-50 μM) to $A_{260}$ = 0.3 (~160 nm). We and others have previously noted that some nucleosome dissociation will occur even at very low ionic strengths if a sample is sufficiently dilute [see Yager and van Holde (1984) for a further discussion of this

Fig. III.2. Time-dependence of core particle dissociation in 0.75 M NaCl.

5 M NaCl in 10 mM Tris, 0.25 mM EDTA, pH 7.5 was mixed, slowly and with stirring, with a stock solution of core particles in 10 mM Tris, 0.25 mM EDTA, pH 7.5. The final core particle concentration was ~140 nM ($A_{260}$ = 0.27), and the final concentration of NaCl was 0.75 M. The ambient temperature was 20.5 ± 1.5°C. Aliquots were examined in the analytical centrifuge in 30 mm cells, at various times. Shown are scans at 44 and 424 min. The direction of sedimentation is from left to right. A, m and r denote absorbance at 265 nm, meniscus, and radial position, respectively. These scans are part of the complete set of data of Figure 3.

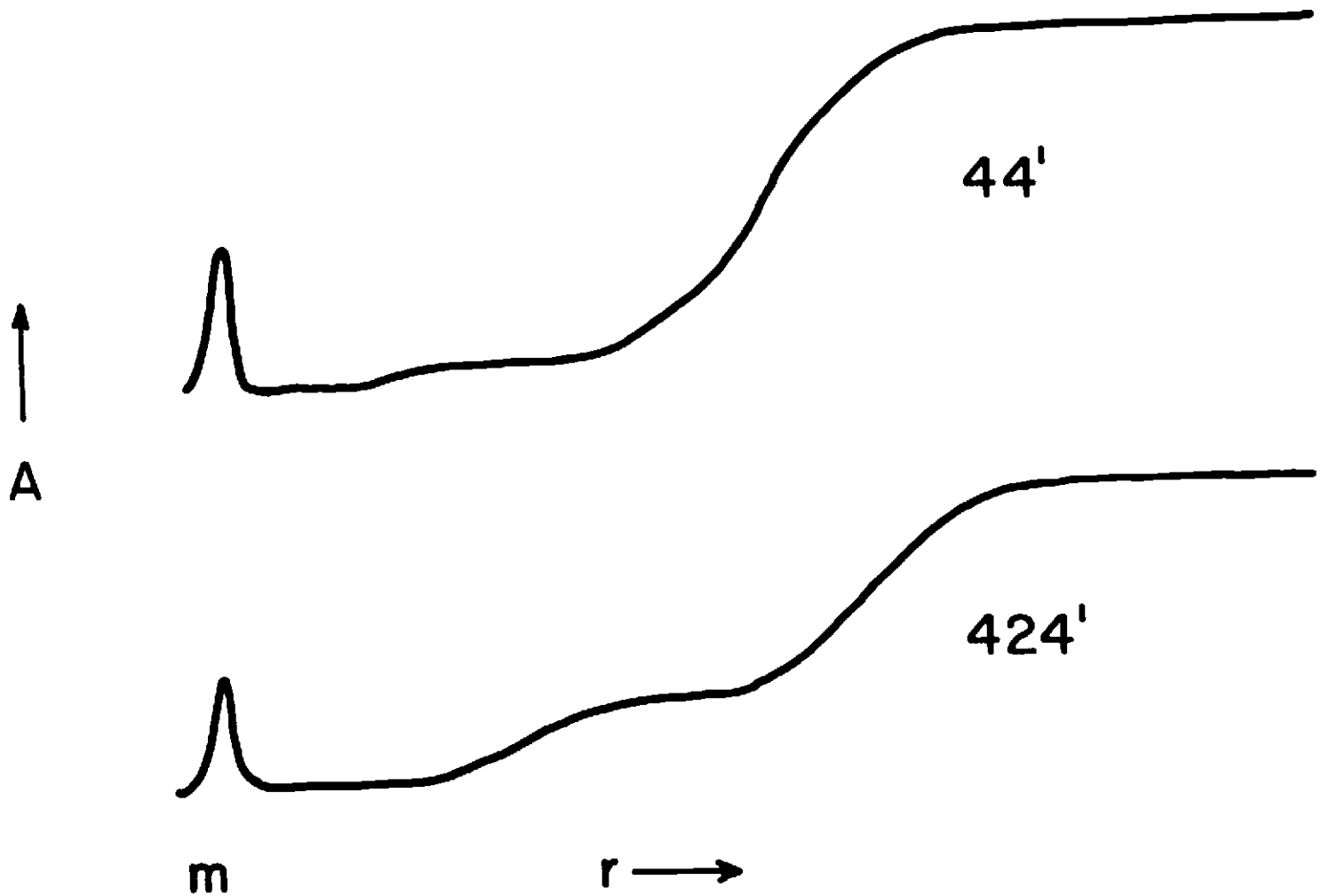


Figure III.2

Fig. III.3. Core particle dissociation, as a function of salt concentration and time of incubation

Core particles and 5 M stock NaCl, each in 10 mM Tris, 0.25 mM EDTA, pH 7.5, were mixed as in the legend of Figure 2, to give solutions containing ~140 nM core particles ($A_{265}$ = 0.27), and 0, 0.1, 0.3, 0.5 or 0.75 M NaCl. The ambient temperature was 20.5 ± 1.5°C. Periodically, aliquots were removed and examined in the ultracentrifuge in 30 mm cells; from scans such as those shown in Figure 2, the % slow boundary was calculated, and corrected for radial dilution. The resultant corrected values were equated with the % free DNA in the samples (see Yager and van Holde, 1984). Each point in Figure 3 is the average of data from 3-5 scans taken in a single centrifuge run.

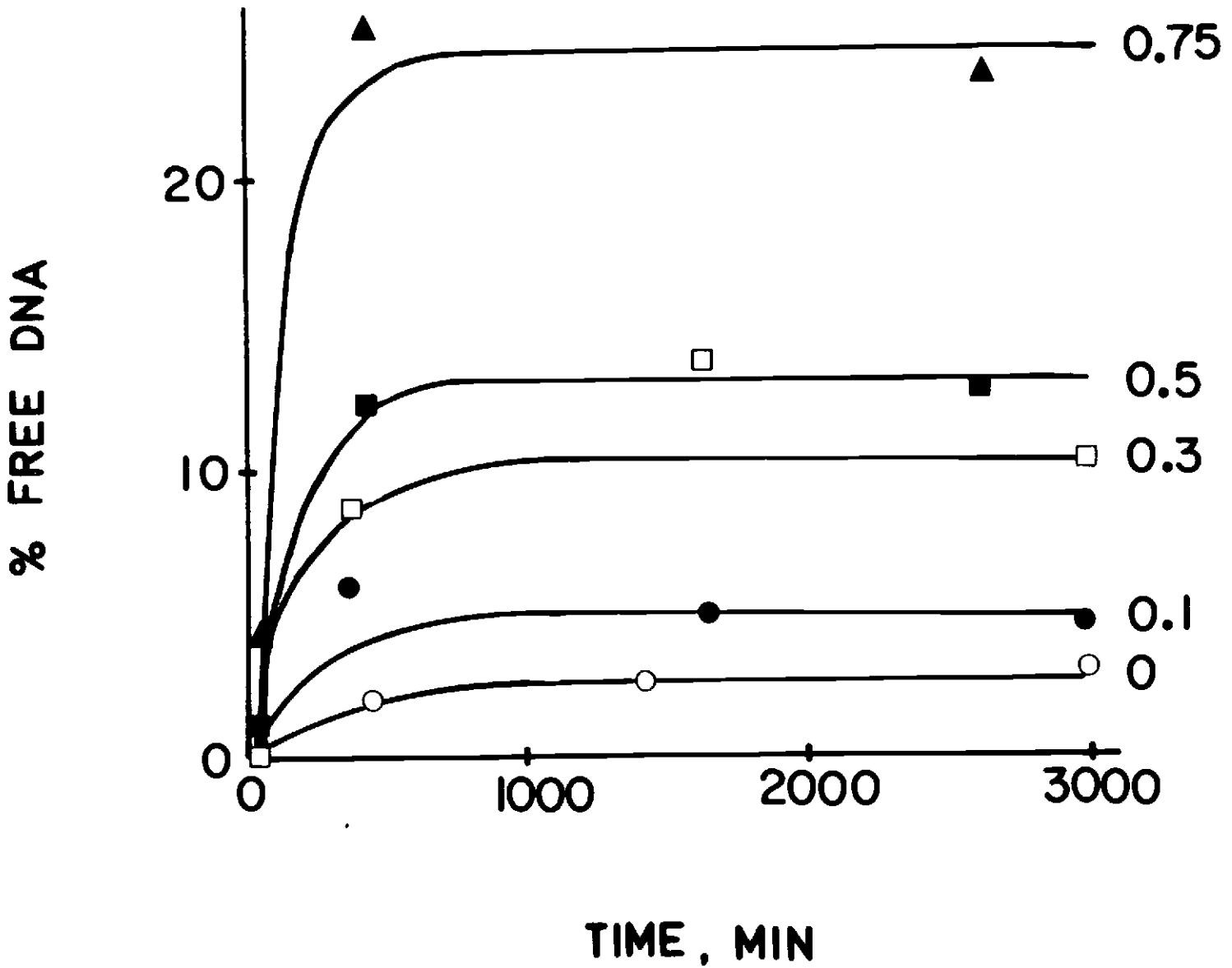


Figure III.3

fact, and for additional references]. Second, we have noticed that, in 10 mM Tris, 0.25 mM EDTA, pH 7.5, the relatively high pressures in the ultracentrifuge induce some core particle dissociation (not shown). This effect is most obvious in the late scans of a series (when the pressure on the fast-sedimenting boundary material is the greatest). It indicates that the specific volume of the core particle decreases upon dissociation. We note that this phenomenon may complicate the interpretation of Figures 2 and 3: if the specific volume decrease upon dissociation occurs also in solutions of higher ionic strength, then all the percentages of free DNA in these figures will be biased high. Third, we have noticed, for core particle solutions having optical densities (at 265 nm) of 0.2-0.3, that if the concentration of sucrose is increased from 0.5% to 1% and then to 2%, there is a progressive decrease in the percentage of slow boundary (not shown). This suggests that, at least in salt-free, highly dilute solutions, a component of the slow boundary may be an artifact due to turbulence.

The plateau values of free DNA approached in Figure 3 probably represent equilibrium values of dissociation, as was demonstrated in our earlier studies using nucleosomes with longer DNA (Yager and van Holde, 1984). These plateau values increase with increasing salt concentration, as has been noted by many researchers [see Ausio et al. (1984) and Yager and van Holde (1984) for recent studies, and for references to earlier studies]. We will explore the kinetics and mechanism of this slow dissociation step further in a future publication.

The remainder of this paper will be concerned with a second salt-induced process, which occurs much faster than dissociation, and probably independently of it. As Figure 4 shows, the sedimentation coefficient of the more rapid (nucleosomal) boundary decreases above ~0.4 M NaCl. This effect can be detected in even the earliest centrifugaton experiments, before dissociation becomes significant (compare the early and late time points in Figure 4). It is more dramatically shown in Figure 5, which compares the sedimentation coefficient distribution of core particles in zero salt with the distributions for core particles in 0.75 M salt, 44 min and 424 min after mixing. By 44 min, all of the core particles had decreased in $s_{20,w}$ from 10.7 S to about 9.0 S, even though little dissociation had yet occurred. This decrease in sedimentation coefficient with increasing salt concentration has been observed by others, also [see Yager and van Holde (1984) for references and discussion]. Thus, the effects of high salt concentration are two fold-a rapid change in sedimentation coefficient, followed by a much slower dissociation process. To further investigate the nature of the fast change, we have turned to another technique.

C. Circular dichroism studies

In the near-UV region, free DNA and nucleosomes each have a maximum in ellipticity in the neighborhood of 280 nm, but the maximum in nucleosomes is strongly suppressed, presumably because of the coiling of the DNA about the nucleosome core (reviewed in Fasman, 1979). The histones contribute virtually nothing to the ellipticity in this wavelength region. We reasoned, therefore, that if the rapid

Fig. III.4. Decrease in sedimentation coefficient of the fast (nucleosomal) centrifuge boundary, with increasing NaCl concentration.

The experiments of Figure 3 were analyzed by the method of van Holde and Weischet (1978). For core particles at each salt concentration and time point in Figure 3, an integral distribution of the sedimentation coefficient was obtained. By this method of analysis, small changes ( ~0.2 S) in the sedimentation coefficient of a homogenous boundary can be detected. Open circles: sedimentation coefficient of the fast (nucleosomal) boundary as a function of NaCl concentration, immediately after mixing (taken from early timepoints of Figure 3). Closed circles: sedimentation coefficient of the fast (nucleosomal) boundary as a function of NaCl concentration, after dissociation equilibrium had been reached (taken from late timepoints of Figure 3). Values have been corrected to conditions of 20°C and water.

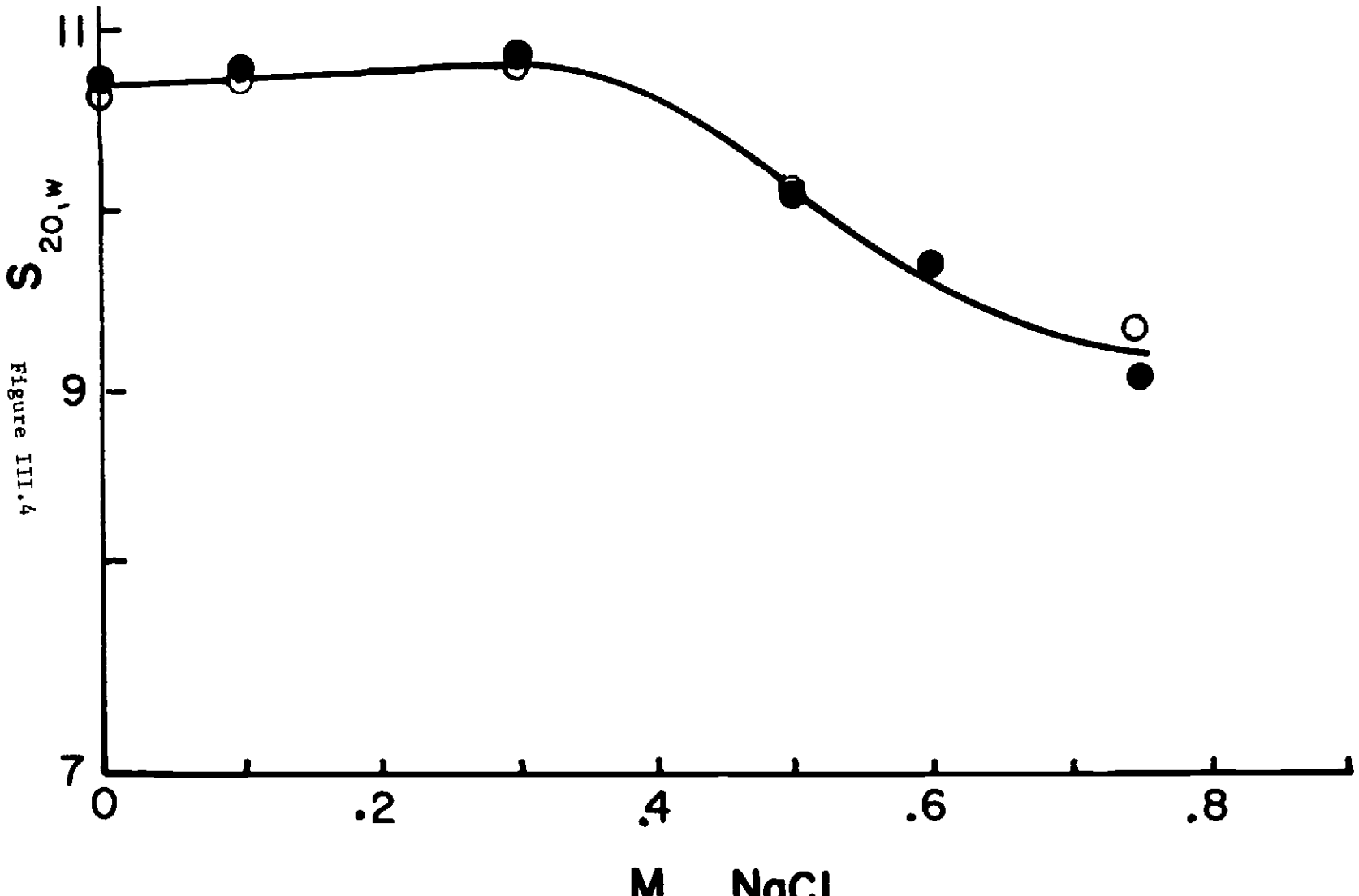


Figure III.4

Fig. III.5. Detail of the integral distribution of $s_{20,w}$ analysis, for the centrifuge data of Figure 2.

Top panel: the integral distribution for core particles in 10 mM Tris, 0.25 mM EDTA, pH 7.5 is centered at 10.7 ± 0.15 S. Immediately after jumping core particles to 0.75 M NaCl in the above buffer, the integral distribution of the fast (nucleosomal) boundary has decreased, so as to be centered on 9.0 ± 0.15 S. The horizontal arrow indicates the percentage free DNA calculated by measuring individual scans and averaging, as in the legend of Figure 3. Bottom panel: after dissociation equilibrium has been reached in 0.75 M NaCl (in the above buffer), the integral distribution of the fast (nucleosomal) boundary is still centered at 9.0 ± 0.15 S. In the integral distribution, a slow species centered at 5.7 ± 0.15 S (free DNA) also is apparent. The horizontal arrow indicates the percentage free DNA calculated by measuring individual scans, correcting for radial dilution, and averaging, as in the legend of Figure 3.

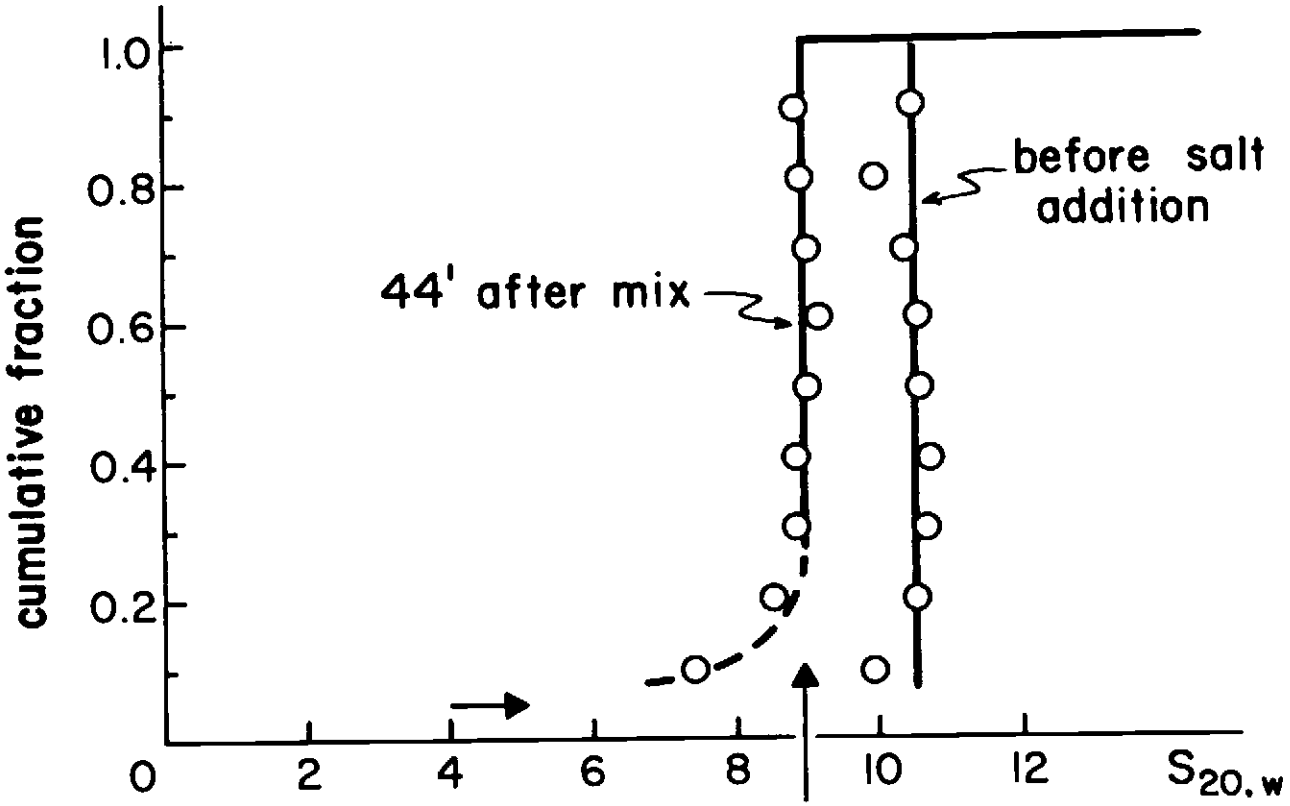
cumulative fraction
1.0
0.8
0.6
0.4
0.2
0
2
4
6
8
10
12
$S_{20,w}$
before salt addition
44' after mix

Figure III.5

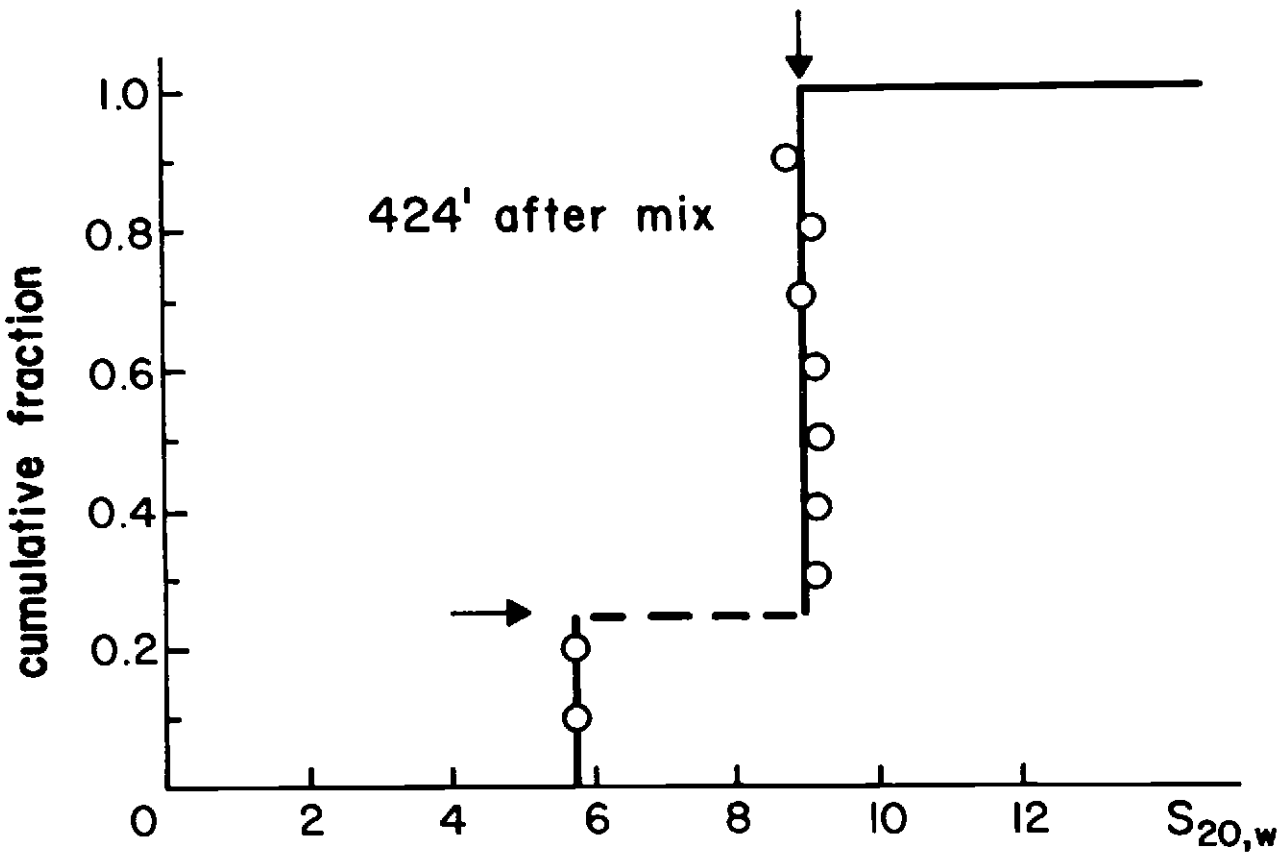
424' after mix
cumulative fraction
1.0
0.8
0.6
0.4
0.2
0
2
4
6
8
10
12
$S_{20,w}$

Figure III.5

change seen in sedimentation velocity studies caused any portion of our core particles' DNA to be converted to a "free DNA"-like conformation, then an increase in ellipticity around 280 nm should be detectable. Furthermore, if such an increase in CD were observed, then the rapid process and the slow dissociation might be resolved well by CD measurements. Accordingly, experiments were designed as follows: The monochromator was set at $\lambda$ = 282.5 nm and a baseline value was recorded for buffer (10 mM Tris, 0.25 mM EDTA, pH 7.5), over 5-10 min. A core particle solution in this buffer was then placed in the cuvette, and the signal was recorded for 5-15 min. Concentrated NaCl in this buffer was then added slowly, with rapid stirring, to the desired final salt concentration. The ellipticity was again recorded, beginning as quickly as possible after mixing. Recording was continued for 5-15 min if only the immediate change was to be observed, or for longer periods if the dissociation process was to be followed as well. Solid NaCl was then added to a concentration of about 2.6 M, to completely dissociate the nucleosomes, and the resultant CD signal monitored for 5-15 min. Finally, baseline was recorded again for the buffer, over 5-10 min. A tracing of such a recording is shown in Figure 6. It is clear that there is an immediate increase in ellipticity upon the first addition of salt. This we identify, for reasons given below, with the change which produces a rapid decrease in core particle sedimentation coefficient (Figures 4 and 5, top panel). In other experiments of this type, a small, slower change also is apparent, which we identify with the

Fig. III.6. Time-dependent changes in the circular dichroism of core particles, at elevated NaCl concentrations

The spectropolarimeter was allowed to warm up for three to six hours, to attain stability. After this, the CD at 282.5 nm was measured for a blank (10 mM Tris, 0.25 mM EDTA, pH 7.5) (point I), and then for a temperature-equilibrated solution of core particles in the same buffer as the blank (point II). The core particles had either a concentration of ~520 nM (optical density at 260 nm = 1.0; this figure, and other experiments), or of ~50 nM (optical density at 260 nm = 0.1; other experiments). Then, slowly and with stirring, 5 M NaCl in 10 mM Tris, 0.25 mM EDTA, pH 7.5 was added to the core particles, to a final concentration of 0.59 M (this figure), or to other final concentrations between 0.1 and 0.75 M (other experiments). The CD signal at 282.5 nm was then monitored over 10-45 min (point III). Solid NaCl was then added to ~2.6 M, and the CD signal remeasured (point IV). FInally, the blank was rechecked (point V). The temperature of this particular experiment was 27.6°C. In general, the temperature was controlled to within 0.1°C during each experiment, although there was some temperature fluctuation between readings, when the cuvette was removed and salt added. There was always a 1.5-3 min gap in recording, during salt additions. Broken line: interpolated baseline. In this particular experiment, there was a ~10% upward drift of the baseline, over the course of measurements. A 10% drift was the maximum observed in any experiment.

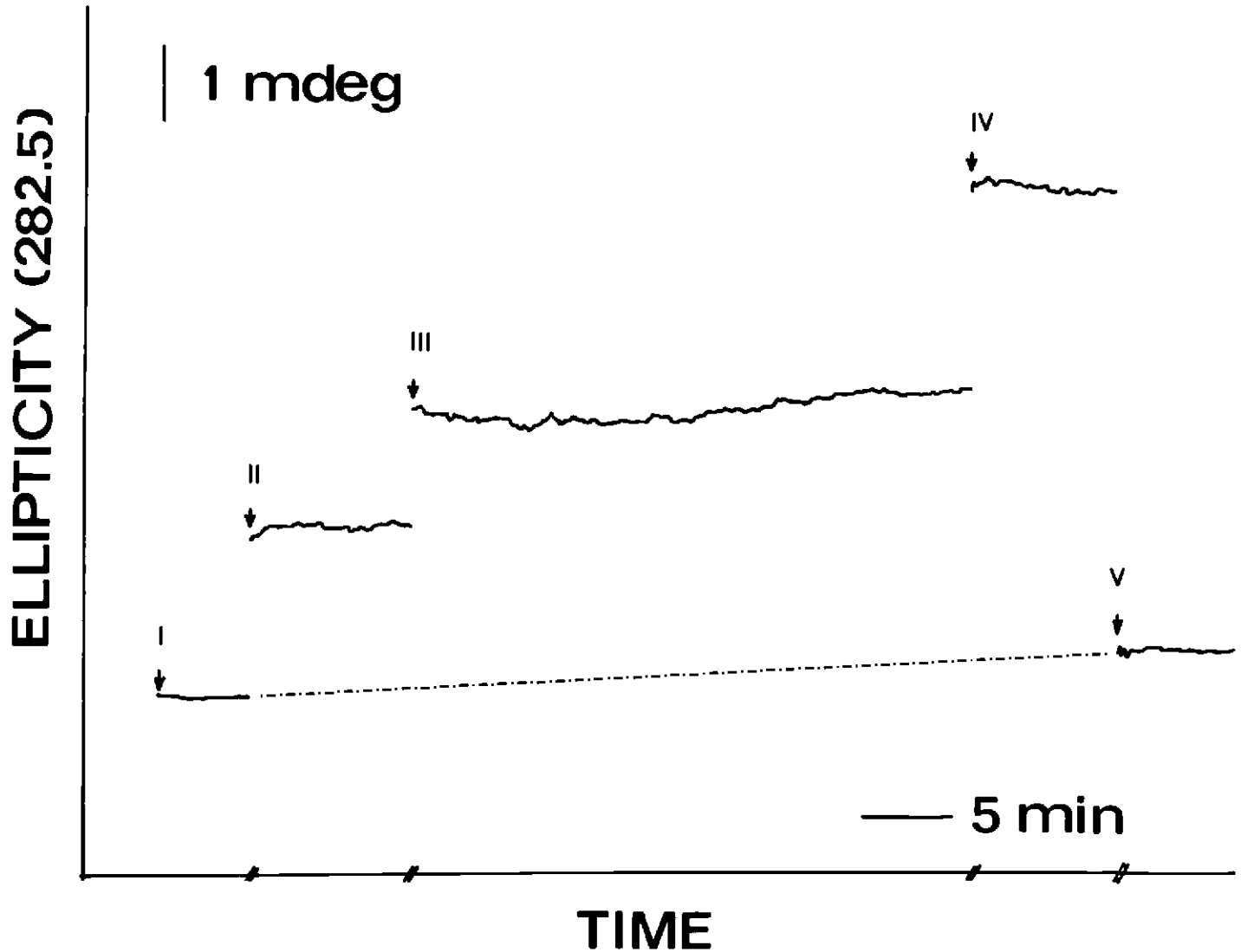


Figure III.6

slow dissociation process depicted in Figures 2, 3 and 5, bottom panel.

Each of these processes apparently involves conversion of DNA from a "nucleosomal" conformation to a "free" conformation. All of the core particles appear to be able to undergo the rapid change, at least at high salt: we see no trace of the original 10.7 S boundary in 0.75 M salt, all material having been converted to a 9.0 S form (Figure 5, top panel). Only a portion of the DNA on each core particle appears to be involved, however, since the total rapid change represents only a fraction of the possible change (Figure 6; see also the theoretical S calculations depicted in Figure 11). On the other hand, the dissociation-associaton reactions are such that only a fraction of the core particles have wholly dissociated at equilibrium (Figures 3 and 5, bottom panel). Therefore, we have chosen to analyze data like that shown in Figure 6 in the following way. At any wavelength, the observed ellipticity $\theta$ is given by

$$\theta = [\theta]lC \qquad (1)$$

where $[\theta]$ is the molar ellipticity in deg $cm^{-1}$ $M^{-1}$, l is the path-length in cm, and C is the molar concentration of bp of DNA. We consider a situation in which a portion of the DNA's base pairs are in a "nucleosomal" state, with molar ellipticity $[\theta]_N$, and another portion are in a "free" state, with molar ellipticity $[\theta]_D{}^{S,T}$. The superscripts S and T signify that the molar ellipticity of the free DNA base pairs is a function of salt concentration and temperature, because of the dependence of DNA winding on these parameters [for a review, see Fasman (1979)]. We assume that $[\theta]_N$ is

independent both of salt concentration over the range 0-0.75 M, and of temperature, because of the constraints on DNA winding in the core particle. For the ellipticity of the partially "modified" and partially dissociated core particle mixture at any salt concentration we may write

$$\theta = l([\theta]_N C_N + [\theta]_D^{S,T} C_D) \qquad (2)$$

where $C_N$ is the molar concentration of base pairs in the nucleosomal state, and $C_D$ is the molar concentration of base pairs in the free state. If we denote by $f_B$ the fraction of base pairs in the bound nucleosomal state, and by $f_R$ the fraction of base pairs released, either by conversion in "modified" core particles of part of the DNA to a "free" conformation, or by the dissociation of core particles, we have $f_B = 1 - f_R$. The $C_N = f_B C$ and $C_D = f_R C$, where C is the total molar concentration of base pairs of DNA. Equation (2) becomes

$$\theta = lC \left([\theta]_N + \left([\theta]_D^{S,T} - [\theta]_N\right) f_R\right) \qquad (3)$$

Since at low salt $f_R = 0$, we may write

$$\theta_0 = lC[\theta]_N \qquad (4)$$

Immediately after addition of NaCl to concentrations between 0.35-0.75 M, the ellipticity increases. We interpret this in terms of the release of some DNA from nucleosomal constraints, and write:

$$\theta_{S,O} = lC' \left([\theta]_N + ([\theta]_D^{S,T} - [\theta]_N) f_{R,O}\right) \qquad (5)$$

where C' is the total concentration of base pairs after dilution in this step, and $f_{R,O}$ is the fraction of base pairs in the system which have at this step been released from nucleosomal constraints.

If sufficient salt is now added to complete the dissociation, $f_R = 1$, and we have

$$\theta_h = 1C'' \, [\theta]_D^{h,T} \qquad (6)$$

where C" is the total concentration of base pairs after this second dilution, and $[\theta]_D^{h,T}$ is the molar ellipticity of free DNA in the "high salt" condition.

Combining equations (4)-(6), we find

$$f_{R,O} = (\theta_{S,O} - r\theta_O)/(r''g\theta_h - r\theta_O) \qquad (7)$$

where $r = C'/C$, $r'' = C'/C''$, and $g = [\theta]_D^{S,T}/[\theta]_D^{h,T}$. The factors r and r" take into account the dilutions accompanying the salt additions, and the factor g corrects for the change in molar ellipticity of DNA with salt concentration (at a fixed temperature).

The factor g was evaluated by measuring, at 20°C, the change in ellipticity of chicken erythrocyte core particle DNA over a range of NaCl concentrations between 0-4 M. The data need not be given here, for they reproduce, with experimental error, the results given by Ivanov et al. (1973) for calf thymus DNA. We have assumed g is independent of temperature.

It seems possible that, in attempting to compare $f_{R,O}$ values observed at different temperatures (as in the temperature-dependence plot of Figure 10, below), one may encounter difficulty. This would be because, in addition to any change in the extent of tail release with temperature, there is also a change, with temperature, in the molar ellipticity of the released DNA tails. To phrase this complication mathematically, we note that both $\theta_{S,O}$, in the numerator, and $g\theta_h$ in the denominator of equation (7) depend on temperature,

each through the parameter $[\theta]_D^{S,T}$. We show in the Appendix that, fortunately, the temperature-dependencies of numerator and denominator exactly cancel, so that no temperature-correction need be made.

The above equations can be extended to follow the effects of dissociation, but we shall consider this in a later publication.

With this basis, we turn now to the analysis of the fast process. The results of a series of measurements at 20, 25 and 27.5°C are depicted by the individual data points of Figure 7. Three salient points should be noted.

First, the rapid increase in ellipticity at 282.5 nm is observable only above 0.3 M NaCl, and appears to plateau at about 0.7-0.75 M. Furthermore, the salt range over which it occurs, as measured by CD, is in good agreement with the range noted for the rapid decrease in S (Figure 4). That is, this transition involves both an increase in the frictional coefficient, and a transformation of a part of the DNA in each particle to a conformation more like that of free DNA. At the plateau, the transformation corresponds to the "release" of about 55 bp of DNA per particle (although there is some uncertainty in the determination of this value; see Discussion).

We did not extend the CD experiments to higher salt concentrations, for there is evidence that the loss of H2A·H2B dimers commences at about 0.8 M (Burton et al., 1978, 1979). On the other hand, we probably were safe in going up to 0.6-0.75 M salt, according to the following two lines of evidence. (i) In elevated NaCl solutions of both core particles and nucleosomes with long DNA, the

Fig. III.7. The salt-induced rapid increase in circular dichroism of core particles.

Core particles were jumped to various concentrations of NaCl and their circular dichroism at $\lambda$ = 282.5 nm monitored, as described in the legend of Figure 6. The observed CD values were corrected for dilution and for salt-dependence, as described in the text. Ordinate on left: $f_{R,0}$, as defined by equation (7) in the text. Ordinate of the right: value for the total concentration of bp released, divided by the total concentration of particles, corresponding to each particular value of $f_{R,0}$ on the left ordinate. Closed circles: core particles at an optical density (at 282.5 nm) of ~0.9, in a 10 cm cell. Temperature: 20°C for all points at 0.2, 0.3, 0.5 and 0.7 M NaCl, and for the solid point at 0.6 M NaCl; 25°C for the lower open point at 0.6 M NaCl; 27.5°C for all other points. The absolute uncertainty in each temperature is $\leq$ 0.25°C. The temperature was held constant to within 0.1°C, during each experiment. The theoretical curves 1 and 2 are calculated from equations (8) and (9), using parameters listed in the first portion of Table I (as described in the text).

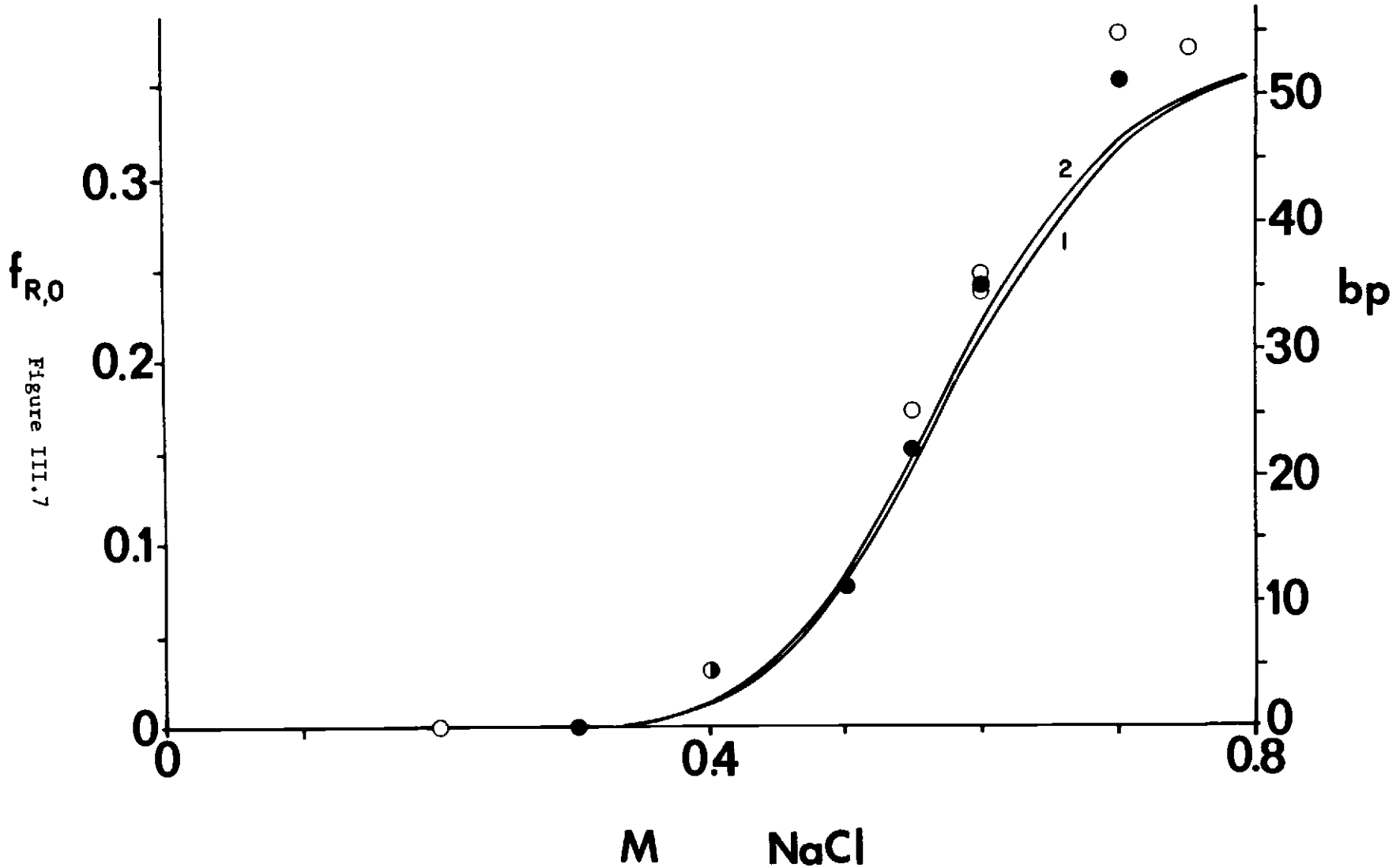


Figure III.7

histone stoichiometry of the non-dissociated subpopulation of particles is preserved until at least 0.6 M salt (Wilhelm and Wilhelm, 1980; Zayetz et al., 1981; Yager and van Holde, 1984). (ii) We observe, both for core particles and for nucleosomes with long DNA, the preservation of a homogenous ~9.0 S sedimentation boundary in 0.6-0.75 M salt, even after dissociation equilibrium has been reached [Figure 5, bottom panel; see also Yager and van Holde (1984)].

Second, this fast transition is independent of concentration, as evidenced by the fact that data obtained at ten-fold different nucleosome concentrations (solid and open circles, Figure 7) superimpose almost exactly. This very strongly supports the idea that the transition is a conformational change, and further distinguishes it from the dissociation process which is concentration-dependent, both for core particles and for long-DNA nucleosomes (Stacks and Schumaker, 1979; Lilley et al., 1979; Cotton and Hamkalo, 1981; Yager and van Holde, 1984; Ausio et al., 1984).

Third, the rapid change is wholly reversible. This is demonstrated by the experiment depicted in Figure 8. The ellipticities of solutions of core particles at a concentration of ~480 nM ($A_{260}$ ≈ 0.9) were first recorded in a 1 cm cuvette. The solutions were then jumped to various salt concentrations and monitored in the 1 cm cuvette. They were then diluted 1:10 with "zero salt" buffer, and monitored in a 10 cm cuvette. The experiment depends on the previous observations that the fast transition is concentration-independent, and is not observed below 0.3 M NaCl. As Figure 8 shows, the final CD signal in the 10 cm cell is virtually the same as that

Fig. III.8. Reversibility of the salt-induced repid increase in circular dichroism of core particles

Core particles were parpared at an optical density (at 282.5 nm) of 0.9 in 10 mM Tris, 0.25 mM EDTA, pH 7.5, and their CD at 282.5 nm was measured (dashed line).

They were then jumped to the concentrations of NaCl shown on the abscissa of this figure (in 10 mM Tris, 0.25 mM EDTA, pH 7.5), and their CD measured again (closed circles). These measurements were made in a 1 cm cell. Each measurement was initated 1.5 min after the salt-jump, and took approximately 10 min to complete. The core particles were then diluted 10-fold with 10 mM Tris, 0.25 mM EDTA, pH 7.5, and their CD measured in a 10 cm cell (open circles). The temperature was held at 20.0°C in the 1 cm cell and at 21.1°C in the 10 cm cell (each with an absolute uncertainty of ± 0.25°C); the variation of temperature was $\leq$ 0.1°C in each cell, except during salt additions, when it was somewhat greater. The data at high salt concentrations (closed circles) were not corrected for the depression of the free-DNA portion of the CD signal with increasing salt concentration (see text), or for any dissociation of core particles which may have occurred during the measurements. All data were corrected for baseline drift. (The error bar in this figure indicates the range of baseline drift which occurred over the course of the experiment). Ordinate: CD signal at 282.5 nm, in millidegrees.

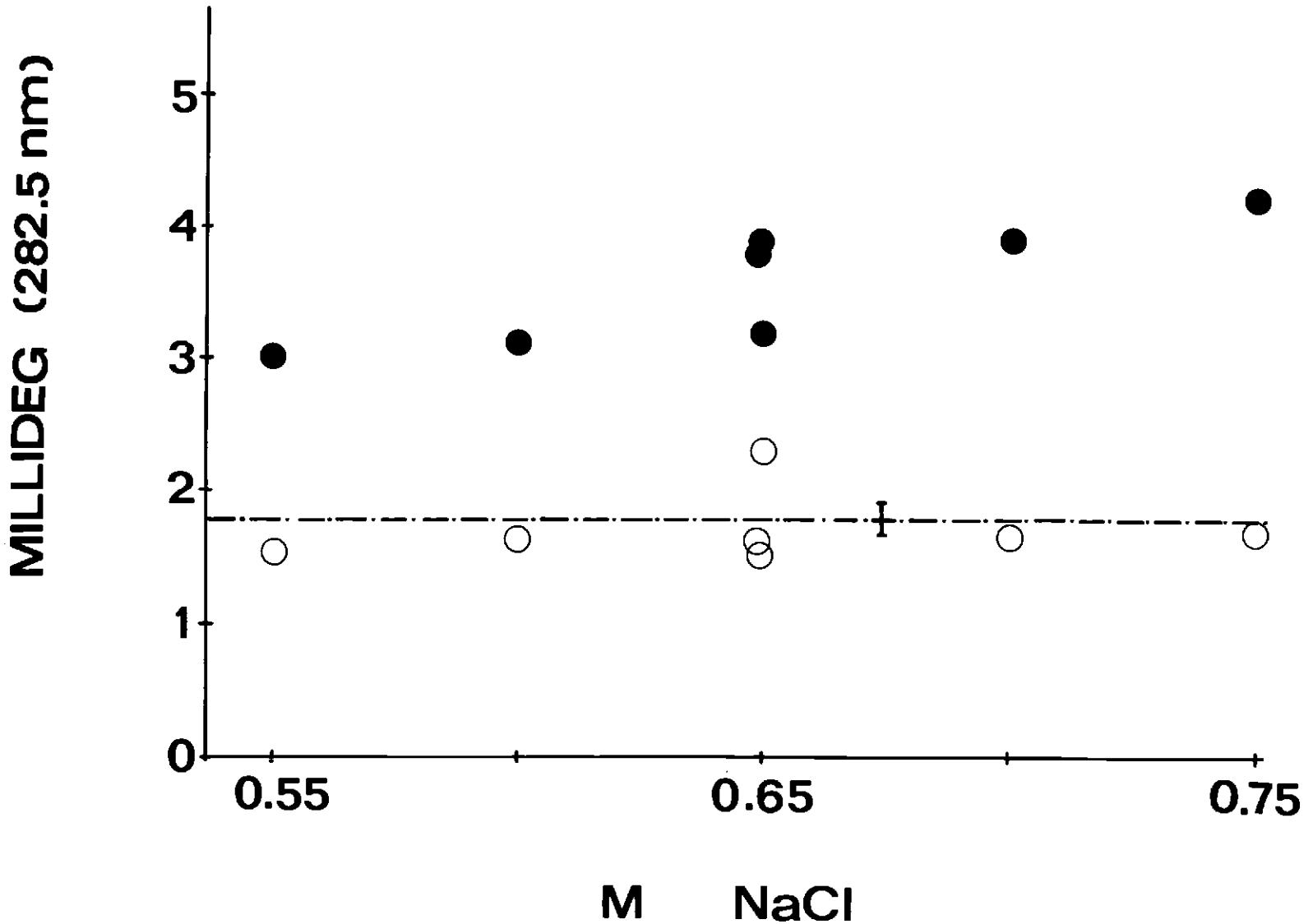


Figure III.8

of the 10-fold more concentrated solution in the 1 cm cell, before the salt jump.

D. Thermodynamic analysis

As will be argued in the Discussion, there are good reasons to believe that this rapid conformational change corresponds to the release of a portion of the DNA from the histone core. At the plateau ( ~0.75 M NaCl), the data are consistent with about 55 bp being released from each nucleosome. We cannot tell, however, whether the values of the ellipticity or sedimentation coefficient observed at a salt concentration between 0.35 and 0.75 M correspond to a partial (< 55 bp) release of DNA from every core particle, or to a mixture of intact core particles and maximally (i.e. 55 bp-) released particles. Conceptually, it is easier to analyze the equilibrium from the latter, "two-state" model, and we shall adopt this point of view. What we are measuring (at least in the CD experiments) is the release of a fraction of the DNA, and unless the energetics of this process are non-linear in its extent, a two-state model should give meaningful results.

Therefore, we interpret the data in the following way. Each value of $f_{R,O}$ in Figure 7 is divided by the plateau value (0.37) to yield the fraction of nucleosomes which have their DNA extended ($f_{out}$). We compute an observed equilibrium contant $K_{obs}$ as

$$K_{obs} = \frac{1-f_{out}}{f_{out}} \qquad (8)$$

We have chosen to consider the binding reaction between the DNA tails and the histone core, rather than the unbinding reaction, so as to

make our analysis compatible with the formalism of Record et al. (1978).

If we then assume that Z/2 sodium ions are released from each of the DNA tails as its binds to the histone core, we can write, for the observed equilibrium constant at a particular NaCl concentration,

$$\ln K_{obs}\left([NaCl]\right) = \ln K_T^{o} + Z\xi^{-1}\ln(\delta\gamma\pm) - Z\psi\ln[NaCl] - (\Delta G_B([NaCl]) - \Delta G_B^{o})/RT \qquad (9)$$

The first term on the right, $\ln K_T^{o}$, is the logarithm of the thermodynamic equilibrium contant at 1 M NaCl for the standard-state tail-binding reaction, in which core particles at 1 M concentration are converted from the "tails released" state to the "tails bound" state. This term includes a contribution for bending the DNA in 1 M NaCl. The second term on the right, $Z\xi^{-1}\ln(\delta\gamma\pm)$, describes essentially the contribution to $\ln K_{obs}$ made by the activity coefficient of the DNA tails. It can be resolved into salt-independent and salt-dependent components (Record et al., 1978). The third term on the right, $-Z\psi\ln[NaCl]$, describes essentially the contribution to $\ln K_{obs}$ made by the dilution of $Na^+$ counterions as they are released during tail-binding. (The parameters $\xi$, $\delta$, and $\psi$ are from Manning's theory of counterion condensation (Manning, 1978; Record et al., 1978). The (dimensionless) parameters $\xi$ and $\delta$ are inversely and directly proportional, respectively, to the axial spacing of the negatively-charged phosphates on the DNA; $\xi = 4.2$, and $\delta = 0.56$. The parameter $\psi$ describes the extent of neutralization of the DNA phosphates by Na+ counterions, as is the sum of contributions by the tightly bound "condensation" layer and the more loosely associated

"screening" layer. It has the value 0.88.) The fourth term on the right, $-(\Delta G_B([NaCl]) - \Delta G_B^o)/RT$ describes the contribution to $\ln K_{obs}$ of the difference between the DNA bending free energy at the given NaCl concentration, and the DNA bending free energy at 1 M NaCl.

Equation (9) can be used to generate theoretical curves fitting the data of Figure 7. The method of generating these curves (curves 1-2 in Figure 7, curves 3-14 in Figure 12A, and curves 15-26 in Figure 12B) will be given in the Discussion.

Differentiating both sides of equation (9) with respect to ln[NaCl], and recognizing that $K_T^o$, Z, $\xi$, $\delta$, $\psi$, $\Delta G_B^o$, R and T are constants under this operation, we have

$$\frac{\partial \ln K_{obs}}{\partial \ln[NaCl]} = Z\xi^{-1} \frac{\partial \ln\gamma^{\pm}}{\partial \ln[NaCl]} - Z\psi - \frac{1}{RT}\frac{\partial \Delta G_B}{\partial \ln[NaCl]} \qquad (10)$$

Equation (10) allows us to estimate Z, the number of counterions released from the DNA in the tail-binding reaction, from the slope of a plot of $\ln K_{obs}$ versus ln[NaCl]. Such a plot, obtained from the data of Figure 7, is shown in Figure 9.

In order to estimate Z from Figure 9, we must first learn something about the relative magnitudes of the terms on the right-hand side of equation (10). The quantity $\ln \gamma^{\pm}$ is a nearly linear function of ln[NaCl], over the range 0.1-1 M NaCl (Lewis and Randall, 1961). Using $\gamma^{\pm}$ versus [NaCl] data (Lewis and Randall, 1961) and the above value of $\xi$, we calculate $\xi^{-1}\ \partial \ln\gamma^{\pm}/\partial \ln[NaCl] = 0.018$ over the 0.1-1 M NaCl range. Since this is only $\sim$2% the magnitude of $\psi$, the first term on the right of equation (10) can be ignored without introducing much error. The third term presents considerably more

Fig. III.9. Sslt-dependence of the observed equilibrium constant for the binding of DNA tails to the histone core

The data of Figure 7 were replotted by setting $f_{R,O}$ / $f_{R,O}$ (plateau) = $f_{out}$ , and $(1-f_{out}/f_{out}) \equiv K_{obs}$, as described in the text [cf. equation (8)]. The highest and lowest salt points from Figure 7 have here been omitted, because of their relatively large experimental uncertainties.

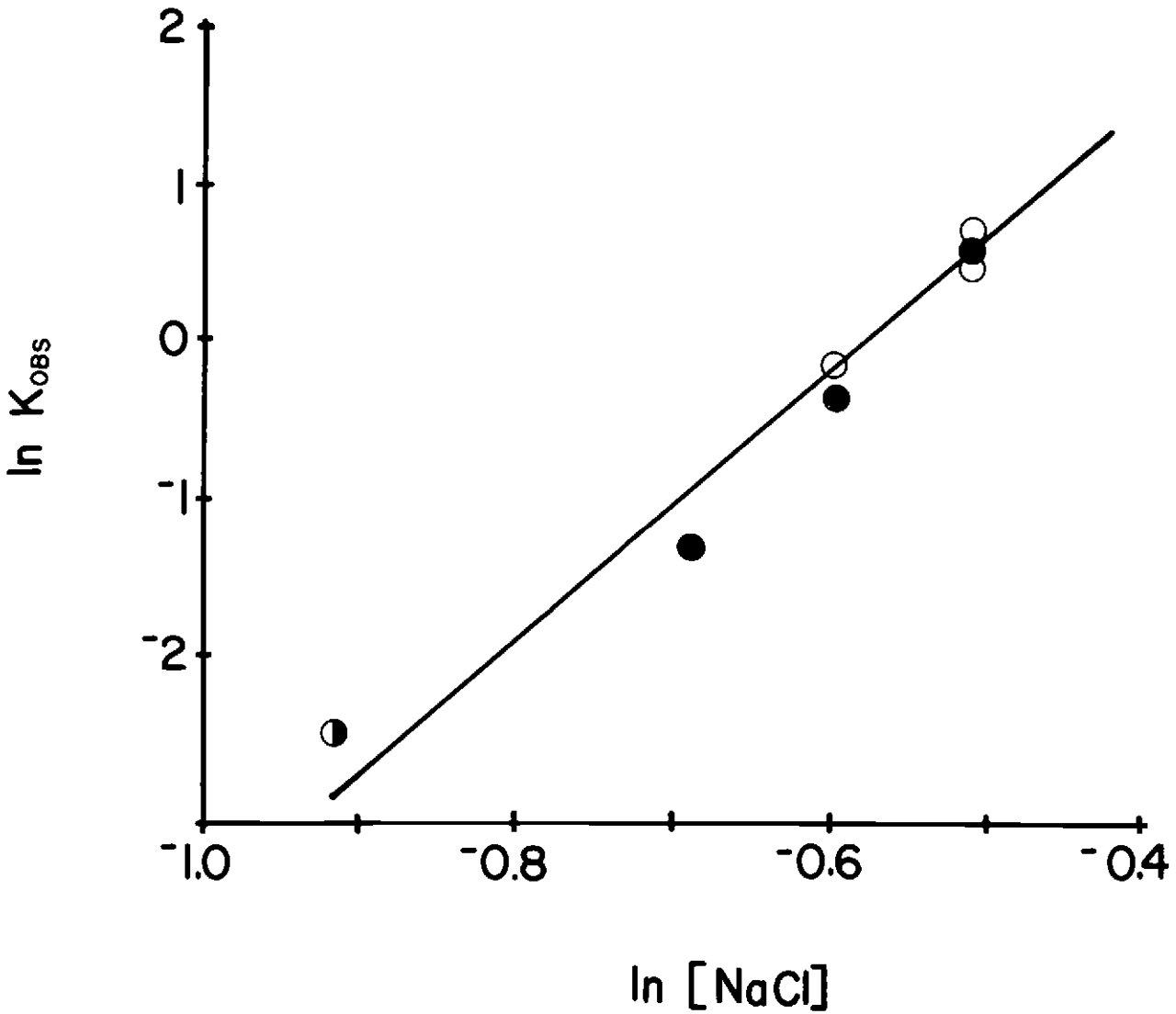


Figure III.9

problem. It is hard to believe that the bending free energy increases with bulk salt concentration, because of Manning's (1978) argument that much of the resistance to DNA bending comes from phosphate-phosphate repulsion in the backbone, which is screened by salt. Therefore, we assume that an upper limit for $(\partial \Delta G_B/\partial \ln[NaCl])/RT$ is zero. A numerical estimate of this term will depend on the particular theoretical model one assumes for the energetics of DNA bending. One general class of models (based on the treatment of small deformations of a thin uniform rod) yields, from persistance length data, the approximate inequality $-4.5 \leq (\partial \Delta G_B/\partial \ln[NaCl])/RT \leq -2.3$ (see Discussion). A second general class of models (based on calculating the potential energy of a deformed piece of DNA, using coordinates of the DNA's atoms and potential functions) yields estimates of $\Delta G_B$, but no indications of how this quantity might vary with bulk NaCl concentration (see Discussion). We therefore assume that a lower limit for $(\partial \Delta G_B/\partial \ln[NaCl])/RT$ is -3.4 (the average of calculations from the persistance length data; see Discussion).

If $(\partial \Delta G_B/\partial \ln[NaCl])/RT$ equals 0, then we calculate, from the slope of Figure 9 and from equation (10), that $Z \approx 9.8$. Similarly, if it equals -3.4, then we calculate $Z \approx 13.6$. We therefore conclude that, as the bulk salt is raised, 5-7 bonds are broken between the histone core and each DNA tail, as the tails come free into solution. Assuming 55 bp of DNA are released in the transition (see above) this equates to one bond every 4-6 bp, or to an involvement of approximately 9-12% of the available DNA phosphates in bonding of the DNA tails to the histone core.

We have examined the temperature dependence of the above equilibrium, by carrying out experiments at 0.65 M NaCl over a range of T. The results are most simply demonstrated by Figure 10: there is no temperature dependence, within experimental error. This means that the unfolding process must be entropy-driven. By this statement, we do not mean to imply that no enthalpy changes occur in the transition. If there are enthalpy changes, though, then they must cancel each other out to make the net driving force entropic. This will be elaborated upon in the Discussion.

## V. Discussion

The results described above delineate and distinguish two processes which occur when core particles are exposed to elevated concentrations of NaCl.

### A. The fast conformational change involves the release of DNA tails

The fast conformational change is detectable only at NaCl concentrations above 0.3 M. It is a rapid, reversible, concentration-independent process which produces a decrease in the sedimentation coefficient of about 15%, and an increase in the ellipticity at 282.5 nm corresponding to the conversion of about 55 bp of DNA in each nucleosome into a "free-DNA"-like state. It appears from the sedimentation experiments that every nucleosome can undergo the change, and that the change is limited to this fraction of the nucleosomal DNA.

Fig. III.10. The temperature-dependence of the unbinding of DNA tails from the histone core, in 0.65 M NaCl

The circular dichroism signal at 282.5 nm was measured for a blank (10 mM Tris, 0.25 mM EDTA, pH 7.5), and for a solution of core particles in this buffer (optical density at 282.5 nm = 0.9). During these measurements, the temperature was set as shown on the abscissa of this figure (uncertainty ± 0.25°C), was controlled to within ± 0.1°C. The core particles were then jumped to 0.65 M NaCl by the addition of 5 M NaCl in 10 mM Tris, 0.25 mM EDTA, pH 7.5 with stirring, and the increase in CD recorded. There was a 1.5-3 min gap in recording while salt was being added; subsequent to this, the first 1 min of recording was somewhat biased, because of temperature-reequilibration. Recording was continued for 10-15 min, during which time core particle dissociation began to occur. The value of the CD about 1 min after resumption of recording was the least biased, because at this time the temperature had reequilibrated, but not much dissociation had yet occurred. Therefore the 1 min values were used in subsequent computation of $f_{R,O}$. The core particle solutions were next made ~2.6 M in NaCl, the temperature reequilibrated, and the CD remeasured. Finally, the blank was recorded again, and the data corrected for baseline drift. $f_{R,O}$ was calculated as described in the text, and plotted against temperature.

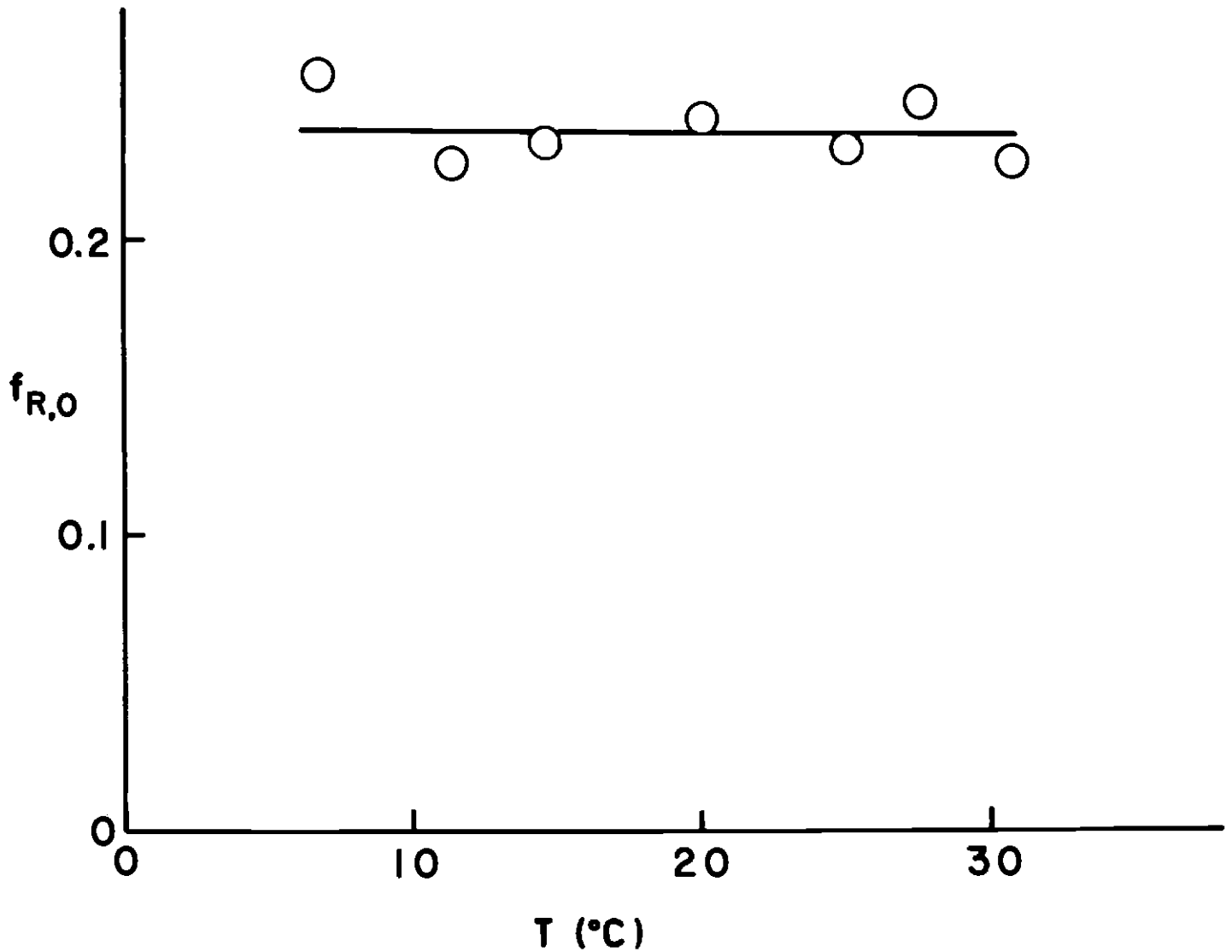


Figure III.10

In many respects, the conformational change resembles the first step in the thermal denaturation of nucleosomal DNA. Various workers have reported that about 40-55 bp of DNA are involved in this thermal transition (Weischet et al., 1978; Simpson, 1979; Simpson and Shindo, 1979; McGhee and Felsenfeld, 1980). It has been shown that the DNA released in this thermal transition lies at the two ends of the coil about the nucleosome core (Simpson, 1979). These earlier calorimetric studies of DNA tail-release, however, are rendered somewhat ambiguous by the fact that they were done under very low salt conditions (0.4-11 mM ionic strength). This range of ionic strength certainly spans the range in which the core particle undergoes an apparent "expansion", brought about by lowered ionic strength [reviewed in Uberbacher, et al. (1983)]. Only in the studies of Simpson (1979) and Simpson and Shindo (1979), in which I ≈ 11 mM, is the core particle undoubtedly in the "moderate salt" state pertinent to the present study. Even in these studies, though, some uncertainty exists, because poly(dA-dT)·poly(dA-dT) core particles were used, and 0.1 mM $Zn^{2+}$, pH 5.1 conditions sometimes prevailed (i.e. in S1 nuclease mapping of single-stranded regions of the DNA).

The decrease in sedimentation coefficient observed in the salt-dependent conformational change (Figure 4) corresponds almost exactly to that reported by Simpson (1979) for the first stage in thermal denaturation. In this context we note that, in hydrodynamic modeling, the decrease in $s_{20,w}$ which we observed is consistent with the "tail release" interpretation of the conformational change. We have employed the Kirkwood (1954) formalism, as detailed by Bloomfield et

al. (1967), to estimate the change in $s_{20,w}$ to be expected with various amounts of DNA tail release. Figure 11 depicts the results of these calculations. The maximum decrease in sedimentation coefficient which we observe in Figures 4 and 5 corresponds, by this model, to about 35 bp at each end of the DNA being released from the core, in fair agreement with the estimate from circular dichroism studies. However, three reservations should be noted with respect to the theoretical sedimentation analysis. First, as had been pointed out in numerous publications [for review, see Bloomfield, et al. (1974)], the model used is not exact. It should, however, be adequate for predicting relative s values. Second, hydration of the nucleosome is assumed to be invariant with NaCl concentration. However, a number of studies on the salt dependencies of DNA and protein hydration suggest that, in fact, hydration should decrease with increasing NaCl concentration [for reviews, see Tunis and Hearst (1968), Bloomfield et al. (1974), Kuntz and Kauzmann (1974)]. This would mean that the net decrease in $s_{20,w}$ which we observe actually has two components: a decrease due to the release of DNA tails, and a (smaller) increase due to diminished hydration. Therefore, in interpreting our observed decrease in $s_{20,w}$ according to the Kirkwood calculations (which account for only the first factor), we might be underestimating the actual extent of tail-release. Third, "DNA tail-release" is not the only model which can accomodate the hydrodynamic data. We have carried out similar calculations which show that the decrease in $s_{20,w}$ could be accounted for equally well by a small expansion of the entire core particle (not shown).

Fig. III.11A. Hydrodynamic Model for the Unbinding of DNA Tails from the Histone Core

The core particle is represented as a central frictional object, enwrapped by a helix of spherical beads. The helix of beads (small solid spheres, in Figure 11A) represents the DNA; it is assigned M = 650/bp x 146 bp = 94,900, and partial specific volume $\overline{v}$ = 0.499 $cm^3/g$ (Cohen and Eisenberg, 1968). The helix has a contour length of 146 bp x 3.4 Å/bp = 496.4 Å. It contains 28 beads of 8.76 Å radius each, equidistantly placed with centers 17.73 Å apart. A gap of 0.22 Å separates the surfaces of two adjacent beads, and there is a gap of 0.11 Å between the surface of each terminal bead and its respective end of the helix. The helix is placed around the central object at a radius R = 44.94 Å in a left-handed orientation, with pitch = 27 Å, in accordance with the model of Klug et al. (1980).

The central object represents the octamer of core histones. It is assigned M = 108,000 and $\overline{v}$ = 0.804 $cm^3/g$ (by calculation, assuming volumes of protein and DNA are additive). This implies a volume of 144 $nm^3$; an equivalent sphere has radius R = 32.5 Å, while a reasonable choice for an equivalent cylinder has height 35.8 Å and diameter 71.6 Å.

The unbinding of small beads at the ends of the helix represents the extension of DNA tails. To release the first bead, we move its center onto a vector that is tangent to the helix at its exit point on the succeeding bead. A comparable procedure is followed for the

last bead, at the other end of the helix. Thus, after unbinding, the first and last beads lie along their respective tangent vectors, with their centers 17.73 Å from the centers of the adjacent beads. Additional pairs of beads are released in a similar fashion.

This model may easily be generalized to nucleosomes with long DNA. Extra DNA beads (dashed spheres) are simply placed along the tangent vectors, such that the distances between beads' centers are always 17.73 Å.

Using the above model we calculate, for an unhydrated core particle of native conformation, a frictional coefficient $f_o$. We then multiply this by a hydration factor $f/f_o$, which takes into account the increase in friction of the particle due to hydration. We pick the hydration factor to yield s = 10.7 S for a core particle, using the Svedberg relation $s = M(1-v\rho)/Nf_o(f/f_o)$, where M, $\bar{v}$, $f_o$, $f/f_o$ are defined as above, $\rho$ = density of solution, and N = Avogadro's number. We find that, to obtain s = 10.7 S, we must assume a hydration of 0.83 g water/g nucleoprotein.

We next release the two DNA tails from the histone core, keeping the hydration constant in this process. This yields a ratio $s/s_o$ of sedimentation coefficients of "DNA tail-released" and "native" particles. We note that s of either particle depends on approximately the inverse 1/3 power of hydration. Thus a change in hydration between the two states should have only a very small effect on the $s/s_o$ ratio.

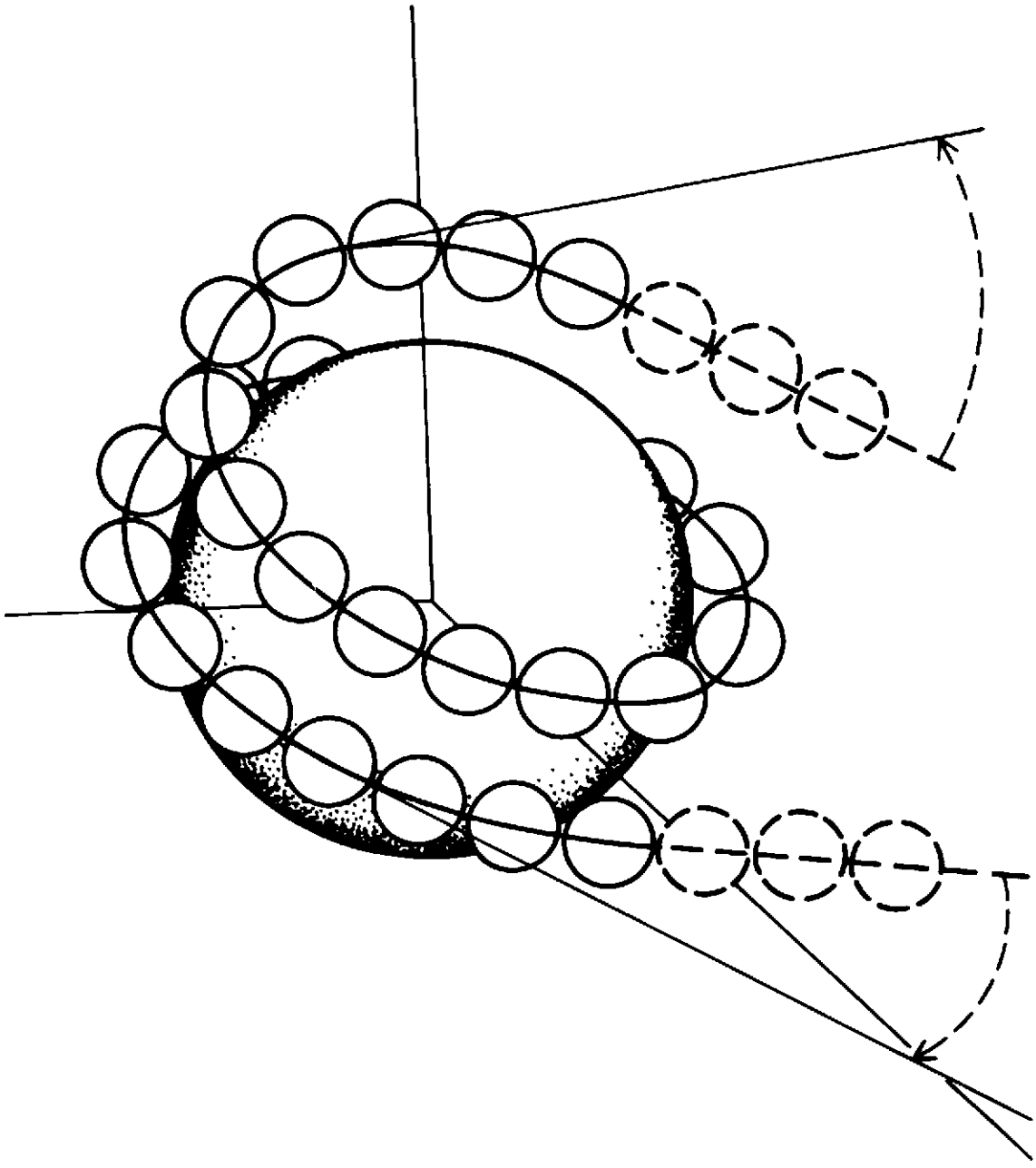

Figure III.11A

Fig. III.11B. Quantitative Predictions of the Hydrodynamic Model of Figure 11A

Two predictions of the above theoretical model are illustrated in Figure 11B. First, the helix termini are allowed to come off the core, one pair of beads at a time. This corresponds to unbinding terminal DNA from the core. Second, extra DNA beads are added. The beads are added in pairs, with each member of a pair going to one of the helix termini. This corresponds to increasing the length of the DNA in the tails, without additional unbinding of core DNA. As these two factors are varied, the ratio of s for a nucleosome of given tail length and extension to $s_o$ for a native core particle is calculated, and graphed.

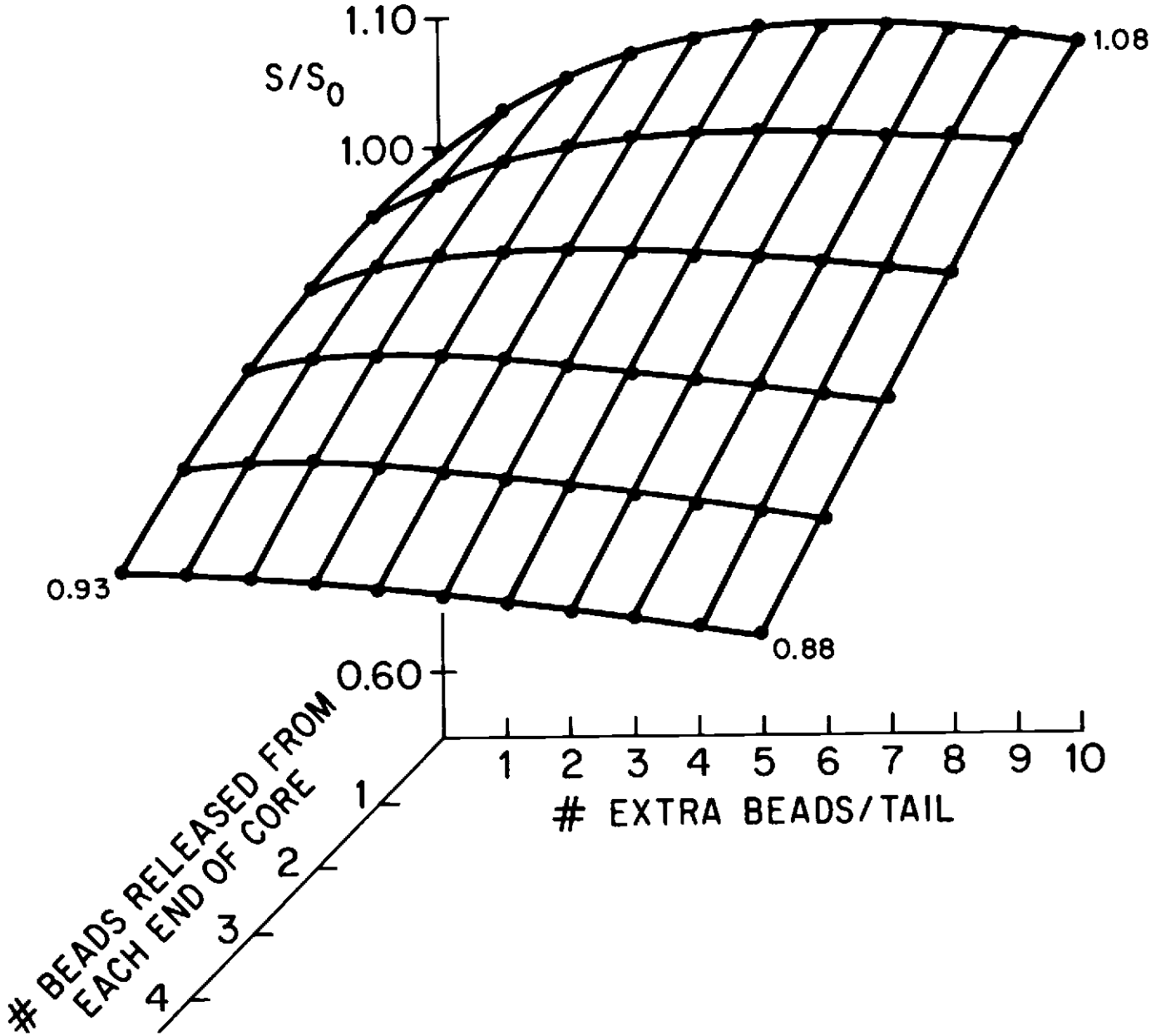


Figure III.11B

From the above discussion, it seems that both the CD and the sedimentation data could be interpreted in a fundamentally different way-that is, according to an "unfolding core particle" model. We therefore have consulted the literature for other studies of relevance, which may help us to decide between the two alternative models of "DNA tail release" and "core particle unfolding".

Cary et al. (1978) have presented proton NMR data to indicate that the N-terminal tails of histones H3 and H4 may become released at NaCl concentrations between 0.3 and 0.6 M. Although this would contribute to the decrease in $s_{20,w}$, it is difficult to see how it would explain the large increase in the circular dichroism of the DNA which we observe. Furthermore, there is evidence that proteolytic removal of the H3/H4 tails does not modify the pattern of bonding between the DNA and the histone core [as assayed by DNase I digestion patterns (Whitlock and Stein, 1978)], or the structure of the histone core itself (Cary et al., 1978; Whitlock and Stein, 1978).

Arguing against a global unfolding of the histone core are the results of H3-thiol reactivity studies (Zama et al., 1977; Wong and Candido, 1978; Bode and Wagner, 1980; Bode et al., 1980) and histone-histone crosslinking experiments (Wilhelm and Wilhelm, 1980). Neither type of study reveals significant rearrangement of the histone core over the salt concentration range studied here.

Recently, Ausio et al. (1984) have reported experiments in which the H3 molecules in core particles were crosslinked together through -S-S- bridges. The decrease in $s_{20,w}$ with increasing salt concentration was unaffected by this modification.

Finally, Libertini and Small (1982) have examined histone tyrosine fluorescence in core particles over a KCl concentration range spanning 0.01-0.75 M (using a core particle concentration high enough to prevent significant dissociation). They find no change in either the intensity or the anisotropy of the fluorescence from 0.01 to 0.60 M KCl. From 0.60 M to 0.75 M KCl, they observe only a slight increase in intensity, and a slight decrease in anisotropy; the magnitude of each change corresponds to about 10% of what would be observed were the salt raised to 1.5 M. The slight increase in intensity presumably is due to a slight "loosening" of the histone/DNA contacts (hence less quenching of fluorescence by DNA), while the slight decrease in anisotropy presumably is due to a slight increase in the "flexibility" of the core. This study therefore suggests that histone core structure changes very little from 0.01 to 0.75 M KCl.

We conclude that there is no evidence for a significant change in histone core structure, other than H3/H4 tail release, over the salt range we have studied. Consequently, we tentatively rule out a global unfolding of the core particle as an explanation for our data. We feel that the "DNA tail-release" model is the only one which can both explain the CD data and still be consistent with the sedimentation experiments. Moreover, it satisfies the prediction from thermal denaturation studies (see above) and from structural considerations (see below) that the DNA tails should be released preferentially to the rest of the DNA, as the salt is raised.

In this connection, it should be noted that Harrington (1982) has interpreted flow birefringence measurements at elevated KCl concentrations in terms of a similar model. There may be some ambiguity in the interpretation of his experiments, though, for the following reasons. (i) His core particles were prepared by sedimentation through a sucrose gradient containing 0.6 M KCl, followed by dialysis into a low ionic strength buffer. Sedimentation through high salt may have caused the generation of non-equilibrating, extra free DNA in his core particle preparation; this effect has been noticed before, in preparation of long-DNA nucleosomes (Yager and van Holde, 1984). Although free DNA was not apparent as a second peak in his sucrose gradient profile, a 10% shoulder in the core particle peak may not have been observable. (ii) Harrington did not take into account possible additional dissociation of the core particles, as the salt concentration was again raised, in preparation for flow birefringence measurements. However, he has informed us (R. E. Harrington, personal communication) that the measurements were carried out less than one hour after mixing, and at 20°C; dissociation would tend to be minimized by the small duration of the lag phase, and by the low temperature (Yager and van Holde, 1984), and unpublished experiments; Ausio et al., 1984).

In our interpretation of the CD studies, there is some uncertainty as to the exact number of DNA base pairs released in the fast step. This uncertainty has at least two sources. (i) There are dilution errors both during the first addition of salt to release the

DNA tails, and during the second addition of salt to give complete dissociation. (ii) It is possible that some dissociation occurs after the first salt addition, but before the cuvette has been replaced in the spectropolarimeter. (A lag time of 1.5-3 min is unavoidable.) We note that, if error source (ii) is significant, our estimate of 55 bp DNA released in the fast step will be biased somewhat high.

B. Estimates of the number of bonds holding the DNA tails to the histone core

Our estimate of the number of bonds holding the DNA tails to the histone core is based on evaluating the slope of Figure 9, according to equation (10). A major uncertainty lies in establishing a numerical value for the term $(\partial \Delta G_B/\partial \ln[NaCl])/RT$, which describes the salt dependence of the free energy change for DNA bending.

One general class of estimates for DNA bending free energy involves the use of the Landau and Lifschitz (1958) theory for small deformations of a thin, uniform rod (Schellman, 1974; Harrington, 1977). A central result of the theory of Landau and Lifschitz is that, for uniform bending, the bending free energy is directly proportional to the Kratky-Porod persistence length. The persistence length of free "B" DNA has been studied as a function of NaCl concentration, both by Harrington (1978) and by Eisenberg and coworkers (Borochev et al, 1981; Kam et al, 1981). When we replot the data of the three studies as persistence length versus ln[NaCl] we find, over the 0.1-1 M NaCl range, that the persistence length is an approximately linear function of ln[NaCl]. Obtaining slopes from these

plots, and inserting them into the formula of Landau and Lifschitz [see Harrington (1977)], we calculate $(\partial \Delta G_B/\partial \ln[NaCl])/RT = -2.3$, $-3.4$ or $-4.5$, from the data of Borochov et al. (1981), Kam et al. (1981) and Harrington (1978), respectively. These data yield a mean value ± S.D. of $-3.4 \pm 1.1$.

It may be questioned as to whether the uniform bending model is appropriate to this problem. The model was developed for small deformations of a uniform long rod, and we are dealing with large deformation of a short segment of DNA. Unfortunately, none of the other models which have been presented for DNA bending (Crick and Klug, 1975; Sobell et al., 1976; Levitt, 1978; Sussman and Trifonov, 1978; Keepers et al., 1982; Tidor et al., 1983) allow a calculation of the dependence of the bending free energy on salt concentration. Since the uniform bending model can be expressed in terms of the persistence length, and this quantity has been reported as a function of salt concentration, an estimate of $(\partial \Delta G_B/\partial \ln[NaCl])/RT$ is possible. Even if the absolute value of $\Delta G_B$ may be incorrect in our calculations, we might presume that the salt dependence, which depends on an experimental parameter, the persistence length, might not be in gross error.

Our estimate of the percent of DNA phospates involved in tail-binding (9-12%) agrees quite well with the earlier estimate by McGhee and Felsenfeld (1980) of 15 ± 6%. The earlier estimate was obtained by analyzing the salt-dependence of the first thermal transition in core particles. We note that it involved calculating relatively small differences between large numbers, and therefore may have been

subject to larger errors than the present study. Also, it was done under conditions where the undenatured core particles probably were in the "low ionic strength expanded state" (see above). Finally, it treated the effects of DNA bending in a rather different way than we have (see below). Thus we feel it is important to have confirmed this earlier estimate by the present method.

Neither our nor McGhee and Felsenfeld's estimates agree very well with one that might be made using data of Mirzabekov and coworkers (Mirzabekov et al., 1978; Shick et al., 1980). These workers, using a DNA/histone crosslinking reaction, estimate about one DNA/histone "contact" every 5 bp for the central 95-105 bp of DNA in the core particle, but only 1-2 "contacts" for each of the DNA "tails". There is a fundamental difficulty, however, in equating a "contact" with a bona fide DNA/histone bond, for the following reason: Mirzabekov and coworkers propose that, in their crosslinking reaction, a deoxyribose aldehyde is generated on the DNA by depurination with dimethyl sulfate. This aldehyde then reacts with the ε-amino group of a histone lysine, to form a stable Schiff's base. If this indeed is the correct mechanism, then we may conclude the following. The deoxyribose aldehyde lies 4-5 bond lengths (about 5 Å) distant from the phosphoryl oxygen presumably involved in the nearest DNA/histone bond. Thus, a reaction at the deoxyribose aldehyde group is not really topographically equivalent to a reaction at the nearest phosphoryl oxygen. Also, we present evidence in the next section suggesting that it is arginines, and not lysines, which are involved in DNA/histone bonding. Thus we feel that the data of

Mirzabekov and coworkers, while accurately reporting positions of stable contact between ε-amino groups of histone lysines and aldehyde groups of DNA deoxyriboses, really do not address the question of bona fide DNA/histone bonds. (It is worth noting, in this discussion, that the crosslinking reaction of Mirzabekov and coworkers was done under conditions where the ionic strength I ≈ 170 mM [see Butler (1964)]. Thus, in their core particles, the DNA tails were bound considerably less tightly to the histone core than they would have been at lower ionic strength [cf. Figure 9 and equation (9)]. This may be the reason Mirzabekov and coworkers observed such a small number of DNA/histone "contacts" in the region of the DNA tails, relative to the number of contacts in the central DNA region).

C. The strength of the bonds holding DNA tails to the core

We may obtain more information from Figure 9, using the analysis developed by Record et al. (1978), and embodied in equation (9). Upon extrapolation of the curve in Figure 9 to 1 M NaCl, we find $\ln K_{obs}$ (1 M) = -4.8. We insert this value into equation (9), together with appropriate values of ξ, δ, $\gamma^{\pm}$ and ψ. with Z = 9.8 and $(\partial \Delta G_B/\partial \ln[NaCl])/RT = 0$ (see above), we calculate $\ln K_T^o$ = -2.4. Similarly, with Z = 13.6 and $(\partial \Delta G_B/\partial \ln[NaCl])/RT = -3.4$ (see above), we calculate $\ln K_T^o = -1.6$. We have used these two sets of values, in conjunction with equations (9) and (8), to generate theoretical curves for $f_{R,O}$ versus NaCl concentration (curves 1 and 2, respectively, in Figure 7; parameters listed in Table I). The curves provide good fit to the experimental points.

Table I. Parameters of the theoretical curves of Figures 7, 12A, and 12B.

| Figure | Qualitative nature of curves | curve # | Z | $\ln K_T^o$ | $\Delta G_B^o$(kcal/mol) | $\frac{1}{RT}\frac{\partial \Delta G_B}{\partial \ln[NaCl]}$ |
|---|---|---|---|---|---|---|
| 7 | Best fit of data of Figs. 7,9 to eqns. (9),(10) | 1 | 9.8 | - 2.4 | * | 0 |
| | | 2 | 13.6 | - 1.6 | * | -3.4 |
| 12A | Model of oligolysine/DNA interaction, with bending terms: eqns. (9), (12), (13) | 3 | 9.8 | -18.7 | 9 | 0 |
| | | 4 | 9.8 | -18.7 | 9 | -3.4 |
| | | 5 | 9.8 | -32.5 | 17 | 0 |
| | | 6 | 9.8 | -32.5 | 17 | -3.4 |
| | | 7 | 9.8 | -73.7 | 41 | 0 |
| | | 8 | 9.8 | -73.7 | 41 | -3.4 |
| | | 9 | 13.6 | -20.1 | 9 | 0 |
| | | 10 | 13.6 | -20.1 | 9 | -3.4 |
| | | 11 | 13.6 | -33.8 | 17 | 0 |
| | | 12 | 13.6 | -33.8 | 17 | -3.4 |
| | | 13 | 13.6 | -75.1 | 41 | 0 |
| | | 14 | 13.6 | -75.1 | 41 | -3.4 |
| 12B | Model of oligoarginine/ DNA interaction, with bending terms; eqns. (9), (12), (13) | 15 | 9.8 | - 9.4 | 9 | 0 |
| | | 16 | 9.8 | - 9.4 | 9 | -3.4 |
| | | 17 | 9.8 | -23.2 | 17 | 0 |
| | | 18 | 9.8 | -23.2 | 17 | -3.4 |
| | | 19 | 9.8 | -64.4 | 41 | 0 |
| | | 20 | 9.8 | -64.4 | 41 | -3.4 |
| | | 21 | 13.6 | - 4.0 | 9 | 0 |
| | | 22 | 13.6 | - 4.0 | 9 | -3.4 |
| | | 23 | 13.6 | -20.8 | 17 | 0 |
| | | 24 | 13.6 | -20.8 | 17 | -3.4 |
| | | 25 | 13.6 | -62.0 | 41 | 0 |
| | | 26 | 13.6 | -62.0 | 41 | -3.4 |

* Not relevant to this calculation. Here $\ln K_T^o$ is the observed quantity, which presumably contains contributions from both DNA/histone association and DNA bending.

It is possible to attempt a more fundamental analysis. Data exist for the binding affinities of various model oligopeptides to DNA. From such binding affinities, the experimentally determined number of binding sites, and estimates of the DNA bending free energy, one may attempt to predict the locations of the experimental points in Figure 7.

An example of such a prediction is the following. We know from the analysis of oligolysine/DNA interactions made by Record et al. (1978) that an assemblage involving Z canonical "lysine/phosphate"-like bonds obeys the formula

$$\ln K_{obs}([NaCl]) = \ln K_T^{o\prime} = Z\xi^{-1}\ln(\delta\gamma\pm) - Z\psi\ln[NaCl] \quad (11)$$

where $\ln K_T^{o\prime} = -0.34 \cdot Z$. Here, we have generalized the binding data of Record et al. (1978) for $(L\text{-}Lys)_5$ and double-stranded "B" DNA at pH 7.63 and 20°C, recognizing that the contributions of the separate lysyl residues are believed to be additive (Record et al., 1978) and that this type of nucleic acid and this pH are closest in nature to those of our own study. It should be noted, however, that, in Formula (11), there are no terms for the bending of the DNA. We indicate this fact by attaching a superscripted prime to the symbol $K_T^o$ in the formula.

For assemblages of Z = 9.8 or 13.6 "lysine/phosphate"-like bonds, $\ln K_T^{o\prime} = -3.3$ or $-4.6$, respectively. We find that these values correspond to standard free energy changes (in 1 M NaCl) of +1.9 or +2.7 kcal/mol, respectively, from the relation:

$$\Delta G_T^{o\prime} = -RT \ln K_T^{o\prime} \quad (12)$$

We next turn to estimating the standard free energy change $\Delta G_B^o$ (in 1 M NaCl) of bending 55 bp of DNA (two "tails") from a "straight" configuration into the configuration it would have in the core particle. Treatment by the theory of Landau and Lifschitz yields estimates of 7.6, 8.1, or 12.4 kcal/mol at 1 M NaCl (mean ± S.D. = 9.4 ± 2.6 kcal/mol), depending on which set of data on DNA persistence length in 1 M NaCl is used (see above). Calculations by Levitt (1978) yield minimum and maximum estimates of 9 and 17 kcal/mol when van der Waal's repulsion is ignored, and an estimate of 41 kcal/mol when van der Waal's repulsion is taken into account.

We will consider separately three families of cases, where $\Delta G_B^o \simeq 9$, 17 or 41 kcal/mol. To investigate the behavior of an assemblage of "lysine/phosphate"-like bonds <u>subject to the bending constraint</u> we write, for the free energy change $\Delta G_T^o$ of the association reaction in the standard state (1 M NaCl),

$$\Delta G_T^o = \Delta G_T^{o\prime} + \Delta G_B^o \qquad (13)$$

Assuming Z = 9.8, $\Delta G_T^{o\prime} = +1.9$ kcal/mol, and the three estimates above for $\Delta G_B^o$, we calculate $\Delta G_T^o = 10.9$, 18.9 or 42.9 kcal/mol. From an analogue to equation (12) (without the superscripted primes), we thus obtain $\ln K_T^o = -18.7$, -32.5 or -73.7, respectively. Similarly, assuming Z = 13.6, $\Delta G_T^{o\prime} = +2.7$ kcal/mol, and the three estimates above for $\Delta G_B^o$, we calculate $\Delta G_T^o = 11.7$, 19.7 or 43.7 kcal/mol, and so $\ln K_T^o = -20.1$, -33.8 or -75.1.

These <u>synthetic</u> values of $\ln K_T^o$, and their companion values of Z, are next inserted into equation (9), along with appropriate

values of $\xi^{-1}$, $\delta$, $\psi$, ln[NaCl], and $\gamma^{\pm}$. The term $(\Delta G_B([NaCl]) - \Delta G_B^o)/RT$ is approximated by $(\ln[NaCl])\cdot(\partial\Delta G_B/\partial \ln[NaCl])/RT$. In this way, we are able to predict curves for the salt-dependence of the association of $(L\text{-}Lys)_{9.8 \text{ or } 13.6}$ with double-stranded DNA, subject to the bending constraint (curves 3-14, Figure 12A; parameters summarized in Table I).

An examination of curves 3-14 in Figure 12A shows that, if the bonds holding the DNA tails to the core are assumed to be of the canonical "lysine/phosphate"-type, then the "associated" or "tails in" state cannot be achieved until the bulk salt concentration is dropped to quite low values (< 0.2 M NaCl). Because this clearly is at odds with our observations (midpoint of transition ≈ 0.6 M), we conclude that, in the actual DNA tail-binding reaction in core particles, the bonding must be considerably stronger than the canonical "lysine/phosphate" type.

This result is not unexpected. Ishimura et al. (1982) have observed that, when core particles in various concentrations of salt are subjected to a reagent which reacts with lysine ε-amino or arginine guanidino groups, the extent of reaction with lysines is independent of salt, while the extent of reaction with arginines increases with increasing salt. They interpret this to mean that, in low salt, certain arginines are protected from reaction by the DNA; at elevated salt concentrations, the DNA is stripped away, allowing these particular arginines to react. A second, though less direct, line of evidence implicating arginines in bonding comes from the study of Rill and Oosterhof (1982). These workers found that, in

Fig. III.12A. Theoretical Curves for the Salt-Dependent Binding of DNA to Oligolysines

An attempt was made to fit the experimental points in Figure 7 with a theoretical model involving binding interactions, plus a contribution to the energetics by DNA bending. The binding interactions were of the "oligolysine/DNA" type. Curves 3-14 (Figure 12A) were generated using equation (9) and the values of $\ln K_T^o$, Z, $\Delta G_B^o$, and $(\partial \Delta G_B / \partial \ln[NaCl])/RT$ given in Table I, 2nd portion. Also shown in Figure 12A are the data of Figure 7 (open and closed circles).

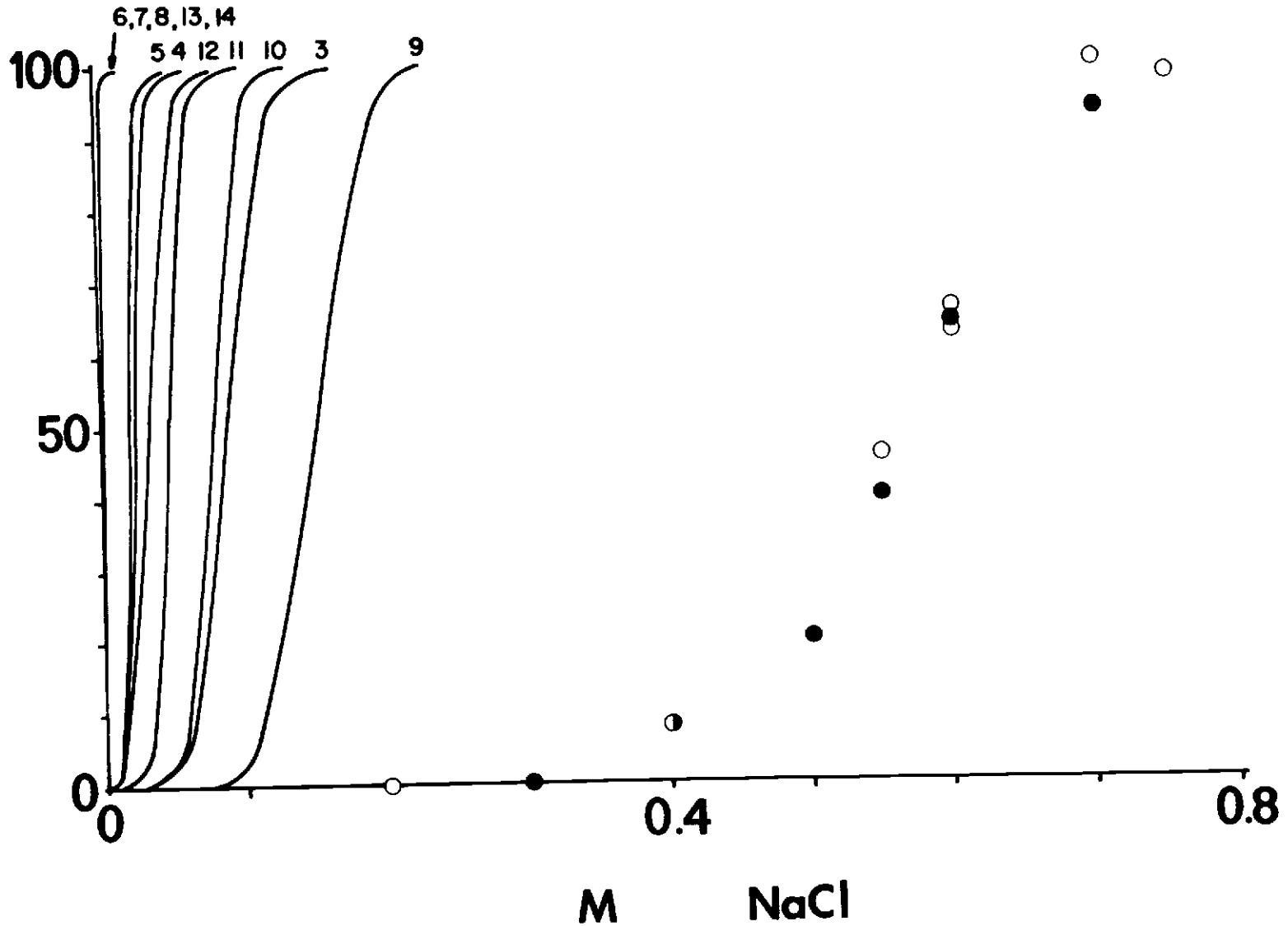


Figure III.12A

core particles, many of the arginines in the core histones are protected from attack by an arginine-specific protease. A third line of evidence for the involvement of histone arginines in the binding of DNA in chromatin comes from the Raman-spectroscopic study of Peticolas and coworkers (Mansy et al., 1976). These workers have identified the 1490 $cm^{-1}$ Raman band as due to a stretching vibration of the $N^7$-C bond in guanine. They find that, in comparison to free DNA, the intensity of this band is decreased (relative to an internal standard of the 1097 $cm^{-1}$ phosphate band), for DNA that is complexed with N-α-acetyl arginine, poly(L-arginine), or the histones (plus contaminating non-histone chromosomal proteins) in chromatin. They ascribe this decrease in intensity of the 1490 $cm^{-1}$ band to the formation of a specific hydrogen bond between the guanidino group of arginine and the $N^7$-amine of guanine. They observe a 10% decrease in intensity, which is the magnitude one would expect if 145/210 ≈ 70% of the DNA in chromatin were comlexed to core histones to form core particles (the remaining 65/210 ≈ 30% being in linker DNA (Lewin, 1980), and if ∼14.5% of the guanines (i.e. 14.5% of all bases, assuming the DNA sequence is random) were involved in bonding to the core histones. We note that both Ishimura's group and Peticolas' group postulate a substantial nonelectrostatic (primarily hydrogen-bonding) component in the interaction of arginyl residues with DNA.

Felsenfeld and coworkers have measured the equilibrium constants for the binding of $(L\text{-}Arg)_3$, $(L\text{-}Arg)_5$ and $(L\text{-}Arg)_7$ to DNA, as a function of NaCl concentration (G. Felsenfeld, personal communication). Extrapolating their ln $K_{obs}$ vs. ln [NaCl] data to 1 M NaCl and

using equation (11), we calculate ln $K_T^{o\prime}$ (mean ± S.D.) = +(0.62 ± 0.10)·Z, for their three sets of data.

We consider once again three families of cases, where $\Delta G_B^o$ = 9, 17 or 41 kcal/mol, and proceed to investigate the behavior of an assemblage of Z = 9.8 or 13.6 "arginine/phosphate"-like bonds, subject to DNA bending. From equations (12) and (13) and the data of Felsenfeld and coworkers, we calculate $\Delta G_T^o$ = +5.5, 13.5 or 37.5 kcal/mol for Z = 9.8, and $\Delta G_T^o$ = +2.3, 12.1 or 36.1 kcal/mol for Z = 13.6. These values translate to ln $K_T^o$ = -9.4, -23.2 or -64.4 (for Z = 9.8), or to ln $K_T^o$ = -4.0, -20.8 or -62.0 (for Z = 13.6). Following the same calculational procedure as for the synthetic oligolysine/DNA curves of Figure 12A, we now generate analogous oligoarginine/DNA curves, which are shown in Figure 12B (curves 15-26; parameters summarized in Table I).

For the synthetic binding curves of $(L\text{-}Arg)_{9.8 \text{ or } 13.6}$ with DNA, the fit to the observed data is much better than for the corresponding oligolysine/DNA curves. In fact, for curve 21 (where Z = 13.6, DNA tail-bending in 1 M NaCl is assumed to cost only 9 kcal/mol, and no dependence of bending free energy on salt concentration is assumed), the synthetic curve lies within experimental error to the observed points. We conclude that the bonds between the histone core and the DNA tails are exceptionally strong-perhaps even stronger than expected from the oligoarginine/DNA model data (see below, also).

Fig. III.12B. Theoretical Curves for the Salt-Dependent Binding of DNA to Oligoarginines

The fitting procedure of Fig. 12A was repeated, except that this time, the binding interactions were of the "oligoarginine/DNA" type. Curves 15-26 (Figure 12B) were generated using equation (9) and the values of $\ln K_T^o$, Z, $\Delta G_B^o$, and $(\partial \Delta G_B / \partial \ln[NaCl])/RT$ given in Table I, 2nd portion. Also shown in Figure 12B are the data of Figure 7 (open and closed circles).

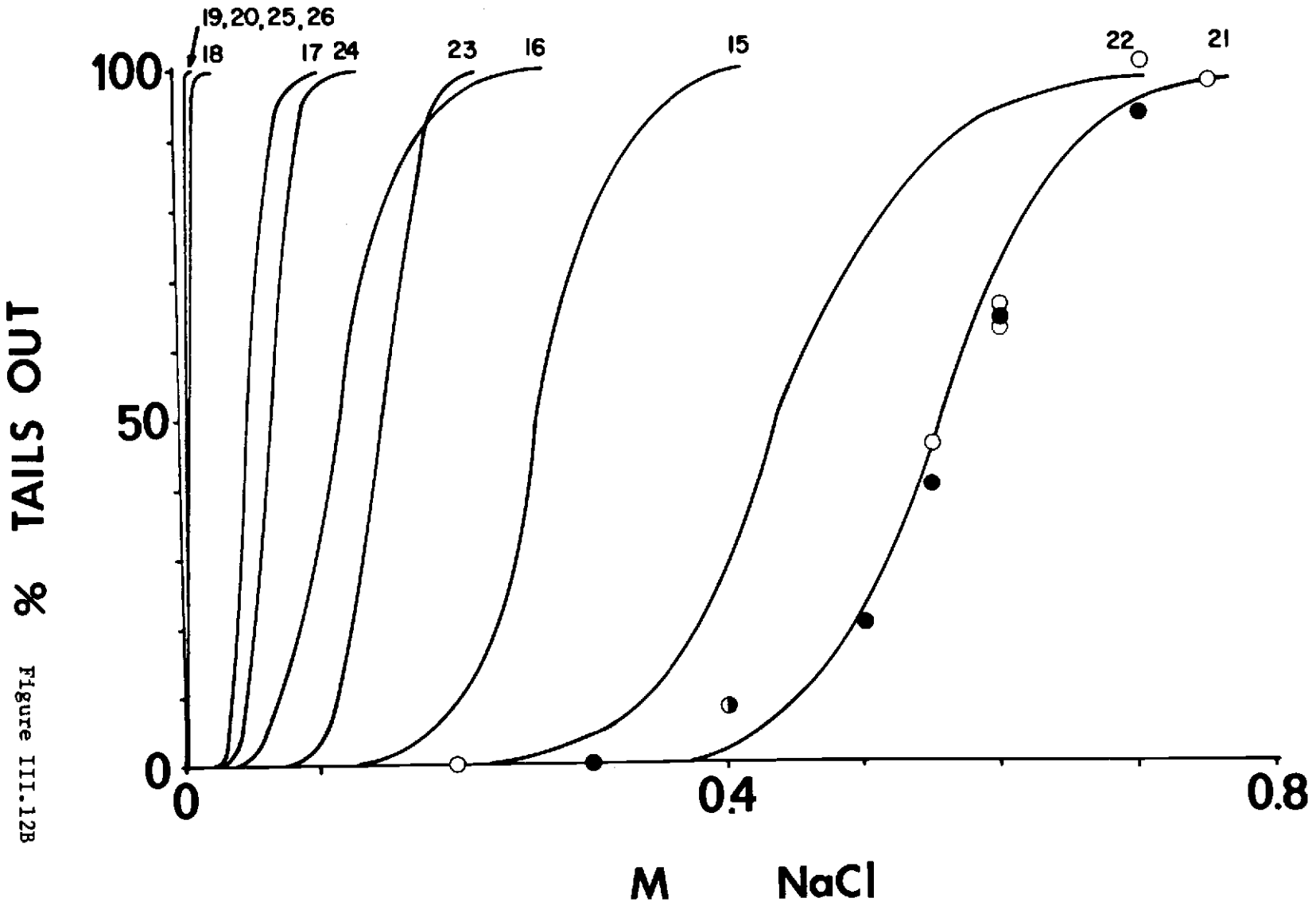


Figure III.12B

D. The problem of DNA topology in the core particle

As pointed out by McGhee and Felsenfeld (1980), the central 80 bp of DNA in the core particle forms one complete turn, or coil, about the histone core. The two DNA tails, ~30 bp each, then lie in additional coils closely apposed to the central one. Assuming the DNA in a core particle to have a pitch of ~27 Å (Klug et al., 1980), and assuming the non-hydrated radius of the DNA to be ~11 Å (Wing et al., 1980; Drew et al., 1981), we calculate that the phosphates of the respective coils approach each other to within ~5 Å. Thus there is a repulsion between adjacent coils, which is relieved when the two tails are allowed to project off the core. We therefore expect, solely on the basis of DNA topology in the core particle, that the bonding between the histone core and the two DNA tails should be of lower stability than that between the histone core and the central portion of the DNA. This in turn predicts that a plateau should be seen, both in the salt-dependence of the tail-release reaction, and in the thermal denaturation of core particles. The former prediction is confirmed in this paper, and the latter is confirmed by the work of Weischet et al. (1978), Simpson (1979), Simpson and Shindo (1979), and McGhee and Felsenfeld (1980) (though note our reservations, above, about the exact state of the core particle in the thermal denaturation studies). We note that this explanation of the plateau phenomena does not require the tail DNA/core bonds and the central DNA/core bonds to be of different chemical types.

When "coil-coil repulsion" is considered, extra uncertainty is introduced into our estimates of $\Delta G_B^o$ and $(\partial \Delta G_B/\partial \ln[NaCl])/RT$.

More importantly, though, we note that the "coil-coil repulsion" effect must always act to destabilize the binding of DNA tails. Thus our conclusion is reinforced that the core/tail bonds are exceptionally strong.

E. The relationship between tail release and dissociation

Are the fast "tail release" reaction and the slow dissociation process interrelated? It was our first impression that tail release might be a necessary prelude to dissociation. But closer inspection of the data shows that this cannot be so. We find no evidence, either by sedimentation or circular dichroism, for the tail release reaction at NaCl concentrations less than 0.3 M (cf. Figures 4, 7). Yet Figure 3 shows that dissociation can be detected in dilute nucleosome solutions even at very low salt concentrations ($\sim$0.1 M). This conclusion is reinforced by observations of dissociation at even lower ionic strengths [as monitored with particle gels (not shown); see also Yager and van Holde (1984)]. Neither is the beginning of dissociation a likely prelude to the tail release reaction, since the latter is observed immediately, even at temperatures low enough that dissociation is slow or non-existant [cf. Figure 10, and Ausio et al. (1984)]. The processes should then be thought of as parallel and independent, at least in core particles.

In H1-depleted long chromatin, the situation may be more complex. When nucleosomes are spaced regularly along a long piece of DNA, the release of 55 bp of DNA from the terminal portion of each nucleosome would allow much more room for sliding of the histone

cores. In particular, it would allow two cores to slide close enough together to form the "compact dimers" which have been reported by several groups (Klevan and Crothers, 1977; Steinmetz et al., 1978; Crothers et al., 1978; Tatchell and van Holde, 1978; Beard, 1978; Weischet, 1979). It is noteworthy that in Weischet's studies, compact dimer formation could only be detected at salt concentrations above 0.3 M. [Beard (1978), however, has shown that some nucleosome sliding occurs in chromatin at ionic strengths as low as 0.15 M]. Such a tail release reaction in bulk chromatin deserves more extensive study. In H1-depleted chromatin, it would result in over half of the DNA in each repeat length being freed from the histone core.

We may ask what the status of the nucleosome is in situ. It has been suggested, on the basis of electrophysiological measurements, that the ionic strength inside of a cell is $I \approx 0.1$ [Hoagland and Davis, 1922-3; Shaw, 1955; Conway, 1957; but see Hodgkin (1958) for a measurement of $I \approx 0.4$. A brief review of these measurements, and of their methodology, is given in Giese (1973)]. Calculations suggest that, at least in the mammalian interphase nucleus, the total volume of chromatin is only about 5-15% of the nuclear volume (Giese, 1973; Lehninger, 1975; Lewin, 1980; Lewin, 1983). Therefore it may still be meaningful to speak of a "solution ionic strength" in the nucleus. We assume, then, that the value $I \approx 0.1$ is applicable to the nucleus. Using the parameters for the theoretical curves in Figure 7, we calculate $K_{obs}$ (0.1 M) $\approx 5 \cdot 10^6$, which corresponds to $\Delta G^o$ (0.1 M) = -9 kcal/mol for the "tails out" $\rightarrow$ "tails in"

reaction. (Note: this free energy change is for the standard state reaction where core particles at a concentration of 1 M change from the "tails out" state to the "tails in" state, but where [NaCl] = 0.1 M.) Thus it appears that the "tails in" state is favored considerably in vivo. However, the moderate magnitude of $\Delta G^{o}$ in 0.1 M salt suggests that DNA tail release, under certain circumstances, could occur-for example, through histone modification, or through interaction with non-histone proteins.

The above analysis suggests a possible role of histone modification and non-histone protein binding on the "DNA tail release" transition. Such effects could be studied using core particles as a model system. If tail release could be induced at physiological ionic strength, it would be implicated as a process possibly of major importance in DNA transcription, repair and replication.

## VI. Appendix - Evaluation of a temperature-correction term in the CD equations

Consider the function

$$Z(T) = \frac{\theta_{S,O} - r\theta_o}{r''g\,\theta_h - r\theta_o} \qquad \text{(A-1)}$$

where the terms on the right-hand side of this equation are defined as in equation (7) and the text. Z(T) is the <u>apparent</u> fraction of DNA base pairs released in the fast step at the given salt concentration, and is assumed to depend on T through containing the term $[\theta]_O^{S,T}$ (which applies to the released DNA tails) in both its numerator and denominator. We want to evaluate Z(T) as T changes. $f_{R,O}$ is the <u>true</u> fraction of DNA base pairs released in the fast step, at a given concentration of salt [see equation (7)]. For purposes of this argument, we assume $f_{R,O}$ to be invariant with temperature. Substituting into equation (A-1) from the equalities $\theta_o = lC\,[\theta]_N$, $r = C'/C$, $r'' = C'/C''$, and $g\theta_h = lC''\,[\theta]_D$ [see equation (7) and text], we obtain

$$Z(T) = \frac{C'l\left([\theta]_N(1-f_{R,O}) + f_{R,O}[\theta]_D^{S,T}\right) - C'l\,[\theta]_N}{C'l\,[\theta]_D^{S,T} - C'l\,[\theta]_N} \qquad \text{(A-2)}$$

Rearranging and cancelling identical terms out of numerator and denominator, we obtain

$$Z(T) = f_{R,O} \qquad \text{(A-3)}$$

which is invariant of temperature, according to our assumption above. Thus no temperature correction to equation (7) is necessary.

## VII. Acknowledgements

In this particular work (thesis, part 3), Cynthia T. McMurray was responsible for designing method #2 for the preparation of nucleosomes, and for obtaining nucleosomes by this method. Thomas D. Yager and K.E. van Holde were responsible for the design and realization of the experiments, for the theoretical analyses, and for writing the manuscript.

We would like to express our appreciation to E.M. Bradbury, H. Eisenberg, G. Fasman, G. Felsenfeld, R.E. Harrington, W.C. Johnson, J.C. Wang, H. Wickman and P.H. von Hippel for discussion and advice, and to G. Felsenfeld for providing us with unpublished data on oligoarginine/DNA interactions. Also, within our own research group, we would like to thank A. Paton for nucleosomes prepared by method #1, C. Poklemba for expert technical help in preparing nucleosomes by method #2, and E. Gillman for certain experiments on nucleosome dissociation using a particle gel assay. Finally, we would like to thank B. Hanson and S. Conte for expert typing of the manuscript.

T.D.Y. was supported during part of this work by a Tartar Fellowship from Oregon State University. K.E. van Holde is recipient of an American Cancer Society Research Professorship. This work was supported in part by American Cancer Society Grant NP355, and by PHS Grant GM22916.

## VIII. List of abbreviations

Abbreviations used in this paper are: bp, base pairs (of DNA); EDTA, (ethylenedinitrilo)-tetraacetic acid; EGTA, ethylene glycol bis (β-aminoethyl ether)-N,N,N',N'-tetraacetic acid; PMSF, phenylmethylsulfonyl fluoride; DMSO, dimethyl sulfoxide; near-UV, long wavelength ultraviolet light; CD, circular dichroism; SDS, sodium dodecyl sulfate; CfoI, restriction endonuclease (Type II) CfoI; pBR322, plasmid pBR322; NaOAc, sodium acetate; S, Svedberg unit ($10^{-13}$ sec); nt, nucleotides (of DNA); H1/5, histones H1 and H5, considered together; NMR, nuclear magnetic resonance; H3/H4, histones H3 and H4, considered together; S.D., standard deviation.

# A Quantitative Assay for Nucleosome Sliding

by

Thomas D. Yager

Department of Biochemistry and Biophysics
Oregon State University
Corvallis, OR 97331

## I. Introduction

The sliding of histone cores along the DNA is a phenomenon which has been well documented to occur in vitro, and which appears also to occur in vivo (for a review of evidence, see van Holde and Yager [1985]). At least one model has been proposed for the mechanism of core sliding (van Holde and Yager, 1985).

At this time, what is needed for a true advancement of knowledge concerning sliding of histone cores is not further documentation of its occurrance, or more theoretical models. Instead, the primary need is that of a simple test system in which sliding can be induced and tracked with high precision.

With the structure of the nucleosome rapidly becoming solved to several angstroms resolution, it has become meaningful to propose sliding mechanisms based on atomic-scale movements and deformations of the histone core and the DNA (see van Holde and Yager [1985]). Thus one cannot overemphasize the need for high precision in a sliding assay.

Below, I relate an attempt to construct a test system for monitoring core sliding. The attempt involves reconstituting histone cores onto single-end-labelled cloned DNA, in a sequence-specific manner. In principle, any cloned DNA which allows sequence-specific (i.e. "phased") nucleosome phasing might have been suitable for use. However, the DNA sequence for

which phasing has been studied in most detail is the 5S rDNA (plus flanking sequences) of Lytichinus variegatus (Simpson and Stafford, 1983). I have worked with this DNA.

The 5S rDNA of L. variegatus has two additional advantages for use in this study. (i) R.T. Simpson has constructed numerous deletion, insertion and substitution variants of this sequence, in preparation for determining the features which cause phasing specificity (R.T. Simpson, personal communication [1983]). In addition to the obvious bonus of working with a DNA sequence for which the "phasing determinants" are known, it may prove advantageous to examine the effects these base changes may have on the ability of cores to slide. (ii) Simpson has also prepared milligram quantities of this DNA, for nucleosome reconstitution and x-ray crystallography (in collaboration with A. Klug). If Klug and coworkers are successful in reconstituting and crystallizing nucleosomes containing this DNA, then a structural map of extremely high resolution may eventually be obtained. (The use of uniquely phased nucleosomes will eliminate that component of the noise in an electron density map which is due to DNA sequence variation.)

From the above two considerations, it is clear that the L. variegatus 5S rDNA is currently the DNA sequence of choice for examining core sliding. I now turn to a detailed description of the progress I have made on the problem of constructing the test system.

## II. Preparation of plasmid pLV405-10

### A. Procedure for isolation of crude plasmid

E. coli HB 101 containing plasmid pLV405-10 (Lu et al., 1980; Simpson and Stafford, 1983) was obtained from Dr. R.T. Simpson, as a streak on an LB-agarose/tetracycline plate.

For early preparations of this plasmid, a single bacterial colony was grown in LB broth + ampicillin, and was then subjected to plasmid amplification by treatment with chloramphenicol, according to the procedure for rich-medium amplification on p. 88 of Maniatis et al. (1982).

It was suspected, however, that chloramphenicol-amplification led to the incorporation of ribonucleotides in the plasmid DNA, and thus to an enhanced sensitivity of the plasmid to hydrolysis (see sections IIE, IVE). Therefore for later preparations of plasmid the chloramphenicol-amplification step was omitted.

For harvesting of plasmid, steps 1-8 of the lysis-by-alkali procedure on pp. 90-91 of Maniatis et al. (1982) were used. The following changes were made in step 4 of the procedure:

(i) The KOAc neutralizing solution, when made by the recipe of Maniatis, et al., has the wrong pH. To obtain a KoAc

solution having the proper pH of 4.8, 6 M KOAc was simply titrated with glacial acetic acid until pH 4.8 was reached. The final volume of solution was about 1.95 X the initial volume of 6 M KOAc.

(ii) 15 ml of the above KOAc solution was added slowly, with agitation, to the bacterial lysate from step 3 of Maniatis, et al. (There was a tendency for the KOAc solution not to mix with the bacterial lysate. Therefore the addition was made with stirring. The most gentle stirring method appeared to be through the intermittent use of a glass rod. After the addition of KOAc was complete, a two-phase lysate/KOAc system was present. This was converted into a uniform suspension by transferrring it to a tube, covering the tube's mouth with parafilm, and turning it gently end-over-end for about 15 min at room temperature.) Once a uniform suspension was obtained, it was placed on ice for 10 min.

The protocol of Maniatis et al. was subsequently followed through step 8 without further changes. The plasmid DNA pellet obtained at the end of step 8 was not contaminated by genomic DNA. It was, however, highly contaminated by KOAc, SDS and RNA, and also possibly by protein. At this point, an attempt to digest the plasmid with Eco RI failed (not shown).

B. Removal of contaminants

Steps 9-11 in the procedure of Maniatis et al. were modified as follows, to produce plasmid that could be cut with Eco RI.

(i) The pellet from approximately 1 L of cells was resuspended in 1.5 ml of 0.1 X "E" buffer. A number of extractions were then done with 1 vol of PCIA. Initially, after each extraction a white interface appeared between the aquaous and hydrophobic layers. The extractions were continued until this interface no longer appeared; usually 2-3 extractions were required. Next, a series of extractions with 1 vol of CIA was performed. As before, this yielded a white interface, and extractions were continued until the interface ceased to appear. Usually, 2-3 extractions were required. Finally, three extractions were done with 2-5 vol ether. Residual ether was removed from the final aqueous phase with $N_2$ gas or air.

(ii) The plasmid DNA (along with contaminating RNA) was precipitated by adding $Mg(OAc)_2$ to 20 mM, NaCl to 0.5 M and EtOH to 65-70% final volume, cooling to -60 °C for 1-2 hours or to -200 °C (liquid N2 temperature) for 10 min, and centrifuging 20 min at 8800 x g. The pellet was dried with $N_2$ gas or air, then resuspended in Tris/EDTA.

At this point the plasmid can be cut with Eco RI, but still is highly contaminated with RNA. Therefore an RNA-degradation step was performed.

(iii) 1/25 vol of stock RNAase mixture (5 mg/ml bovine

pancreatic RNAase + 5,000 U/ml RNAase T1, pre-heated to 80 °C for 10 min) was added, and the resultant solution incubated 2 hours at 37 °C. It was then extracted once with 1 vol PCIA, once with 1 vol CIA, and 2-3 times with 2-5 vol ether. The aquaeous phase was cleared of residual ether with $N_2$ gas or air.

The plasmid DNA was reprecipitated with $Mg(OAc)_2$, NaCl and EtOH, as above. The pellet was dried with N2 gas or air, and was then resuspended in Tris/EDTA.

At this point, the plasmid DNA is free of RNA contamination, and can easily be cut to completion with Eco RI.

C. Estimated potential yield of the 260 bp Eco RI fragment

When taken through the above procedure with plasmid amplification, 1 L of cells was observed to produce about 1 mg of plasmid DNA. Of this, the desired insert (10 head-to-tail copies of a 260 bp Eco RI repeat) comprises about 400 ug. Thus 1 L of cells, when taken through plasmid amplification, should ultimately yield about 2 nmol of the Eco RI repeat. If the amplification step is omitted, one may expect roughly a 10-fold decrease in the yield of plasmid (Davis et al., 1980; Maniatis et al., 1982).

III. Characterization of the plasmid

A. Extent of RNA contamination

The clean-up procedure above was carried to the RNAase step (step (iii) above), and a portion of the material was examined on a 2% agarose "E" gel, by ethidium fluorescence photography. A highly heterogeneous population of nucleic acid molecules was seen (Figure 1A, lanes 2,7). The same material after RNAase treatment is shown on a 1% agarose "E" gel in Figure 1B, lanes 2,3,4 (at a much higher loading than in Figure 1A). The non-discrete, fast-running smear in lanes 2,7 of Figure 1A (> 99% of the total fluorescent material) has been degraded by the RNAase treatment. I conclude that the resistant 1% of the fluorescent material (the discrete high MW bands in Figure 1A) must be DNA.

If the bands in lanes 2,3,4 of Figure 1B are numbered 1-7 from top to bottom, then bands 3,4 and 5, by their relative intensities and positions, seem to correspond to the top,middle and bottom discrete high MW bands of lanes 3-5, 8-10 in Figure 1A.

B. Variability of the pattern of plasmid bands; identities of the bands

There is a variability in the pattern of DNA bands produced

Fig. IV.1A. Preparation I of plasmid pLV405-10 (and contaminating RNA), before RNAase treatment. The effect of alkaline heat treatment.

Plasmid was taken through step (ii) of my modification of the purification procedure of Maniatis et al. (see sction I B, (ii)). Aliquots were removed, were made pH 10, and were heated to 100 $^{o}$C for 1, 3, or 10 min. The control (neutral pH, unheated) and the treated samples were examined on a 2% agarose "E" gel. Lanes 2,7: control; lanes 3,8: 1 min; lanes 4,9: 3 min; lanes 5,10: 10 min; lanes 1,6,11: pBR322/Cfo I marker (neutral pH, unheated).

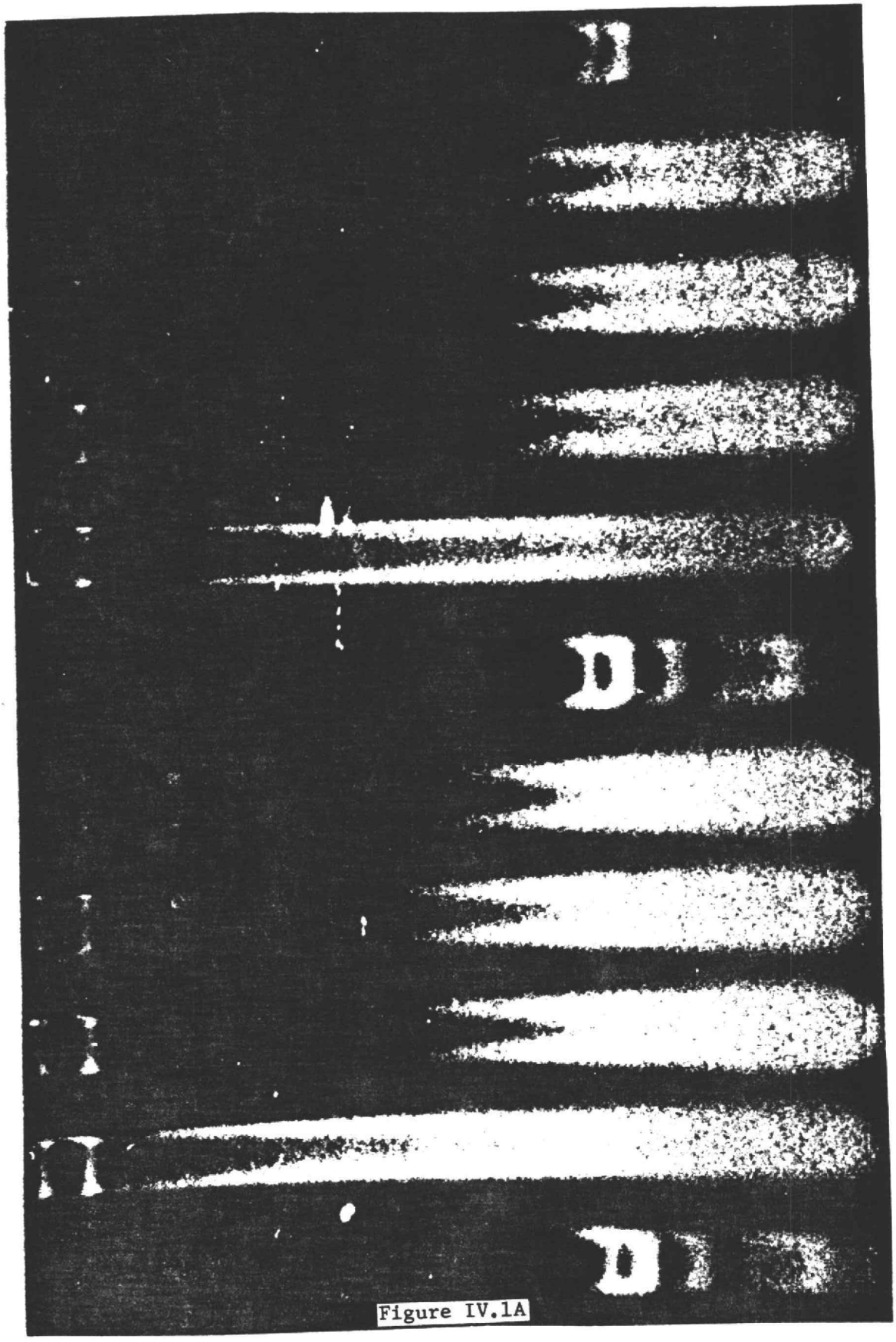

Figure IV.1A

Fig. IV.1B. Purified plasmid of preparation I, after RNAase treatment. 7% supercoiled form.

The plasmid of Figure 1A was taken through step (iii) of my modification of the purification procedure of Maniatis et al. (see section I B, [iii]). An aliquot was removed, was made pH 10, and was heated to 100 °C for 10 min. The control (neutral pH, unheated) and the treated sample were examined on a 1% agarose "E" gel. Lanes 2,3,4: successively lower loadings of control. Lanes 7,8,9: successively lower loadings of treated sample. Lanes 1,5,6,10: lambda/Hind III marker (neutral pH, unheated).

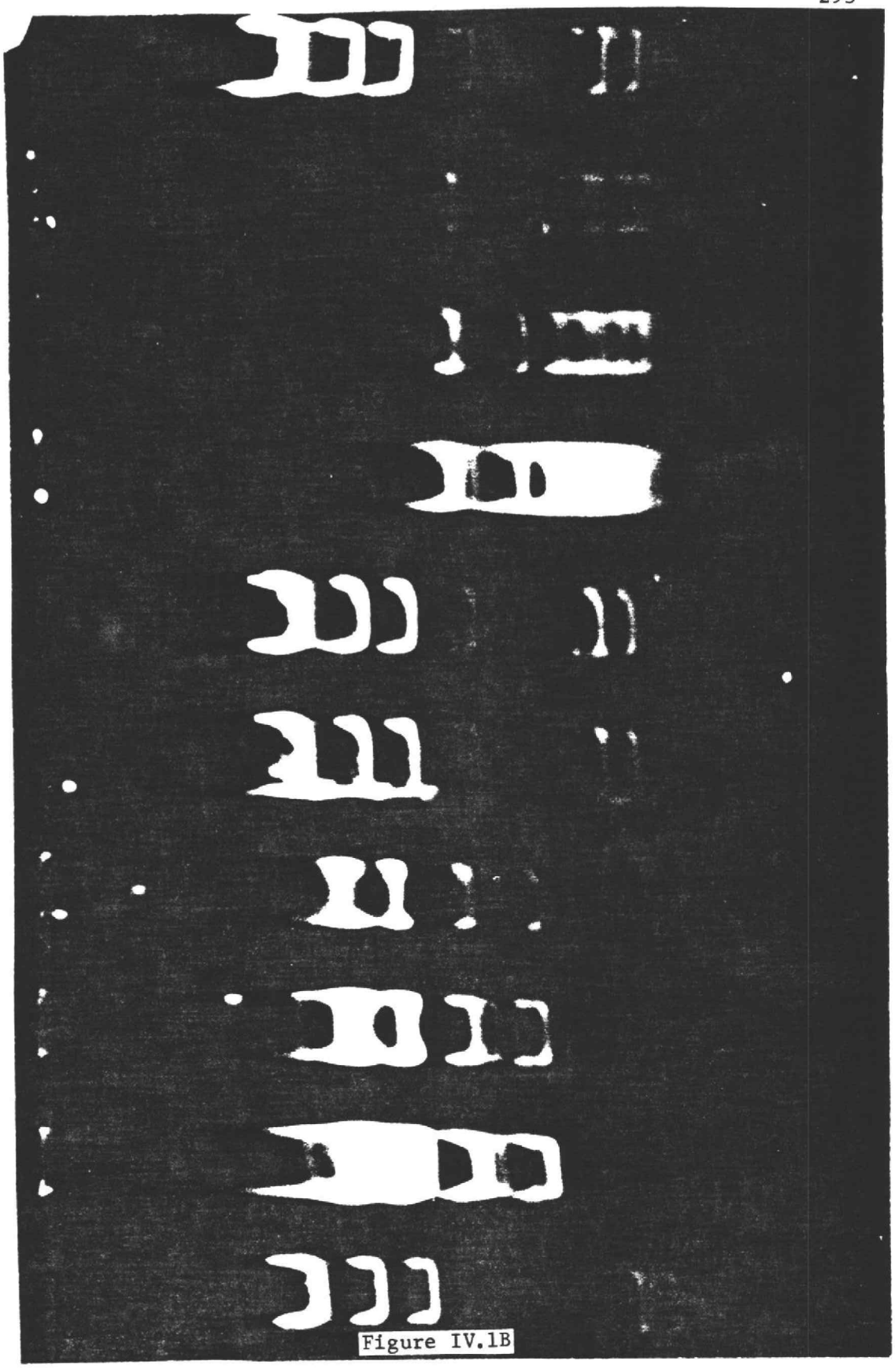

Figure IV.1B

by the above preparative procedure. In the most contaminated preparation (preparation "I"), seven bands are visible (Figure 1B, lanes 2-4; numbered as above). Roughly 90-95% of the material is present in bands 3,4 and 5. The cleanest preparation ever obtained (preparation "II") is shown in Figure 1C, lanes 3-5. Bands 1,2 and 7 are absent, and bands 3,4 and 5 together contain > 99% of the material.

It is of interest to identify the bands in Figures 1B and 1C. Band 5 (numbered as above) almost certainly is the supercoiled plasmid. Bands 3 and 4 probably are nicked-circular and linear plasmid, respectively. The basis for these identifications is as follows:

(i) Band 4 runs at about 6900 bp (relative to lambda/Hind III), which is expected for the linear molecule.

(ii) Under almost all reported conditiona of electrophoresis in "native" agarose gels, the supercoiled form of an arbitrary plasmid, having a smaller radius of gyration, runs more quickly than either the linear- or the relaxed-circular form (reviewed in Serwer and Allen, 1984).

Bands 1,2,6 and 7, from their very narrow widths, appear to be other plasmids. Of these, all except band #1 appear to be supercoiled, because of their partial resistance to degradation by treatment with heat and alkali (lanes 7-9 in Figure 1B; see section III E for further explanation of methods).

(iii) I have studied the mobilities of the supercoiled,

Fig. IV.1C. Purified plasmid of preparation II, after RNAase treatment. 47% supercoiled form; no contaminant DNAs.

A preparation of plasmid different from that of Figures 1A and 1B was carried through step (iii) of my modification of the purification procedure of Maniatis et al. (see section I B, [iii]). Successively smaller aliquots of the purified plasmid were examined on a 1% agarose "E" gel (lanes 3,4,5). Note the high percentage of supercoiled form (lower band), and the absence of DNA species besides the three forms (supercoiled, linear and nicked-circular) of this plasmid. For calibration, lambda/Hind III markers were run in lanes 1,2,6.

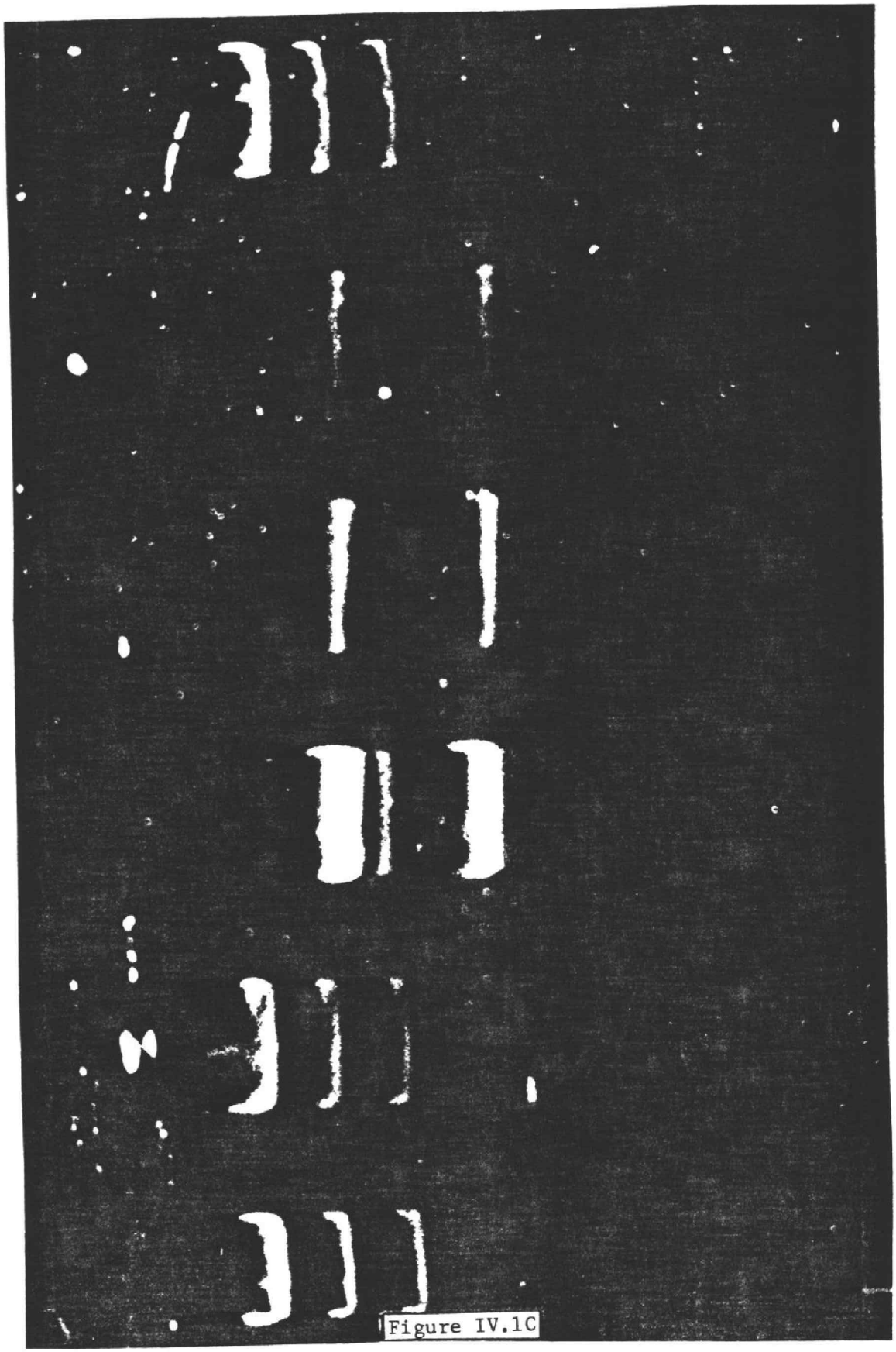

Figure IV.1C

nicked-circular, and linear forms of plasmid pBR322 (which is identical to the above plasmid, except that it lacks the 2600 bp insert), in a 1% agarose "E" gel, at field strengths comparable to those used above (about 10 V/cm). In this study (not shown), various preparations of pBR322 yielded 3 bands on the gel. The center band (when present in the preparation) ran at about 4400 bp, as expected for linear DNA. Treatment of the pBR322 with Eco RI (to make one double-stranded cut in each plasmid molecule) caused all material to be driven into the center band. I conclude that the center band is the linear molecule. Treatment of the pBR322 preparation with calf thymus topoisomerase I (which relaxes supercoiled plasmid molecules) caused a disappearance of the lower band, and a simultaneous increase in the amount of the upper band. This indicates that the lower and upper bands are supercoiled- and relaxed-circular plasmid, respectively.

I assume that this study, done on pBR322 (which is 4362 bp in size), is directly applicable to pLV405-10 (which is 6962 bp in size). This seems reasonable, because the gel and electrophoretic field strength were comparable to those described above. I have not performed an analogous study on pLV405-10.

C. Extent of genomic DNA contamination

In this laboratory, preparations of other plasmids (obtained by the "SDS" and "heat" methods [see Maniatis et al., 1982]) have been plagued by contamination with sheared genomic DNA. Such contaminant DNA is large, running on the above gels with a lower mobility that the 23,190 bp lambda/Hind III marker (not shown). It seems likely that the preparative method used in the present study is no more destructive of genomic DNA than are the other methods. From the absence of stained material above the 23,130 bp marker band (see Figures 1B,1C), I conclude that the present method gives plasmid uncontaminated by genomic DNA.

D. Estimated nicking of the 260 bp Eco RI fragment within the amplified plasmid

It has been suggested that a considerable amount of ribose-substitution occurs during amplification of a plasmid with chloramphenicol (Maniatis et al., 1982). Also, it is well-known that RNA, by virtue of its 3' hydroxyl group, is much more susceptible to acid- or alkaline hydrolysis than is DNA. It therefore seems reasonable to think that plasmid DNA will tend to become nicked at the sites of its ribosylation during the brief exposure to alkalinity in the above preparative procedure.

It is possible to estimate the extent of nicking in the 260

bp Eco RI fragment within the plasmid, through using the following statistical argument.

Assume ribose-substitution to occur at random with respect to the sequence of the plasmid, with respect to the two DNA strands, and with respect to different plasmid molecules. Assume further that the probability of a ribose-substitution event in a particular plasmid molecule is independent of previous substitution events in that same molecule. To the extent that these assumptions hold, ribose-substitution is a Poisson-type process (Feller, 1957). The probability p(k') of k' ribosylation events per plasmid molecule is then given by:

$$p(k') = e^{-t'} t^{k'} / k'! \qquad (1),$$

where t' is a "ribosylation density parameter" (to be discussed further below).

Assume that, during exposure of the plasmid to alkalinity, DNA strand breakage occurs at some randomly selected subpopulation of ribosylation sites. Then nicking also is a Poisson process, and the probability p(k) of k nicks per plasmid molecule is described by an equation analogous to that for ribosylation:

$$p(k) = e^{-t} (t)^{k} / (k)! \qquad (2),$$

where t is a "nicking density parameter".

The fraction of plasmid which remains in supercoiled form after the purification procedure must equal the fraction which has escaped being nicked - i.e. the fraction of the plasmid population for which, in equation (2), k=0. The probability of the event $\{k=0\}$ is given by this equation as $p(0) = \exp(-t)$. Therefore, the "nicking density parameter" t characterizing the Poisson distribution of nicks in the plasmid population can be obtained by measuring the fraction of supercoiled plasmid left after purification, and setting this fraction equal to p(0) in equation (2). (Note: this argument assumes that strand-breakage never occurs at sites which are not ribosylated.)

To estimate the yield of supercoiled plasmid, I consider the ratio of the ethidium-fluorescence of band 5 to the sum of the ethidium-fluorescences of bands 3, 4 and 5 in either Figure 1B or 1C. (Note: this is a biased estimate of yield to the extent that ethidium binding and/or fluorescence per molecule of plasmid differs for the three plasmid forms. However, as a rough estimate, it will suffice.)

The yield of supercoiled plasmid seems to be quite variable. For the plasmid of Figures 1A and 1B (preparation "I"), the supercoiled form constitutes about 7% of the total. (Note: there is a fair amount of uncertainty in this yield estimate, because of the problem of determining the baseline between the bands of Figure 1B. A more realistic estimate would be that the supercoiled form constitutes 5-10% of the total.) For the plasmid of Figure 1C (preparation "II"), the supercoiled form constitutes about 47% of the total. (This value is considerably more certain that that reported for the plasmid of Figure 1B, because in this case the baseline between the bands is easier to determine.) Taking 47% and 7% as two separate estimates of p(0) in equation (2), I predict the distributions of p(k) versus k that are given in Figure 2A (first and second panels, respectively). These distributions describe the probability p(k) that, after purification, a particular plasmid molecule will contain k nicks. Note that the sum of p(k) over all values of k equals 1.

Out of k nicks in a plasmid molecule, some number l of these will fall within the 2600 bp cloned insert. What is the rule governing the random partitioning of nicks from the entire plasmid molecule into the 2600 bp insert? The length of the insert (10 head-to-tail copies of a 260 bp repeat) is 2600 bp, and the length of the remainder of the plasmid is 4362 bp. The probability therefore is $a = (2600)/(2600+4362) = 0.374$ that a

Fig. IV.2A. Probability density functions for nicking in the plasmids of preparation I and II. 1. The distribution of nicks throughout the entire plasmid molecule.

Film negatives from Figures 1B and 1C were scanned, and the fraction of pLV405-10 remaining in supercoiled form was estimated for each plasmid preparation. This "fraction of supercoiled plasmid" was set equal to p(0) in equation (2), and t , the "nicking density parameter", was determined. Using this value of t , Poisson distributions for nicking were calculated, for each preparation of the plasmid.

Left panel (A): distribution of nicks for the plasmid having 47% supercoiled form. Right panel (B): distribution of nicks for the plasmid having 7% supercoiled form.

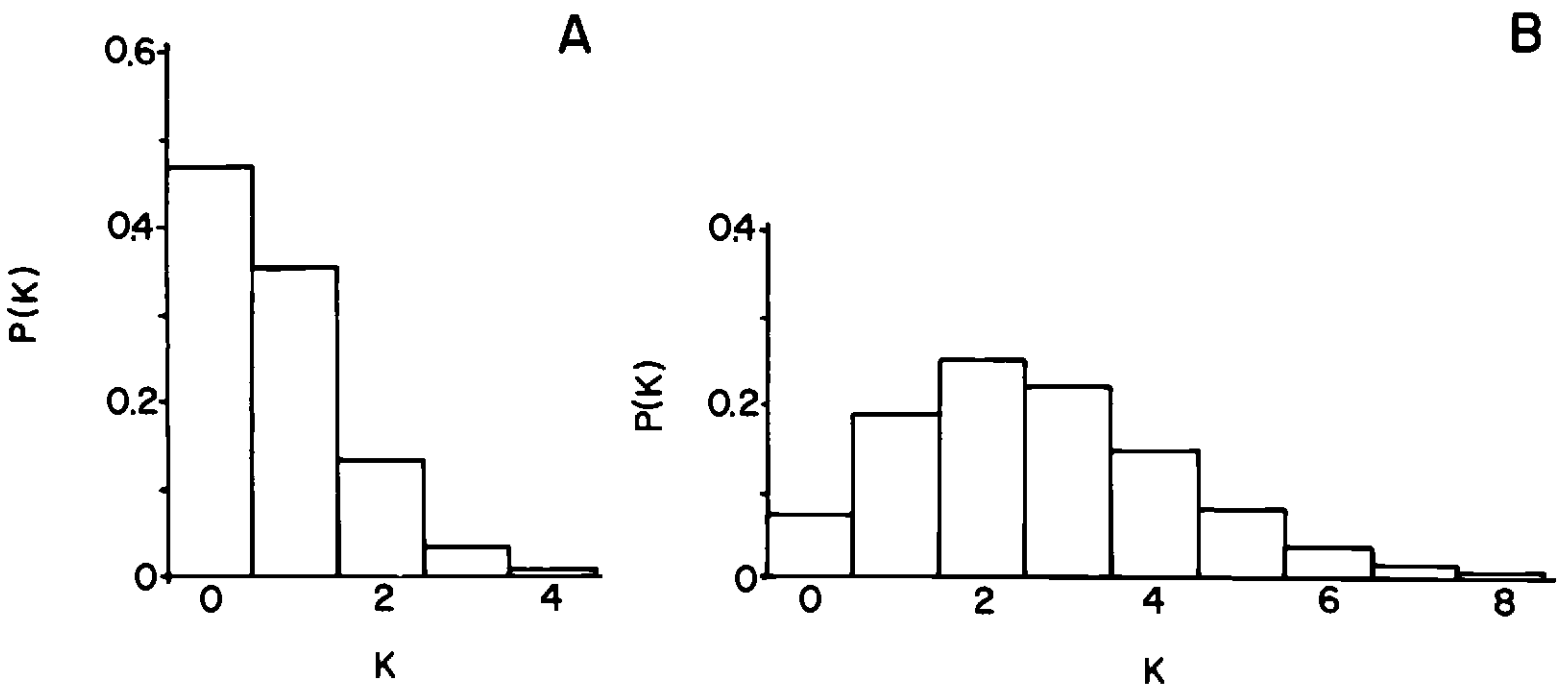


Figure IV.2A

particular nick in a plasmid molecule will fall at random in the insert. For k nicks in the entire plasmid, the probability that l of these will fall in the 2600 bp insert is given (Feller, 1957) by the binomial distribution:

$$p(l;k,a) = a^{l} (1-a)^{k-l} \quad k! \;/\; l!\,(k-l)! \qquad (3).$$

What is the (cumulative) probability P(l) that there are l nicks in the 2600 bp insert, regardless of the total number k of nicks in the entire plasmid? This probability is obtained by weighting each binomial-type term above by the probability of that term's occurrance, and then summing:

$$P(l) = \quad p(k) \;\; p(l;\, k,\, a) \qquad (4).$$

(Note: in my formalism, the use of an upper-case "P" for a probability means that a summation has been done.) The left and right panels of Figure 2B display distributions of P(l) versus l, for the plasmid preparations having 47% supercoiled- and 7% supercoiled forms, respectively.

Fig. IV.2B. Probability density functions for nicking in the plasmids of preparations I and II. 2. The distribution of nicks in the 2600 bp insert.

Within a plasmid molecule, the partitioning of nicks into a subdomain - in this case, the 2600 bp cloned insert - follows a binomial distribution, as described by equation (3) in the text. Equation (3) was convoluted with the Poisson distribution for nicks in the entire plasmid molecule (from Figure 2A). The resultant distribution of nicks in the 2600 bp insert (equation [4] in the text) was plotted for the plasmids having 47% supercoiled form and 7% supercoiled form (left and right panels [A and B], respectively).

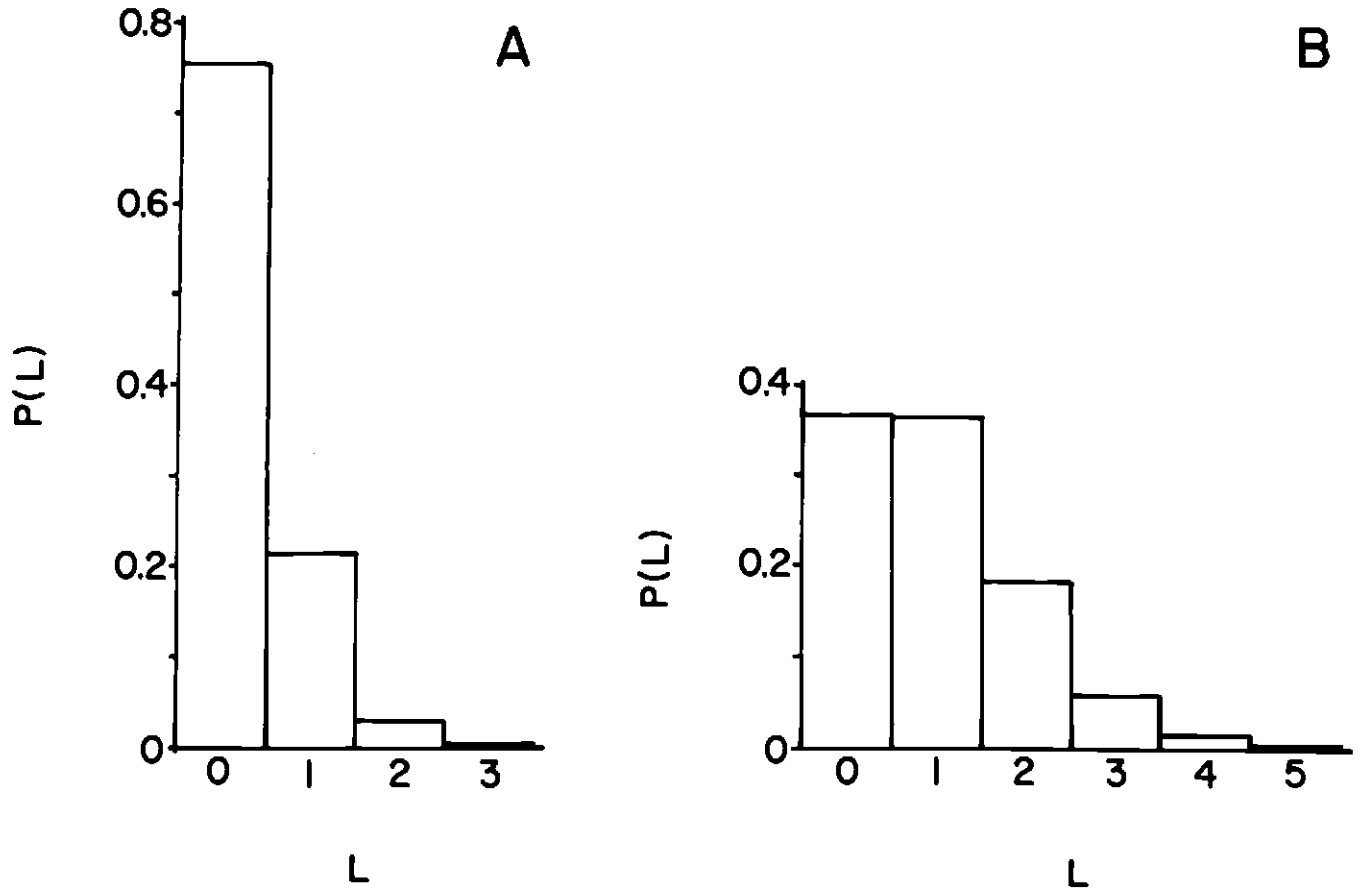


Figure IV.2B

The probability distribution of nicks for an individual 260 bp repeat is calculated as follows.

(i) The repeat can be divided naturally into $n = 260$ subintervals, each 1 bp long. Every such subinterval has a small, finite probability $r$ of both carrying a ribose moiety and of being nicked.

(ii) Mathematically speaking, the 260 bp repeat may therefore be considered to be a sequence of n Bernoulli trials (Feller, 1957). The probability of the event {ribose substitution and nicking at any single position} is equal to the probability of the event {success in a particular Bernoulli trial}, which in turn is equal to $r$. The product of $n$ and $r$ is finite and of a moderate value. Therefore (Feller, 1957) the probability of m successes (i.e. nicks in the 260 bp repeat) is approximated by the Poisson distribution:

$$p(m; nr) = e^{-nr} (nr)^{m} / m! \qquad (5).$$

(iii) $nr$ is approximately equal to $l/N$ (the average "linear density" of nicks, or # [nicks] per insert), where $l$ is the total number of nicks in the entire 2600 bp insert, and $N$ is the number (= 10) of 260 bp repeats in the insert (Feller,

1957).

(iv) From above, l has the probability distribution given by equation (4). Therefore, to obtain the probability that m nicks occur in an arbitrary 260 bp repeat regardless of the number of nicks either in the 2600 bp insert or in the entire plasmid molecule, each Poisson-type term from equation (5) is weighed by the appropriate (cumulative) factor P(l) from equation (4), and summed:

$$P(m) = P(l) \; e^{-l/N} \; (l/N)^{m} \; / \; m! \qquad (6).$$

The left and right panels of Figure 2C display P(m) versus m distributions, for the plasmid preparations having 47% supercoiled- and 7% supercoiled forms, respectively.

E. Estimated ribose substitution in the 260 bp Eco RI fragment within the amplified plasmid

The above statistical argument allows one to estimate how severely the 260 bp repeat becomes nicked during preparation of the plasmid. Thus some knowledge of its structural integrity is obtained. It is quite likely, however, that not all of the ribosylation sites in the plasmid are converted into nicks

Fig. IV.2C. Probability density functions for nicking in the plasmids of preparations I and II. 3. The distribution of nicks in the 260 bp repeat.

The partitioning of nicks in the 2600 bp insert into a single 260 bp repeat follows the Poisson distribution, as described by equation (5) in the text. Equation (5) was convoluted with the probability distribution of nicks in the 2600 bp insert (from Figure 3B). The resultant distribution of nicks in the 260 bp repeat (equation [6] in the text) is plotted for plasmids having 47% supercoiled form and 7% supercoiled form (left and right panels [A and B], respectively).

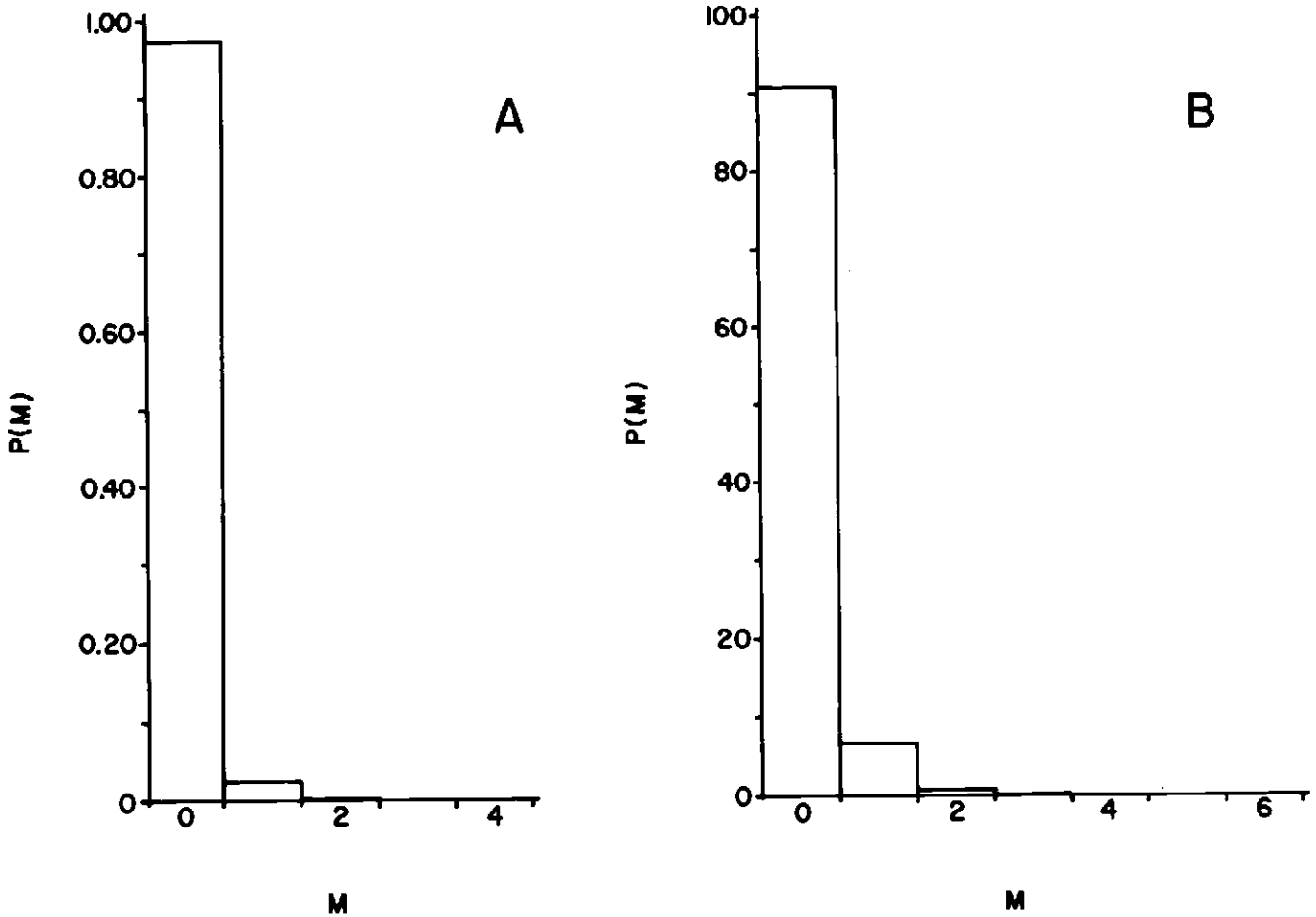


Figure IV.2C

during the brief exposure to alkalinity in the preparative procedure. Thus one would expect the purified 260 bp repeat to undergo additional spontaneous degradation with time, as nicking occurred at "hidden" ribosylation sites.

The frequency distribution of ribosylation sites in the 260 bp repeat may be estimated by an approach similar to the above. In this case, however, the estimate depends critically upon causing quantitative strand breakage at all the ribosylation sites in the plasmid. I have attempted to quantitatively convert ribosylation sites into nicks, through treating the plasmid with heat and alkali.

A sample of (RNA-free) plasmid of preparation I (lanes 2-4 in Figure 1B) was brought to pH 10 and heated at 100 °C for 10 min. After this treatment, aliquots of the sample were run in lanes 7-9 of the gel of Figure 1B. Using the band-identification scheme described previously, I note that only bands 2,6 and 7 remain in their original positions. I assume that each of these bands, displaying a high resistance to degradation, contains a supercoiled plasmid which is not ribosylated. (Note: these bands have not been positively shown to represent supercoiled DNA species. A critical test would be to treat the samples with topoisomerase I; a decreased mobility of these bands would indicate that they were supercoiled.)

The loadings of lanes 2 and 7, of lanes 3 and 8, and of lanes 4 and 9 of Figure 1B were carefully matched. Thus it was

possible to determine the percentage of plasmid remaining in supercoiled form after the treatment with heat and alkali, by taking the ratio of ethidium-fluorescence of band 5 after treatment to that of the sum of bands 3,4 and 5 before treatment. In this way, I calculate that only 46 +- 19 % of the plasmid that was originally in supercoiled form remains supercoiled after the alkaline heat treatment.

Using 0.46 X 0.07 = 0.03 as p(0) in equation (1), and carrying out an analysis similar to the one done above for nicking, I obtain Figures 3A, 3B and 3C. Figure 3A describes the probability of finding k' ribosylation events per plasmid. Figure 3B describes the probability of finding l' ribosylation events per 2600 bp insert. Finally, Figure 3C describes the probability of finding m' ribosylation events per 260 bp repeat. These Figures suggest that about 9 out of 10 260 bp "repeats" has 0 ribosylations, that 1 out of 10 repeats has 1 ribosylation, and that 1 out of 100 repeats has 2 ribosylations.

The above assay for ribosylation depends upon the premises that: (i) only sites which are ribosylated are attacked during the alkaline heat treatment; and (ii) conversion of these ribosylation sites into nicks is quantitative (i.e. complete). I have no information on the validity of premise (i), although the well-known stability of pure DNA to heat and alkalinity argues for it. As suggested below, premise (ii) probably is not

Fig. IV.3A. Probability density functions for ribosylation in the plasmid of preparation I. 1. The distribution of ribosylation events throughout the entire plasmid molecule.

From the data shown in Figure 1B it was calculated that, for preparation #1, only 46+-19% of the plasmid which originally was in supercoiled form remained supercoiled, after a 10 min heating at 100 $^{o}$C, pH 10. Using 0.46 x 0.07 = 0.03 as p(0) in equation (1), the probability distribution of ribosylation "hits" in the entire plasmid molecule was computed, and graphed.

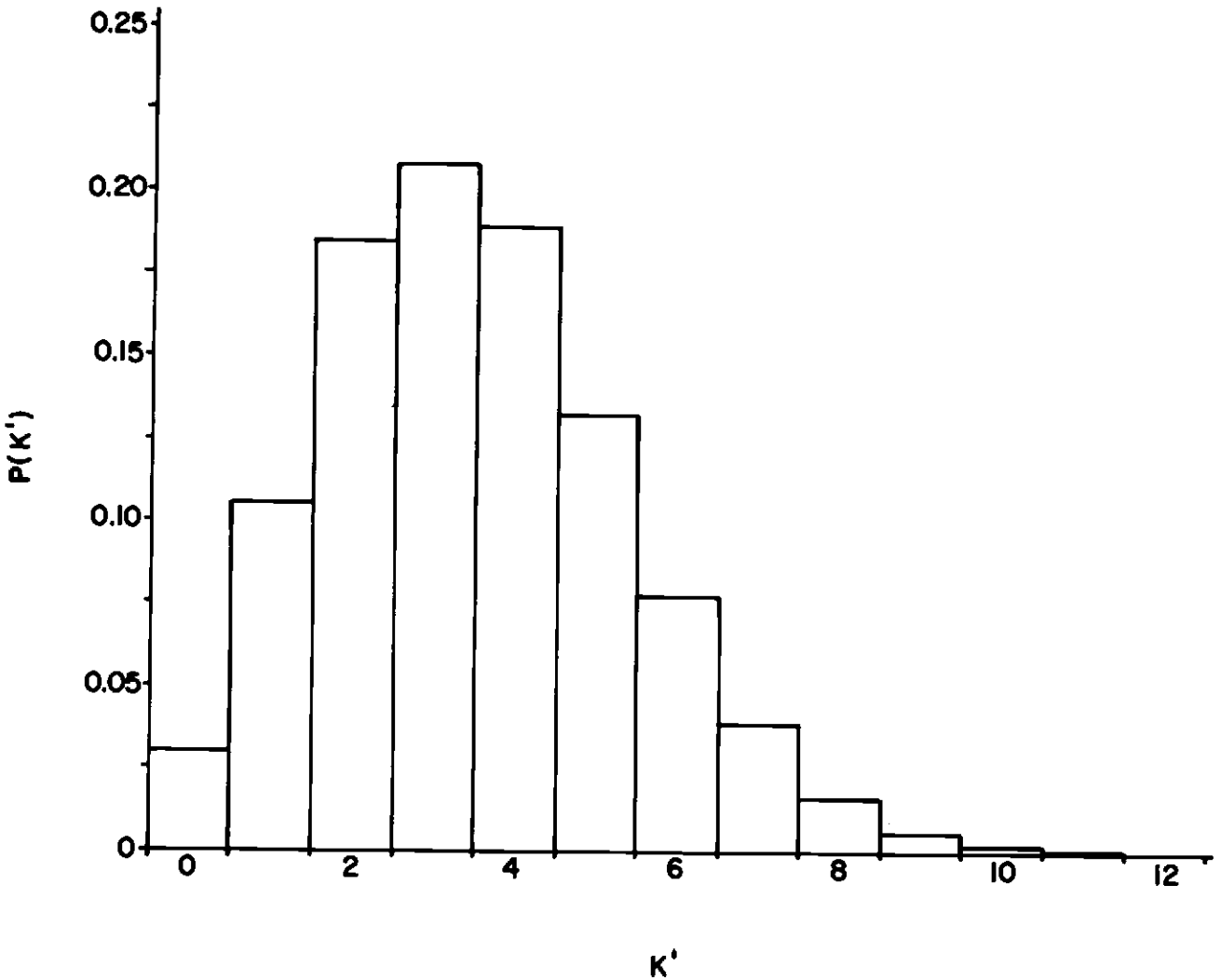


Figure IV.3A

Fig. IV.3B. Probability density functions for ribosylation in the plasmid of preparation I. 2. The distribution of ribosylation events throughout the 2600 bp insert.

The probability distribution of ribosylation "hits" in the 2600 bp insert was computed by convoluting the "plasmid hit distribution" of Figure 3A with a binomial formula for partitioning "hits" from the plasmid into the 2600 bp insert (analogous to binomial equation [4] for the partitioning of "nicks").

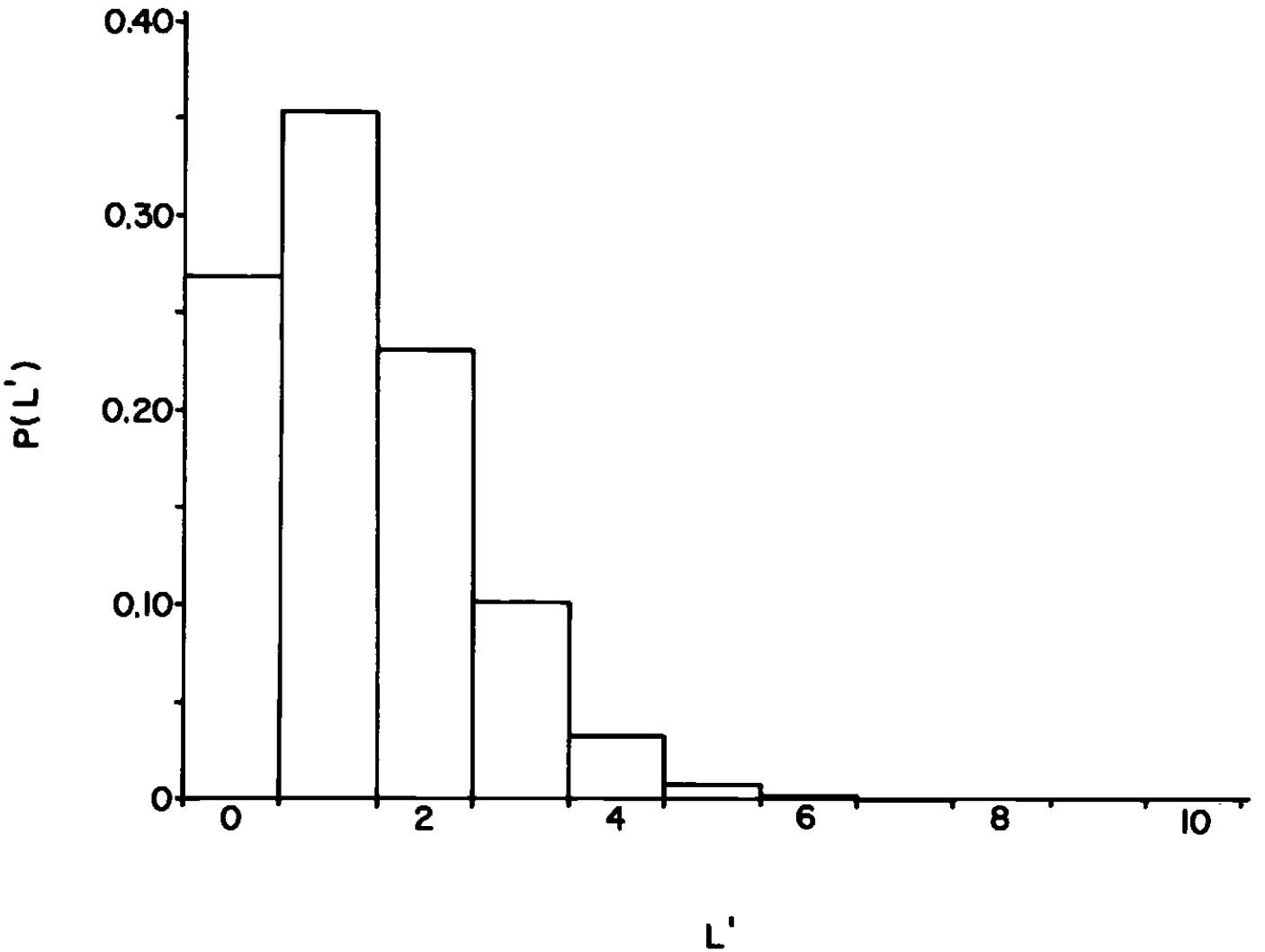


Figure IV.3B

Fig. IV.3C. Probability density functions for ribosylation in the plasmid of preparation I. 3. The distribution of ribosylation events throughout the 260 bp repeat.

The probability distribution of ribosylation "hits" in the 260 bp repeat was computed by convoluting the "hit distribution" of the 2600 bp insert (Figure 3B) with a Poisson formula for partitioning hits from the 2600 bp insert into a single 260 bp repeat (analogous to Poisson equation (5) for the partitioning of "nicks").

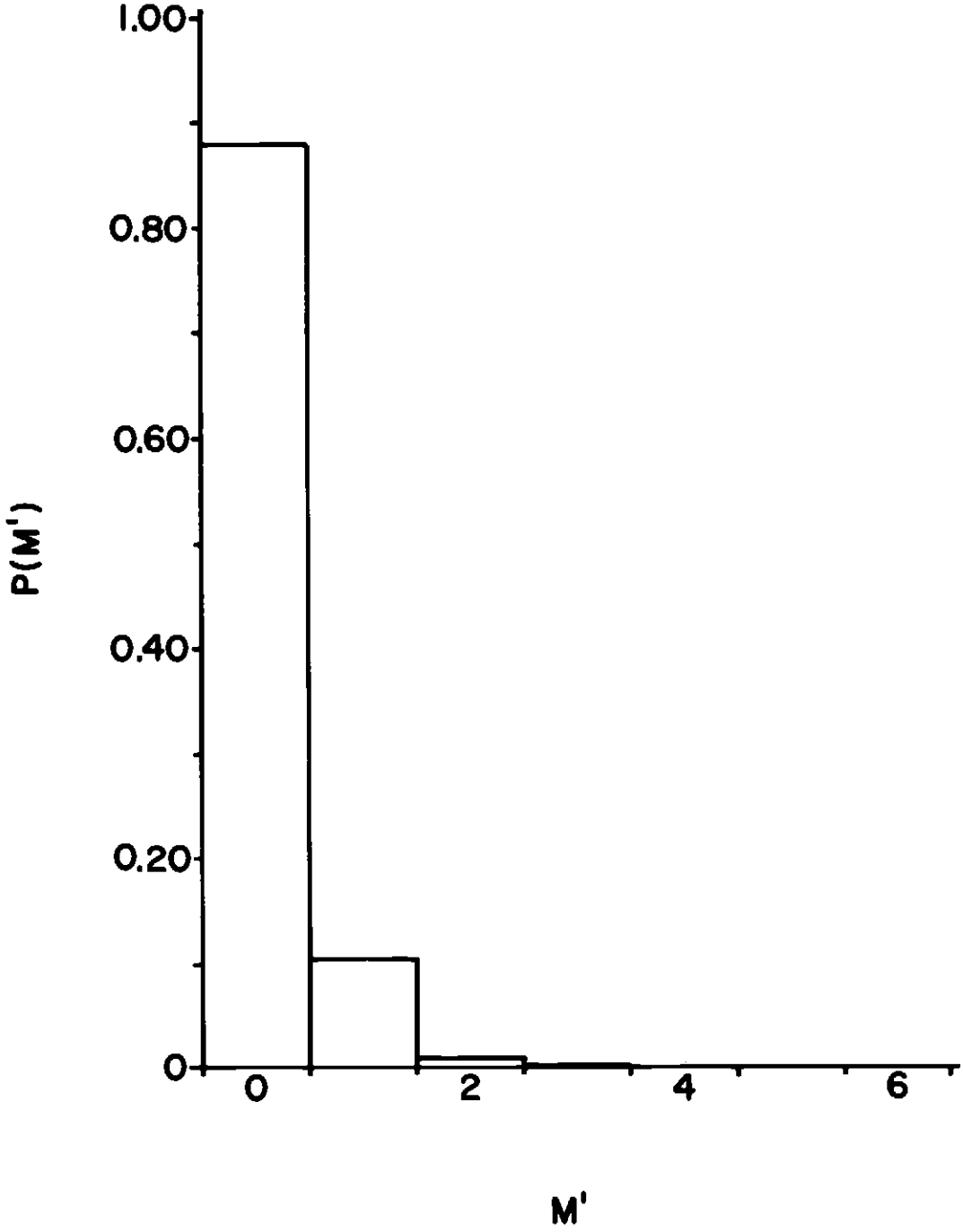


Figure IV.3C

true.

An idea of how completely the plasmid's ribosylation sites are converted into nicks may be obtained by examining the extent of destruction, upon treatment with heat and alkali, of the contaminant RNA in Figure 1A. One method of examination involves gel electrophoresis. An untreated sample is shown in lanes 2,7 of Figure 1A. The results of heating at pH 10, 100 °C for 1,3 or 10 min are shown in lanes 3 and 8, 4 and 9, or 5 and 10, respectively, of the same figure. Examination of this maximally-degraded RNA on a "SS" gel, against DNA standards, reveals a broad distribution of sizes, spanning at least the 60-400 nt range (not shown). It is clear from these results that only partial destruction of the RNA has occurred.

A second method of examination involves the analytical centrifuge. When the untreated sample (lanes 2,7 of Figure 1A) is examined (in Tris/EDTA), the midpoint of the sedimenting boundary has $s_{20,w}$ = 1.5. When the sample is heated to 100 °C at pH 10, for 10 min (lanes 5,10 of Figure 1A), then diluted into Tris/EDTA, the boundary midpoint has $s_{20,w}$ = 1.0. From a log-log plot of $s_{20,w}$ versus #(nucleotides) (based on the data: 4S = 70-80 nt, 5S = 120 nt, 16S = 1520 nt, 23S = 3000 nt [Watson, 1976]), the above values of $s_{20,w}$ are found to correspond to approximate mean RNA sizes of 10 nt before alkaline heat treatment, and 4 nt after treatment. I note that these sedimentation coefficients and size estimates appear to

be inconsistent with the gel data, above. There are at least two possible reasons for this: (i) The S values may be somewhat low because of turbulence in the centrifuge cells (the samples were run at a concentration of only $A_{260}$ = 0.2 - 0.3). Correction for this effect, however, would raise the S values by only a factor of 2 or so (Yager and van Holde [1984], unpublished observations). (ii) The midpoint-S analysis reveals only the most common size of RNA molecule which is present. A distribution-of-S analysis, which is sensitive to heterogeneity, would reveal more accurately the true range of molecular sizes (see van Holde and Weischet, 1978).

Regardless of the seeming inconsistencies between the gel- and the centrifugation- analyses, one must conclude also from the latter investigative technique that alkaline heat treatment does not convert the RNA into single nucleotides, but instead introduces only a few cuts per molecule. Thus it is reasonable to believe that not all the ribosylation sites in the plasmid are detected by this assay technique. In consequence, the estimate of ribosylation made by the above statistical argument probably is too low. This conclusion is reinforced by the finding that the 195 bp Eco RI - Nci I fragment is highly susceptible to degradation (see section V E).

IV. Preparation of the 260 bp Eco RI fragment

A solution of 1 mg plasmid in 100 ul Tris/EDTA was brought to the appropriate conditions for restriction digestion by adding 10-fold concentrated stock solutions of BSA and "medium salt restriction digestion buffer" (Davis et al., 1980). After thorough mixing and preheating to 37 $^{o}$C, Eco RI was gently added. The approximate concentrations of chemical species in the reaction were:

DNA, 10 mg/ml (20 uM Eco RI recognition sites);

Eco RI, 1 U/ul;

$MgSO_4$, 10 mM;

NaCl, 50 mM;

Tris, 10 mM, pH 7.4;

DTT, 1 mM;

BSA, 100 ug/ml;

EDTA, 0.25 mM.

The pH was approximately 7.4. Periodically, aliquots were analyzed by electrophoresis on a polyacrylamide "E" gel (Figure 4A). The reaction appeared virtually complete after 24 hours.

After 24 hours, the reaction was stopped by adding EDTA to an excess of 15 mM. The entire sample was then made 20% in glycerol, 0.005% in xylene cyanol and 0.005% in bromophenol blue, and was loaded in 100-200 ug (10-20 ul) aliquots onto separate lanes of a 0.8 mm thick, 15 cm long polyacrylamide "E"

Fig. IV.4A. The digestion of plasmid pLV405-10 with Eco RI. 1. Intermediate timepoint in the digestion. Proof that the cloned insert is comprised of 10 tandem repeats of a 260 bp unit.

The plasmid of Figure 1C (preparation "II") was cleaved with Eco RI in "medium salt buffer", at 37 °C (see text). An intermediate timepoint in the cleavage reaction was sampled on a 3.5 % polyacrylamide "E" gel. Lane 1: pBR322/Cfo I markers. Lane 2: intermediate digestion timepoint. Within the ladder of bands, one may find each of the 10 n-mers of the 260 bp repeat (n = 1 to 10).

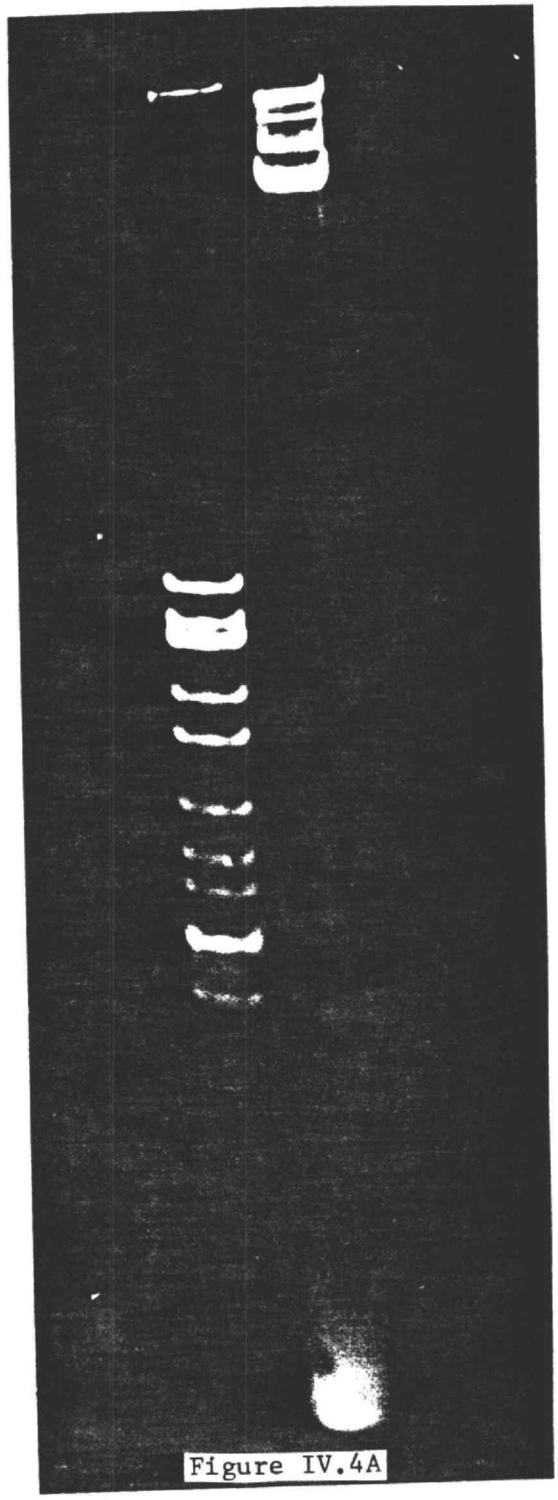

Figure IV.4A

gel. The gel was electrophoresed at 10-15 V/cm for 2-3 hours, until the xylene cyanol band was 2/3 of the way to the bottom. (On a 5% gel, xylene cyanol co-migrates with the 260 bp fragment; on a 3.5% gel it runs somewhat more slowly than this [Maniatis et al., 1982].)

A slice of the gel 1 cm in height (either slightly below or centered on the xylene cyanol band, depending on whether a 3.5% or 5% gel was used) was cut out. A check of the remaining portion of the gel by ethidium-fluorescence photography revealed that >95% of the 260 bp fragment had been removed. The 260 bp fragment was either electroeluted with 1/10 x "E" buffer, then lyophilized and resuspended in water, or it was allowed to diffuse from the gel into 0.5 M $NH_4OAc$, 10 mM EDTA, pH 7.0 (Maniatis et al., 1982). To remove contaminants carried through from electrophoresis, one extraction with PCIA, one extraction with CIA, and two extractions with ether were done. The DNA was then precipitated, and the DNA pellet was dried with N2 gas or air and resuspended in Tris/EDTA.

On a polyacrylamide "E" gel, the purified fragment runs as a single band, just above the 259 bp pBR322/Cfo I marker (Figure 4B). No contamination by other DNA species can be seen. On a "SS" gel, only a single band, running at about 260 nt, can be seen (not shown). (Note: these tests involve only the detection of ethidium fluorescence. Thus they are not nearly as sensitive to contaminant DNAs or to DNA degradation as is

Fig. IV.4B. The digestion of plasmid pLV405-10 with Eco RI. 2. purified Eco RI fragment, 260 bp in length, on a 3.5% polyacrylamide "E" gel. Ethidium-fluorescence photograph.

After the digestion of Figure 4A had gone to completion, the 260 bp Eco RI/Eco RI fragment was purified as described in the text, and run on a 3.5 % polyacrylamide "E" gel (lane 1). Lane 2 displays pBR322/Cfo I markers.

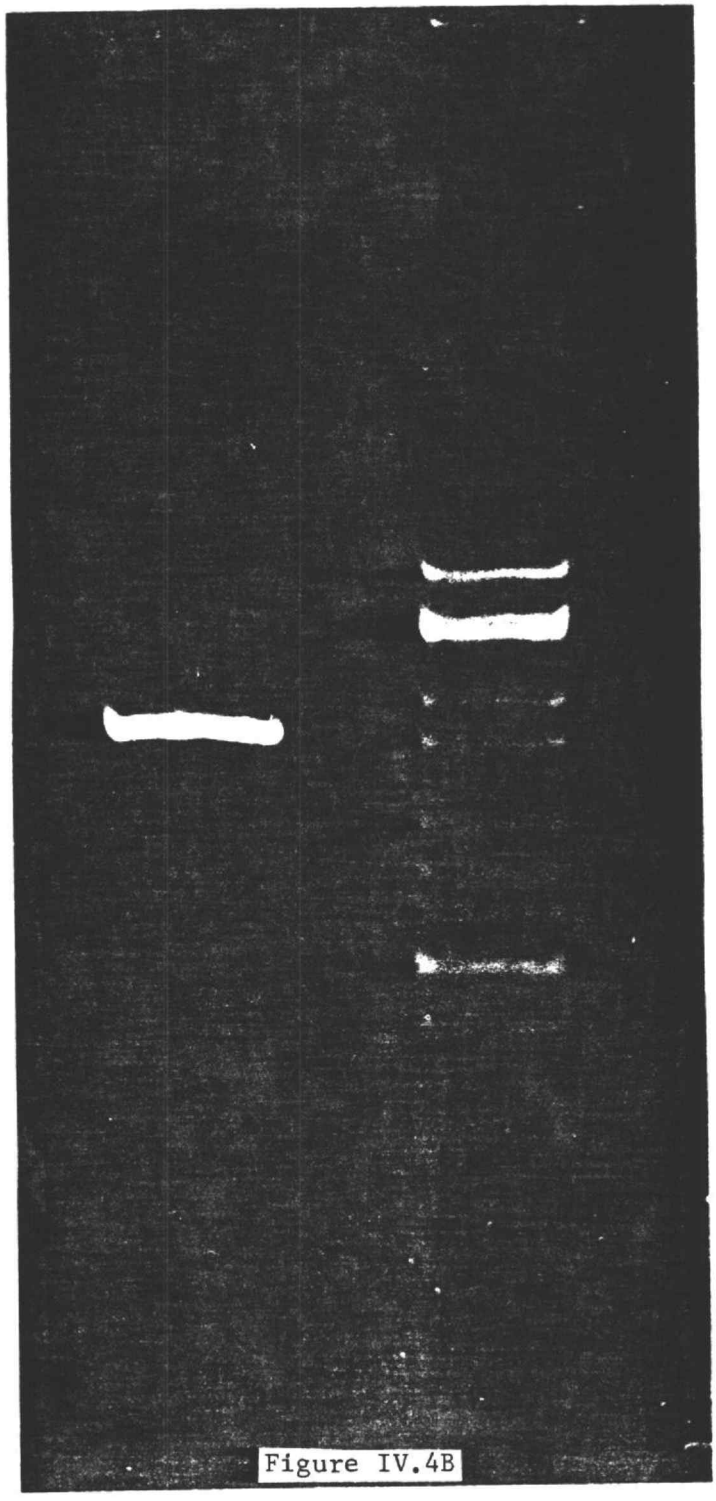

Figure IV.4B

radioautography; see section V E.)

V. End-labelling and secondary restriction of the 260 bp Eco RI fragment; purification and characterization of the 195 bp Eco RI - Nci I fragment

A. 3' end labelling

I have introduced label into the recessed 3' ends of the 260 bp Eco RI fragment, using the end-filling (5'-to-3' polymerase) activity of the Klenow fragment of DNA polymerase I (Maniatis et al., 1982). This method of end-labelling has the advantage that the "sticky" Eco RI ends tend to be made "blunt". This helps eliminate the fundamental problem of not knowing the effects of the "sticky" ends on either nucleosome reconstitution, or on the subsequent dynamic behaviors of the reconstituted nucleosomes. There is, however, a serious potential drawback to this method of radiolabelling DNA: it may generate microheterogeneity by incompletely filling the recessed ends. This problem is treated in detail in section V A,3.

1. End-filling with [$\alpha$32P]-dATP

End-filling with [$\alpha$32P]-dATP was done as described in

Maniatis et al. (1982), with minor modifications. It was found to be a completely reliable reaction, by the criterion that radiolabelled DNA was generated. As discussed in section V A, 3, however, this criterion is not very rigorous.

The following reagents were added together:

0.2 to 0.4 vol of 220+-50 ng/ul DNA (1.3 +- 0.3 uM Eco RI fragment), in Tris/EDTA;

0.1 vol of "10 X nick-translation buffer", which consisted of 0.5 M Tris (pH 7.2), 0.1 M $MgSO_4$, 1 mM DTT, 0.5 mg/ml BSA (Maniatis et al., 1982);

0.4 to 0.6 vol of [$\alpha$-32P]-dATP, 800 Ci/mmol, 13 uM in 10 mM Tricine, pH 7.6;

0.02 to 0.03 vol each of (unlabelled) 2 mM dATP and 2 mM dTTP in water.

After thorough mixing, 0.02 to 0.03 vol of 5-6 U/ul Klenow fragment, in 100 mM $KHPO_4$ (pH 6.5), 1 mM DTT, 50% glycerol, was then gently mixed in.

In this end-filling reaction, the approximate final

concentrations the of reagents were:

DNA, 70+-20 ng/ul (0.8+-0.3 uM Eco RI recognition sites);

[$\alpha$32P]-dATP, 50-70 uM (with a specific activity of 50-100 Ci/mmol);

dTTP, 40-60 uM;

Klenow Fragment, 0.1-0.2 U/ul;

Tris, 52-54 mM;

Tricine, 4-6 mM;

DTT, 0.12-0.13 mM;

EDTA, 0.05-0.1 mM;

$MgSO_4$, 10 mM;

$KHPO_4$, 2-3 mM;

BSA, 50 ug/ml;

glycerol, 1-1.5% v/v.

A typical reaction was 40-80 ul in volume, and contained a total radioactivity of 50-200 uCi. The pH was approximately 7.2. The reaction was allowed to proceed 30 min at 20 $^{o}$C.

2. End-Filling with [$\alpha$35S]-dATP

Although the end-filling reaction was not done with [$\alpha$35S]-dATP in this study, distinct advantages would be gained by using it instead of [$\alpha$32P]-dATP. These advantages include a

longer half-life (87.9 days, as opposed to 14.3 days) and the generation of sharper bands in radioautography (see section VII B,2). Deborah Ornstein (New England Nuclear Corp.) has graciously supplied the following (unpublished) list of approximate reagent concentrations for end-filling with [α35S]-dATP:

DNA, 1.2 uM "recessed ends" (e.g. 170 ng/ul of a pBR322/Hinf I digest);
[α35S]-dATP, 3 uM (with a specific activity 500-1000 Ci/mmol);
dTTP, 20 uM;
Klenow Fragment, 0.25 U/ml;
Tris, 30 mM;
DTT, 1 mM;
$MgCl_2$, 4 mM;
BSA, 3 ug/ml.

The pH should be approximately 7.4. The reaction should be allowed to proceed 60 min at 15 °C.

3. The potential generation of microheterogeneity in the end-filling reaction

At either terminus of the 260 bp fragment of interest, Eco RI has generated the 5' protruding end -TpTpApAp. Thus, if 3'

end-filling does not proceed to completion, each of the two strands will give rise to the following radiolabelled variants (read 5' to 3'):

Rp*AOH

Rp*Ap*AOH

Rp*Ap*ApTOH

Rp*Ap*ApTpTOH.

Here, the distal [i.e. 5'] portion of each strand is indicated by the symbol "R". The asterisk denotes the presence of radioactivity in the phosphate it is adjacent to.

Thus, for each of the two strands, a four-fold heterogeneity of (labelled) variants is expected. This will cause ambiguity in the subsequent analysis of nucleosome phasing on gels (see section VII), due to the superpositioning of 4 phasing patterns, shifted from one another by 1 nt. This is a fundamental limitation of the method of 3' end-filling. The problem therefore is raised of attempting to eliminate such potential for heterogeneity, while still using this labelling reaction. Three solutions readily suggest themselves:

(i) if $\alpha$-labelled dTTP were used instead of $\alpha$-labelled dATP, the problem would be reduced to that of a two-fold heterogeneity.

(ii) It might be possible to use, instead of Eco RI, a

restriction enzyme which generated a smaller "sticky end" - e.g. one that was only 1 nt long.

The three commercially available restriction endonucleases which cut outside of the region where the histone core apparently is phased (Simpson and Stafford, 1983) are Nci I, Xmn I, and Mnl I (R.T. Simpson, personal communication). Relative to position 1 in the Eco RI site, their recognition and cutting specificities are (read 5' to 3'):

1

G¦AATTC (Eco RI);

194

CC¦GGG (Nci I);

10

GAATA¦ACTTC (Xmn I);

229

249

CCTCNNNNNNN (Mnl I; cutting specificity not known).

Thus, if Nci I is used as the primary restriction endonuclease, a 5' "sticky end" only 1 nt in length (-GOH) will be generated.

There are, however, at least three complications with this approach. First, Nci I cleaves pBR322 in 10 places; if some other fragment from the pLV 405-10 plasmid happens to be similar in size to the 260 bp fragment of interest, the latter's purification will be made more difficult. Second, Nci I apparently generates a 3' phosphate when it cuts (Bethesda Research Laboratories, 1983-84); before end-filling is attempted, this 3' phosphate would have to be removed (for example, with T4 kinase [Bethesda Research Laboratories, 1983-84]). Third, the Klenow fragment of DNA polymerase I might not be able to fill a 3' end that is recessed by only 1 nt.

(iii) A third solution to the threat of heterogeneity is suggested by a closer examination of the paper of Simpson and Stafford (1983). These workers labelled the Eco RI fragment at the 3' end using the Klenow fragment of DNA polymerase I, and then secondarily restricted it with Mnl I. Tracks 1 and 10 of their Figure 3 show (replicate) G-ladders generated by the action of dimethyl sulfate on this labelled DNA. One "ghost" band 1 nt shorter than the main band is readily observed, at several percent of the main band's intensity. No additional

"ghosts" are seen. Thus the species present (read 5'-to-3') are either RA (ghost) and RAA (main), RAA (ghost) and RAAT (main), or RAAT (ghost) and RAATT (main).) Clearly, in the hands of Simpson and Stafford, the labelled DNA is >95% homogeneous. The crucial point to note is that these workers performed the end-filling step in a slightly different way than I have above. First, DNA, [α32]P-dATP of high specific activity, and the Klenow fragment were mixed together and incubated. Then a chase with cold dATP and cold dTTP was performed.

The above discussion suggests that, after purification of the secondarily-restricted fragment but before nucleosome reconstitution, a Maxam/Gilbert sequencing ladder should be generated, to test for heterogeneity of end-filling. One should proceed to subsequent steps only if, say, <5% heterogeneity is seen.

B. 5' end labelling

A completely different approach to end-labelling the fragment of interest is to use T4 polynucleotide kinase and [γ32P]-dATP (Maniatis et al., 1982). This places a radioactive phosphate group on each 5' end of the DNA fragment. There are both advantages and disadvantages to this approach. One advantage is that no possibility arises for the generation of microheterogeneity of sequence, in contrast to the case of

3'-end-filling. A second advantage is that, when nucleosomes are reconstituted on this DNA and are then digested with DNAase I, the phasing pattern is more distinctive than for nucleosomes reconstituted on 3' end-labelled DNA (Simpson and Stafford, 1983). This makes it easier to check for correct phasing. A disadvantage is that the "sticky ends" (generated by Eco RI) remain after labelling. As noted previously, the effects of these "sticky ends" on nucleosome reconstitution and on the subsequent dynamic behaviors of the nucleosomes are unknown.

In collaboration with R. Moyer at Oregon State University, I have recently tried 5' end-labelling the 260 bp Eco RI fragment with [$\alpha$32P]-dATP and T4 polynucleotide kinase [unpublished results, 1984]. Using the procedure given on pp. 122-123 of Maniatis et al. [1982], successful labelling to a high specific activity was achieved [not shown]. After purification of the labelled fragment on a polyacrylamide "E" gel, secondary restriction with Nci I also was successfully performed [not shown; see sections V C,D]. Thus there appears to be no fundamental difficulty in preparing single-end-labelled Eco RI - Nci I fragment, bearing 5' end-label at the Eco RI side.

C. Preparation for the secondary restriction step

To stop the 3'-end-filling reaction above, the Klenow

fragment was denatured by adding 1 vol PCIA, and vortexing. The aquaeous and hydrophobic phases were separated by centrifugation, and the former was collected. The cloudy interface contained a considerable proportion (10-50%) of the radiolabel, possibly incorporated into DNA. So as not to possibly lose radiolabelled DNA at this step, the interface was extracted 3 times with 5 ul of Tris/EDTA, and the aquaeous extracts were combined with the original aquaeous phase. This procedure allowed the recovery of >95% of the radioactivity. Next, residual phenol, chloroform and isoamyl alcohol were removed from the aquaeous phase by 3 extractions with ether. After removing residual ether with $N_2$ gas or air, the labelled DNA was precipitated with NaCl, $Mg(OAc)_2$ and EtOH, as above. The DNA pellet was dried with N2 or air, and was then resuspended in Tris/EDTA.

There are a number of points to note about the above procedure:

(i) The conditions for the 3'-end-filling reaction (30 min, at 20 C) reflect a trade-off between maximizing the end-filling, and minimizing the 3'-to-5' exonuclease activity of the Klenow fragment (Maniatis et al., 1982). I have not determined how much exonucleolytic removal of label and degradation of DNA occurs at this step.

(ii) Denaturation of the Klenow fragment is necessary before proceeding to the secondary restriction step. This must

be done both to prevent its 3'-to-5' exonuclease activity from removing the label and further degrading the DNA, and also to prevent its polymerase activity from introducing label into the secondary restriction site.

(iii) The denatured Klenow fragment and BSA must be removed, to prevent subsequent denaturation of the secondary restriction enzyme (see section V D). The extractions with phenol accomplish both the goals of (ii) and (iii).

(iv) I have found that, if the secondary restriction is attempted in the buffer remaining after steps (i) and (ii), the specificity of the restriction endonuclease may be altered. (An altered specificity was observed for Nci I; data not shown.) Therefore it is prudent (and may even be necessary) to change buffers at this point.

(v) It is best to do the secondary restriction digest in as small a volume as possible, for ease of subsequent purification of the DNA fragment on a gel (see section V D). Therefore the volume of the solution should be decreased. The ethanol precipitation achieves the goals of both (iv) and (v).

(vi) In the precipitation with ethanol, a significant proportion (about 50%) of the unincorporated label (and probably also some cold dATP and dTTP) is brought down, along with the DNA.

The free nucleotide triphosphates do not interfere with the secondary restriction cut, at least for Nci I. (However, the

observed inability to completely cut the DNA with Xmn I or Mnl I [see section V D] may be due to this factor.)

Free label does generate an intense smear in autoradiography, when the secondarily-restricted DNA fragment is purified on a preparative gel (see section V D). This smear prevents one from detecting, in radioautography, exactly where the DNA fragment lies in the gel. Thus, a dialysis step is necessary to remove the free label. I have performed this dialysis after the secondary restriction step; it may actually be better to perform it at this point (to prevent potential interference with the secondary restriction).

D. Secondary restriction; purification of the 195 bp Eco RI - Nci I fragment

A solution of about 4 ug double end-labelled Eco RI fragment in 10-20 ul Tris/EDTA was brought to the appropriate conditions for restriction digestion, by adding 10-fold concentrated stock solutions of BSA and "restriction digestion buffer" (Davis et al., 1980; New England Biolabs catalog, 1983). After thorough mixing and pre-heating to 37 °C, Nci I was gently added. The concentrations of chemical species in the reaction were:

DNA, 0.15 - 0.2 ug/ul (0.9 - 1.2 uM recognition sites);

Nci I, 2-3 U/ul;

$MgSO_4$, 5 mM;

NaCl, 25 mM;

Tris, 10 mM;

DTT, 0.5 mM;

BSA, 100 ug/ml;

EDTA, 0.25 mM.

The pH was approximately 7.4. The reaction was allowed to proceed 10-24 hours at 37 °C. Periodically, progress was monitored by removing an aliquot, performing one extraction with PCIA and two extractions with ether, and then running the aliquot on a polyacrylamide "E" gel. Both the disappearance of the 260 bp band, and the appearance of new bands at 195 bp and 65 bp could be followed.

After the enzymatic digestion was complete, one extraction was done with PCIA. About 50% of the radioactivity remained in a cloudy interface, possibly in the form of radiolabelled DNA. So as not to discard this component, the interface was extracted 3 times with 5 ul Tris/EDTA, and the aqueous extracts combined with the original aqueous phase.

The aqueous sample of DNA was then placed in a small (200-500 ul) capless polypropylene tube, a dialysis membrane (cutoff 3000-8000 daltons) was fastened around the open end of the tube with a rubber band, and the sample was forced against

the dialysis membrane by shaking the tube once. The sample was then dialyzed against 4 L of Tris/EDTA for 24 hours, to remove free [$\alpha$32P]-dATP.

The dialyzed sample was made 10% in glycerol and 0.0025% in bromophenol blue, and was run on a 0.8 mm thick, 15 cm long polyacrylamide "E" gel. To detect the 195 bp band by radioautography, one glass plate was removed, and the gel (still attached to the other glass plate) was covered with plastic wrap. Radioautography was done with Kodak X-OMAT film and a DuPont "Cronex Lightning Plus" (calcium tungstate) fluorescent "intensifying" screen, at -60 to -80 °C (Swanstrom and Shank, 1978). A 15-60 min exposure was sufficient to generate an image of the 195 bp band.

Before the gel had a chance to thaw, the developed film was placed under the glass plate/gel/plastic wrap assemblage, and a clean razor blade was used to cut out the 195 bp gel band, through the plastic wrap.

Elution of the DNA was performed by the "NH4OAc" method as described in Maniatis et al. (1982), but with minor modifications. The (still frozen) gel slice containing the 195 bp fragment was placed in a 1.5 ml polypropylene tube. One volume of 0.5 M $NH_4OAc$, 1 mM EDTA, pH 7.0 was added, and the gel slice was mashed into fine particles. The suspension was incubated 4 hours at 37 °C. The eluent, containing about 50% of the radioactivity, was then removed with a Gilson 200 ul

Pipetman. This procedure was repeated 3 more times, leading to a removal from the gel slice of 90-95% of the radioactivity. The pooled eluent was centrifuged 15 min at 8800 x g to remove acrylamide fragments. The DNA (about 4 ug) was precipitated with NaCl, $Mg(OAc)_2$ and EtOH as described above, dried with $N_2$ gas or air, and resuspended in 10-20 ul of Tris/EDTA. Several extractions with ether were then done, to help remove any organic contaminants from electrophoresis.

Figure 5A shows an ethidium-fluorescence photograph of this repurified, single-end-labelled DNA fragment, run on a polyacrylamide "E" gel. It appears to be perfectly homogeneous, except for some aggregated material at the top of the gel. In radioautography (Figure 5B), more contaminaion is apparent. The contamination may be divided into three categories. First, as in the ethidium-fluorescence photograph, there is aggregated material at the top of the gel. Second, there appears to be a trace of 65 bp DNA, which must have been generated during the secondary restriction step. Presumeably, this 65 bp DNA fragment had base-paired with the 195 bp fragment, to form a 260 bp double-nicked entity which was carried through the gel electrophoresis; poor aim in cutting out the 195 bp band then allowed inclusion, in the sample, of this 260 bp entity, which subsequently fell apart. Third, there appear to be degradation products of the 260 bp- and 195 bp fragments. Thus the (chloramphenicol-amplified) cloned DNA may be subject to fairly

Fig. IV.5A. Purified 195 bp Eco RI - Nci I fragment, labelled with $^{32}$P at the Eco RI end, on a 3.5 % polyacrylamide "E" gel. 1. Ethidium-fluorescence photograph.

The 260 bp Eco RI fragment was double-end-labelled with [$\alpha$32P]-dATP, using the end-filling activity of the Klenow fragment of DNA polymerase I. It was then cleaved to completion with Nci I, generating a 195 bp fragment with label just at the Eco RI end. This secondary restriction fragment was purified as described in the text, run on a 3.5 % polyacrylamide "E" gel, and stained with ethidium bromide (lane 2; lanes 1,3 display pBR322/Cfo I markers).

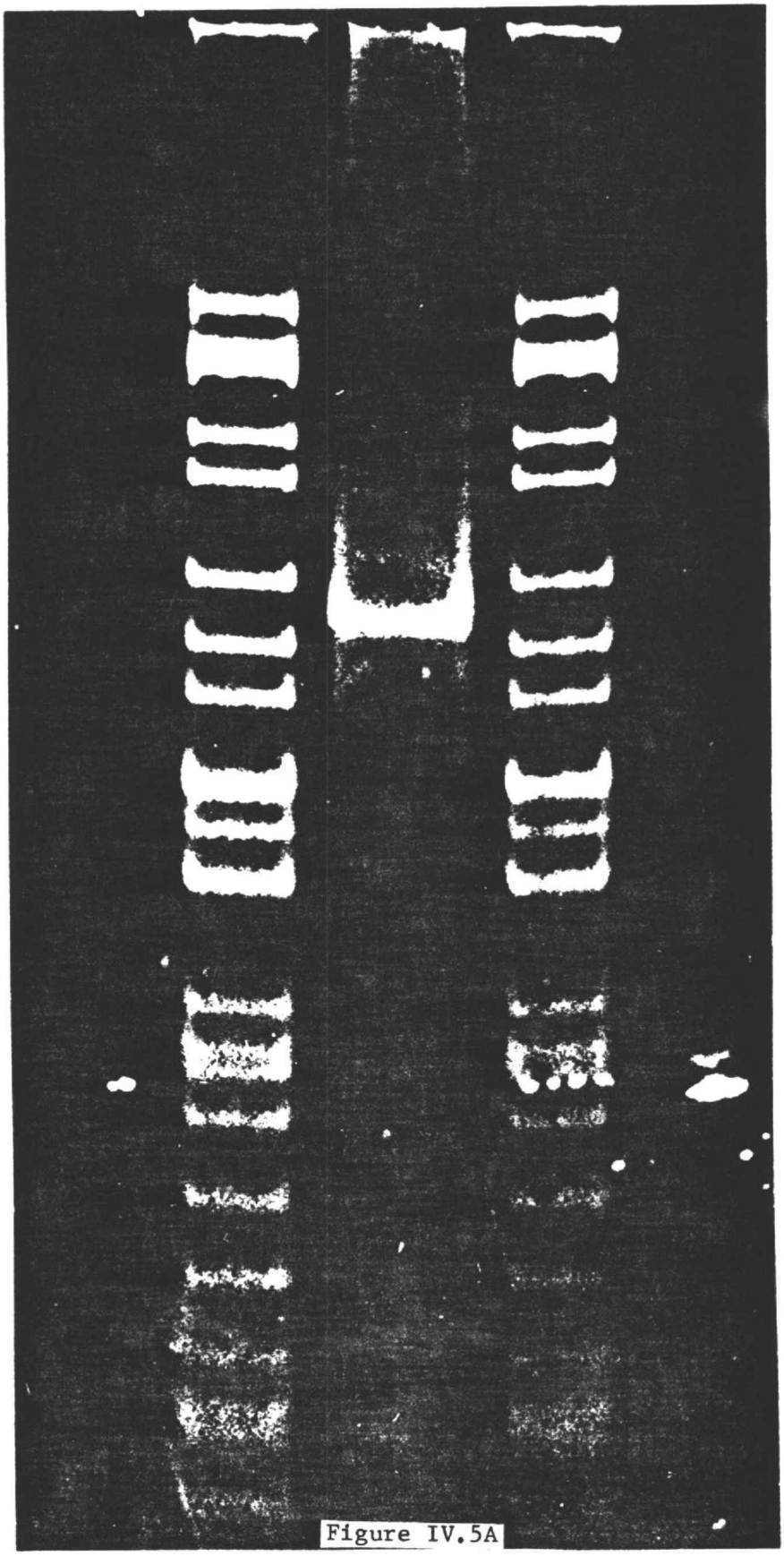

Figure IV.5A

Fig. IV.5B. Purified 195 bp Eco RI - Nci I fragment, labelled with $^{32}P$ at the Eco RI end, on a 3.5 % polyacrylamide "E" gel. 2. Radioautograph.

The gel from Figure 5A was dried and subjected to radioautography. Note traces of DNA bands other than the 195 bp band, in this radioautograph.

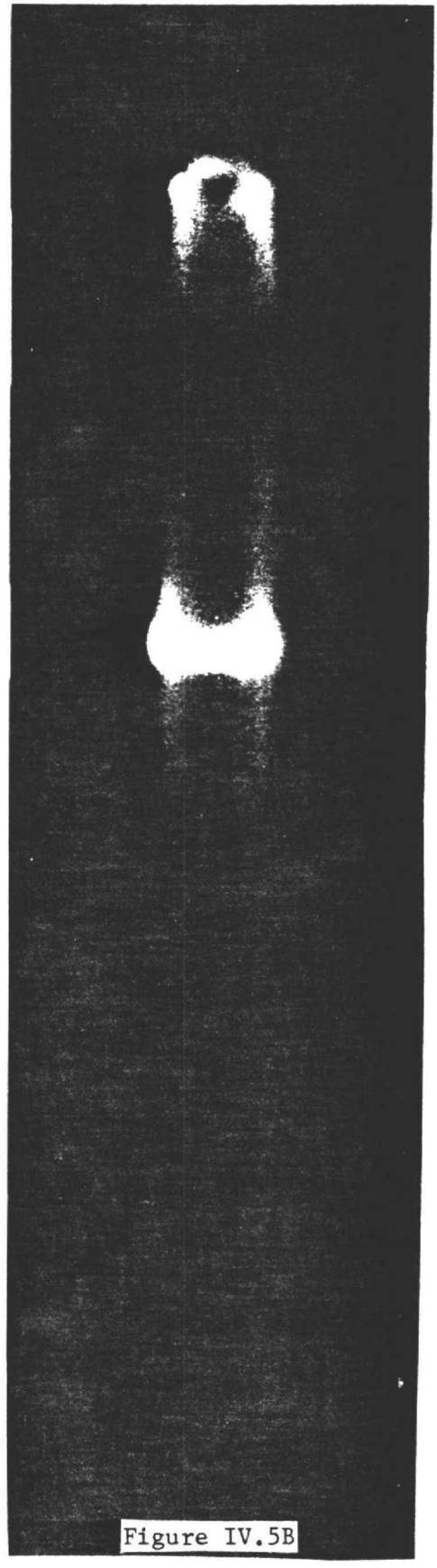

Figure IV.5B

rapid spontaneous degradation, even during its purification. This possibility is investigated further in section IV E.

The following points should be noted about the above protocol:

(i) The secondary restriction reaction always goes to completion with Nci I. In contrast, I have been unable to consistently get more than about 10% secondary restriction with either Xmn I or Mnl I (cf. section V A, 3), when these restriction enzymes were used under the appropriate buffering conditions. Three possible sources of difficulty come to mind. One is that free dATP and dTTP, carried through the previous ethanol precipitation step, may inhibit these enzymes. Another is that Xmn I or Mnl I may not be able to cleave sites which lie close to the ends of a target DNA molecule. A third possibility is that the small DNA fragments released by digestion with these enzymes may act as competetive inhibitors in the cleavage reaction. I have not attempted to critically test any of these possibilities.

(ii) Before either the initial gel diagnosis or the large-scale gel purification of 195 bp DNA, it is crucial to extract the samples with PCIA and ether, to prevent aggregation. In the first of these extractions, an interface is generated between the hydrophobic and aquaeous phases, which traps up to 50% of the radiolabel. To recover the label, it is necessary to extract this interface 2-4 times with Tris/EDTA.

(iii) In order to see the 195 bp band in the preparative gel, the free [$\alpha$32P]-dATP, which was carried through the previous precipitation step, must be removed. This is accomplished through dialysis.

(iv) To obtain the 195 bp fragment from the preparative gel, one may utilize diffusion into $NH_4OAc$, in place of electroelution. (Because of the large volumes of eluent involved, however, electroelution is relatively inconvenient.)

E. The stability of the 195 bp Eco RI - Nci I fragment

Both from the statistical "nicking" and "ribose substitution" analyses of Figures 2 and 3, and from the direct examination of 195 bp DNA in radioautography (Figure 5B), it seemed to me that chloramphenicol-amplified plasmid DNA may be quite subject to spontaneous degradation.

The problem of stability was examined more thoroughly as follows. Single-end-labelled 195 bp DNA was obtained using the above purification scheme, and was diluted to about 20 ng/ul in Tris/EDTA. It was then incubated either (i) at 0 °C for 3 days, (ii) at 22 °C for 3 days, or (iii) at 37 °C for 1 day, and then at 22 °C for 2 more days. Aliquots of these incubated samples were then run on a polyacrylamide "E" gel.

For each incubation condition, only a single band at 195 bp was observed in ethidium-fluorescence photography (Figure 6A).

Fig. IV.6A. Stability of the end-labelled 195 bp fragment. 1. Stability over 3 days' incubation in buffer. Polyacrylamide "E" gel; ethidium-fluorescence photograph.

Purified 195 bp single-end-labelled fragment was incubated in Tris/EDTA at 0 °C or 22 °C for 3 days, or at 37 °C for 1 day and then at 22 °C for 2 more days. The three samples were then run on a 3.5 % polyacrylamide "E" gel, and stained with ethidium bromide. (Lanes 3,4,5: samples incubated at 0, 22 or 37/22 °C, respectively; lanes 1,2 6: pBR322/Cfo I marker.)

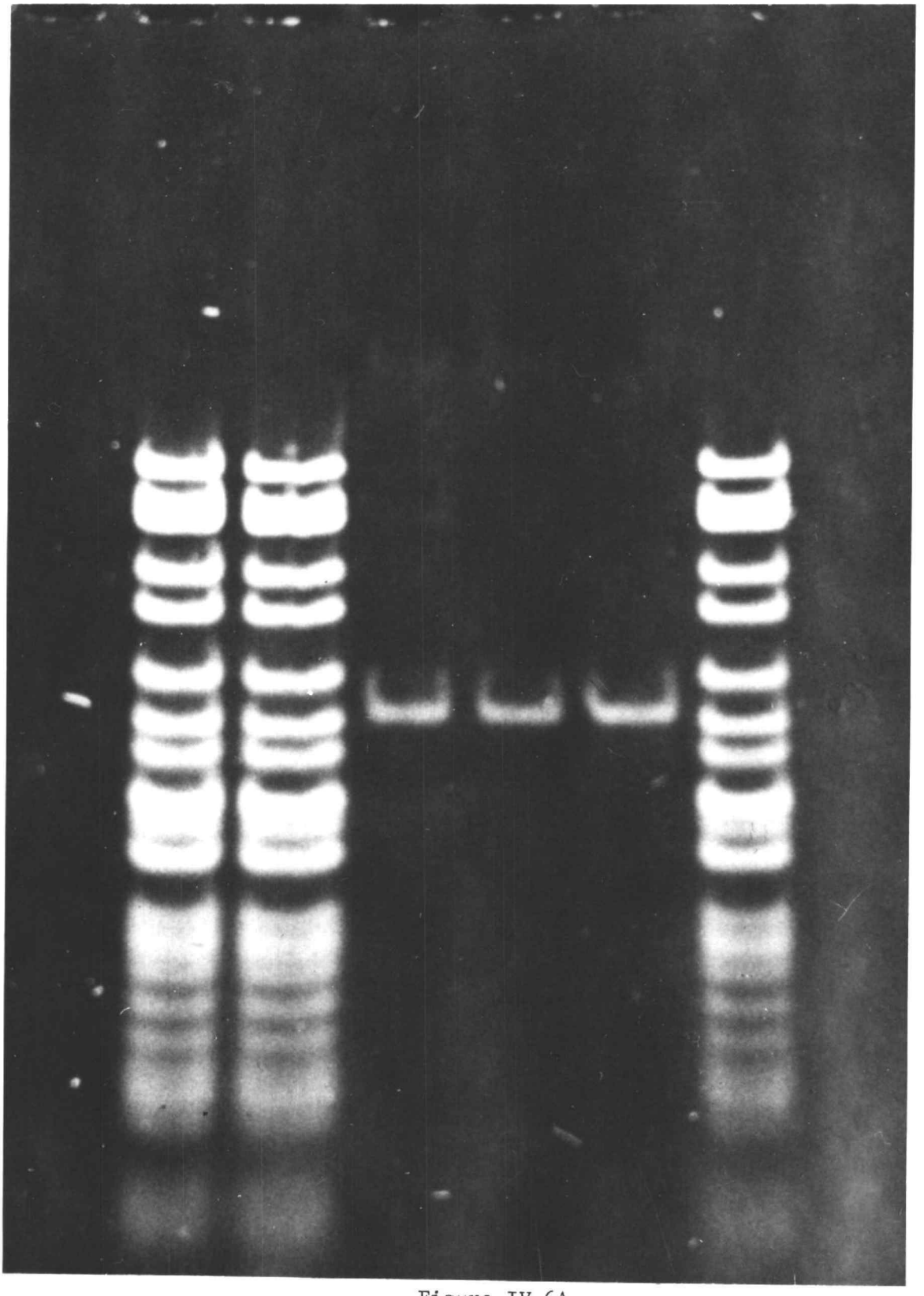

Figure IV.6A

In radioautography also, the DNA samples appeared mostly intact, although there may have been some generation of heterogeneity with increasing temperature of incubation (Figure 6B). (I note that, in the radioautograph, there are what appeared to be "dimer" bands. Thus the "sticky ended" 195 bp fragment may have had a tendency to form catemers in Tris/EDTA, which are not disrupted by electrophoresis in "E" buffer. This is consistent with my hypothesis, above, about how a trace of the 65 bp restriction fragment can be carried through preparative electrophoresis by base-pairing with the 195 bp fragment [see section V D and Figure 5B].)

At this point, it worth digressing to ask how sensitive electrophoresis in polyacrylamide "E" gels is as an assay for DNA degradation. The following statistical argument suggests that, in such gels, even fairly extensively nicked DNA molecules might not be resolved from unnicked molecules.

Suppose that there is a probability $p=1/2$ of one strand of a 200 bp DNA molecule being nicked once at random. Then the probability of a nick occurring in some particular 10 bp segment of the molecule is $p = 1/2 \times 10/200 = 1/40$. Suppose now that, for a 200 bp molecule which is nicked once on each strand, a separation into two half-molecules (each double stranded) will occur only if the two nicks are within the same 10 bp segment. For a particular 10 bp segment, the joint probability of this occurrance is $p = 1/40 \times 1/40 = 1/1600$.

Fig. IV.6B. Stability of the end-labelled 195 bp fragment. 1. Stability over 3 days' incubation in buffer. Polyacrylamide "E" gel; radioautograph.

After photography, the gel from Figure 6A was dried, and an autoradiogram made. (Lanes 1,2,3: samples incubated at 0, 22, or 37/22 $^{o}$C, respectively.) Note: the 195 bp fragment apparently had a tendency to form a hydrogen-bonded dimeric structure under the first two incubation conditions (but not under the third condition): bands in the correct position for a dimer can be seen in the autoradiogram.

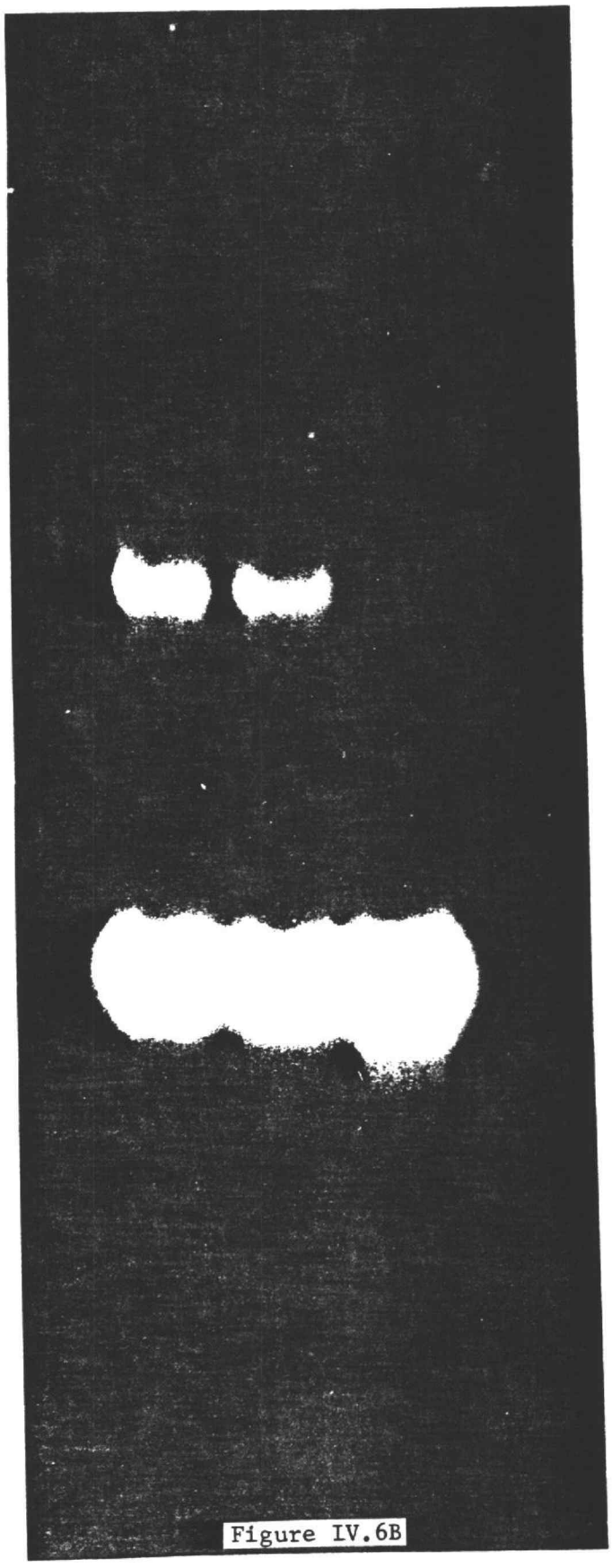

Figure IV.6B

Since there are 20 choices of a 10 bp segment within the 200 bp molecule, the total probability for generating two half-molecules is p = 20 x 1/1600 = 1/80. Thus if every DNA molecule in a sample has two nicks, one placed at random in each strand, then only about 1% of these molecules will run differently from the intact molecule, on a polyacrylamide "E" gel. Clearly, one needs a more critical test for nicking than an examination on this type of gel.

Aliquots from the incubations of Figures 6A/6B were brought to 30% DMSO, heated 5 min at 100 $^{o}$C, and run on a "SS" gel. In staining by ethidium, the "195 bp" band appeared non-Gaussian (Figure 6C). Such an apperance might not have been due to degradation, however: it could instead simply have been an artifact of electrophoresis. A more critical test for degradation was provided by radioautography. When the "SS" gel was allowed to expose a film, a striking degradation pattern emerged (Figure 6D). A significant fraction of the radioactivity was seen to reside in discrete bands smaller than 195 bp. Some of these bands were much more prominent than others. Thus there seemed to be "hot spots" for nicking.

At what point in this "nick-detection experiment" was such extensive DNA damage introduced? In the radioautograph, the three samples were virtually identical in their extent and patterns of nicking. This lack of a strong difference suggests that the majority of the nicking occured either before or after

Fig. IV.6C. Stability of the end-labelled 195 bp fragment. 2. Stability over 3 days' incubation in buffer, followed by 5 min heating at 100 $^{o}$C. "SS" gel; ethidium fluorescence photograph.

After 3 days, samples from Figures 6A and 6B were made 30% in DMSO, were heated 5 min at 100 $^{o}$C, and were then put on ice. They were next run on a 6% polyacrylamide "SS" gel and stained with ethidium bromide. (Lanes 3,4,5: samples from Figures 6A and 6B incubated at 0,22 or 37/22 $^{o}$C, respectively; lanes 1,2,6: pBR322/Cfo I marker.)

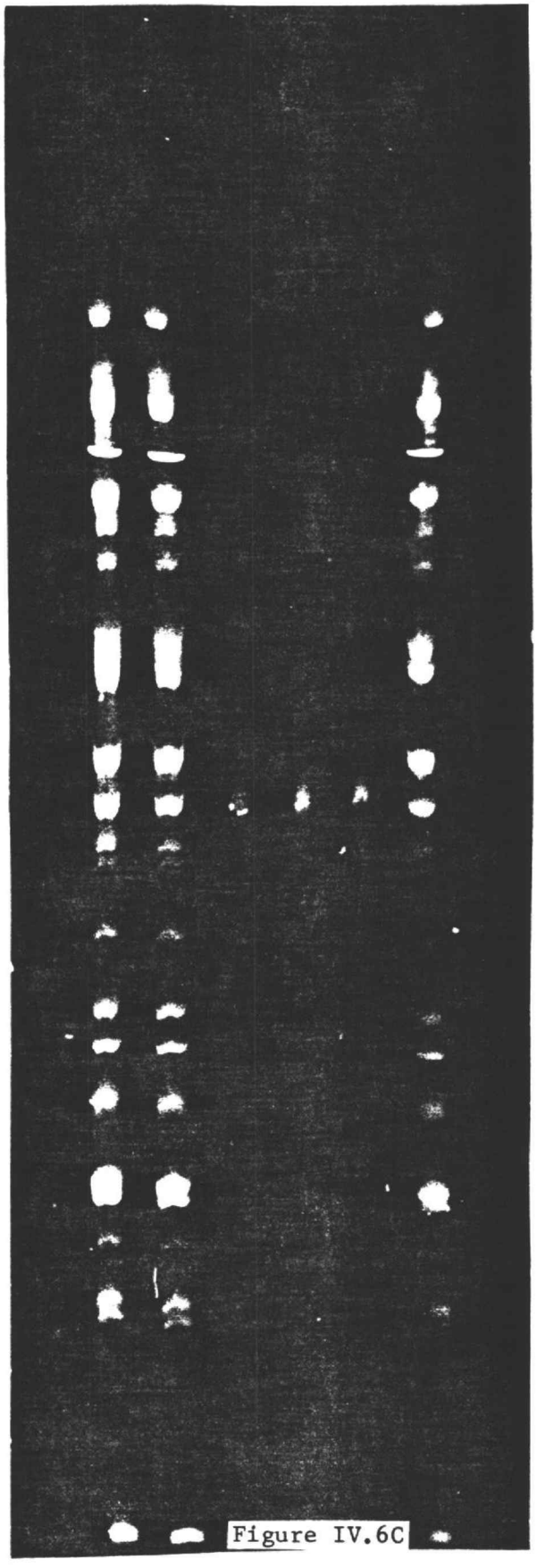

Figure IV.6C

Fig. IV.6D. Stability of the end-labelled 195 bp fragment. 2. Stability over 3 days' incubation in buffer, followed by 5 min heating at 100 $^{o}$C. "SS" gel; radioautograph.

The gel from Figure 6C was dried and subjected to radioautography. (Lanes 1,2,3: same as Figure 6C, lanes 3,4,5.) Note the presence of specific degradation bands in the radioautograph.

Figure IV.6D

the 3-day incubation step. It seems quite plausible to suppose that most of the nicking occurred during heating to 100 °C in 30% DMSO, in preparation for the "SS" gel analysis.

The incubation of samples at 0, 22 or 37 °C was continued for an additional 10 days. During this time, the water in the 37 °C sample evaporated onto the top of the (closed) incubation vial, leaving at the bottom a dried pellet of DNA, Tris and EDTA. This pellet ultimately was resuspended in the original amount of water at the end of the experiment, before gel analysis. After the 10 day incubation period, the samples were run on a polyacrylamide "E" gel. An ethidium-fluorescence photograph and radioautograph are shown in Figures 6E and 6F, respectively. The sample from 0 °C appeared almost completely intact. In contrast, there was a large amount of degradation in the 22 °C sample (observable even on a polyacrylamide "E" gel!). The 37 °C pellet appeared hardly damaged. I conclude that a significant amount of nicking probably occurs spontaneously in Tris/EDTA, if the temperature of incubation is around 20 °C. The DNA appears fairly stable in this buffer at 0 °C, or (surprisingly) as a dried pellet with EDTA and Tris at 37 °C.

Two practical conclusions arise from the above tests. First, the radiolabelled DNA fragment should be stored either dry or, if in solution, at 0 °C. Second, it seems likely that, even if degradation can be avoided during storage and

Fig. IV.6E. Stability of the end-labelled 195 bp fragment. 3. Stability over 13 days' incubation in buffer at 0 or at 22 °C, or over 3 days' incubation in buffer at 27°C, followed by 10 days incubation in solid form at 37 °C. Polyacrylamide gel; ethidium fluorescence photograph.

The incubation from Figures 6A, 6B was continued an additional 10 days. During this period, the liquid in the 37/22 °C sample evaporated to the top of its tube. Thus, at the end of the incubation, the samples had been kept either: (i) at 0 °C in buffer, for 13 days; (ii) at 22 °C in buffer for 13 days; or (iii) at 37 °C in buffer for 1 day, next at 22 °C in buffer for 2 days, and finally at 37 °C in solid form for 10 days. The samples were run on a 3.5% polyacrylamide "E" gel, and stained with ethidium bromide. Samples (i), (ii), (iii) are in lanes 1,2,4. Lane 3 shows pBR322/Cfo I markers.

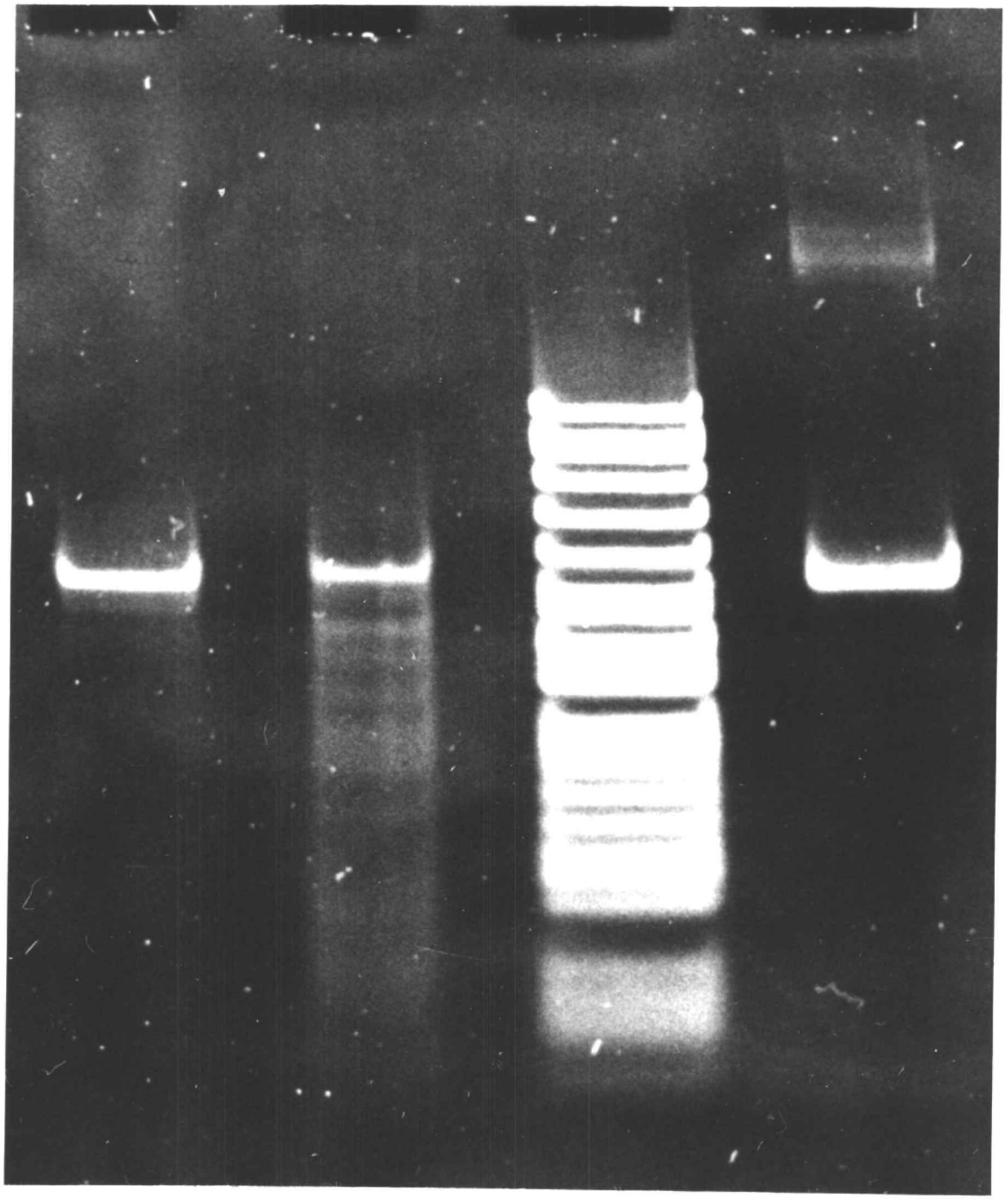

Figure IV.6E

Fig. IV.6F. Stability of the end-labelled 195 bp fragment. 3. Stability over 13 days' incubation in buffer at 0 or at 22 °C, or over 3 days' incubation in buffer at 27°C, followed by 10 days incubation in solid form at 37 °C. Polyacrylamide gel; radioautograph.

The gel from Figure 6E was dried and subjected to radioautography. Samples (i), (ii), (iii) are in lanes 1,2,4. Lane 3 is blank because the pBR322/Cfo I markers were not radiolabelled.

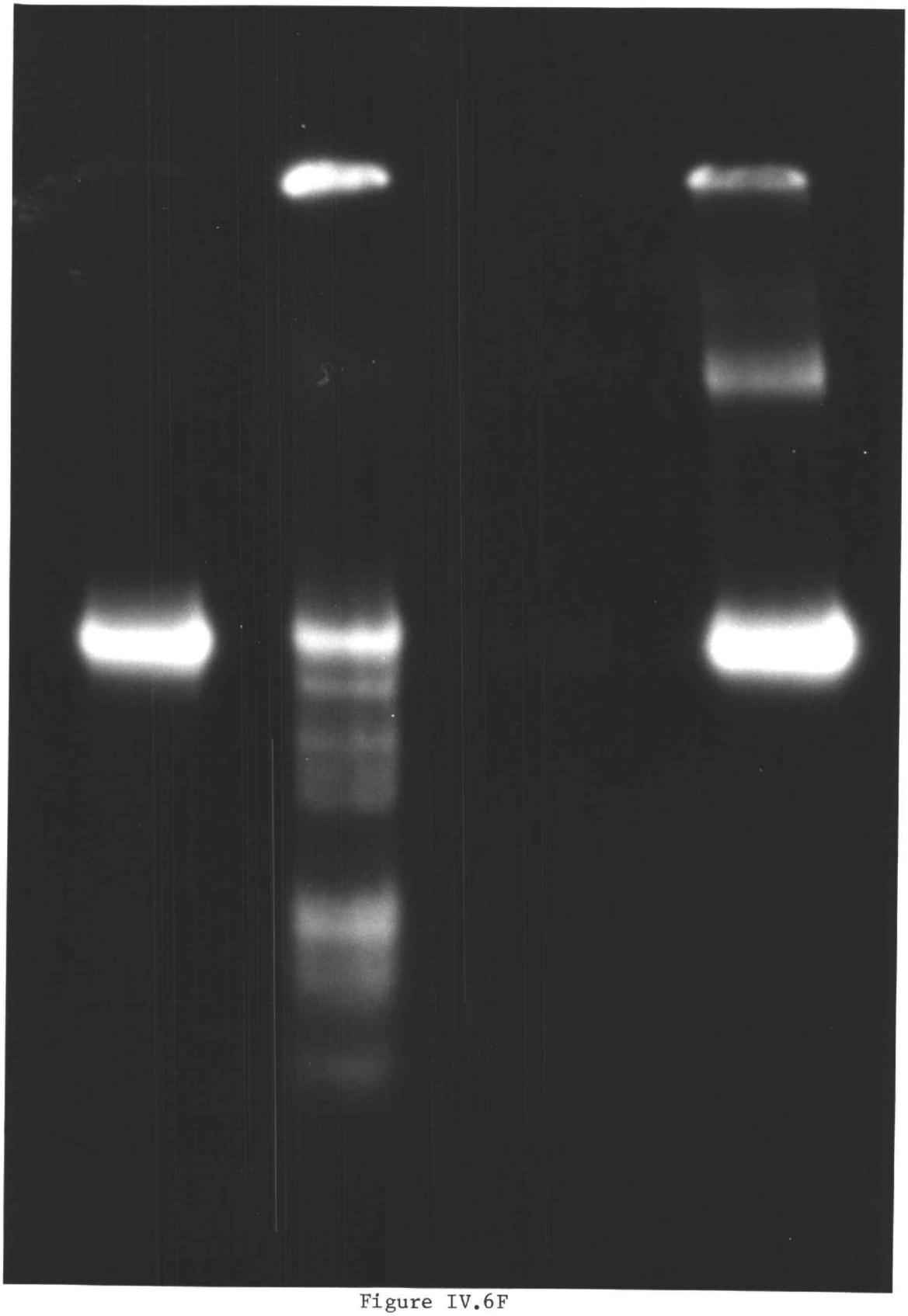

Figure IV.6F

experiments, it will occur spontaneously during the preparation of DNA samples for electrophoresis on a "SS" gel.

A somewhat superficial solution to the problem of stability would be to store DNA at 0 °C, to do experiments at low temperature, and then, if analysis on "single-stranded DNA" gels is necessary, to denature the samples by a route that avoids heating (if possible). A more satisfactory solution undoubtedly will involve changing the procedure for plasmid amplification, so that less ribose-substitution occurs. It may be necessary to actually omit the amplification step, and work with "indiginous" plasmid.

## VI. Reconstitution of nucleosomes

I have examined two methods of reconstitution of nucleosomes onto the 195 bp Eco RI - Nci I fragment. The first involves transfer of purified histones to the radiolabelled DNA, using the (nucleoplasmin-like) histone carrier poly(L-glutamic acid) (Stein et al., 1979; Simpson and Stafford, 1983). The second reconstitution method involves histone transfer from intact core particles to the radiolabelled DNA.

Of the two methods, I found the second to be simpler and more reliable, and to give a higher efficiency of reconstitution. I note, however, that it suffers from a

fundamental limitation: the radiolabelled nucleosomes will be present in only trace amounts, relative to cold carrier nucleosomes. Separation of the two species, as a prelude to physical studies, will be difficult or impossible.

A. The "histone transfer from core particles" method

Briefly, the "transfer from core particles" method involves mixing unlabelled core particles with a trace amount of radiolabelled DNA, raising the salt by dialysis to allow histone transfer from the core particles to the radiolabelled DNA (by some unknown mechanism[s]), and then lowering the salt concentration again. With respect to the phasing pattern on an Eco RI - Xmn I fragment or on a Eco RI - Mnl I fragment, the nucleosomes produced by the "transfer from core particles" method and the "poly(L-glutamic acid)" method appear to be identical (R.T. Simpson, personal communication, 1983).

There are a number of variables in the "transfer from core particles" method which may critically affect the reconstitution process. These are: (i) the molar concentration of (unlabelled) core particles; (ii) the molar concentration of radiolabelled DNA; (iii) the molar ratio of core particles to radiolabelled DNA (determined by [i] and [ii], above); (iv) the concentration of salt in the first dialysis step; and (v) the duration of the first dialysis step. I assume (but do not

attempt to demonstrate) that the temperatures of the first and second dialysis steps, and the duration of the second dialysis step are less critical variables. In the course of this work, I have found one or two other, much less obvious variables which greatly affect the reconstitution process. These are: (vi) the ratio of the dialysis volume to the dialysis membrane's surface area, and/or (vii) the ratio of the dialysis volume to the area of the air/liquid interface, in the two dialysis steps.

A rough idea of values to use for these variables, and of a reasonable reconstitution procecure, was obtained from Dr. R.T. Simpson (personal communication, 1983). Thus the first dialysis step always lasted 75-90 min. It was always done against a 1 L bath of Tris/EDTA which was initially at 20 $^{o}$C, and was then lowered toward 4 $^{o}$C during the dialysis. Similarly, the second dialysis always lasted > 3 hours. It was always done against a 1 L bath of Tris/EDTA which was initially at 20 $^{o}$C, and was lowered toward 4 $^{o}$C during the dialysis.

The problem of finding optimum values for the concentration of core particles, the concentration of radiolabelled DNA, and the core particle/DNA ratio was approached next. This is formally equivalent to the problem of maximizing a function (the reconstitution yield), when this function depends simultaneously upon two independent variables (two of the three variables of core particle concentration, radiolabelled DNA concentration, and core particle / radiolabelled DNA ratio).

This problem may be solved through a "grid search" (Bevington, 1969). A grid search involves: (i) fixing the first independent variable at an arbitrary value; (ii) finding the optimum of the second independent variable; (iii) holding the second independent variable at its newly-found optimum, and then determining the resultant optimum of the first independent variable. Successive rounds of iteration are made, leading eventually to both independent variables being optimized.

There are three points to note about using a grid search to optimize nucleosome reconstitution. First, more than one round of iteration probably will be required for true optimization, as this method converges slowly (Bevington, 1969). A search by a "simplex" method should converge to an optimum considerably more quickly (Backman and Shanbhag, 1984). Second, the reconstitution maximum found by the grid search may not be a global maximum, but instead only a local maximum (Bevington, 1969). (In other words, there may be other combinations of the two independent variables' values which also yield [local] reconstitution maxima.) Third, the optimum found by the above method probably will only hold within the particular constraints of the reconstitution procedure. Thus, for example, were the first dialysis step done for a different length of time, or against a different concentration of NaCl, other values of the two independent variables might be optimum.

B. Dependence of reconstitution yield upon the concentration of core particles

A reconstitution was attempted in which the concentration of core particles was varied, while the concentration of radiolabelled DNA was held constant. This experiment was done by placing 30 ul of a solution of core particles and radiolabelled DNA in a 200 ul polypropylene centrifuge tube, fastening a dialysis membrane over the top of the tube with a rubber band, shaking the tube once to force the liquid against the membrane, and then dialyzing. Thus the reconstitution occurred in a 30 ul hemispherical bead against the dialysis membrane. (In this situation, the calcuated ratio of bead volume to membrane surface area was about 0.16 cm. The calculated ratio of bead volume to liquid/air interfacial area was about 0.082 cm. The particular values these two ratios have very likely are critical in the reconstitution; see section VI E.)

Figures 7A and 7B, respectively, show both an ethidium-fluorescence photograph and a radioautograph of a polyacrylamide "E" gel on which the reconstitution was analyzed. For calibraton, Cfo I-cut pBR322 was run in lane 3 of the gel, as shown in the ethidium-fluorescence photograph. From left to right in either 7A or 7B, the concentration of core particles in the reconstitution was 320, 400, 480, 560 or 640

Fig. IV.7A. Reconstitution of nucleosomes, by the method of "histone transfer from (unlabelled) core particles". 1. The effect of changing the concentration of the core particles. "Native" gel; ethidium-fluorescence photograph.

Unlabelled core particles and 3'-end-labelled 195 bp Eco RI-Nci I fragment, each in Tris/EDTA, were mixed together. After mixing, the concentration of radiolabelled DNA was about 3 ng/ul (24 nM), and the concentration of core particles was 320, 400, 480, 560, or 640 nM. Each sample was dialyzed against Tris/EDTA + 0.7 M NaCl for 1.25-1.5 hours, and then against Tris/EDTA for >3 hours. In each dialysis step, the temperature was lowered from an initial 20 $^{o}$C toward 4 $^{o}$C. The ratio of sample volume to dialysis membrane area was always about 0.16 cm, and the ratio of sample volume to liquid/air interfacial area was always about 0.082 cm.

After dialysis, aliquots of the samples were run on a 3.5% polyacrylamide "E" gel. The gel was stained with ethidium bromide and photographed under long-wave UV transillumination.

Lanes 1,2,4,5,6: samples with 320, 400, 480, 560 or 640 nM core particles, respectively. Lane 3: Cfo I-cut pBR322, as marker.

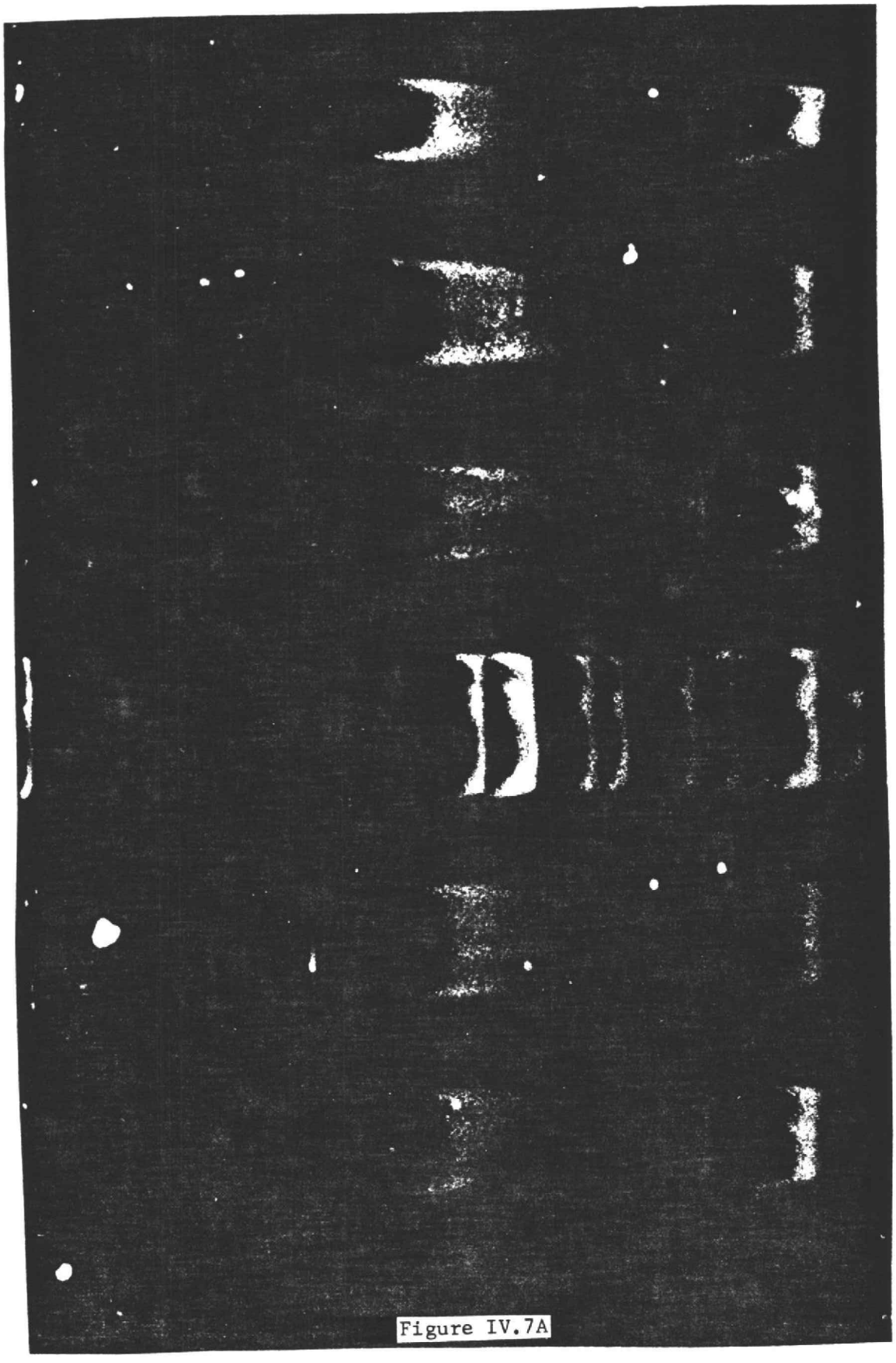

Figure IV.7A

Fig. IV.7B. Reconstitution of nucleosomes, by the method of "histone transfer from (unlabelled) core particles". 1. The effect of changing the concentration of the core particles. "Native" gel; radioautograph.

The gel from Figure 7A was dried and subjected to radioautography.

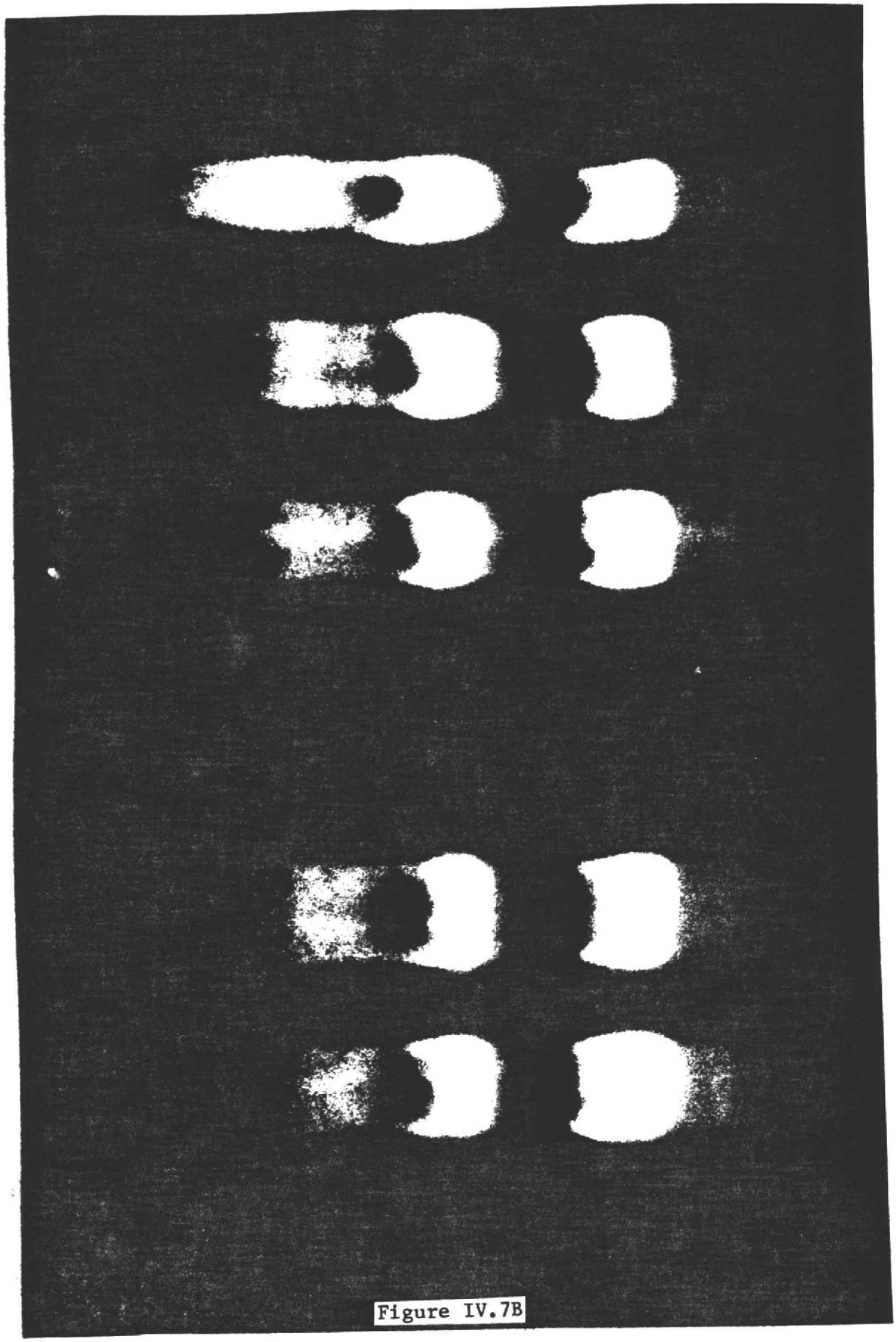

Figure IV.7B

nM, respectively (optical densities of 0.64, 0.80, 0.96, 1.13 or 1.29 at 260 nm, known by spectral analysis to an uncertainty of about 1-3%). The concentration of radiolabelled DNA was always about 3 ng/ul (24 nM). (The concentration of the radiolabelled DNA was measured by loading several different-sized aliquots on a polyacrylamide "E" gel along with spectrally-measured DNA standards, staining the gel with ethidium bromide, taking a fluorescence photograph, and scanning the film negative. There is about 30% uncertainty in the concentrations of radiolabelled DNA estimated in this fashion.) From above, I calculate the molar ratio of core particles to radiolabelled DNA to be about 13, 17, 20, 23 or 27, respectively, in the different trials.

There are a number of features to note about this reconstitution attempt:

(i) The yield of the reconstituted nucleosomes (second band from the top, in Figure 7B) increases approximately linearly with core particle concentration, from a low of 29% at 320 nM, to a high of 41% at 640 nM (cf. Figure 7C).

(ii) A second DNA/histone complex is also generated (first band from the top, in Figure 7B). The yield of this unidentified and undesireable complex also increases linearly with core particle concentration, from a low of 7% at 320 nM to a high of 24% at 640 nM (cf. Figure 7C). It is critical to keep the production of this unidentified complex to a minimum,

Fig. IV.7C. Reconstitution of nucleosomes, by the method of "histone transfer from (unlabelled) core particles". 1. The effect of changing the concentration of the core particles. Quantitation of the radioautograph of Figure 7B.

The radioautograph from Figure 7B was scanned, to determine the percentage of radiolabelled DNA incorporated into nucleosomes (middle band), or into an unidentified "histone/DNA complex" (upper band). This percentage, or yield, was graphed versus the concentration of unlabelled core particles present at the start of reconstitution. Circles: nucleosomes. Triangles: unidentified "histone/DNA complex".

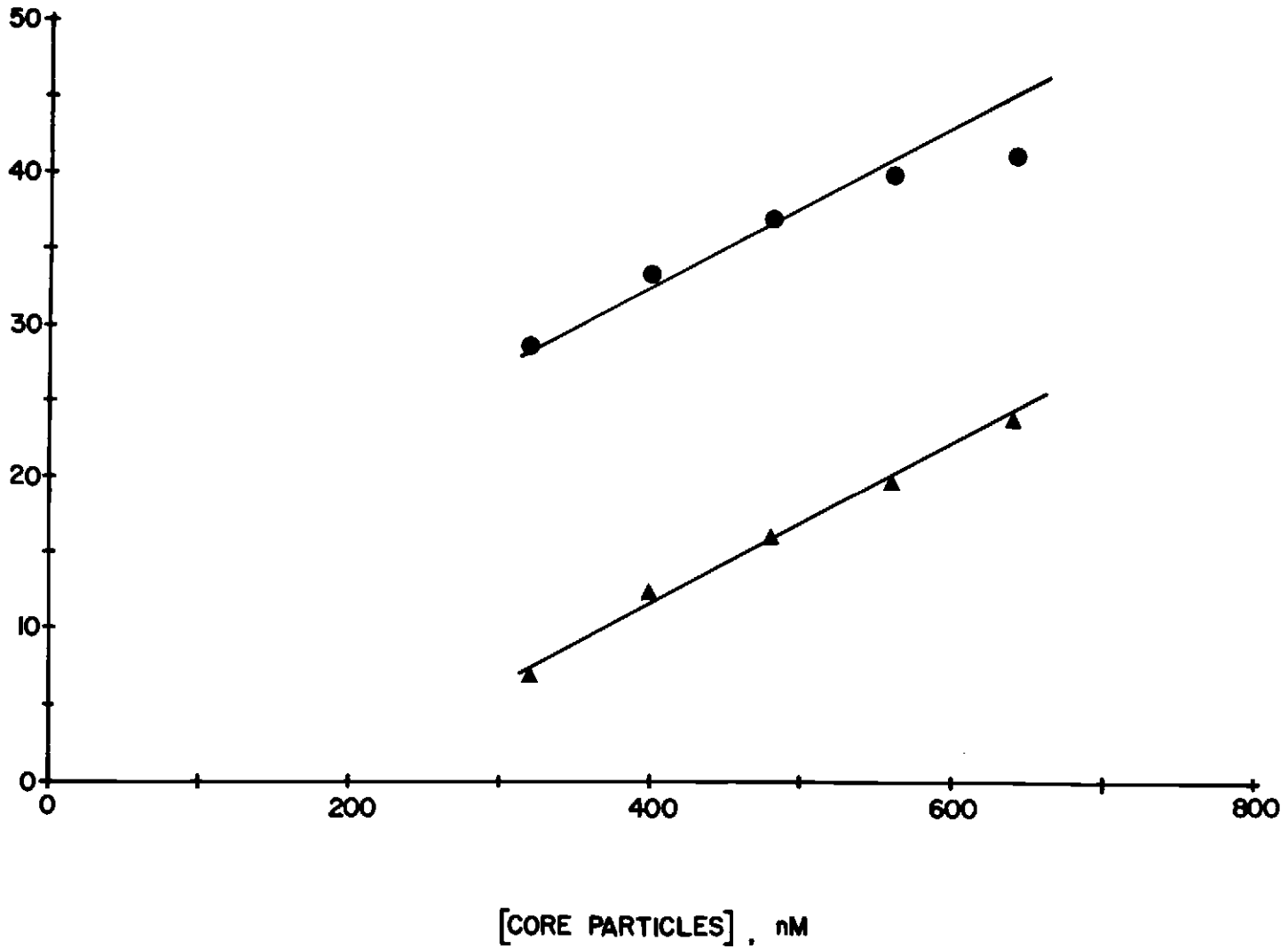


Figure IV.7C

because it will introduce artifacts into the subsequent DNAase I analyses of the reconstituted nucleosomes (see section VIII).

(iii) In the radioautograph (Figure 7B), some heterogeneity in the radiolabelled DNA may be apparent. For a discussion of the probable causes of this heterogeneity, see sections V D and E.

(iv) From the ethidium-stained gel (Figure 7A), it is apparent that the transient exposure to high salt concentration generates more free DNA from core particles that can be accounted for by the stoichiometry of the histone-transfer reaction. Also, the core particle band possible displays more heterogeneity than it did before the experiment began (original core particle band not shown). Thus a transient exposure to high salt causes the unlabelled components in the reconstitution system to become less well defined.

C. Dependence of reconstitution yield upon the concentration of radiolabelled DNA

A second reconstitution experiment was done in the same fashion as above, to explore the dependence of reconstitution yield on the concentration of the radiolabelled DNA. This and the previous experiment together comprise one iteration of a "grid search" for the reconstitution maximum (see above). In this second experiment, the core particle concentration was

held constant at 480 nM (an optical density of 0.96 at 260 nm), and the concentration of radiolabelled DNA was varied. In Figures 8A and 8B, this reconstitution attempt is displayed on a polyacrylamide "E" gel (ethidium-fluorescence photography and radioautography, respectively). For calibration, Cfo I-cut pBR322 was run in lane 4 of the gel. The concentration of radiolabelled DNA in the reaction was 0.75, 1.5, 3, 6, or 12 ng/ul (lanes 1,2,3,5 and 6, respectively, in 7A or 7B; concentrations known with an absolute uncertainty of about 30%). This translates to 6, 12, 24, 48 and 96 nM, respectively. Thus the molar ratios of core particles to radiolabelled DNA are 80, 40, 20, 10, and 5.

The following points should be noted:

(i) The yield of reconstituted nucleosomes (the second band from the top, in Figure 8B) increases monotonically as the concentration of radiolabelled DNA is decreased (cf. Figure 8C). The effect is dramatic: at the lowest concentration of radiolabelled DNA (and so at the highest core particle/DNA ratio), the yield is about 75%.

(ii) A second histone/DNA complex (possibly heterogeneous) is always generated (cf. the upper band in Figure 8B). About 25-30% of the input radiolabelled DNA ends up in this complex, regardless of the initial concentration of radiolabelled DNA (cf. Figure 8C).

(iii) In the radioautograph (Figure 8B), in addition to the

Fig. IV.8A. Reconstitution of nucleosomes by the method of "histone transfer from (unlabelled) core particles". 2. Effect of changing the concentration of radiolabelled DNA. "Native" gel; ethidium fluorescence photograph.

Unlabelled core particles and 3-end-labelled 195 bp Eco RI-Nci I fragment, each in Tris/EDTA, were mixed together. After mixing, the concentration of core particles was 480 nM, and the concentration of radiolabelled DNA was approximately 0.8, 1.5, 3, 6 or 12 ng/ul (6, 10, 24, 50 or 100 nM, respectively). Each sample was dialyzed against Tris/EDTA + 0.7 M NaCl for 1.25-1.5 hours, and then against Tris/EDTA for >3 hours. In each dialysis step, the temperature was lowered from an initial 20 °C toward 4 °C. The ratio of sample volume to dialysis membrane area was always about 0.16 cm, and the ratio of sample volume to liquid/air interfacial area was always about 0.082 cm.

After dialysis, aliquots of the samples were run on a 3.5% polyacrylamide "E" gel. The gel was stained with ethidium bromide and photographed under long-wave UV transillumination.

Lanes 1,2,3,5,6: samples with 0.8, 1.5, 3, 6 or 12 ng/ul radiolabelled DNA, respectively. Lane 4: Cfo I-cut pBR322, as marker.

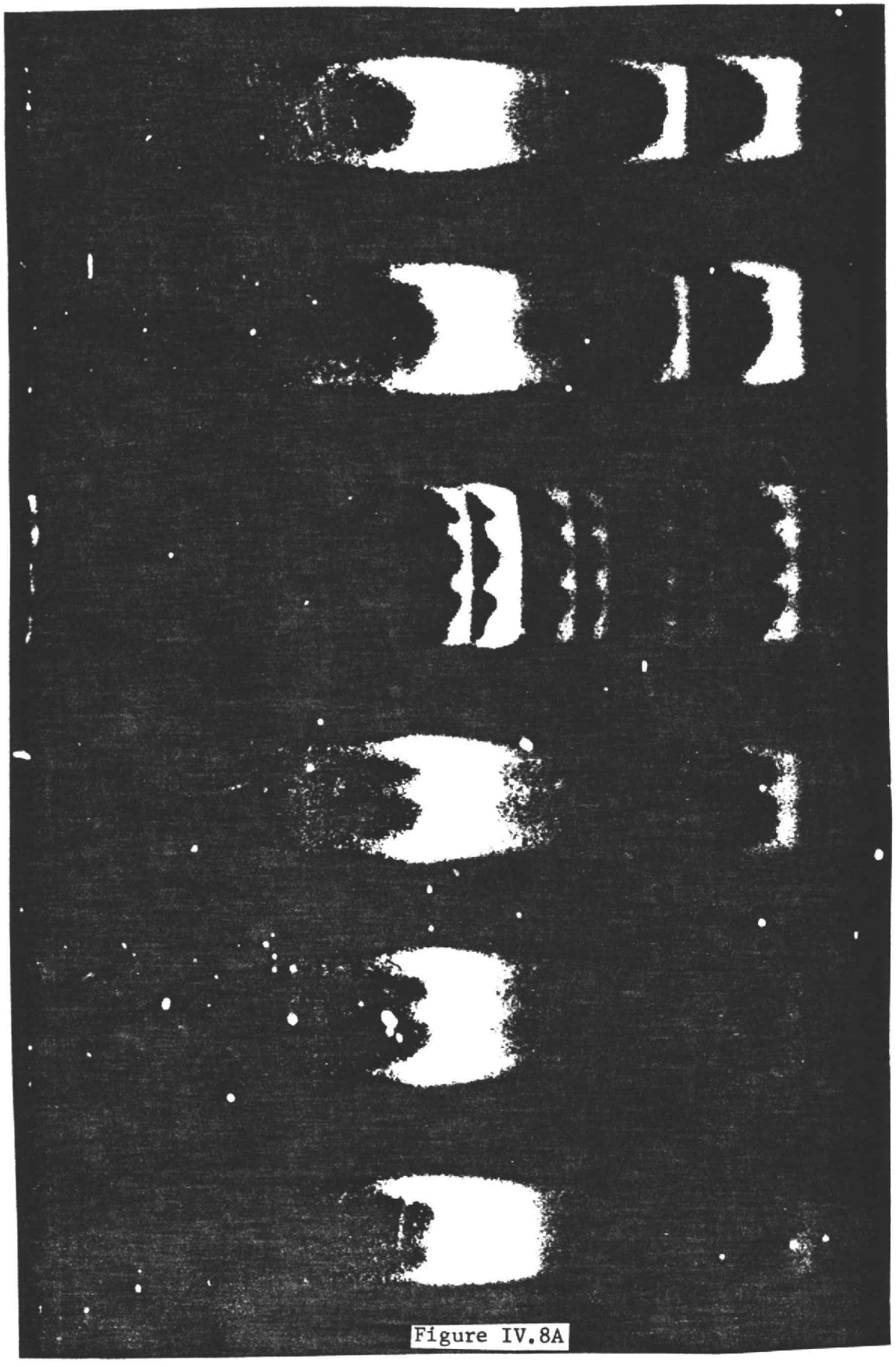

Figure IV.8A

Fig. IV.8B. Reconstitution of nucleosomes by the method of "histone transfer from (unlabelled) core particles". 2. Effect of changing the concentration of radiolabelled DNA. "Native" gel; radioautograph.

The gel from Figure 8A was dried and subjected to radioautography.

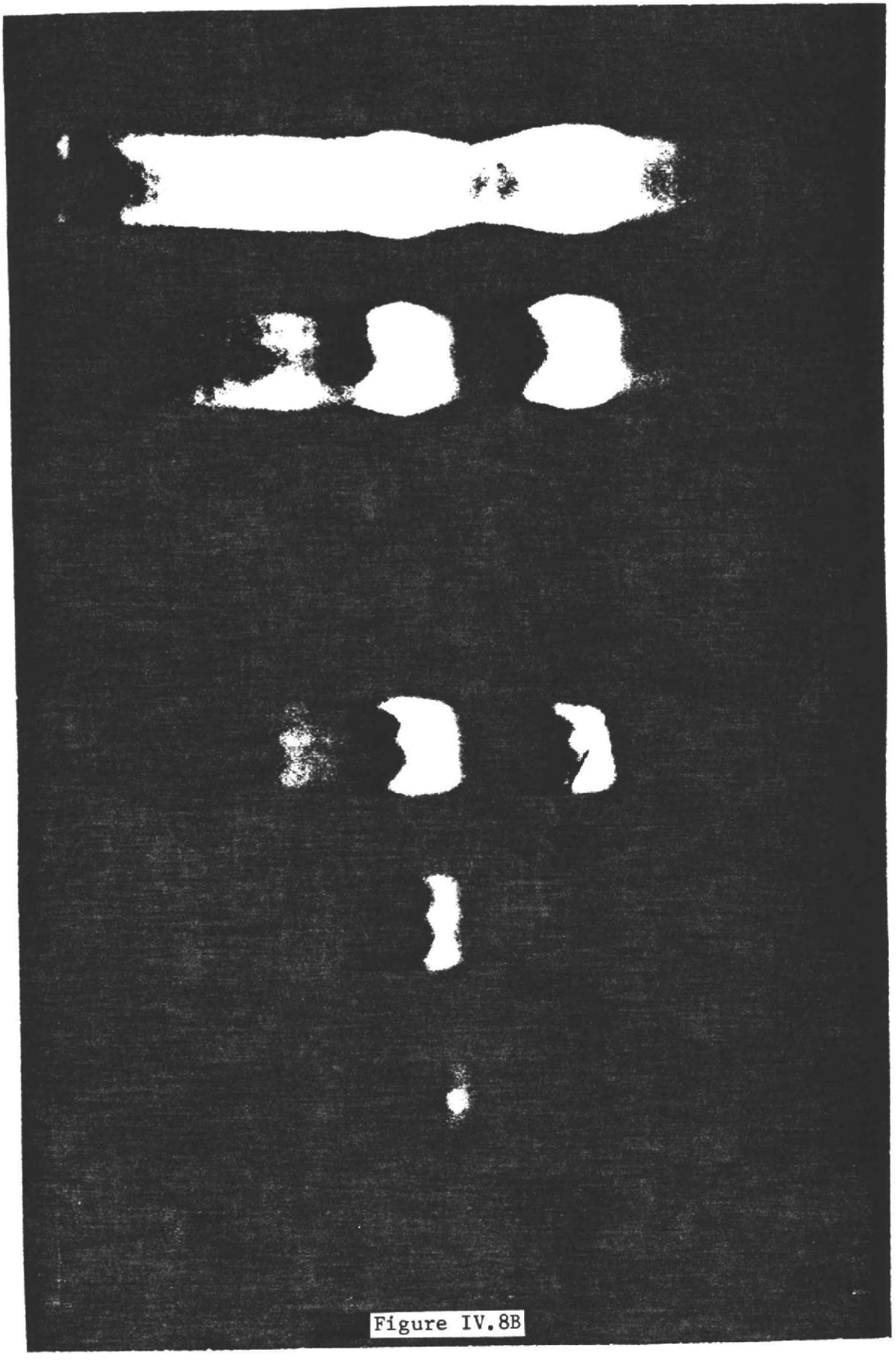

Figure IV.8B

Fig. IV.8C. Reconstitution of nucleosomes by the method of "histone transfer from (unlabelled) core particles". 2. Effect of changing the concentration of radiolabelled DNA. Quantitation of the radioautograph of Figure 8B.

The radioautograph from Figure 8B was scanned, to determine the percentage of radiolabelled DNA incorporated into nucleosomes (middle band), or into an unidentified "histone/DNA complex" (upper band). This percentage, or yield, was graphed versus the concentration of unlabelled core particles that was present at the start of reconstitution. Circles (curve #1): nucleosomes. Triangles (curve #2): unidentified "histone/DNA complex".

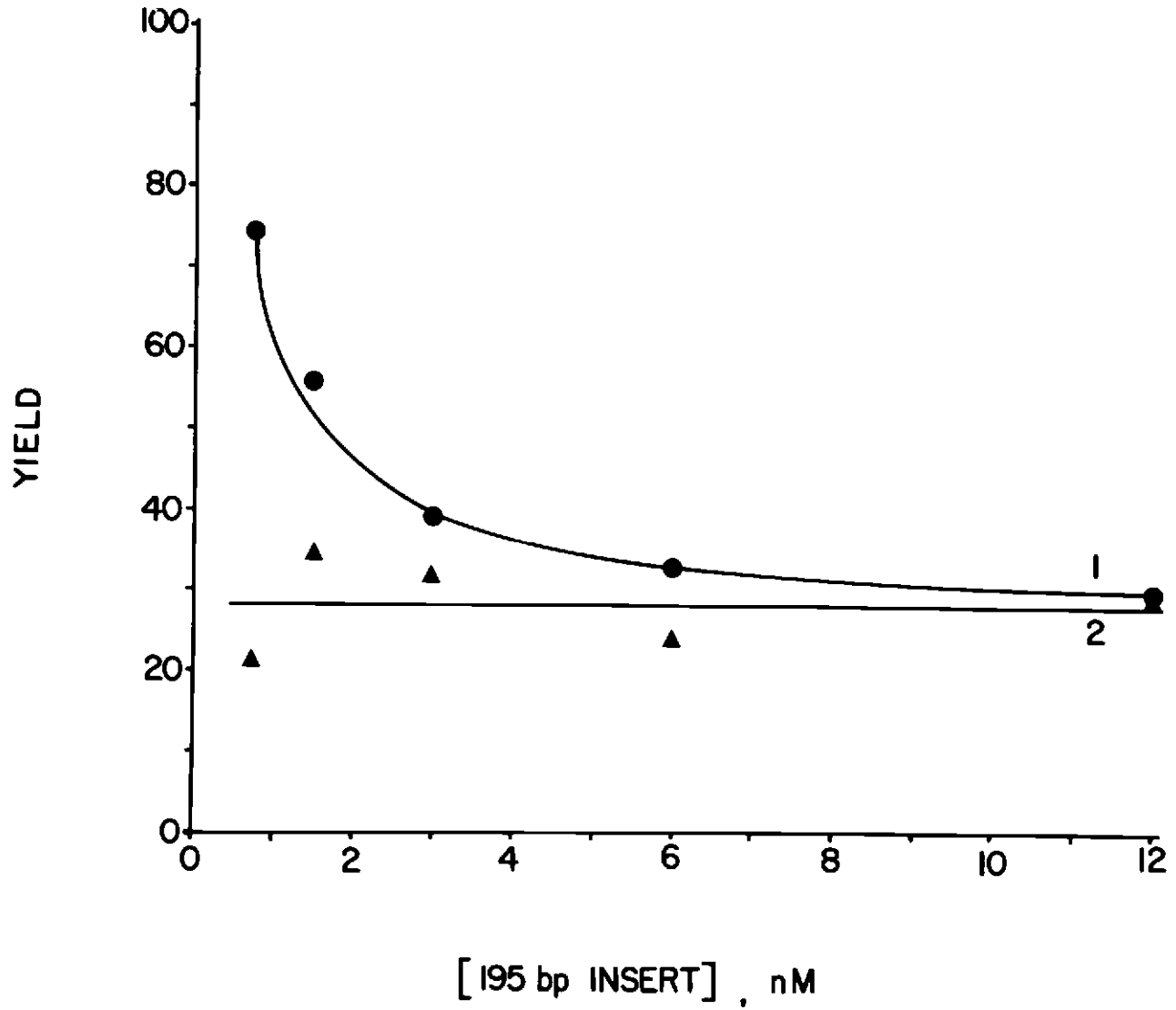


Figure IV.8C

bands from the nucleosome and the unidentified "histone/DNA complex", there are a large number of other discrete bands (especially evident at the higher DNA loadings). These other bands seem to fall into discrete size classes: (a) The bottommost band probably is the 65 bp fragment generated by Nci I cleavage of the 260 bp fragment, and carried through the procedure for isolating the 194 bp fragment (see above). (b) The other discrete bands below 194 bp may reflect "hot spots" for DNA degradation (cf. Figure 6D). (c) The identities of the discrete bands above 195 bp are unknown. Some of them may have arisen through imperfect purification of the 195 bp DNA (see section V D).

D. Joint dependence of reconstitution yield upon core particle concentration and radiolabelled DNA concentration

Is it possible, from the above, to predict the conditions giving a maximum yield of core particles, and simultaneously a minimum yield of the unidentified "histone/DNA complex"? On the basis of my limited data, I predict that this situation will occur as a limiting case, when both the core particle concentration is decreased below 0.64 A260 unit (320 nM) and the radiolabelled DNA concentration is decreased below 0.8 ng/ul (12 nM). I also predict the additional requirement that the ratio of core particles to radiolabelled DNA lie above 80.

E. The effects of dialysis geometry on nucleosome reconstitution

Using exactly the same materials as in the previous two experiments, an attempt was made to scale up the nucleosome reconstitution reaction. By reference to Figures 7-8, a core particle concentration of 480 nM, and a concentration of radiolabelled DNA of 0.8 ng/ul (6 nM) were used, with the expectation of a high yield of nucleosomes, and a low yield of the unidentified "histone/DNA complex". The reconstitution volume was increased from 30 ul to 2.3 ml (a factor of about 76), with a corresponding increase in the absolute amounts of materials. As noted above, the former reconstitution reactions were done in a hemispherical drop against a dialysis membrane, with a ratio of drop volume to membrane surface area of about 0.16 cm, and a ratio of drop volume to air-liquid interfacial area of about 0.082 cm. The scaled-up reconstitution was done in an approximately cylindrical dialysis tube, with radius = 0.5 cm and height = 3 cm. Thus the ratio of liquid volume to membrane surface area was about 0.23 cm, and the ratio of liquid volume to air-liquid interfacial area was about 3.3 cm.

Figures 9A and 9B, respectively, show the ethidium-fluorescence photograph and radioautograph of this reconstitution attempt, analyzed on a polyacrylamide "E" gel.

Fig. IV.9A. The effect of dialysis geometry on the reconstitution reaction. Ethidium-fluorescence photograph.

Using the knowledge gained from Figures 7 and 8, an attempt was made to scale up the reconstitution reaction, so as to generate a large quantity of radiolabelled nucleosomes.

Unlabelled core particles and 3'-end-labelled 195 bp Eco RI-Nci I fragment, each in Tris/EDTA, were mixed together. After mixing, the concentration of radiolabelled DNA was about 0.8 ng/ul (6 nM), and the concentration of core particles was 480 nM. The sample was next dialyzed against Tris/EDTA + 0.7 M NaCl for 1.25-1.5 hours, and then against Tris/EDTA for >3 hours. In each dialysis step, the temperature was lowered from an initial 20 $^{o}$C toward 4 $^{o}$C. After dialysis, an aliquot of the sample was run on a 3.5% polyacrylamide "E" gel. The gel was stained with ethidium bromide and photographed under long-wave UV transillumination.

The volume (hence absolute amount of each component) in this reconstitution attempt was about 76-fold greater than in the attempts of Figures 7-8. In consequence, the ratio of sample volume to dialysis membrane area was increased from 0.16 cm to 0.23 cm, and the ratio of sample volume to liquid/air interfacial area was increased from 0.082 cm to 3.3 cm.

Lane 1: Cfo I-cut pBR322, as marker. Lane 2: an aliquot from the reconstitution sample. Note that, in this

ethidium-stained gel, the "nucleosome" band is considerably more heterogeneous than is the corresponding band in the ethidium-stained gel of either Figure 7A or Figure 8A. Note also that there is no free 146 bp (core particle-sized) DNA; in contrast, free 146 bp DNA is seen in the ethidium-stained gels of both Figures 7A and 8A.

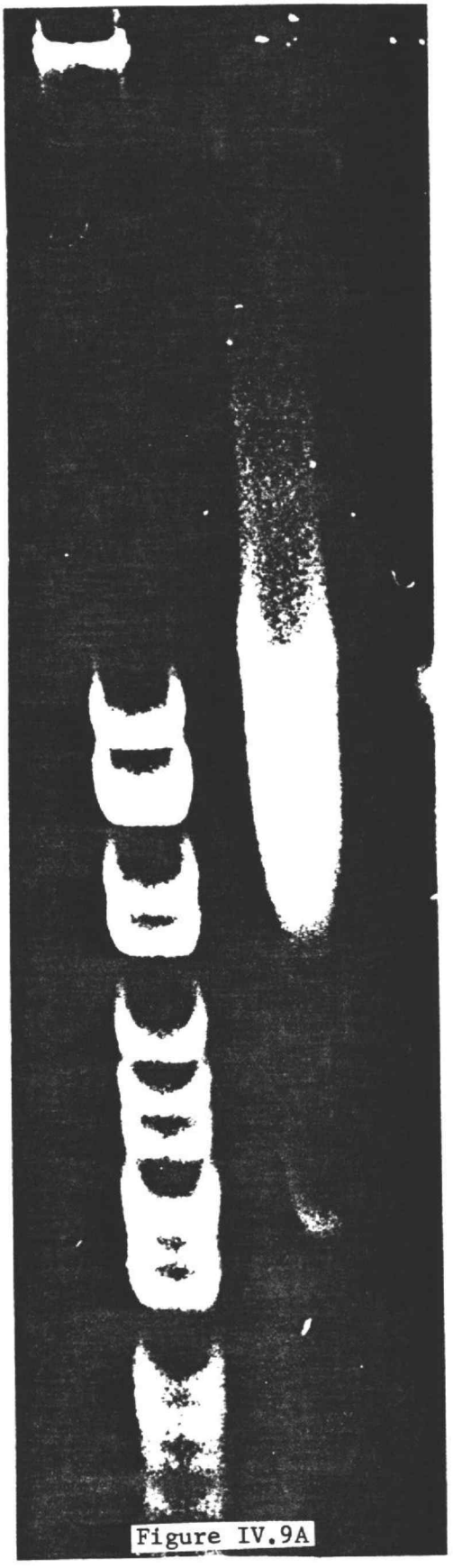

Figure IV.9A

Fig. IV.9B. The effect of dialysis geometry on the reconstitution reaction. Radioautograph.

The gel from Figure 9A was dried and subjected to radioautography. In the radioautograph, the first (fastest-migrating) band is free 195 bp DNA, the second band is the reconstituted nucleosome, the third band is the unidentified "DNA/histone complex", and the fourth "band" is aggregated material at the top of the gel. Note that the yield of authentically reconstituted nucleosomes is much lower than expected on the basis of Figures 7-8. Note also that the unidentified "DNA/histone complex" is more heterogeneous than expected, and that there is considerable aggregated material.

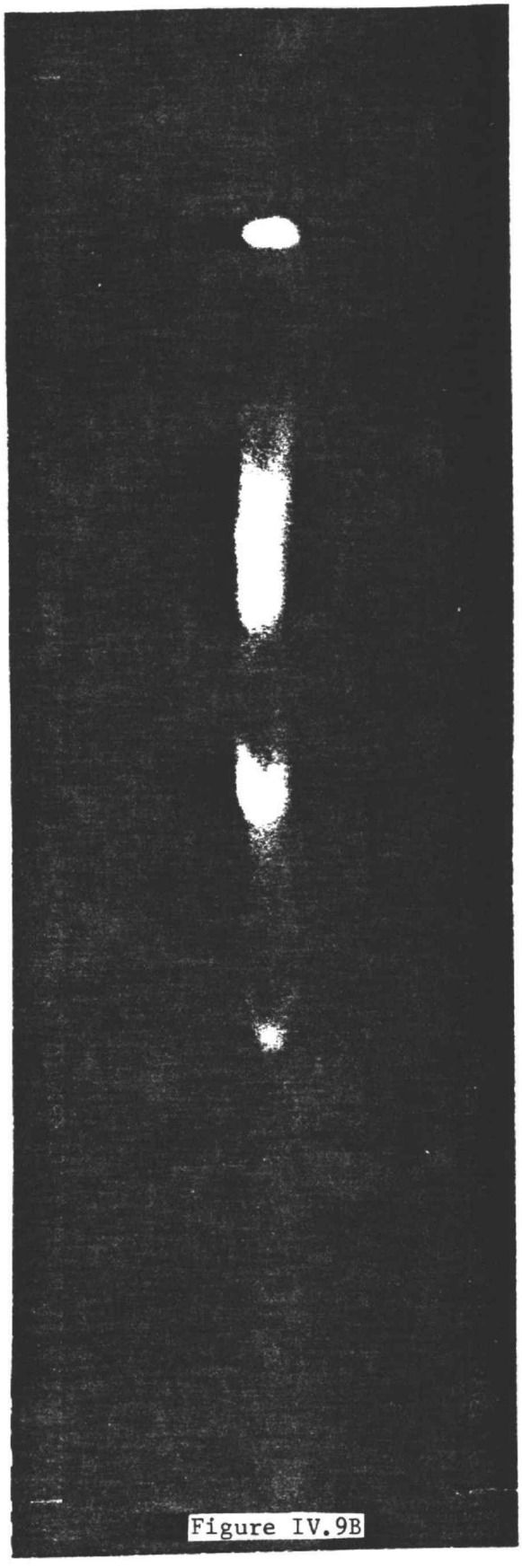

Figure IV.9B

It is clear that the reconstitution yield is substantially lower here than for the most closely related small-scale experiment (cf. Figures 7-8). Also, here there is a considerably higher proportion of the "histone/DNA complex". Thus it is best to work with small-scale reconstitution, as described above.

## VIII. Analysis of the phasing of reconstituted nucleosomes

The previous sections' chief concern was to develop a reliable procedure for nucleosome reconstitution. This was essentially a problem in preparative biochemistry. I now change focus, and concentrate on the task of determining whether or not nucleosomes reconstituted as above are phased correcly (see Simpson and Stafford, 1983).

### A. Outline of theory

In the study of Simpson and Stafford (1983), nucleosome phasing was detected by a DNAase I digestion. After digestion of nucleosomes with this nuclease, the radiolabelled, fragmented DNA was purified, and analyzed by high-resolution electrophoresis and radioautography. The pattern of radioactive bands was compared to a ladder of radioactive marker bands, to determine the placement of the histone core with respect to the

DNA sequence.

DNAase I, and other nucleases as well, can be used also to investigate the loss of phasing. The histone core is allowed to slide at random for a short time, through transiently raising, then lowering the bulk salt concentration. The population of nucleosomes is then digested with some combination of nucleases. An increase in the dispersion of the digestion pattern, as assayed by electrophoresis and radioautography, is then related to the loss of phasing of the histone core. (In section VIII, these methods are elaborated more completely.)

In these types of assays, problems are raised ranging from the very concrete (optimizing electrophoretic and autoradiographic systems), to the abstract (quantitatively analyzing the dispersion of bands in a digestion pattern, to determine the microheterogeneity of core placement).

B. Technical problems encountered in practice

1. The choice of a gel system for analyzing nuclease digestion patterns

For use in this part of the project, a gel system must be able to hold the DNA in single-stranded form, and not allow renaturation or the formation of intrastrand secondary structure. This insures that the mobilities of the various DNA

fragments fall monotonically in inverse proportion to their sizes. Thus any gel system, to be useable, must involve some denaturant, such as urea or formamide.

There are two more specific considerations in the design of a gel system for this project. First, the gel must have an inherently high resolving capability in the DNA size region of interest. Second, the gel must be able to tolerate loadings of relatively high volume and absolute amount, without much loss of resolution. (A typical nuclease digestion of a reconstitute may involve the loading of 10 ul x 50 ng/ul = 500 ng of [mostly unlabelled carrier] DNA per well.) The ultimate factors that determine whether or not these two additional requirements are met are far from obvious. (They undoubtedly relate to the maximizing of differences in electrophoretic mobility between similarly-sized DNA fragments, while holding the tendency for random diffusion to a minimum.) Thus the problem of finding the optimal gel system is somewhat one of trial and error.

Lutter (1978, 1979) has developed a gel system which can resolve single-stranded fragments of random-sequence DNA differing in length by single nucleotide amounts. An entire DNAase I digest, spanning 0-150 nt, sometimes can be resolved on a single gel. The unique feature about this type of gel, which affords such great resolution, is the use of a relatively high crosslinking ratio (1:12 or even 1:6 bisacrylamide:acrylamide). F. Ziemer (Oregon State University)

has further refined this gel system by adding a "stacking gel" (personal communication, 1984). In this preliminary work, I always used a 4-8% acrylamide (1:12 crosslinking ratio) Lutter-type gel, made in 7 M urea, 0.045 - 0.09 M Tris/Borate, 1-2 mM EDTA, pH 8.4 (a "SS" gel buffer; see List of abbreviations). For reasons detailed in section VII C, it seems best to concentrate future efforts on finding a Lutter- or Ziemer - type gel that optimizes resolution in the 0-40 nt region.

2. The need to optimize the radiographic process

There are at least four ways to improve the resolution of bands in radioautography, over the conventional approach:

(i) Instead of performing radioautography with wet, frozen gels that are several millimeters thick, one should compress the gels to effectively zero thickness, by drying them. This operation causes a particular DNA band in a gel to act, in B-emission, as a geometrical line of zero depth, and not as a rectangle extended perpindicularly to the plane of the film. The consequence is that the solid angle of film subtended by the radiation from the band is reduced (see Figure 10). One must be careful not to shear the gel sideways while drying it. This will convert each DNA band into a rectangle lying parallel to the film, and so will cause an increase in the solid angle

Fig. IV.10. Film geometry is a critical variable in the radioautography of gels of DNase I digestion fragments.

This figure illustrates three sources of "band broadening" in radioautography.

I (conventional methodology): wet gel, containing a radioactive band, is placed on one side of film; a fluorescent "intensifying" screen is placed on the other side. Radiation passes from the (thick) band in the gel through the film, and into the intensifying screen; fluorescence photons pass back from the screen to the film. d1, d2, d3 refer to gel thickness, distance between gel and film, and distance between film and screen, respectively; w1 refers to predicted width of film image of the band. Dispersion occurs (i) because the gel is thick, (ii) because the intensifying screen is on the far side of the film, and (iii) because the interfaces in the system cause refraction. Effects (i) and (ii) are "distance effects", while (iii) is a "refraction effect". The consequence of these effects is that w1 is large.

II: dried gel, containing a radioactive band, is placed on one side of film; an "intensifying" screen is placed on the other side. d2, d3 are defined as above. w2 = predicted width of film image of band. Breadth of band on film is decreased (that is, w2 < w1) because "distance" effect (i), due to gel thickness, is eliminated.

III: dried gel, containing a radioactive band, is placed on one side of film, and a fluorescent "enhance" compound is sprayed between the gel and the film; no intensifying screen is used. d2 is defined as above. w3 = predicted width of film image of band. The breadth of the band on the film is decreased beyond case II (i.e. w3 < w2) because "distance effect" (ii) is eliminated, and because "refraction effect" (iii) is lessened (since there are fewer interfaces to pass across).

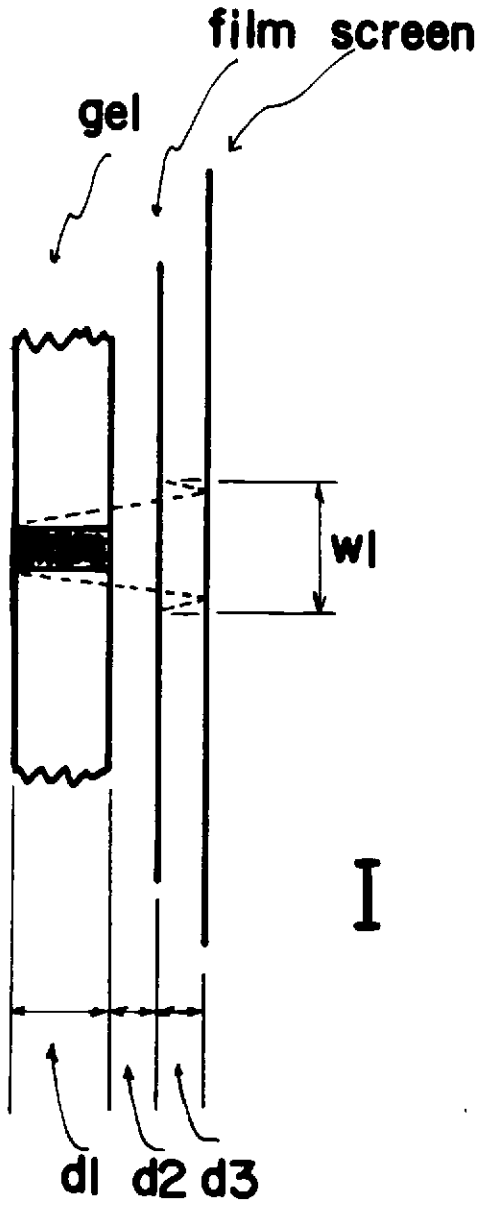


Figure IV.10

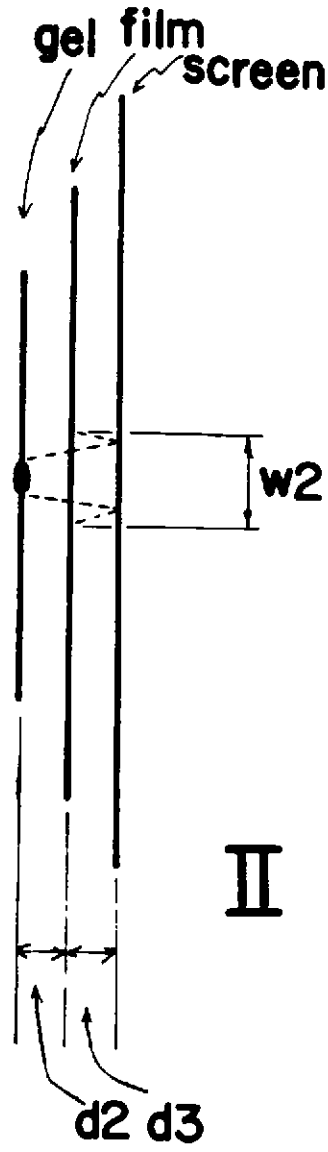


Figure IV.10

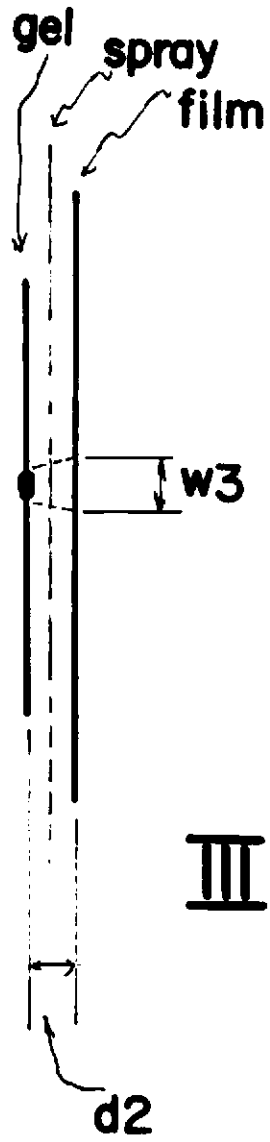


Figure IV.10

of film subtended by each band's radiation. I have found that Lutter-type gels cannot be dried on a "vacuum/heat" type drying apparatus without cracking. One may, however, dry them by placing them between a plastic slab and a taut sheet of cellulose, and letting the liquid phase evaporate away.

(ii) An overexposure in radioautography causes the apparent breadth of bands (on the film) to be greater that their actual breadth (in the gel). Thus a light exposure of film is often preferable to a heavy exposure. For each gel, one should make several different exposures, to optimize the intensities and breadths of the various bands on the film.

(iii) Radioautography with $^{32}P$ is commonly enhanced by placing a fluorescent "intensifying" screen on the side of the film opposite the gel's side. $\beta$- electrons passing through the film cause showers of photons to originate in the screen, which then strike the film from behind. It very probably is better to coat the gel directly with a fluorescent "enhancing" spray. The argument for this is the following. $\beta$- electrons from a single DNA band, although travelling quite close together when first striking the film, become spread out considerably by the time they leave its far side. Thus the shower of photons originating in the screen and moving back into the film from behind, although due to a single DNA band, will have a large dispersion in space. On the other hand, $\beta$- electrons passing through an "enhancing" layer on the gel's surface would not yet have been

dispersed by the film. Thus, in the latter case, the fluorescence photons' contribution to the film image will be of higher resolution (cf. Figure 10).

(iv) The range of penetration of any type of radiation into an arbitrary "stopping material" increases sharply with increasing average energy of the radiation, and decreases with increasing density of the stopping material (Wang et al., 1975). $\beta$- electrons from $^{35}S$ have a considerably lower average energy than those from $^{32}P$ (E = 0.05 Mev, as compared to 0.70 Mev [Wang et al., 1975]). I have measured the density of Kodak X-OMAT film to be 1300 $mg/cm_3$ (not shown). The "average areal ranges" of $\beta$- emission from $^{35}S$ and $^{32}P$ (expressed in cm of penetration x density ($mg/cm_3$) of stopping material) have been reported as 3 and 200 cm-$mg/cm_3$ , respectively (Wang et al., 1975). Therefore the average penetration range of $\beta$- electrons in this film is calculated to be 2.3 um for $^{35}S$, and 1.5 mm for $^{32}P$. The maximum penetration ranges are rougly 3 X greater than this (Wang et al., 1975).

The consequence of such a difference in penetration range is that, upon entering the film and being deflected by molecules of the film, some $\beta$- electrons from a $^{32}P$ source will be able to travel sideways a large distance, before causing a silver grain to blacken. In contrast, the $\beta$- electrons from a $^{35}S$ source will not be able to travel sideways nearly as far. Thus the film bands in $^{35}S$ radioautography should be inherently

narrower that those in $^{32}P$ radioautography.

Biggin et al. (1983) have demonstrated, in DNA sequencing applications, a considerable increase in the resolution of radioautographs, when $^{35}S$ label is used instead of $^{32}P$. [$\alpha$35]S-dATP is recognized by Klenow fragment in the end-filling reaction (see section V A,2), and is commercially available. Thus it seems best to do all high-resolution studies with $^{35}S$ label, instead of with $^{32}P$. I note that, because of its low $\beta$-energy, $^{35}S$ label cannot work with fluorescent screens, and may require the use of fluorescent "enhancing" spray.

3. Calibration Markers

One encounters two complications in attempting to assign sizes to the radioautograph bands from a DNAase I digest. First, due to uncertainty in the extent of end-filling (see section V A, 3), one does not know exactly the lengths of any of the DNA fragments carrying end-label. Second, one does not know if electrophoresis of the various DNA fragments is distorted by any sequence-dependent mobility effects in the gel.

If one uses calibration markers derived from the same sequence of DNA that reconstitution is done on, both problems are compensated for. A logical choice for the method of generating the calibration markers from this sequence is one of

the (base-specific) chemical DNA sequencing reactions (cf. Maxam and Gilbert, 1977). There is a particular advantage to the "G reaction": this reaction has already been used successfully for calibrating the DNAase I digestion patterns of the phased nucleosomes of Simpson and Stafford (1983).

4. Background problems

One cannot expect reconstituted nucleosomes as prepared above to have completely unambiguous DNAase I digestion patterns. There are two reasons for this. First, additional patterns will be generated by digestion of the free DNA and of the unidentified "histone/DNA complex" which are present in the reconstitution mixture (cf. Figures 7B, 8B). These additional patterns will be superimposed upon the pattern from the authentic reconstituted nucleosomes. Second, if the DNA from the DNAase I digestion is heated in preparation for electrophoresis (as is necessary for examination on a "SS" gel), considerable degradation may be induced, due to nicking at sites of ribose-substitution (cf. section V E and Figure 6D).

The first problem may in principle be solved by purifying the nucleosomes on a sucrose gradient or gel-filtration column after reconstitution, to eliminate the contaminating species. The second problem could perhaps be sidestepped by finding a

very mild way to prepare the samples for electophoresis. A fundamental solution, however, will have to involve changing (or eliminating) the plasmid-amplification step, so as to produce much less ribose-substitution. In the event that both of the above proposals fail, one may gain some compensation by subtracting the background patterns away from the observed digestion pattern. For an attempt at this, see section VII D and Figures 12D, 12F-12H.

C. The DNAase I digestion pattern expected for phased nucleosomes

1. The global features of the pattern

If reconstituted nucleosomes are phased according to the model of Simpson and Stafford (1983), then they should yield a very particular type of DNAase I digestion pattern.

A 10 bp repeat should begin with the first DNAase I cut lying about 0 bp in from the proximal end of the histone core - i.e. roughly at position 20, relative to the (presumeably blunted) Eco RI end of the 195 bp DNA fragment. The pattern should propagate roughly to position 165 (about 0 bp in from the distal end of the histone core). On either side of this region, the DNAase I pattern should be that of the equivalent sequence of free DNA.

2. The fine structure of the pattern

DNAase I, as is well known, does not have absolute specificity for cutting exactly once in every 10 bp stretch of DNA in a nucleosome. It is more accurate to view the DNAase I cutting pattern as having a probability for cutting that is non-zero at every position, but that has (fairly broad) maxima approximately every 10 bp (see Lutter [1979]). One would like, therefore, to be able to predict the breadth and internal structure of each of the "bands" spaced 10 bp apart in the DNAase I pattern of a phased nucleosome.

If the histone cores of the different nucleosomes of a population are phased identically (i.e. to the nucleotide), then each of these "bands" should have approximately 1/2 the variance of the corresponding "band" from the best available preparation of double-end-labelled core particles (such as that of Lutter [1978, 1979]). (The basis for this assertion is given below, in section VII C, 4.) Any higher variance will indicate microheterogeneity in the phasing of the histone cores.

From the above discussion, it is clear that, if the dispersion of the start of the phasing pattern is determined with enough accuracy and precision, then no additional information from other regions of the pattern is required to estimate the microheterogeneity in the placement of cores.

(This conclusion, however, requires that the core be phased uniquely in a global sense. To determine global phasing, both the start and stop points of the 10 bp DNase I ladder must be measured; see section VII C, 1.) The chief advantage of concentrating on the start point of the phasing pattern, and not on some other region, is that the resolution of neighboring bands is decidedly much better in the low MW region of a "SS" gel than in the high MW region (cf. Figures 6A, 6B, 11A, 12A-12D, and the papers of Lutter [1978, 1979]).

3. A reexamination of Lutter's DNAase I digestion patterns

As mentioned above, each "10 bp ladder band" in the DNAase I digestion pattern of a nucleosome has well-defined internal structure. This is clearly shown in Figures 1 and 2 of the 1979 paper of Lutter, for the case of random-sequence core particles (very homogeneous in length around 146 bp), which have been radiolabelled at both ends. (The fact that these nucleosomes are labelled only at the ends implies that the bands in autoradiography reflect only those cutting events which leave either end intact. Thus double-end-labelling simplifies the analysis enormously, to a point where precise discussion is possible.)

Lutter's radioautograph scan (Figure 2 of his 1979 paper) is shown in my Figure 11A. The "S1" region (the first "10 bp

Fig. IV. 11A. Fine structure of radioautographs of phased nucleosomes: the problem of microheterogeneity. 1. Lutter's radioautograph of the DNAase I digestion of double-end-labelled core particles.

Reproduction of Figure 2 of the 1979 paper of Lutter. To obtain this figure, 146 bp chicken erythrocyte core particles were double-5'-end-labelled and digested with DNAase I. The resultant fragments of DNA were separated from the histones, were denatured, and were resolved on a "SS" gel. The gel then underwent radioautography. Shown is the radioautograph of those fragments of single-stranded DNA ranging in length from 7 to 27 nt.

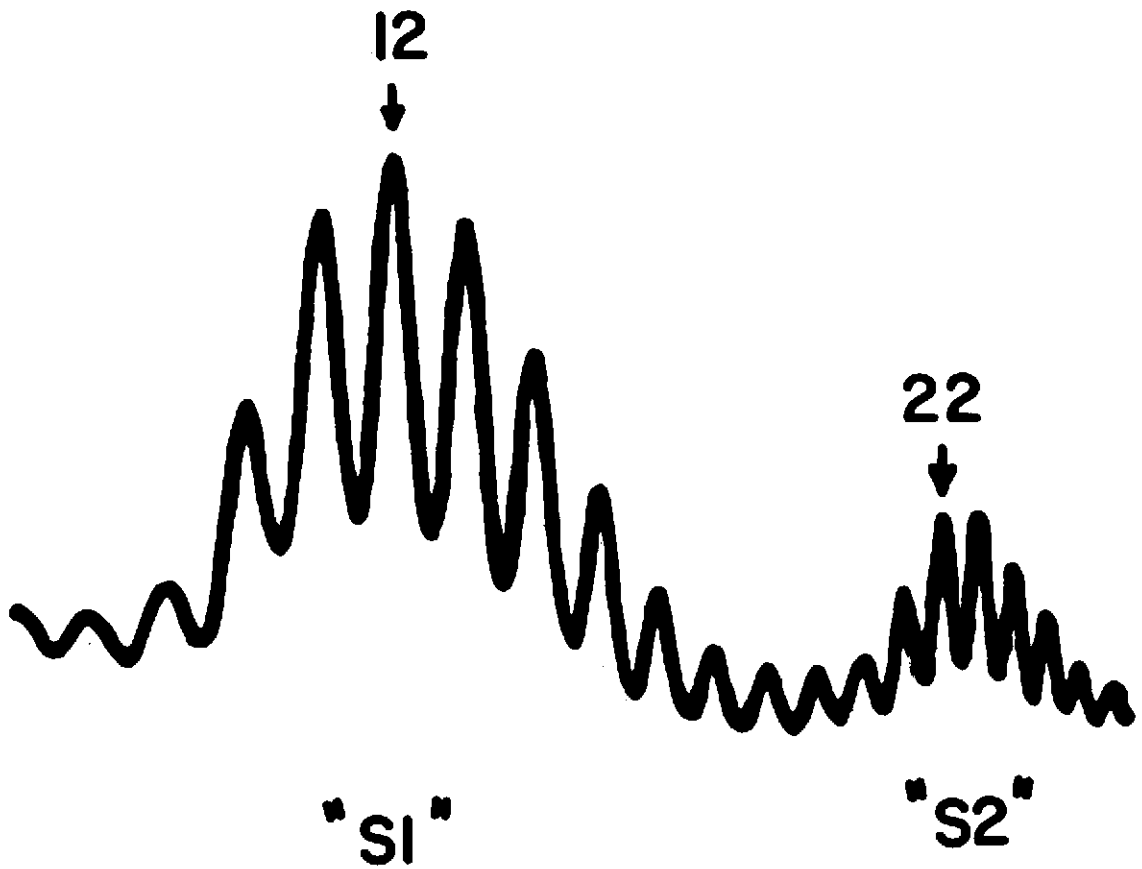


Figure IV.11A

ladder band") spans at least nucleotide positions 7-18, while the "S2" region (the second "ladder band") spans at least positions 18-27. "S1" is centered on position # 12, and "S2" is centered on positions # 22-23.

I make the following assumptions in the quantitative analysis of his "S1" and "S2" patterns:

(i) I am forced to assume, by incompleteness of data, that the "S1" and "S2" regions of his DNAase I pattern are completely represented by bands 7-27. This assumption is inaccurate to the extent that other bands make significant contributions to "S1" or "S2".

(ii) Lutter presented only the upper half of band #7 in his figure 2. I have drawn in the missing half in my Figure 11A, assuming symmetry for the band.

(iii) There clearly is an overlap in the "S1" and "S2" patterns, because of each one's dispersion. I assume that the overlap is completely confined to band #18. I further assume that 85% of the intensity of this band is due to "S1", and the remaining 15% is due to "S2". (These percentages are roughly the same as the relative contributions of "S1" and "S2" to the total integrated intensity of the 7-27 nucleotide region.)

(iv) There is a problem in trying to integrate the intensity of single "sub-bands" within "S1" or "S2", because each sub-band overlaps its two nearest neighbors. Instead of using a numerical fitting routine for resolving overlapping

Gaussian curves, I have simply dropped verticals at the points of zero slope between the sub-bands, and integrated between these verticals. This "shortcut" undoubtedly causes some error to arise, but should not greatly interfere with the ultimate conclusions of the anaylsis.

Under the above assumptions, I have calculated the proportionate amount of each sub-band within either "S1" or "S2". I have replotted the distributions of intensities for the "S1" and "S2" patterns in terms of these proportions in Figure 11B. In this figure, the two patterns are plotted one above the other, in such a way that their similarities are stressed.

4. A mathematical description of Lutter's data

I seek next a mathematical description of Lutter's DNAase I patterns. The reason for this is to gain the ability to predict fine detail in the cutting patterns for (i) a nucleosome sample in which the histone cores are identically phased on the DNA, and (ii) a nucleosome sample for which the cores have been allowed to slide out of their phased positions. The following model (which I note is only one of many possible alternatives) is presented in four parts.

a. The frequency of DNAase I cutting in the "central region" of a susceptible site

Fig. IV.11B. Fine structure of radioautographs of phased nucleosomes: the problem of microheterogeneity. 2. Frequency distributions of cutting within the "S1" and "S2" sites of double-end-labelled core particles, computed from Lutter's data.

The radioautographic scan of Figure 11A was resolved into "S1" and "S2" regions. The intensities of the "sub-bands" in each region were integrated and normalized, as described in the text.

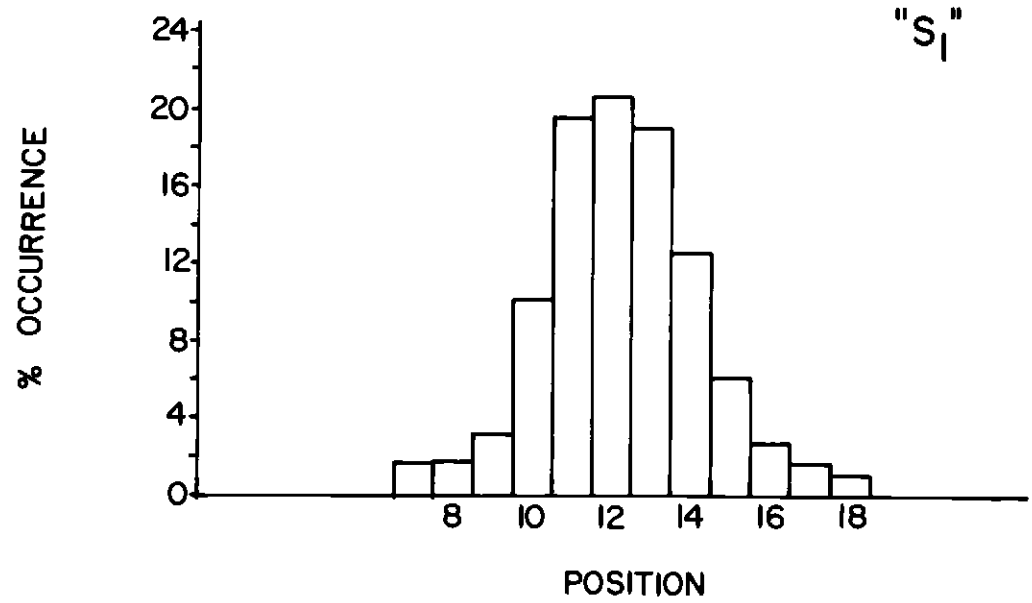


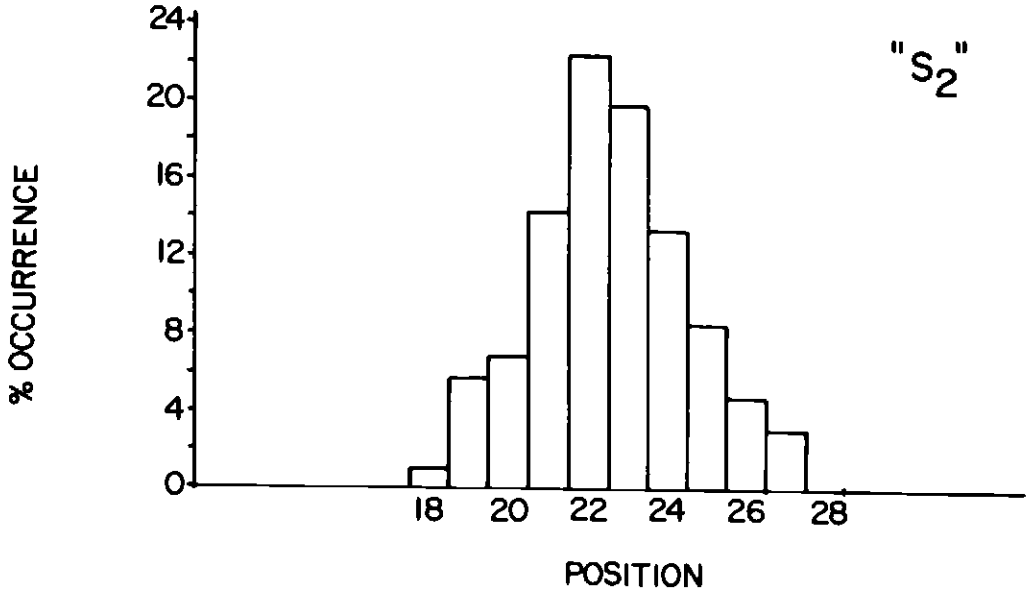


Figure IV.11B

In the DNA on a nucleosome, there is a rotation angle of only about 34.5-36 degrees between successive base pairs. It therefore seems reasonable to believe that, in a particular DNAase I-sensitive site on the nucleosome (e.g. the "S1" or "S2" site), the nuclease may have practically equal access to as many as three phosphodiester bonds.

Assume, then, for such a DNAase I-susceptible site, that the probability of cutting is maximum in a 1-3 bp "central region". Under this assumption, for k positions in this "central region" (k = 1,2 or 3), the cutting probabilities are equal at the value Po/k. This view fits qualitatively with what Lutter observes: in "S1", the central three positions are cut with almost equal frequencies, and in "S2", the central two positions are cut almost equally (see my Figure 11B).

b. The frequency of DNAase I cutting in the "outlying region" of a susceptible site

Assume that the DNAase I cutting probability falls off in constant ratio at successive positions outside the "central region" discussed above. If the probability of cutting at each of the k positions in the "central region" is Po/k, then the probability Pi of cutting a position located i base pairs outside this central region is given by

$$Pi = (1/a)^{|i|} \quad Po/k \qquad (7),$$

where 1/a is a "fall-off ratio" (a>1).

How might the assumption of a constant "fall-off ratio" be tested against the data of Figure 11B? Taking logarithms of both sides of equation (7), I obtain

$$\ln Pi = \ln (Po/k) - |i| \ln a \qquad (8).$$

Thus a plot of ln Pi versus |i| should be linear. Figure 11C shows this type of plot for Lutter's normalized data from Figure 11B. For both "S1" and "S2", assuming "central regions" 3 or 2 positions wide, respectively, the data fall on straight lines, within experimental limits of error. Thus this model seems to describe Lutter's data reasonably well.

I note that the above probability distribution bears some resemblance to the exponential distribution of continuous probability theory (see, for example, McClave and Dieterich [1979]).

Fig. IV.11C. Fine structure of radioautographs of phased nucleosomes: the problem of microheterogeneity. 3. Frequency distributions for DNAase I cutting within the "S1" and "S2" sites of Lutter's double-end-labelled core particles, graphed under the assumption of a constant "fall-off ratio".

The integrated, normalized DNAase I data of Figure 11B were regraphed according to Formula (8) in the text. This formula derives from a model of DNAase I cutting in which: (i) for each DNAase I-susceptible site in a nucleosome (e.g. "S1" or "S2"), the probability of cutting is assumed maximal and equal for a number of "central" positions in the site; and (ii) for successive positions outside such a "central" region, the cutting probability is assumed to fall off with a constant ratio.

In Figure 11C, the solid points come from the lower portions of "S1" and "S2" in Figure 11B (positions 7-12 and 18-22); the open points come from the upper portions of these regions (positions 12-18 and 22-27). Linear plots would indicate agreement of the cutting pattern with the theoretical model outlined above. In Figure 11C, straight lines with an adequate fit to the data have been drawn by assuming a central region of 3 positions for "S1" and a central region of 2 positions for "S2".

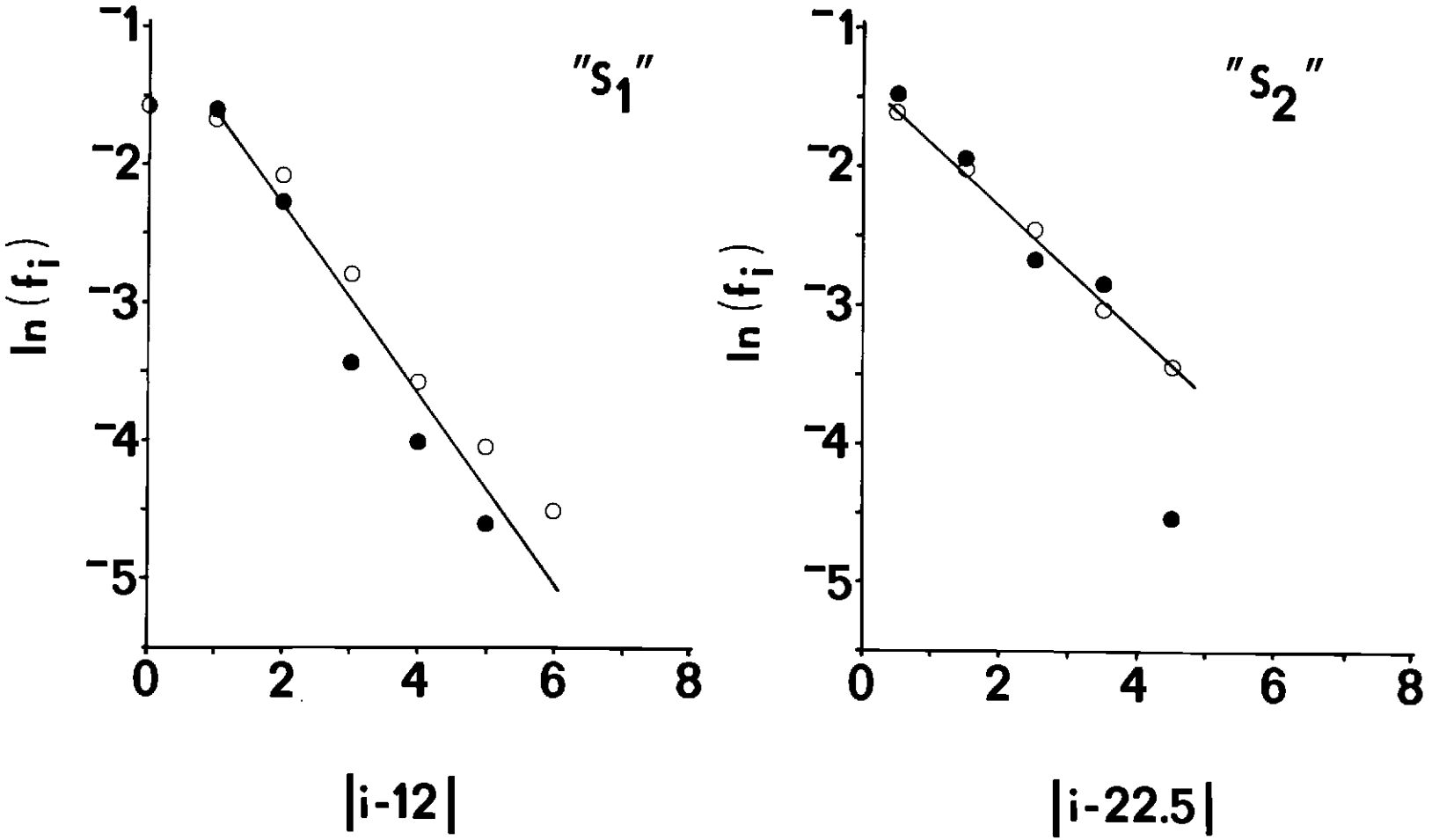


Figure IV.11C

The sum of cutting probabilities within either "S1" or "S2" must equal 1:

$$k\,(Po/k) + 2 \sum_{i=1}^{\infty} (1/a)^{i} (Po/k) = 1 \quad (9).$$

This implies the following relations between Po and a:

$$Po = \begin{cases} (a-1)/(a+1) & \text{if } k = 1 \\ (a-1)/a & \text{if } k = 2 \\ (a-1)/(a - 1/3) & \text{if } k = 3 \end{cases} \quad (10).$$

c. The variance of Lutter's "S1" and "S2" sites; the variance predicted for analogous sites from single-end-labelled, uniformly phased nucleosomes.

From the frequency distributions of Figure 11B, the variance of Lutter's "S1" site is calculated as 4.1 bp, while that of his "S2" site is calculated as 3.8 bp. For Lutter's particles, however, each radioautograph band is the sum of contributions from two DNA fragments, originating at the two ends of the core particle. I assume that the two contributions to each radioautograph band are equal (i.e. that the core particle has an exact dyad symmetry with respect to DNAase I digestion). I further assume that cutting by the nuclease is independent at the two ends of the core particle. If these assumptions are in fact true, then each of the "S1" and "S2" patterns in Figures 11A and 11B represents the probability distribution of the sum of two identical random variables (from the nuclease's cutting actions at either end of the core).

The variance of the sum of two independent random variables is equal to the sum of the individual variances (Feller, 1957). Therefore a preparation of single-end-labelled core particles would give "S1" and "S2" distributions like those of Figure 11B, but with only half of their variances.

In Figure 11D, I have graphed three predicted probability distributions for DNAase I cutting at an "S1"- or "S2"-like site in single-end-labelled core particles. The distributions were predicted from equations (7) and (10), assuming a total variance of 2.0, and $k = 1$, 2 or 3 bp, respectively, in the "central region".

Fig. IV.11D. Fine structure of radioautographs of phased nucleosomes: the problem of microheterogeneity. 4. Predicted frequency distributions for cutting within "S1" and "S2", for single-end-labelled mononucleosomes which are uniformly phased. Effect of varying the selectivity of DNAase I (source I of variance).

The "S1" and "S2" distributions of Figure 11B were calculated to each have a variance of about 4. Therefore one expects a variance of about 2 for the "S1" and "S2" distributions of either single-end-labelled core particles or single-end-labelled, uniformly phased mononucleosomes (see text). The "S1"- or "S2"-like distributions of Figure 11D were calculated assuming K = 1, 2 or 3 positions, respectively, in the "central region" of the DNAase I site.

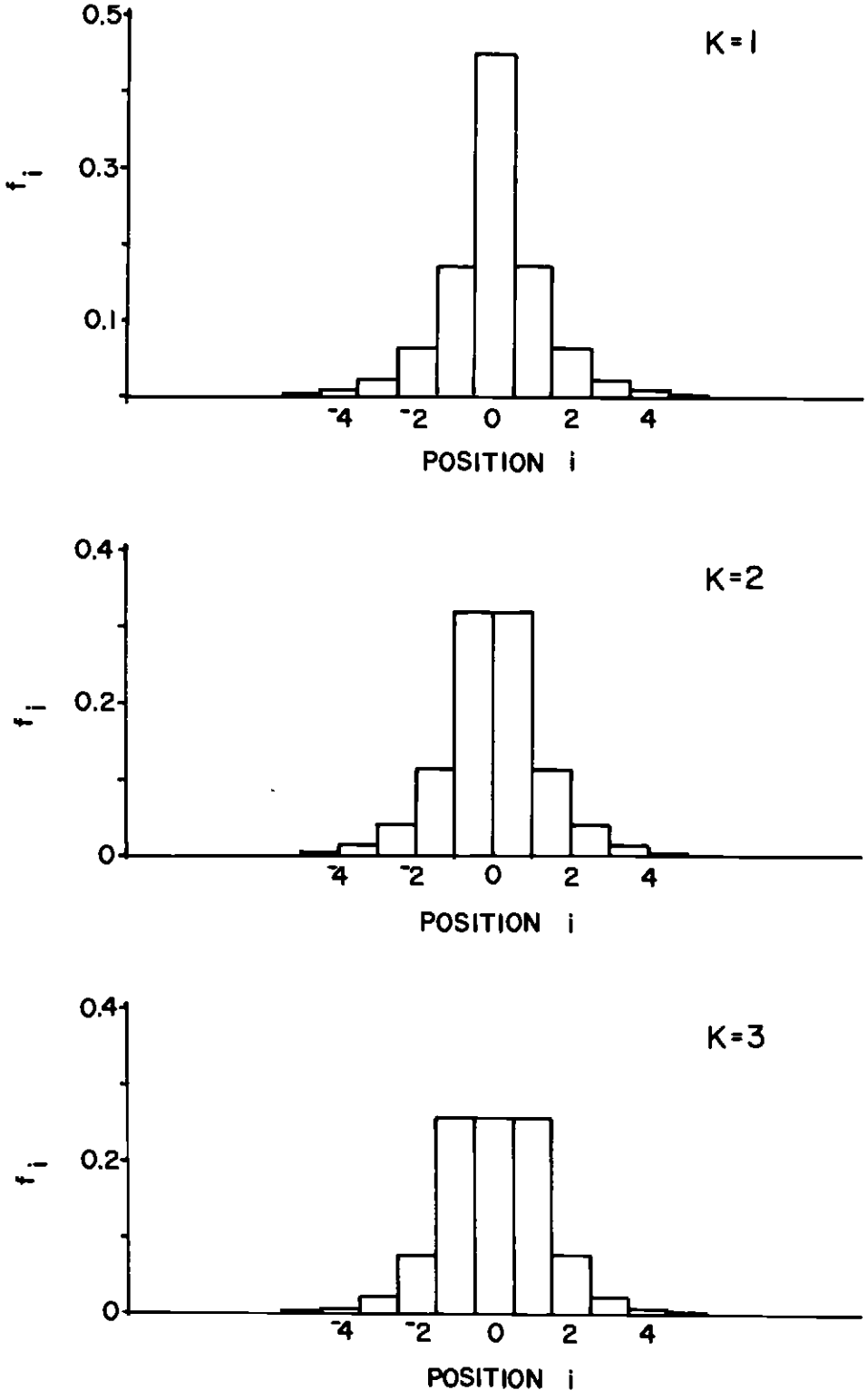


Figure IV.11D

What are the predicted DNAase I patterns for digestion of a population of single-end-labelled mononucleosomes having heterogeneity in the placement of cores with respect to the DNA sequence? In Figure 11E, I have calculated the patterns predicted for cores distributed equally between 1,2,3 and 4 phasing positions that are 1 bp apart. In this calculation, the "central region" of DNAase I cutting was assumed to be 1 bp wide (k=1).

Figure 11F shows four "statistics" which are sensitive to heterogeneity in core placement (for further explanation, see the legend of the figure). From this figure, it seems that one should be able to detect even as little as 1 bp of microheterogeneity in core placement.

5. A technical comment on the foregoing mathematical description

It is of interest to determine whether the variance of the probability distribution given in equations (7-10) is finite and so, whether the distribution is "well-behaved" in a statistical sense. I calculate the variance by splitting it into two terms: one term for the "central region" ("VARcen"), and one term for the outlying region ("VARout").

Fig. IV.11E. Fine structure of radioautographs of phased nucleosomes: the problem of microheterogeneity. 5. Predicted frequency distributions for cutting within "S1" and "S2", for single-end-labelled mononucleosomes having different amounts of microheterogeneity with respect to phasing position (source II of variance). DNAase I selectivity assumed maximal (k = 1 in "central region").

DNAase I was assumed to cut single-end-labelled, uniformly phased mononucleosomes in such a way as to produce, at each cutting site, the pattern shown in panel (i) of Figure 11D. This pattern is reproduced in panel A of Figure 11E. Under this assumption, DNAase I cutting patterns were predicted for single-end-labelled mononucleosomes having microheterogeneity with respect to phasing position.

For mononucleosomes distributed equally between two adjacent positions, the distribution of panel A was added to an image of itself offset by 1 position, and the resultant distribution was renormalized (panel B). For mononucleosomes distributed equally between three adjacent positions, three images of panel A, offset by single positions from each other, were added together, and the resultant distribution was renormalized (panel C). To treat four-fold heterogeneity, four singly-offset images of panel A were added together, and the resultant was renormalized (panel D).

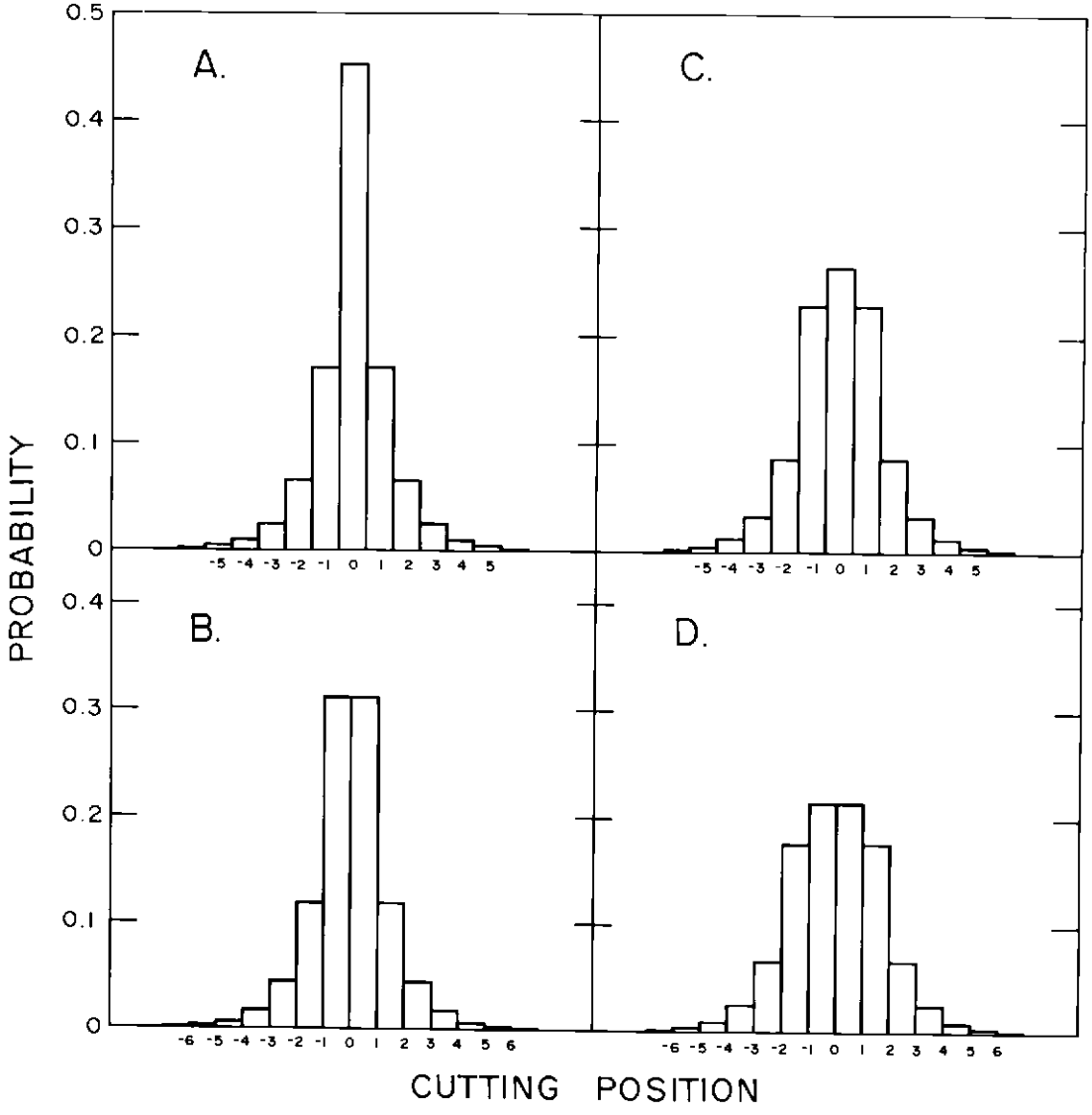


Figure IV.11E

Fig. IV.11F. Fine structure of radioautographs of phased nucleosomes: the problem of microheterogeneity. 6. Four statistical parameters, defined on the basis of the data of Figure 11 E, which are sensitive to the existance of phasing microheterogeneity.

One would like to be able to determine the microheterogeneity of phasing of nucleosomes at a particular position, by comparing the "S1" or "S2" pattern actually observed to the patterns calculated theoretically in Figure 11E. Four statistics were devised, with the aim of achieving such a comparison.

Left panel: (A) The ratio of the variances of the "S1" bands (or, equivalently, of the "S2" bands) of uniformly phased- and j-fold degenerately phased nucleosomes. (B) The ratio of the relative intensity of a "central" band in a j-fold degenerately phased nucleosome, and the relative intensity of the central band in a uniformly phased nucleosome. (C) The ratio of the number of central bands in a uniformly phased nucleosome (=1), and the number of central bands in a j-fold degenerately phased nucleosome (=j). (D) The product of the ratios described in (A), (B), and (C) above. In the left panel of Figure 11F, each of the above statistics is plotted as a function of the "heterogeneity index" j.

Right panel: each of the above statistics decreases

monotonically as the "heterogeneity intex" j increases. The sharper the decrease, the more sensitive is the parameter. The relative magnitude of decrease in each parameter ("discriminant ratio") is shown as a function of a change in j, in this panel. Clearly (D) - the product of parameters (A), (B) and (C) - is more "discriminating" than any of the parameters alone. Thus, to determine the microheterogeneity of phasing of a sample of nucleosomes, (D) should be used.

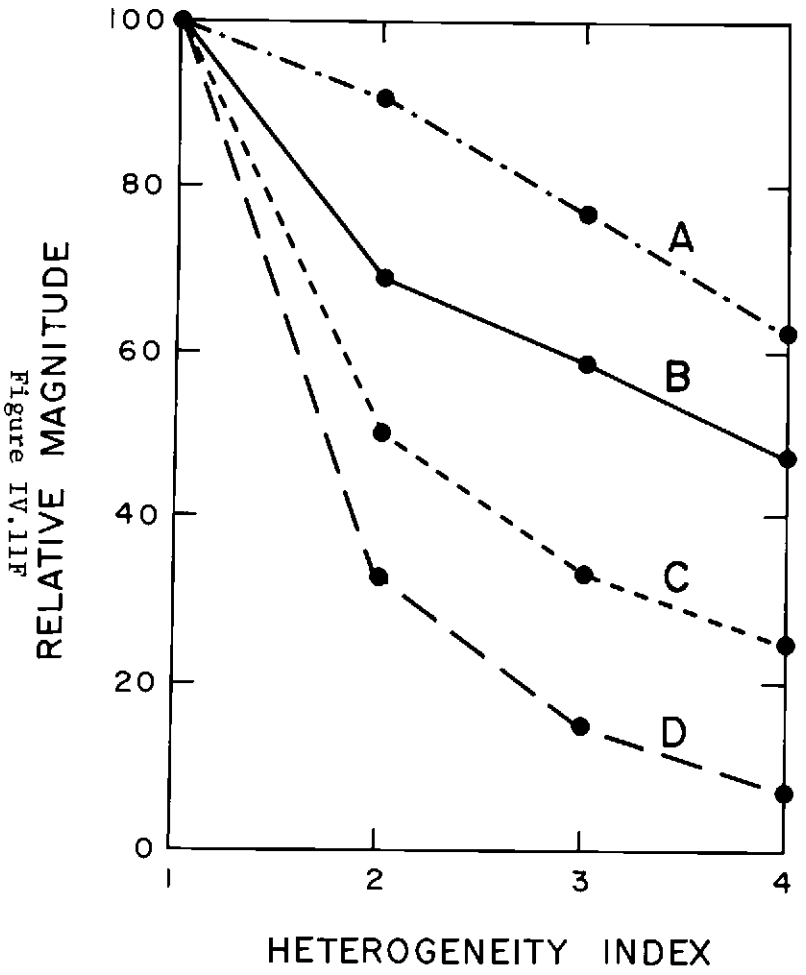


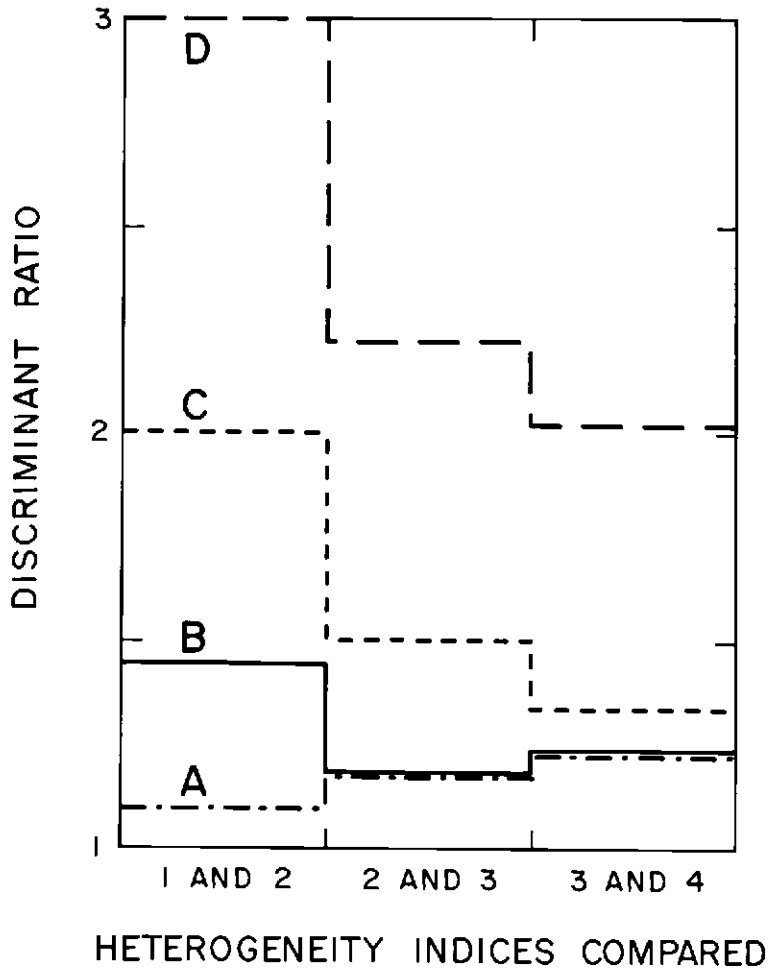


Figure IV.11F

For the central region,

$$\text{VARcen} = \left\{ \begin{array}{ll} 0 & \text{for } k=1 \\ Po/4 & \text{for } k=2 \\ 2Po/3 & \text{for } k=3 \end{array} \right\} \qquad (11),$$

as can be calculated from the definition of the variance (see McClave and Dieterich [1979], and Equation [7]).

For the outlying region,

$$\text{VARout} = \left\{ \begin{array}{lll} 2Po & \sum_{i=1}^{\infty} i^2 / a^i & \text{for } k=1 \\ Po & \sum_{i=1}^{\infty} (i+1/2)^2 / a^i & \text{for } k=2 \\ 2Po/3 & \sum_{i=1}^{\infty} (i+1)^2 / a^i & \text{for } k=3 \end{array} \right\} (12)$$

as also can be calculated from the definition of the variance, and Equation (7).

It is necessary to learn whether the series in equation (12) are convergent. To find out, I apply the ratio test of d'Alembert and Cauchy to a slightly more general problem (see Sokolnikoff, 1939).

Consider the series:

$$\sum_{i=1}^{\infty} (i+m)^2 / a^i \quad , \text{ where } m >= 0,\ a>1 \qquad (13).$$

Define $R_{i+1}$ as the ratio of the (i+1)st to the (i)th term:

$$R_{i+1} = [(i+m+1)^2 / a^{i+1}] / [(i+m)^2 / a^i]$$

$$= a^{-1} [(i+m+1)/(i+m)]^2 \qquad (14).$$

Letting $j = i+m$, I have:

$$R_i = a^{-1} (1 + 1/j)^2 \qquad (15).$$

I know that $1/a < 1$, from definition.

It is possible to pick some small positive d such that

$(1+d)^2/a < 1$ also. Then:

$$R_i = (1 + 1/j)^2/a < (1+d)^2/a < 1 \text{ when } j > 1/d \qquad (16).$$

From the definition $j = i+m$, Equation (16) must hold when $i > (1/d)-m$.

For large enough i, the ratio $R_{i+1}$ is less than 1. Therefore, by the ratio test of d'Alembert and Cauchy (Sokolnikoff, 1939),

the series in formula (13) must be convergent. From this argument, all the series in equation (12) are convergent.

D. Analysis of preliminary phasing data

1. DNAase I digestion fragments, resolved on a "SS" gel

I have made one attempt to reconstitute single-end-labelled nucleosomes by the "histone transfer" method, and then to determine their phasing by DNAase I digestion. Unfortunately, in this attempt the "scaled up" reconstitution procedure, and the particular nucleosome sample described in Figure 9 were used. Therefore a considerable fraction of the radiolabelled material either was in the form of free DNA, or was in the form of an unidentified "histone/DNA complex" (see Figure 9). Because of this lack of homogeneity of sample, the following conclusions must be viewed with some reservation.

Figures 12A-12C show the DNAase I - digestion profile of this reconstitution mixture (and of the cold carrier nucleosomes that also are present), on a "SS" denaturing gel. There are several points to note.

(i) In this gel, cold pBR322/Cfo I marker fragments were mixed in with the material in each lane. This is the origin of the multitude of high MW bands running above the DNAase I "ladder" in Figures 12A, 12B.

Fig. IV.12A. Analysis of preliminary data on phasing in reconstituted nucleosomes. 1. Time-course of DNAase I digestion; "SS" gel; ethidium-fluorescence photograph.

Aliquots of the nucleosome reconstitution mixture shown in Figure 9 (A260 = 0.96) were made 5 mM in $MgCl_2$ by adding 0.1 vol of 50 mM $MgCl_2$. They were then cooled to 0 C and DNAase I was added to a concentration of 50 U/ml, from a stock solution of 1200 U/ml in 50% glycerol. DNAase I digestions were allowed to proceed at 0 $^{o}$C for 0.5,1,2,3,5,10,30,60 or 120 min, and were then quenched by adding EDTA to a free concentration of 10 mM. A control was made by adding EDTA to a sample which had not received DNAase I. The samples were deproteinized by digestion with pronase, followed by extraction with PCIA and ether. The purified, fragmented nucleosomal DNA was precipitated with NaCl/$MgCl_2$/EtOH, and was resuspended in Tris/EDTA. The DNA next was mixed with (unlabelled) Cfo I-cut pBR322, was made 30% in DMSO, was heated to 100 $^{o}$C for 5 min, and was then placed on ice. Samples were run on a "SS" gel. The gel was stained with ethidium bromide and photographed using long-wave UV transillumination. Digestion times increase from left to right.

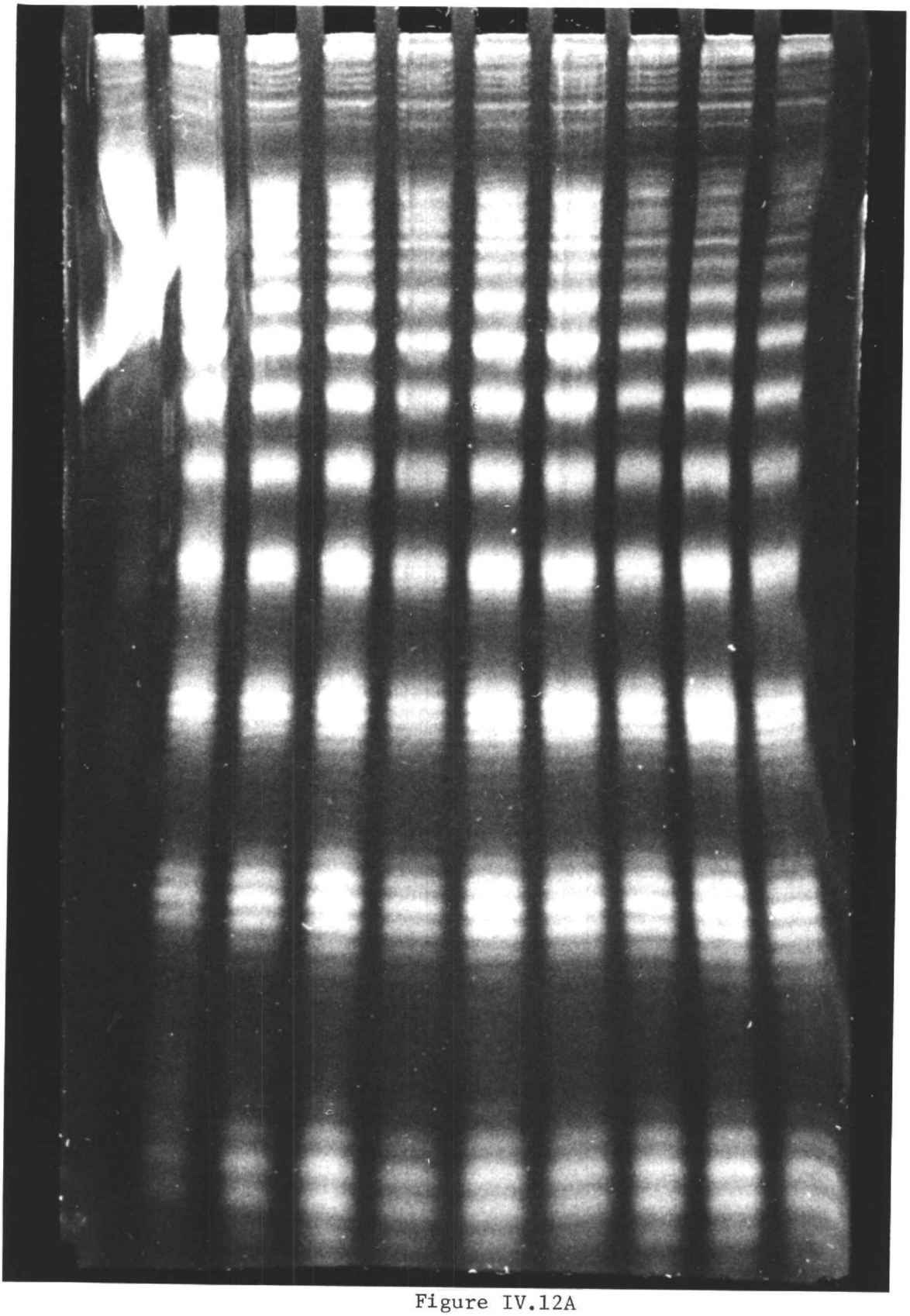

Figure IV.12A

Fig. IV.12B. Analysis of preliminary data on phasing in reconstituted nucleosomes. 2. Time-course of DNAase I digestion; "SS" gel; close-up of a portion of the ethidium-fluorescence photograph of Figure 12A.

This close-up photograph of Figure 12A shows the 1,2,3,5,10 and 30 minute digestion lanes.

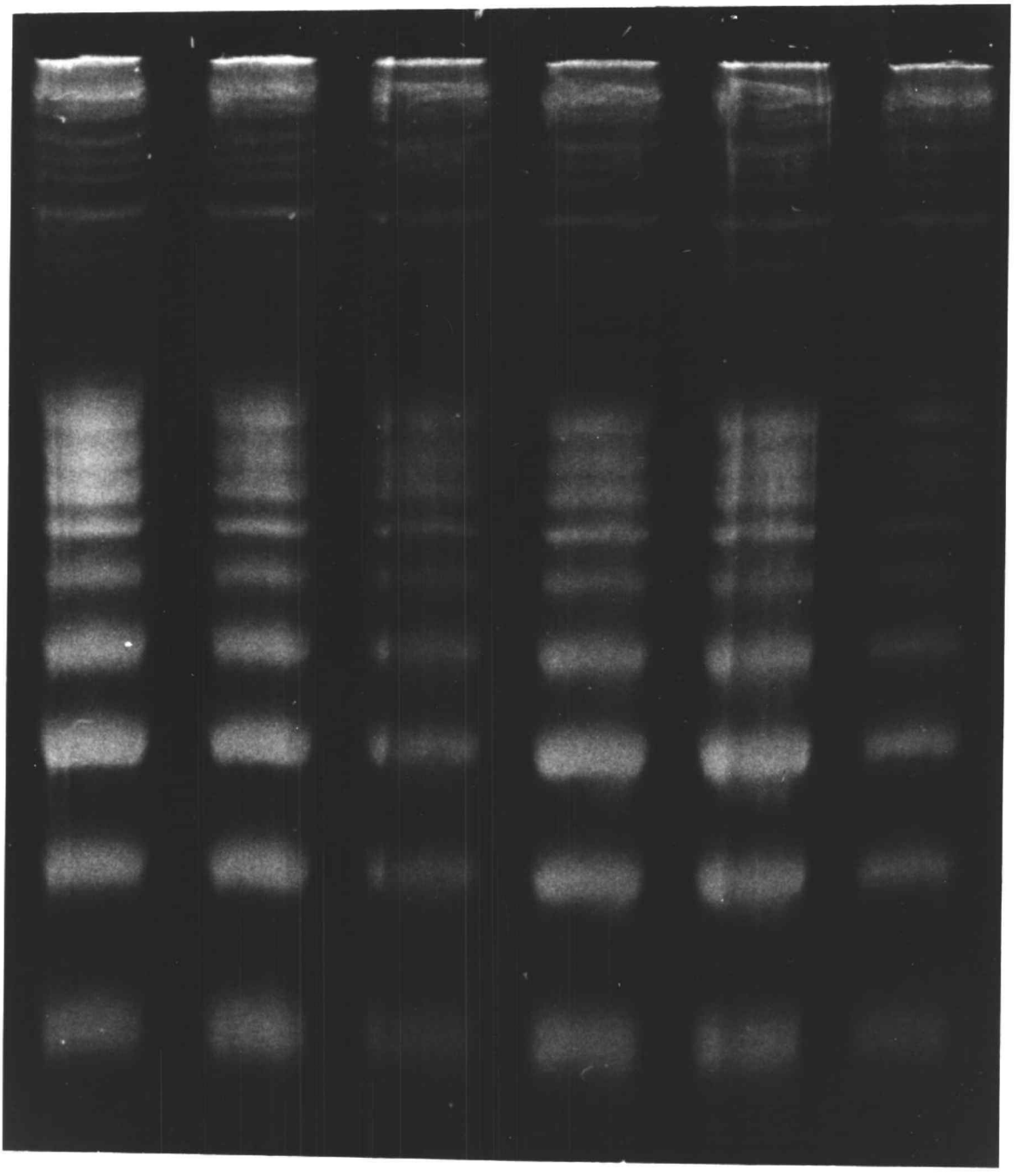

Figure IV.12B

Fig. IV.12C. Analysis of preliminary data on phasing in reconstituted nucleosomes. 3. Time-course of DNAase I digestion; "SS" gel; radioautograph.

The gel from Figures 12A/12B was dried and subjected to radioautography. As discussed in the text, the bottommost "sub-band" on this radioautograph (just running off the gel) is considered to be 18 nt long.

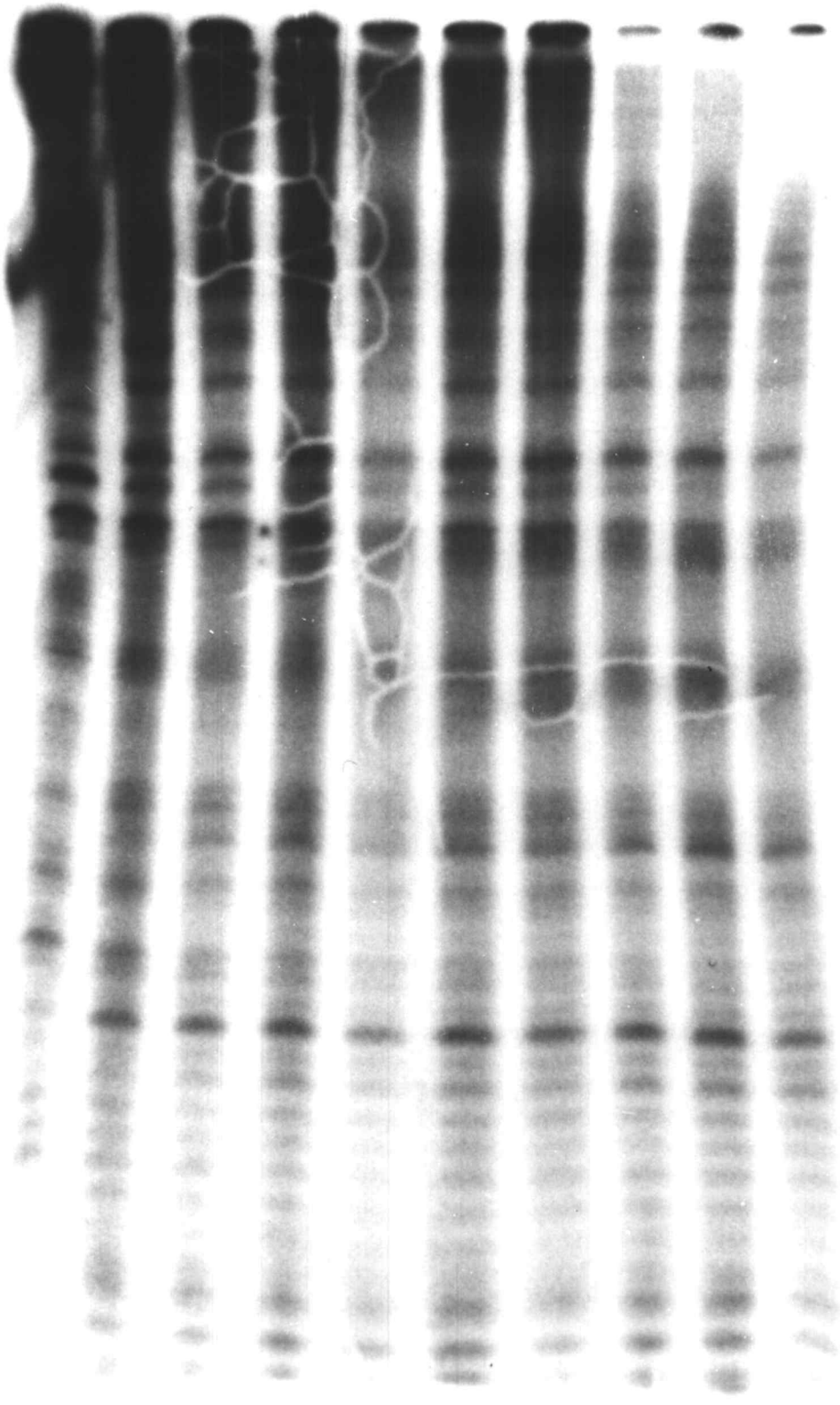

Figure IV.12C

(ii) The extensive background in the zero DNAase I lane of the radioautograph (Figure 12C) probably is due to destruction of the radiolabelled DNA during heat-denaturation, in preparation for electrophoresis (see sections V E, VII B,4).

(iii) The gel cracked during drying, in a "vacuum/heat" drying apparatus (see section VII B,2). This is the origin of the "cracked" appearance of the radioautograph in Figure 12C.

2. Quantitation of the radioautograph

Figure 12D shows a laser-scan of the radioautograph of Figure 12 C. In this scan, a very wide (1000 um) slit was used. Thus, although 9,000-10,000 points were sampled from each lane of the gel, adjacent points are highly correlated (i.e. contain much the same information). This strategy was taken to blur out sharp features in each lane of the radioautograph (spikes due to single DNA "sub-bands"): thus broad features (such as "10 bp DNAase I ladder bands") should be emphasized.

A series of regularly-spaced bands is quite apparent in the later DNAase I digestion lanes, but is not so apparent in the zero DNAase I lane. It is my hypothesis that this series of bands is an authentic "DNAase I 10 bp ladder" arising from the digestion of phased nucleosomes.

One way to test this hypothesis is to see if the series of bands in the radioautograph displays the same relationship

Fig. IV.12D. Analysis of preliminary data on phasing in reconstituted nucleosomes. 4. Low-resolution scan of individual lanes of the radioautograph of Figure 12C; preliminary assignment of bands.

Figure 12C was scanned using a Zenith laser densitometer and digitization computer program. 9000-10000 sampling points were taken per lane, using a beam width of approximately 1000 um. This combination of a large number of sampling points and a wide beam was picked so that adjacent points would contain much the same information (i.e. would be highly correlated). The goal was to average out sharp, localized features of the scan, while emphasizing global features. The heavy vertical lines joining two or more scans indicate the peaks which were used for reference to align the scans. S0, S1, ... , S11, S12 are defined and discussed in the legend of Figure 12E.

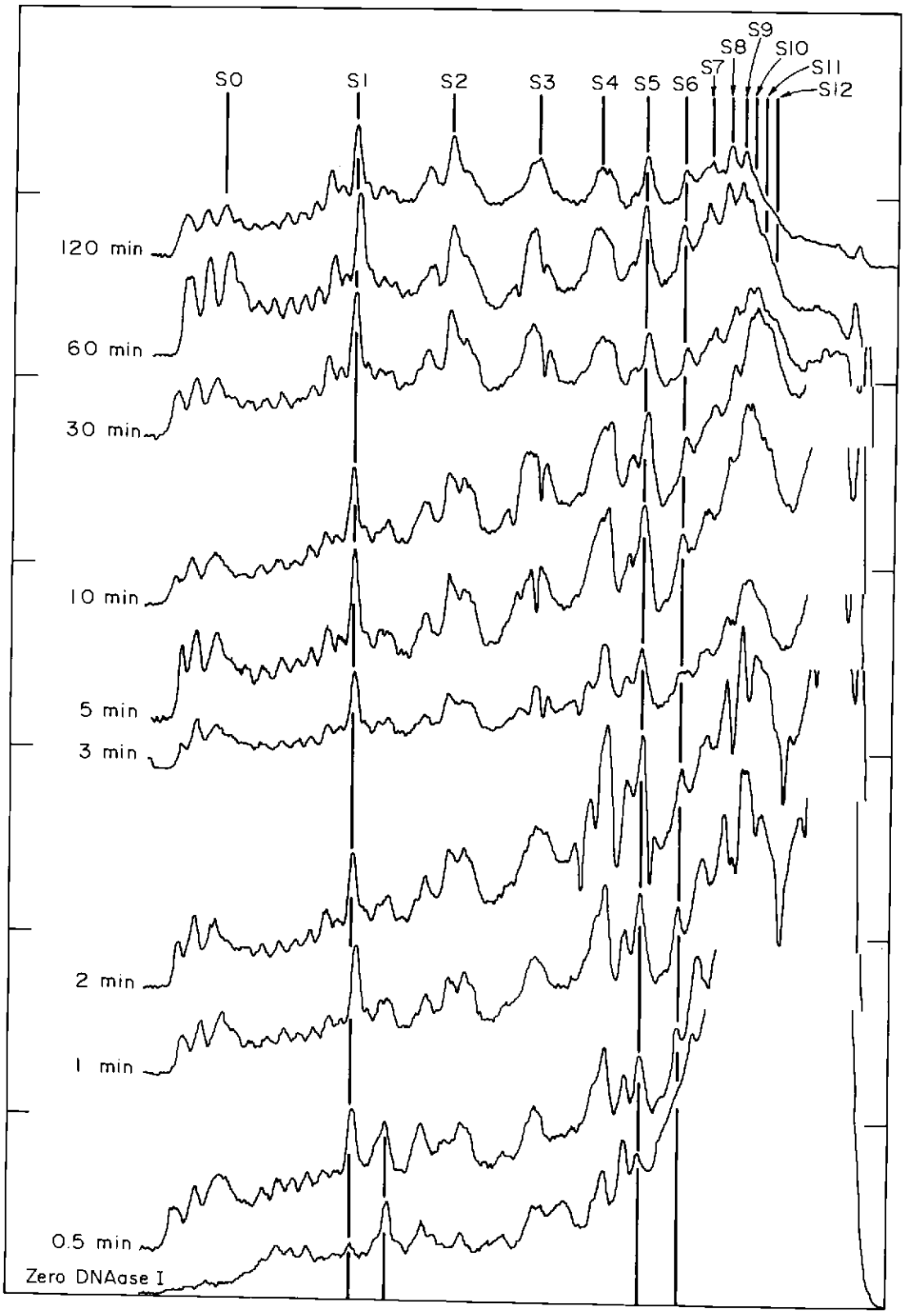


Figure IV.12D

between band size and mobility as does the set of authentic DNAase I bands from the carrier core particles.

The assignment of band sizes in the ethidium-stained gel (i.e. for the carrier core particles) was made as follows. I assumed, from the analysis of Lutter (1979), that 10.5 bp of DNA lies between adjacent points of maximum DNAase I cleavage probability, in a core particle. Therefore, ignoring "end effects", the set of bands generated by DNAase I digestion of core particles is predicted to have maxima at 10.5, 21, 31.5, 42, 52.5, 63, 73.5, 84, 94.5, 105, 115.5, 126, and 136.5 bp. In addition, there should be bands at 0-2 bp and at 144-146 bp, due to "nibbling" at the ends of otherwise intact core particles.

Assigning these values to the maxima of the DNAase I bands in the ethidium-stained gel of Figures 12A and 12B, I concluded that the bottommost "sub-band" of Figure 12A (on the verge of running off the bottom of the gel) is 18 nt long.

Guided by this size-assignment, I next measured, on the ethidium-stained gel of Figure 12A, the mobilities of the individual "sub-bands" # 18-54, and also the mobilities of the midpoints of the higher "DNAase I ladder bands". In Figure 12 E, I have plotted mobility versus ln(# of nucleotides), for each of these "sub-bands" and "DNAase I ladder bands" (closed circles). Both the high- and the low-molecular weight regions display linear behavior, while the mid-molecular weight

Fig. IV.12E. Analysis of preliminary data on phasing in reconstituted nucleosomes. 5. Plot of band mobility versus ln(# of nucleotides), for the DNAase I - digested cold carrier nucleosomes and single-end-labelled nucleosomes of Figures 12A-12C. Band sizes assigned on the basis of Lutter's proposal for the positions of cutting sites.

Lutter's model for the DNAase I cutting sites in 146 bp core particles was used to assign sizes to the bands in panel I of Figure 12A. In Lutter's model, DNase I sites lie about 10.5 bp apart; thus, from a 146 bp core particle, 15 sets of fregments are generated, having most probable lengths of 0-2, 10.5, 21, 31.5, 42, 52.5, 63, 73.5, 84, 94.5, 105, 115.5, 126, 136.5, and 144-146 bp (see text). These are called, respectively, the "S0", "S1", "S2", ..., "S12", "S13", and "c.p." bands.

Counting bands down Figures 12A and 12B, I conclude that the bottommost band in Figure 12A is the "S2" band. From Lutter's model (above), sub-band # 21 is predicted to have maximal intensity within "S2". I use this prediction to assign a size of 18 nt to the sub-band just migrating off the bottom of the gel.

(Note: there is some ambiguity in this size assignment, because: (i) Figure 12A displays two sub-bands of equal maximal intensity in "S2"; and (ii) for double-end-labelled core

particles, Lutter observes sizes of 22 and 23 nt for the two maximal-intensity sub-bands in "S2" [see Figure 11A].) My assignment maximizes the agreement of Figure 12C with the phasing pattern of Simpson and Stafford [see text].)

Using the above assignment of sizes (bottommost sub-band = 18 nt), and measuring mobilities in Figures 12A and 12C, the mobility-vs.-ln(# of nucleotides) graph of Figure 12E was constructed (solid circles = unlabelled core particles; open circles = single-end-labelled nucleosomes). There appears to be a curvilinear relationship between mobility and ln(# of nucleotides).

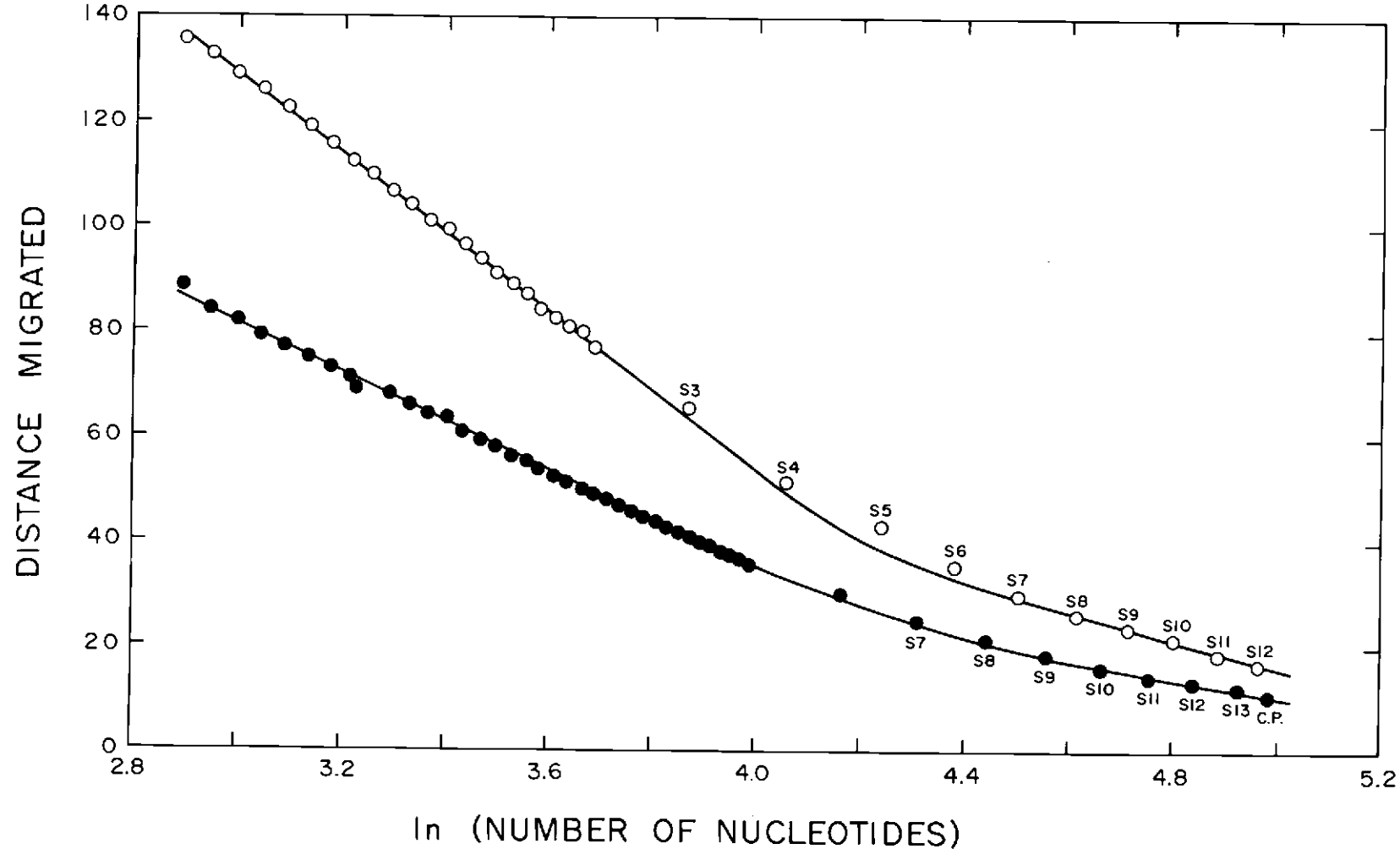


Figure IV.12E

"connecting region" of this graph has a curvilinear character. (Cautionary note: on the same type of gel, the DNAase I digestion of a different preparation of core particles gave a completely linear plot of mobility vs. ln(# of nucleotides) [not shown]. The discrepancy between these two results is puzzling. In the digestion that is not shown, the loading of the gel was very light. Thus the overall mobility pattern of a set of DNA fragments may be influenced by gel loading.)

Under the same assignment of band sizes, Figure 12 E also gives a plot of mobility vs. ln(# of nucleotides) for the radioautograph bands of Figure 12C (open circles). I find that the radioautograph displays the same linear/curvilinear/linear character as does the ethidium-stained gel, and shows the same break points between the various regions of the graph. This similarity between the two plots supports my hypothesis that the regular pattern of bands observed in the radioautograph scan is an authentic DNAase I ladder.

To further strengthen this conclusion, I computed the difference between the radioautograph's "2 hour" scan and either the full "zero DNAase I" scan, or the "zero DNAase I" scan reduced to half-intensity. The results are displayed in Figures 12 F,G and H. Six regularly-spaced maxima are apparent in the "difference scan" of Figure 12H. These correspond, in the above assignment scheme, to DNAase I ladder bands "SO" - "S5".

Fig. IV.12F. Analysis of preliminary data on phasing in reconstituted nucleosomes. 6. The zero DNAase I scan and 2 hour scan from Figure 12 D, with proposed baselines; acans cut into 41 "channels" each, for purposes of a "difference" calculation.

The zero DNAase I scan and the 2 hour DNAase I scan from Figure 12D were aligned more precisely than in Figure 12D, by expanding the former by a factor of 1.017. Baselines were drawn (somewhat arbitrarily) as indicated by the dotted lines. Each scan was chopped into 42 "channels", as indicated by the light vertical lines.

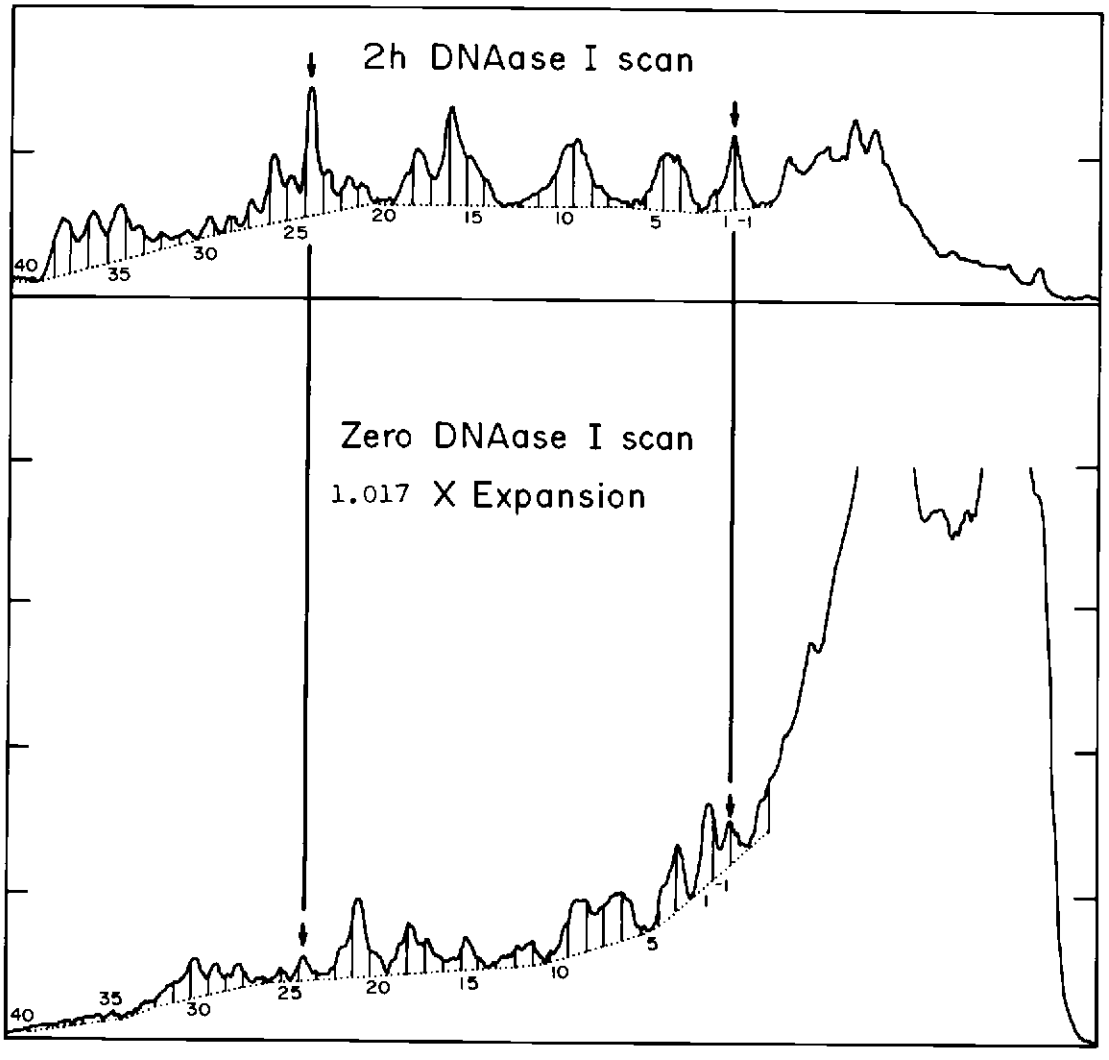


Figure IV.12F

Fig. IV.12G. Analysis of preliminary data on phasing in reconstituted nucleosomes. 7. Normalized scans from Figure 12F.

The "channels" in each of the scans of Figure 12F were individually integrated. The two scans were then reconstructed by placing the integrated values of the various "channels" on flat baselines.

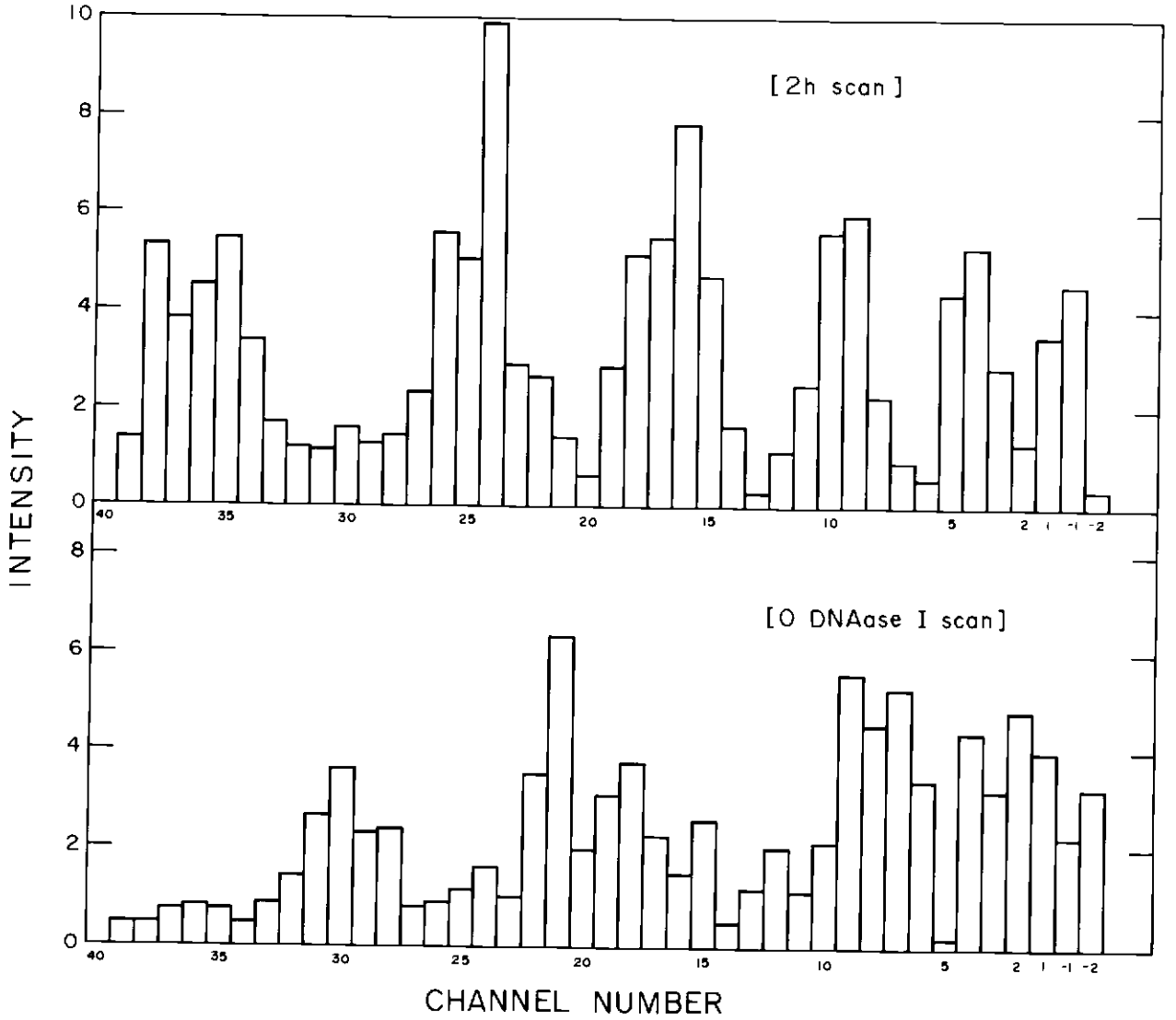


Figure IV.12G

Fig. IV.12H. Analysis of preliminary data on phasing in reconstituted nucleosomes. 8. Calculated difference between the 2 h DNAase I- and the zero DNAase I- scans of Figure 12 G. "Difference" calculation with either full weight or half weight assigned to the zero DNAase I scan.

Upper panel: the difference between the reconstructed 2 hour DNAase I scan and the reconstructed zero DNAase I scan of Figure 12G was calculated, and graphed. Lower panel: the difference between the reconstructed 2 hour DNAase I scan and a half-intensity image of the reconstructed zero DNAase I scan was calculated, and graphed.

A series of peaks is especially apparent in the lower panel of this figure; I hypothesize these peaks to be authentic DNAase I ladder bands.

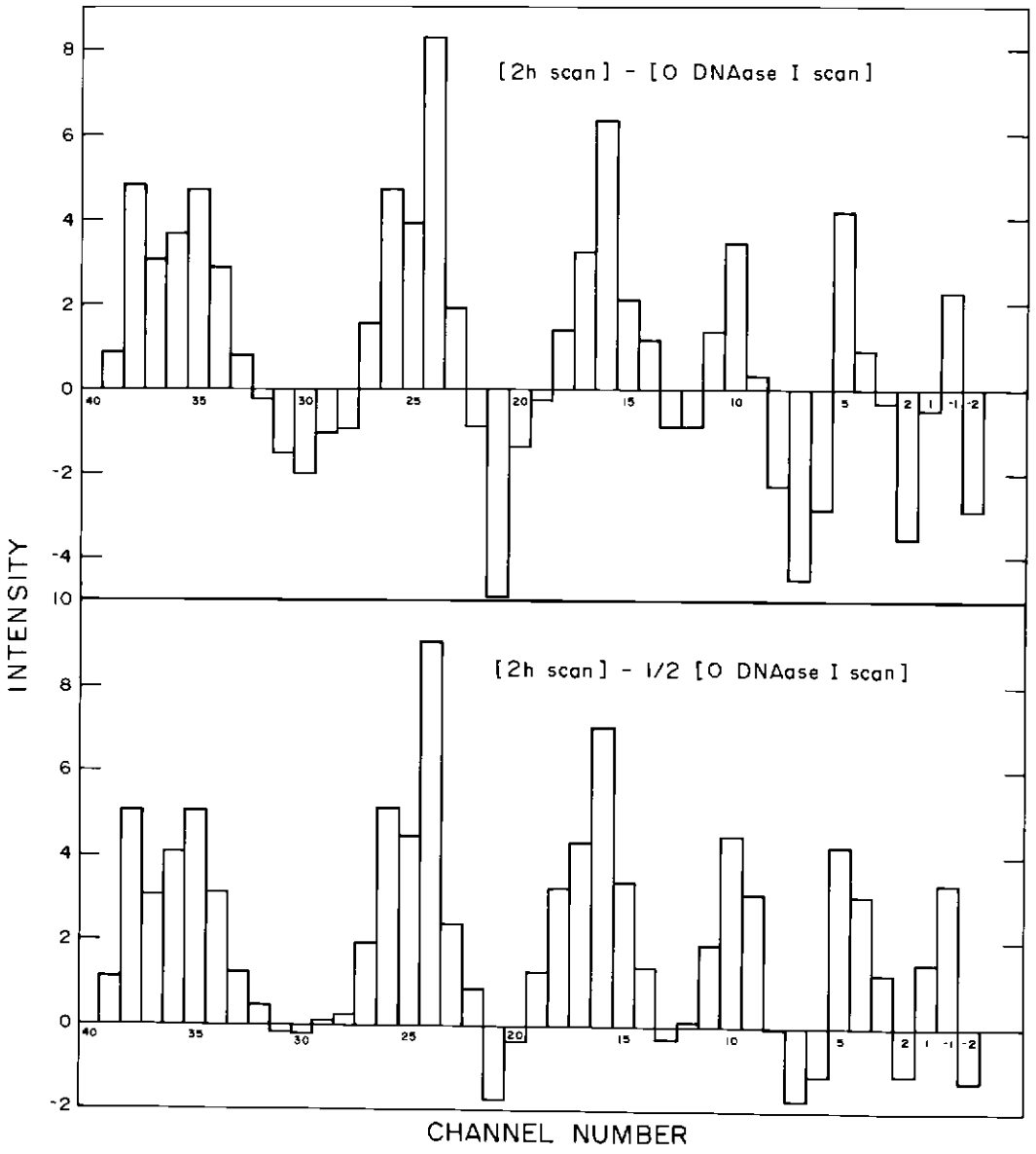


Figure IV.12H

3. Comparison with the results of Simpson and Stafford

The above observations suggest a phasing pattern in which one end of the histone core lies 20 bp from the 5' end of the Eco RI - Nci I fragment. Is this assignment compatable with the phasing data of Simpson and Stafford? To answer this question, I have made a careful examination of Figures 3 and 5B in their 1983 paper. There are three points of agreement between my results and theirs.

(i) Agreement in the "S1" region

Simpson and Stafford observe very strong cutting at (the 3' end of) position A30, both in free DNA, and in their phased nucleosomes. I see a very strong band at position A30 in my DNAase I lanes, but not in my control (Figure 12 C).

Simpson and Stafford observe moderately strong cutting at the 3' ends of positions A28 and T32 in their nucleosomes, and very strong cutting at these positions in free DNA. I observe moderately strong cutting at position A28 in my nucleosomes (2', 5', 30', and 60' lanes of Figure 12 C), and at positions T32 and C33 (1/2' and 2' lanes of Figure 12 C). In my zero DNAase I lane, band C33 is very strong, while bands A28 and T32 are relatively weak.

(ii) Agreement in the "S2" region

Simpson and Stafford observe position A38 to be very strongly cut, and position C36 to be moderately strongly cut, in both DNA and nucleosomes. I observe strong bands at positions C36 and A38 in my DNAase I digestion lanes (Figure 12 C). In my zero DNAase I lane, band C36 is strong, while band A38 is very weak.

(iii) Agreement in the "S3"/"S4" region

Simpson and Stafford observe a sharp band at about position T65 in both free DNA and in nucleosomes, just under the strong "S4" (T68/C69) band. I also observe a sharp band at position 55, in all lanes (most evident in the zero DNAase I lane; cf. Figure 12 C).

From the above comparisons, it seems reasonable to conclude that my reconstituted nucleosomes are phased identically to those of Simpson and Stafford. More work must be done, however, before this conclusion can be considered unassailable. In particular, one should examine the pattern produced by digesting 5'-end-labelled nucleosomes; this pattern is more distinctive than the digestion pattern of 3'-end-labelled

nucleosomes (see Simpson and Stafford [1983]).

## VIII. Possible approaches to detecting core movement

This section seeks to critically evaluate three "nuclease-mapping" approaches to measuring the movement of histone cores along the DNA. The approaches are based on the use of the nucleolytic enzymes DNAase I, MNase, and lambda exonuclease. One should not view the three approaches as being the only possible ones, but rather just as ones that are highly obvious. Also, they should not be viewed as mutually exclusive: it may prove advantageous to use two or even all three of them in concert, to obtain the most thorough possible analysis of core movement.

### A. General requirements of a "sliding" assay

Any sliding assay must meet two criteria, if data of quality sufficient for the testing of theoretical models are to be obtained.

#### 1. The assay must not disrupt nucleosome structure

There are at least two ways in which a sliding assay could disrupt the structure of phased nucleosomes.

First, the nuclease used in the assay could "drive" the sliding of histone cores along the DNA. (This hypothesis was first put forth by Weischet [1979], to explain the generation of "spacerless dinucleosomes" during MNase digestion of chromatin in 0.35 M NaCl.) If, however, the salt concentration always is dropped to a low value before digestion is done, such rearrangement of histone cores should not be a problem (see Weischet's paper for the salt-dependence of the "driving" effect).

Second, the nucleases used for mapping may have additional, undesireable catalytic activities, or strong preferences for certain DNA sequences. An example of an undesireable catalytic activity is the (contaminant?) 5'-to-3' exonucleolytic activity of the nominally 3'-to-5' exonuclease Exo III (Riley and Weintraub, 1978). This activity probably will remove 5' end-label from DNA in reconstituted nucleosomes; thus Exo III is unsuitable for use in a "sliding assay". An example of strong, undesired sequence-specificity is that exhibited by MNase (Horz and Altenburger, 1981; Dingwall et al., 1981).

2. The assay must be able to detect small sliding events

The ultimate goal of this project is to gain the ability to detect movement of histone cores by single nucleotide amounts (if, indeed, the "quanta" of core sliding are this small).

Because of the high precision demanded, it may be necessary to use a combination of different assay techniques, and not just a single one. (As discussed in section VII C, 4, the use of DNAase I may allow detection of single-bp sliding events. A different nuclease assay will be necessary to detect sliding events greater than several bp in extent. See below for more discussion.)

B. Mapping of sliding by digestion with MNase and restriction enzymes

Imagine a unique restriction site lying within the phasing sequence of a nucleosome. For every member of a population of uniformly phased nucleosomes, this site will lie in the same position, relative to the two stop points for MNase digestion. For a population of nucleosomes in which the core has been allowed to slide at random, however, there will be some distribution of distances between the restriction site and either MNase stop point. The problem is to obtain a measure of the core's sliding rate, from data on how this distribution of distances changes with time.

An experimental procedure for this is as follows:

(i) Histone cores are reconstituted onto uniformly labelled DNA in such a way that they are phased uniformly with respect to sequence. The reconstituted nucleosomes are then placed

transiently under conditions which favor sliding of the cores (e.g. elevated salt concentration and temperature).

(ii) After the nucleosomes are put back under conditions favoring the stability of the core, the are "trimmed" with MNase. (In this laboratory, with practice, trimming has been done precisely enough that only a 1-2 bp heterogeneity results in the lengths of the DNA of the resultant core particles (see part 3 of this thesis).

(iii) The histones are removed by pronase digestion and PCIA extraction, and the DNA is precipitated. The DNA is then cleaved to completion with a type II restriction endonuclease that recognizes a unique site in the DNA. (Note: it is best, experimentally, if the restriction site lies toward one side of the phasing sequence, and not toward its center. This allows the production of short restriction fragments, which can be sized on a gel more accurately than can long fragments.)

(iv) The following argument, which is a classical one from probability theory (Feller, 1957), shows that, under certain assumptions, the average rate of core sliding bears a simple relation to the rate of increase in the variance of the short fragment's size distribution.

Suppose, for a mobile core, that, in a time interval $t$, $n$ sliding steps occur, each 1 bp long. Suppose further that, of these $n$ steps, $r$ are to the right, each with probability $p$, and $(n-r)$ are to the left, each with probability $q$. Then the net

displacement X from the starting position (where rightwards movement is positive) is given by:

$$X = r - (n-r) = 2r - n \qquad (17).$$

But r is a binomial random variable, with distribution:

$$Pr,n = p^r q^{n-r} \; n! / r! \, (n-r)! \qquad (18).$$

The expectation value of X is therefore given by:

$$E(X) = E(2r-n) = 2E(r) - E(n) = 2(n/2) - n = 0 \qquad (19),$$

and the variance of X is given by:

$$VAR(X) = VAR(2r-n) = 4 \, VAR(r) - VAR(n) = 4npq - 0 \qquad (20).$$

If p is assumed unequal to q, then the walk is non-random, and the principle of microscopic reversibility is violated (see Moore [1972]). Therefore p must equal q. Consequently, the (average) sliding rate is given by:

$$\text{sliding rate} = n/t = \mathrm{VAR}(X)^2 / 4tp \qquad (21),$$

where p = the probability, in one step, of core movement in either direction. If one assumes core movement to occur continuously (i.e. without pauses), then p = 1/2, and the "sliding rate" equals the rate of increase of variance. (Note: if, instead, one assumes that the core "pauses" at each step, then p < 1/2, and formula (21) yields non-sensical results. To admit such "pausing", a more subtle random-walk analysis, admitting pausing, will have to be made (see Feller [1957]).

C. Mapping of sliding by DNAase I digestion

The fine structure of the DNAase I digestion pattern of phased nucleosomes is predicted to be very sensitive to slight

heterogeneities in phasing position (see Figure 11 F). This suggests that DNAase I digestion could be used to monitor very small amounts of core sliding.

1. Upper limit of detection

The separate "10 bp ladder bands" of a DNAase I digestion pattern should begin to blur together after only about 3-5 bp of random displacement of cores from the initial phasing position. This problem of overlap between adjacent "ladder bands" sets the upper limit on the extent of core sliding which can be monitored with DNAase I. If the minimal increment, or "quantum", of core sliding is less than about 2-3 bp, DNAase I may thus be a useful mapping enzyme.

2. Lower limit of detection

Core sliding may occur through the propagation of local regions of over- and under-twisting of the DNA through the one-dimensional lattice of bonds between the DNA and the histone core (see van Holde and Yager [1985], and part 1 of this thesis). If this view is correct, then core movement should occur in increments, or "quanta" 1 bp in size. From the arguments in section VII C and the calculations in Figures 11E and 11F, it should be possible to detect 1 bp of core movement,

using DNAase I.

It seems reasonable to suppose that, in the DNA/core bonding lattice, "sub-quantum movements" also occur, in which the twist (and therefore the length) of DNA between fixed bonding sites on the core fluctuates. Might it be possible to detect such movement with nucleases? The following argument suggests the affirmative. Suppose the twist of the DNA can fluctuate to a greater extent at the ends of the core/DNA bonding lattice, than in the central part of the lattice. Then the variance of the "S0" and "S1" ladder bands for single-end-labelled phased nucleosomes should be greater than the variances of the higher ladder bands, when measured before core sliding has destroyed the coherence of the pattern.

D. Mapping of sliding by lambda-exonuclease digestion

Lambda exonuclease has been shown to possess a 5'-to-3' exonucleolytic activity, but no other nucleolytic activitites (Maniatis et al., 1982). Thus this enzyme may be useful for monitoring the movement of histone cores along 3'-end-labelled DNA.

The experimental steps in a sliding assay would be:

(i) to prepare 3'-end-labelled, uniformly phased mononucleosomes;

(ii) to allow core sliding, by transient exposure of the

nucleosomes to conditions of high salt and/or temperature;

(iii) to then digest the nucleosomes with lambda exonuclease under conditions of low salt;

(iv) to denature the resultant fragmented DNA and size it on a "SS" gel, with reference to calibration markers;

(v) to calculate the rate of core sliding by the mathematical argument of section VIII B.

I note that, when applied to the 195 bp Eco RI - Nci I fragment with cores phased as in Simpson and Stafford (1983), this technique is expected to yield DNA about 165 bp long. Because of the large size of these fragments, it will be difficult to perform high-resolution analyses on gels. Also, I have observed a tendency for lambda exonuclease to digest into nucleosome core particles in 10 bp increments (not shown). These two points render the lambda exonuclease approach generally less useful than the MNase or DNAase I approaches. Nonetheless, under certain conditions, it may be worth using (for example, when one one wants to monitor the sliding of cores along very long stretches of DNA).

# IX. List of abbreviations

bp - base pair(s) (of DNA)

BSA - bovine serum albumin

CIA - 24:1 chloroform:isoamyl alcohol

DNAase I - bovine pancreatic DNAase I (I.U.B. # 3.1.4.5)

DTT - dithiothrietol

"E" (buffer) - 40 mM Tris, 20 mM NaOAc, 1 mM EDTA, pH 7.2

EDTA - ethylene diamine N,N,N',N'-tetraacetic acid, sodium salt

ether - anhydrous diethyl ether

EtOH - ethanol

Exo III - exonuclease III from E. coli (a 3'-to-5' exonuclease)

lambda exonuclease - the 5'-to-3' exonuclease synthesized by bacteriophage lambda during lytic infection of E. coli

lambda/Hind III - set of defined-length DNA fragments produced by digesting phage lambda DNA with the type II restriction endonuclease Hind III; sizes are 23190,

$Mg(OAc)_2$ - magnesium acetate

MNase - Staphylococcus aureus (Foggi) nuclease (I.U.B. # 3.1.4.7)

NaOAc - sodium acetate

nt - nucleotide(s) (of DNA or RNA)

pBR322/cfo I - set of defined-length DNA fragments produced by digesting plasmid pBR322 with type II restriction endonuclease Cfo I; sizes are 393, 348, 337+332, 270, 259, 206, 190, 174, 153+152+151, 141, 132+131, 109, 103, 100, 93, 83, 75+67+62+60.

PCIA - 25:24:1 phenol (equilibrated with 1 M Tris, pH 8.0):chloroform:isoamyl alcohol

"SS" (gel) - a 4-8% polyacrylamide, 7M urea gel poured and run in 0.09 M Tris-borate, 2 mM EDTA, pH 8.4

Tris/EDTA - 10 mM Tris, 0.25 mM EDTA, pH 7.5 (measured at 22°C)

Bibliography

Albright, S.C., Wiseman, J.M., Lange, R.A. & Garrard, W.T. (1980). Subunit Structures of Different Electrophoretic Forms of Nucleosomes. J. biol. Chem. 255, 3673-3684.

Allan, J., Cowling, G.J., Harborne, N., Cattini, P., Craigie, R. & Gould, H. (1979). Regulation of the Higher-order Structure of Chromatin by Histones H1 and H5. J. Cell Biol. 90, 279-288.

Anderson, P. & Bauer, W. (1978). Supercoiling in Closed Circular DNA: Dependence upon Ion Type and Concentration. Biochemistry 17, 594-601.

Arnott, S., Chandrasekaran, R., Birdsell, D.L., Leslie, A.G.W. & Ratliff, R.L. (1980). Left-handed DNA helices. Nature, Lond. 283, 743-745.

Ashikawa, I., Kinosita, K., Jr., Ikegami, A., Nishimura, Y., Tsuboi, M., Watanabe, K. & Iso, K. (1983a). Dynamics of DNA in Chromatin and DNA Binding Mode to Core Protein. J. Biochem. (Tokyo) 93, 665-668.

Ashikawa, I., Kinosita, K., Jr., Ikegami, A., Nishimura, Y., Tsuboi, M., Watanabe, K., Iso, K. & Nakano, T. (1983b). Internal Motion of Deoxyribonucleic Acid in Chromatin. Nanosecond Fluorescence Studies of Intercalated Ethidium. Biochemistry 22, 6018-6026.

Ausio, J., Seger, D. & Eisenberg, H. (1984). Nucleosome Core Particle Stability and Conformational Change. Effect of Temperature, Particle and NaCl Concentrations, and Crosslinking of Histone H3 Sulfhydryl Groups. J. molec. Biol. 176, 77-104.

Backman, L. & Shanbhag, V.P. (1984). Simplex Optimization in Biochemistry: Application of the Method in Two-Phase Partition. Anal. Biochem. 138, 372-379.

Baer, B.W. & Rhodes, D. (1983). Eukaryotic RNA polymerase II binds to nucleosome cores from transcribed genes. Nature, Lond. 301, 482-488.

Barkley, M.D. & Zimm, B. (1979). Theory of twisting and bending of chain macromolecules; analysis of the fluourscence depolarization of DNA. J. chem. Phys. 70, 2991-3007.

Bates, D.L. & Thomas, J.O. (1981). Histones H1 and H5: one or two molecules per nucleosome? Nucl. Acids Res. 9, 5883-5894.

Beard, P. (1978). Mobility of Histones on the Chromosome of Simian Virus 40. Cell 15, 955-967.

Behe, M. & Felsenfeld, G. (1981). Effects of methylation on a synthetic polynucleotide: The B-Z transition in poly(dG-m5cC).poly(dG-m5dC). Proc. natl. Acad. Sci., U.S.A. 78, 1619-1623.

Bendel, P. & James, T.L. (1983). Structural and dynamic differences between supercoiled and linear DNA from proton NMR. Proc. natl. Acad. Sci., U.S.A. 80, 3284-3286.

Benedict, R.C., Moudrianakis, E.N. & Ackers, G.K. (1984). Interactions of the Nucleosomal Core Histones: A Calorimetric Study of Octamer Assembly. Biochemistry 23, 1214-1218.

Bensadoun, A. & Weinstein, D. (1976). Assay of Proteins in the Presence of Interfering Materials. Anal. Biochem. 70, 241-250.

Bentley, G.A., Finch, J.T. & Lewitt-Bentley, A. (1981). Neutron Diffraction Studies on Crystals of Nucleosome Cores Using Contrast Variation. J. molec. Biol. 145, 771-784.

Bernues, J., Querol, E., Martinez, P., Barris, A., Espel, E. &

Lloberas, J. (1983). Detection by Chemical Cross-linking of Interaction between High Mobility Group Protein 1 and Histone Oligomers in Free Solution. J. biol. Chem. 258, 11020-11024.

Bethesda Research Laboratories. (1983-1984). Catalog. Gaithersburg: Bethesda Research Laboratories.

Bevington, P.R. (1969). Data Reduction and Error Analysis for the Physical Sciences. New York: McGraw-Hill.

Biggin, M.D., Gibson, T.J. & Hong, G.F. (1983). Buffer gradient gels and 35S label as an aid to rapid DNA sequence determination. Proc. natl. Acad. Sci., U.S.A. 80, 3963-3965.

Bina-Stein, M. & Simpson, R.T. (1977). Specific Folding and Contraction of DNA by Histones H3 and H4. Cell 11, 609-618.

Bleam, M.L., Anderson, C.F. & Record, M.T. (1980). Relative binding affinities of monovalent cations for double-stranded DNA. Proc. natl. Acad. Sci., U.S.A. 77, 3085-3089.

Bleam, M.L., Anderson, C.F. & Record, M.T. Jr. (1983). Sodium-23 nuclear magnetic resonance studies of cation-deoxyribonucleic acid interactions. Biochemistry 22, 5418-5425.

Bloomfield, V., Crothers, D.M. & Tinoco, I. Jr. (1974). Physical Chemistry of Nucleic Acids. New York: Harper and Row.

Bloomfield, V., Dalton, W.O. & van Holde, K.E. (1967). Frictional Coefficients of Multisubunit Structures. I. Theory. Biopolymers 5, 135-148.

Bode, J., Gomez-Lira, M. & Schroter, H. (1983). Nucleosomal Particles Open as the Histone Core becomes Hyperacetylated. Eur. J. Biochem. 130, 437-445.

Bode, J., Henco, K. & Wingender, E. (1980). Modulation of the Nucleosome Structure by Histone Acetylation. Eur. J. Biochem. 110, 143-152.

Bode, J. & Wagner, K.G. (1980). Cooperative exposure of histone H3 thiols in core particles. Int. J. Biol. Macromol. 2, 129-136.

Bonner, W.M. & Stedman, J.D. (1979). Histone 1 is proximal to histone 2A and to A24. Proc. natl. Acad. Sci., U.S.A. 76, 2190-2194.

Borochov, N., Eisenberg, H. & Kam, Z. (1981). Dependence of DNA

Conformation on the Concentration of Salt. Biopolymers 20, 231-235.

Boulikas, T., Wiseman, J.M. & Garrard, W.T. (1980). Points of contact between histone H1 and the histone octamer. Proc. natl. Acad. Sci., U.S.A. 77, 127-131.

Bram, S. (1971). The Secondary Structure of DNA in Solution and in Nucleohistone. J. molec. Biol. 58, 277-288.

Bram, S. & Beerman, W.W. (1971). On the Cross-section Structure of Deoxyribonucleic Acid in Solution. J. molec. Biol. 55, 311-324.

Bram, S., Kouprach, S. & Baudy, P. (1977). DNA Structure in Chromatin and in Solution Studied by Electron Microscopy and Neutron and X-ray Scattering. Cold Spring Harb. Symp. quant. Biol. 42, 23-29.

Britten, R.J., Graham, D.E. & Neufeld, B.R. (1974). Analysis of Repeating DNA Sequences by Reassociation. Meth. Enzymol. 29, 363-418.

Burlingame, R.W., Love, W.E. & Moudrianakis, E.N. (1984). Crystals of the Octameric Histone Core of the Nucleosome.

Science, N.Y. 223, 413-414.

Burton, D.R., Butler, M.J., Hyde, J.E., Phillips, D., Skidmore, C.J. & Walker, I.O. (1978). The interaction of core histones with DNA: equilibrium binding studies. Nucl. Acids Res. 5, 3643-63.

Burton, D.R., Butler, M.J., Hyde, J.E., Phillips, D., Skidmore, C.J. & Walker, I.O. (1979). The Interaction of Histones with DNA: Equilibrium Binding Studies. In Chromatin Structure and Function, Part A (NATO Advanced Study Institute Series A, Vol. 21a) (ed. C. Nicolini), pp. 137-165. New York: Plenum.

Bustin, M. (1978). Binding of E.coli RNA polymerase to chromatin subunits. Nucl. Acids Res. 5, 925-932.

Butler, J.N. (1964). Solubility and pH Calculations. Reading, MA: Addison-Wesley.

Cantor, C.R. & Schimmel, P.R. (1980). Biophysical Chemistry, Vol. II. San Francisco: W.H. Freeman & Co.

Carlson, R.D. (1973). X-ray studies of nucleic acid conformations. Ph.D. thesis, University of Wisconsin, Madison, WI.

Caron, F. & Thomas, J.O. (1981). Exchange of Histone H1 between Segments of Chromatin. J. molec. Biol. 146, 513-537.

Cartwright, I.L., Abmayr, S.M., Fleischmann, G., Lowenhaupt, K., Elgin, S.C.R., Keene, M.A. & Howard, G.C. (1981). Chromatin Structure and Gene Activity: The Role of Nonhistone Chromosomal Proteins. CRC Crit. Rev. Biochem. 13, 1-86.

Cary, P.D., Moss, T. & Bradbury, E.M. (1978). High-Resolution Proton-Magnetic-Resonance Studies of Chromatin Core Particles. Eur. J. Biochem. 89, 475-482.

Chambon, P. (1977). Summary: The Molecular Biology of the Eukaryotic Genome is Coming of Age. Cold Spring Harb. Symp. quant. Biol. 42, 1209-1234.

Chan, A., Kilkuskie, R. & Hanlon, S. (1979). Correlations between the Duplex Winding Angle and the Circular Dichroism Spectrum of Calf Thymus DNA. Biochemistry 18, 84-91.

Chen, H.H., Behe, M.J. & Rau, D.C. (1984). Critical amount of oligovalent ion binding required for the B-Z transition of poly(dG-m5dC). Nucl. Acids Res. 12, 2381-2389.

Cohen, G. & Eisenberg, H. (1968). Deoxyribonucleate Solutions: Sedimentation in a Density Gradient, Partial Specific Volumes, Density and Refractive Index Increments, and Preferential Interactions. Biopolymers 6, 1077-1100.

Conway, E.J. (1957). Membrane Equilibrium in Skeletal Muscle and the Active Transport of Sodium. In Metabolic Aspects of Transport Across Cell Membranes (ed. Q.R. Murphy), pp. 73-114. Madison: University of Wisconsin Press.

Cotton, R.W. & Hamkalo, B.A. (1981). Nucleosome dissociation at physiological ionic strength. Nucl. Acids Res. 9, 445-457.

Crick, F.H.C. & Klug, A. (1975). Kinky Helix. Nature, Lond. 255, 530-533.

Crothers, D.M., Dattagupta, N., Hogan, M., Klevan, L. & Lee, K.S. (1978). Transient Electric Dichroism Studies of Nucleosomal Particles. Biochemistry 17, 4525-4533.

D'Anna, J.A., Jr. & Isenberg, I. (1973). A Complex of Histones IIb2 and IV. Biochemistry 12, 1035-1043.

D'Anna, J.A., Jr. & Isenberg, I. (1974a). Interactions of Histone LAK (f2a2) with Histones KAS (f2b) and GRK (f2a1).

Biochemistry 13, 2098-2104.

D'Anna, J.A., Jr. & Isenberg, I. (1974b). A Histone Cross-Complexing Pattern. Biochemistry 13, 4992-4997.

Davie, J.R. & Saunders, C.A. (1981). Chemical Composition of Nucleosomes among Domains of Calf Thymus Chromatin Differing in Micrococcal Nuclease Accessibility and Solubility Properties. J. biol. Chem. 256, 12574-12580.

Davis, R.W., Botstein, D. & Roth, J.R. (1980). Advanced Bacterial Genetics: a manual for genetic engineering. Cold Spring Harbor: Cold Spring Laboratory.

Dieterich, A.E., Axel, R. & Cantor, C.R. (1977). Dynamics of Nucleosome Structure Studied by Fluorescence. Cold Spring Harb. Symp. quant. Biol. 42, 199-206.

Dieterich, A.E., Axel, R. & Cantor, C.R. (1979). Salt-induced Structural Changes of Nucleosome Core Particles. J. molec. Biol. 129, 587-602.

Dingwall, C., Lomonossoff, G.P. & Lasky, R.A. (1981). High sequence specificity of micrococcal nuclease. Nucl. Acids Res. 9, 2659-2673.

Drew, H.R., Wing, R.M., Takano, T., Broka, C., Tanaka, S., Itakura, K. & Dickerson, R.E. (1981). Structure of a B-DNA dodecamer: Conformation and dynamics. Proc. natl. Acad. Sci., U.S.A. 78, 2179-2183.

Drew, H.R., Samson, S. & Dickerson, R.E. (1982). Structure of a B-DNA dodecamer at 16 K. Proc. natl. Acad. Sci., U.S.A. 79, 4040-4044.

Dubochet, J. & Noll, M. (1978). Nucleosome Arcs and Helices. Science, N.Y. 202, 280-286.

Dwek, R.A. (1973). Nuclear Magnetic Resonance (NMR) in Biochemistry. Applications to Enzyme Systems. Oxford: Clarendon Press.

Early, T.A. & Kearns, D.R. (1979). 1H nuclear magnetic resonance investigation of flexibility in DNA. Proc. natl. Acad. Sci., U.S.A. 76, 4165-4169.

Early, T.A., Kearns, D.R., Hillen, W. & Wells, R.D. (1981). A 300- and 600-MHz Proton Nuclear Magnetic Resonance Investigation of a 12 Base Pair Deoxyribonucleic Acid Restriction Fragment: Relaxation Behavior of the Low-Field

Resonances in Water. Biochemistry 20, 3756-3764.

Earnshaw, W.C., Honda, B.M., Lasky, R.A. & Thomas, J.O. (1980). Assembly of Nucleosomes: the Reaction Involving X laevis Nucleoplasmin. Cell 21, 373-383.

Edsall, J.T. (1953). The Size, Shape and Hydration of Protein Molecules. In The Proteins, Vol. 1B, 1st ed. (ed. H. Neurath and K. Bailey), pp. 549-726. New York: Academic Press.

Ehrlich, M. & Wang, R.Y.H. (1981). 5-Methylcytosine in Eukaryotic DNA. Science, N.Y. 212, 1350-1357.

Eickbush, T.H. & Moudrianakis, E.N. (1978). The Histone Core Complex: An Octamer Assembled by Two Sets of Protein-Protein Interactions. Biochemistry 17, 4955-4964.

Eisenberg, H. & Felsenfeld, G. (1981). Hydrodynamic Studies of the Interaction Between Nucleosome Core Particles and Core Histones. J. molec. Biol. 150, 537-555.

Elgin, S.C.R. & Weintraub, H. (1975). Chromosomal Proteins and Chromatin Structure. A. Review Biochem. 44, 725-774.

Ellison, M.J. & Pulleyblank, D.E. (1983a). The Assembly of an

H2A2,H2B2,H3,H4 Hexamer onto DNA under Conditions of Physiological Ionic Strength. J. biol. Chem. 258, 13307-13313.

Ellison, M.J. & Pulleyblank, D.E. (1983b). Internal Structure of Discrete Nucleohistone Complexes Which Form in Vitro under Conditions of Physiological Ionic Strength. J. biol. Chem 258, 13314-13320.

Ellison, M.J. & Pulleyblank, D.E. (1983c). Pathways of Assembly of Nucleohistone Complexes Formed in Vitro under Physiological Conditions. Implications for the structure of the nucleosome. J. biol. Chem. 258, 13321-13327.

Erard, M., Pouyet, J., Mazen, A., Champagne, M. & Daune, M. (1981). Core particle stability critically depends upon a small number of terminal nucleotides. Biophys. Chem. 14, 123-133.

Espel, E., Bernues, J., Querol, E., Martinez, P., Barris, A. & Lloberas, J. (1983). Interaction between histone H1 and non-histone HMG 14 detected by chemical cross-linking. Biochem. Biophys. Res. Commun. 117, 817-822.

Falk, M., Hartman, K.A. Jr. & Lord, R.C. (1963a). Hydration of DNA. II. A Infrared Study. J. Am. Chem. Soc. 85, 387-391.

Falk, M., Hartman, K.A. Jr. & Lord, R.C. (1963b). Hydration of DNA. III. A Spectroscopic Study of the Effect of Hydration on the Structure of Deoxynucleic Acid. J. Am. Chem. Soc. 85, 391-394.

Fasman, G.D. (1979). Circular Dichroism of DNA, Protein, and Chromatin. In Chromatin Structure and Function, Part A (NATO Advanced Study Institute Series A, Vol. 21A) (ed. C. Nicolini), pp. 67-107. New York: Plenum.

Feller, W. (1957). An Introduction to Probability Theory and Its Applications, Vol. I, 2nd edn. New York: J. Wiley and Sons.

Felsenfeld, G. (1978). Chromatin. Nature, Lond. 271, 115-122.

Finch, J.T., Lutter, L.C., Rhodes, D., Brown, R.S., Rushton, B., Levitt, M. & Klug, A. (1977). Structure of Nucleosome Core Particles of Chromatin. Nature, Lond. 269, 29-36.

Finch, J.T., Brown, R.S., Rhodes, D., Richmond, T., Rushton, B., Lutter, L.C. & Klug, A. (1981). X-ray Diffraction Study of a New Crystal Form of the Nucleosome Core Showing Higher Resolution. J. molec. Biol. 145, 757-769.

Fujii, S., Wang, A. H.-J., van der Marel, G., van Boom, J.H. &

Rich, A. (1982). Molecular structure of (m5 dC - dG)3: the role of the methyl group on 5-methyl cytosine in stabilizing Z-DNA. Nucl. Acids Res. 10, 7879-7892.

Genest, D., Wahl, P., Erard, M., Champagne, M. & Daune, M. (1982). Fluorescence Anisotropy Decay of Ethidium Bromide Bound to Nucleosomal Core Particles. Biochimie 64, 419-427.

Germond, J.-E., Bellard, M., Oudet, P. & Chambon, P. (1976). Stability of nucleosomes in native and reconstituted chromatins. Nucl. Acids Res. 3, 3173-3192.

Giese, A.C. (1973). Cell Physiology, 4th ed. Philadelphia: W.B. Saunders.

Godfrey, J.E., Eickbush, T.H. & Moudrianakis, E.N. (1980). Reversible Association of Calf Thymus Histones to Form the Symmetrical Octamer (H2A H2B H3 H4)2: A Case of a Mixed-Associating System. Biochemistry 19, 1339-1346.

Grigoryev, S.A., and Krasheninnikov, I.A. (1982). Transient Unfolding of Trypsin-Digested Chromatin Core Particles. Eur. J. Biochem. 129, 119-125.

Harrington, R.E. (1977). DNA chain flexibility and the

structure of chromatin v-bodies. Nucl. Acids Res. 4, 3519-3535.

Harrington, R.E. (1978). Opticohydrodynamic Properties of High-Molecular-Weight DNA. III. The Effects of NaCl Concentration. Biopolymers 17, 919-936.

Harrington, R.E. (1982). Optical Model Studies of Salt-Induced Conformational Transitions in the Nucleosome. Biochemistry 21, 1177-1186.

Harrington, R.E., Uberbacher, E.C. & Bunick, G.J. (1982). Conformation of the HMG 14 nucleosome core complex from flow birefringence. Nucl. Acids Res. 10, 5695-5709.

Hearst, J.E. & Vinograd, J. (1961). The Net Hydration of T-4 Bacteriophage Deoxyribonucleic Acid and the Effect of Hydration on Bouyant Behavior in a Density Gradient at Equilibrium in the Ultracentrifuge. Proc. natl. Acad. Sci., U.S.A. 47, 1005-1014.

Hearst, J.E. (1965). Determination of the Dominant Factors Which Influence the Net Hydration of Native Sodium Deoxyribonucleate. Biopolymers 3, 57-68.

Hoagland, D.R. & Davis, A.R. (1922-1923). The Composition of the Cell Sap of the Plant in Relation to the Absorption of

Ions. J. Gen. Physiol. 5, 629-646.

Hodgkin, A.L. (1958). Ionic movements and electrical activity in giant nerve fibres. Proc. Roy. Soc. B 148, 1-37.

Hogan, M.E. & Jardetzsky, O. (1979). Internal motions in DNA. Proc. natl. Acad. Sci., U.S.A. 76, 6341-6345.

Hogan, M.E. & Jardetzsky, O. (1980). Effect of Ethidium Bromide on Deoxyribonucleic Acid Internal Motions. Biochemistry 19, 2079-2085.

Hogan, M., Wang, J., Austin, R.H., Monitto, C.L. & Hershkowitz, S. (1982). Molecular motion of DNA as measured by triplet anisotropy decay. Proc. natl. Acad. Sci., U.S.A. 79, 3518-22.

Holbrook, S.R. & Kim, S.-H. (1984). The local motion of nucleic acids as determined from crystollographic data. J. molec. Biol., in press.

Honda, B.M., Baillie, D.L., & Candido, E.P.M. (1975). Properties of Chromatin Subunits from Developing Trout Testis. J. biol. Chem. 250, 4643-4647.

Horz, W. & Altenburger, W. (1981). Sequence specific cleavage

of DNA by micrococcal nuclease. Nucl. Acids Res. 9, 2643-2658.

Houssier, C., Lasters, I., Muyldermans, S. & Wyns, L. (1981). Influence of histones H1/H5 on the DNA coiling in the nucleosome - electric dichroism and birefringence study. Int. J. biol. Macromol. 3, 370-376.

Hull, W.E. & Sykes, B.D. (1975). Fluorotyrosine Alkaline Phosphatase: Internal Mobility of Individual Tyrosines and the Role of Chemical Shift Anisotropy as a 19F Nuclear Spin Relaxation Mechanism in Proteins. J. molec. Biol. 98, 121-153.

Hurley, I., Osei-Gyimah, P., Archer, S., Scholes, C.P. & Lerman, L.S. (1982). Torsional Motion and Elasticity of the Deoxyribonucleic Acid Double Helix and Its Nucleosomal Complexes. Biochemistry 21, 4999-5009.

Igo-Kemenes, T., Horz, W. & Zachau, H.G. (1982). Chromatin. A. Rev. Biochem. 51, 89-121.

Igo-Kemenes, T., Omori, A. & Zachau, H. (1980). Non-random arrangement of nucleosomes in satellite I containing chromatin of rat liver. Nucl. Acids Res. 8, 5377-5390.

Isenberg, I. (1979). Histones. A. Rev. Biochem. 48, 159-191.

Ishimura, S., Mita, K. & Zama, M. (1982). Essential Role of Arginine Residues in the Folding of Deoxyribonucleic Acid into Nucleosome Cores. Biochemistry 21, 5329-5334.

Ivanov, V.I., Minchenkova, L.E., Schyolkina, A.K. & Poletayev, A.I. (1973). Different Conformations of Double-Stranded Nucleic Acid in Solution as Revealed by Circular Dichroism. Biopolymers 12, 89-110.

Javaherian, K. & Liu, L.F. (1983). Association of eukaryotic DNA topoisomerase I with nucleosomes and chromosomal proteins. Nucl. Acids Res. 11, 461-472.

Johns, E.W. (ed.) (1982). The HMG Chromosomal Proteins. London: Academic Press.

Jorcano, J.L. & Ruiz-Carillo, A. (1979). H3.H4 Tetramer Directs DNA and Core Histone Octamer Assembly in the Nucleosome Core Particle. Biochemistry 18, 768-774.

Kallenbach, N.R., Mandel, C. & Englander, S.W. (1980). Structure, Fluctuations, and Interactions of Base Pairs in Nucleic Acids Monitored by NMR, Tritium Exchange and Stopped-Flow Hydrogen Deuterium Exchange Measurements. In

Nucleic Acid Geometry and Dynamics (ed. R.H. Sarma), pp. 233-250. New York: Pergamon.

Kam, Z., Borochov, N. & Eisenberg, H. (1981). Dependence of Laser Light Scattering of DNA on NaCl Concentration. Biopolymers 20, 2671-2690.

Keepers, J.W., Kollman, P.A., Weiner, P.K. & James, T.L. (1982). Molecular mechanical studies of DNA flexibility: Coupled backbone torsion angles and base-pair openings. Proc. natl. Acad. Sci., U.S.A. 79, 5537-5541.

Kelley, R.I. (1973). Isolation of a histone IIb1-IIb2 complex. Biochem. Biophys. Res. Commun. 54, 1588-1594.

Kirkwood, J.G. (1954). The General Theory of Irreversible Processes in Solutions of Macromolecules. J. Polymer Sci. 12, 1-14.

Klevan, L., Dattagupta, N., Hogan, M. & Crothers, D.M. (1978). Physical Studies of Nucleosome Assembly. Biochemistry 17, 4533-4540.

Klevan, L. & Crothers, D.M. (1977). Isolation and characterization of a spacerless dinucleosome from H1-depleted

chromatin. Nucl. Acids Res. 4, 4077-4089.

Klug, A., Rhodes, D., Smith, J., Finch, J.T. & Thomas, J.O. (1980). A low resolution structure for the histone core of the nucleosome. Nature, Lond. 287, 509-516.

Kopka, M.L., Fratini, A.V., Drew, H.R. & Dickerson, R.E. (1983). Ordered Water Structure around a B-DNA Dodecamer - A Quantitative Study. J. molec. Biol. 163, 129-146.

Kornberg, A. (1980). DNA Replication. San Francisco: W.H. Freeman.

Kornberg, R.D. & Thomas, J.O. (1974). Chromatin Structure: oligomers of the histones. Science, N.Y. 184, 865-868.

Kornberg, R.D. (1977). Structure of Chromatin. A. Rev. Biochem. 46, 931-954.

Kovacic, R.T. (1977). Hydrodynamic Properties of Homogeneous Double-Stranded DNA. Ph.D. Thesis, Oregon State University, Corvallis, OR.

Kovacic, R.T. & van Holde, K.E. (1977). Sedimentation of Homogeneous Double-Strand DNA Molecules. Biochemistry 16,

1490-1498.

Kuntz, I.D. & Kauzmann, W. (1974). Hydration of Proteins and Polypeptides. Adv. Prot. Chem. 28, 239-345.

Laemmli, U.K. (1970). Cleavage of Structural Proteins during the Assembly of the Head of Bacteriophage T4. Nature, Lond. 227, 680-685.

Landau, L.D. & Lifschitz, E.M. (1958). Statistical Physics. Reading, MA: Addison-Wesley.

Laskey, R.A., Mills, A.D. & Morris, N.R. (1977). Assembly of SV40 Chromatin in a Cell-free System from Xenopus Eggs. Cell 10, 237-243.

Laskey, R.A. & Earnshaw, W.C. (1980). Nucleosome assembly. Nature, Lond. 286, 763-767.

Lattman, E., Burlingame, R., Hatch, C. & Moudrianakis, E.N. (1982). Crystallization of the Tetramer of Histones H3 and H4. Science, N.Y. 216, 1016-1018.

Launer, R.L. & Wilkinson, G.N. (eds.). (1979). Robustness in Statistics. New York: Academic Press.

Lee, J.C. & Timasheff, S.N. (1981). The Stabilization of Proteins by Sucrose. J. biol. Chem. 256, 7193-7201.

Lee, K.P., Baxter, H.J., Guillemette, J.G., Lawford, H.J. & Lewis, P.N. (1982). Structural studies on yeast nucleosomes. Can. J. Biochem. 60, 379-388.

Lehninger, A.L. (1975). Biochemistry, 2nd ed. New York: Worth.

Levinger, L. & Varshavsky, A. (1980). High-resolution fractionation of nucleosomes: Minor particles, "whiskers", and separation of mononucleosomes containing and lacking A24 semihistone. Proc. natn. Acad. Sci., U.S.A. 77, 3244-3248.

Levitt, M. (1978). How many Base-pairs per turn does DNA have in solution and in chromatin? Some theoretical calculations. Proc. natl. Acad. Sci., U.S.A. 75, 640-644.

Lewin, B. (1980). Gene Expression, vol. II, 2nd. ed. New York: J. Wiley & Sons.

Lewin, B. (1983). Genes. New York: J. Wiley & Sons.

Lewis, G.N. & Randall, M. (1961). Thermodynamics, 2nd ed.

(revised by K.S. Pitzer and L. Brewer). New York: McGraw-Hill.

Libertini, L.J. & Small, E.W. (1980). Salt induced transitions of chromatin core particles studied by tyrosine fluorescence anisotropy. Nucl. Acids Res. 8, 3517-3534.

Libertini, L.J. & Small, E.W. (1982). Effects of pH on Low-Salt Transition of Chromatin Core Particles. Biochemistry 21, 3327-3334.

Lilley, D.M.J., Jacobs, M.F. & Houghton, M. (1979). The nature of the interaction of nucleosomes with a eukaryotic RNA polymerase II. Nucl. Acids Res. 7, 377-399.

Lilley, D.M.J. & Pardon, J.F. (1979). Structure and Function of Chromatin. A. Rev. Genet. 13, 197-233.

Lilley, D.M.J. & Tatchell, K. (1977). Chromatin core particle unfolding induced by tryptic cleavage of histones. Nucl. Acids Res. 4, 2039-2055.

Lohr, D., Kovacic, R.T. & van Holde, K.E. (1977). Quantitative Analysis of the Digestion of Yeast Chromatin by Staphylococcal Nuclease. Biochemistry 16, 463-471.

Lu, A.L., Steege, D.A. & Stafford, D.W. (1980). Nucleotide sequence of a 5S ribosomal RNA gene in the sea urchin Lytechinus variegatus. Nucl. Acids Res. 8, 1839-1853.

Lutter, L.C. (1978). Kinetic Analysis of Deoxyribonuclease I Cleavages in the Nucleosome Core: Evidence for a DNA Superhelix. J. molec. Biol. 124, 391-420.

Lutter, L.C. (1979). Precise location of DNAase I cutting sites in the nucleosome core determined by high resolution gel electrophoresis. Nucl. Acids Res. 6, 41-56.

Mandel, C., Kallenbach, N.R. & Englander, S.W. (1979). Base-pair Opening and Closing Reactions in the Double Helix. A Stopped-Flow Hydrogen Exchange Study in Poly(rA).Poly(rU). J. molec. Biol. 135, 391-411.

Maniatis, T., Fritsch, E.F. & Sambrook, J. (1982). Molecular Cloning - A Laboratory Manual. Cold Spring Harbor: Cold Spring Harbor Laboratory.

Maniatis, T., Jeffrey, A. & van de Sande, H. (1975). Chain Length Determination of Small Double- and Single-Stranded DNA Molecules by Polyacrylamide Gel Electrophoresis. Biochemistry 14, 3787-3794.

Manning, G.S. (1978). The molecular theory of polyelectrolyte solutions with applications to the electrostatic properties of polynucleotides. Quart. Rev. Biophys. 11, 179-246.

Manning, G.S. (1979). Counterion Binding in Polyelectrolyte Theory. Acc. chem. Res. 12, 443-449.

Mansy, S., Engstrom, S.K. & Peticolas, W.L. (1976). Laser raman identification of an interaction site on DNA for arginine containing histones in chromatin. Biochem. Biophys. Res. Commun. 68, 1242-1247.

Mardian, J.K.W., Paton, A.E., Bunick, G.J. & Olins, D.E. (1980). Nucleosome Cores Have Two Specific Binding Sites for Nonhistone Chromosomal Proteins HMG 14 and HMG 17. Science, N.Y. 209, 1534-1536.

Maxam, A.M. & Gilbert, W. (1977). A new method for sequencing DNA. Proc. natl. Acad. Sci., U.S.A. 74, 560-564.

McCammon, J.A. (1984). Protein Dynamics. Rep. Prog. Phys. 47, 1-46.

McCarty, K.S. Jr., Vollmer, R.T. & McCarty, K.S. (1974).

Improved Computer Program Data for the Resolution and Fractionation of Macromolecules by Isokinetic Sucrose Density Gradient Sedimentation. Anal. Biochem. 61, 165-183.

McCarthy, M.P., Steffen, P.K., Allewell, N.M., Benedict, R.C., Moudrianakis, E.N. & Ackers, G.K. (1984). Effects of Ionic Strength and State of Assembly on Kinetics of Hydrogen Exchange of Calf Thymus Histones. Biochemistry 23, 2227-2230.

McClave, J.T. & Dietrich, F.H. II. (1979). Statistics. San Francisco: Dellen.

McGhee, J.D. & von Hippel, P.H. (1974). Theoretical Aspects of DNA-Protein Interactions - Cooperative and Non-Cooperative Binding of Large Ligands to a One-Dimensional Homogeneous Lattice. J. molec. Biol. 86, 469-489.

McGhee, J.D. & Felsenfeld, G. (1979). Reaction of nucleosome DNA with dimethyl sulfate. Proc. natl. Acad. Sci., U.S.A. 76, 2133-2137.

McGhee, J.D. & Felsenfeld, G. (1980a). Nucleosome Structure. A. Rev. Biochem. 49, 1115-1156.

McGhee, J.D. & Felsenfeld, G. (1980b). The number of

charge-charge interactions stabilizing the ends of nucleosomal DNA. Nucl. Acids Res. 8, 2751-2769.

McGhee, J.D., Felsenfeld, G. & Eisenberg, H. (1980). Biophys. J. 32, 261-270.

Mengeritsky, G. & Trifonov, E.N. (1983). Nucleotide Sequence-Directed Mapping of the Nucleosomes. Nucl. Acids Res. 11, 3833-3851.

Miles Laboratories, Inc. (1980). Canalco SAGE Disc Electrophoresis. Elkhart, IN: Miles Laboratories, Inc.

Millar, D.P., Robbins, R.J. & Zewail, A.H. (1980). Direct observation of the torsional dynamics of DNA and RNA by picosecond spectroscopy. Proc. natl. Acad. Sci., U.S.A. 77, 5593-5597.

Miller, K.I. & van Holde, K.E. (1982). The Structure of Octopus dofleini Hemocyanin. Comp. Biochem. Physiol. B 73, 1013-1018.

Mills, A.D., Lasky, R.A., Black, P. & DeRobertis, E.M. (1980). An Acidic Protein Which Assembles Nucleosomes in vitro is the Most Abundant Protein in Xenopus Oocyte Nuclei. J. molec. Biol. 139, 561-568.

Mirzabekov, A.D. (1980). Nucleosomes Structure and its Dynamic Transitions. Quart. Rev. Biophys. 13, 255-295.

Mirzabekov, A.D., Shick, V.V., Belyavsky, A.V. & Bavykin, S.G. (1978). Primary organization of nucleosome core particle of chromatin: Sequence of histone arrangement along DNA. Proc. natl. Acad. Sci., U.S.A. 75, 4184-4188.

Moore, W.J. (1972). Physical Chemistry, 4th edn. Englewood Cliffs: Prentice-Hall.

Moss, T., Cary, P.D., Crane-Robinson, C. & Bradbury, E.M. (1976). Physical Studies on the H3/H4 Histone Tetramer. Biochemistry 15, 2261-2267.

New England Biolabs. (1983-1984). Catalogue. Beverly, MA: New England Biolabs.

Nickol, J., Behe, M. & Felsenfeld, G. (1982). Effect of the B-Z transition in poly(dG-m5dC).poly(dG-m5dC) on nucleosome formation. Proc. natl. Acad. Sci., U.S.A. 79, 1771-1775.

Nicolini, C. (1983). Chromatin Structure: From Nuclei to Genes. Anticancer Res. 3, 63-86.

Olins, A.L., Carlson, R.D., Wright, E.B. & Olins, D.E. (1976). Nucl. Acids Res. 3, 3271-3291.

Olins, D.E. & Olins, A.L. (1978). Nucleosomes: The Structural Quantum in Chromosomes. Amer. Scientist 66, 704-711.

Patel, D.J., Kozlowski, S.A., Marky, L.A., Broka, C., Rice, J.A., Itakura, K. & Breslauer, K.J. (1982). Premelting and Melting Transitions in the d(CGCGAATTCGCG) Self-Complementary Duplex in Solution. Biochemistry 21, 428-436.

Paton, A.E., Wilkinson-Singley, E. & Olins, D.E. (1983). Nonhistone Nuclear High Mobility Group Proteins 14 and 17 Stabilize Nucleosome Core Particles. J. biol. Chem. 258, 13221-13229.

Pech, M., Igo-Kemenes, T. & Zachau, H. (1979). Nucleotide sequence of a highly repetitive component of rat DNA. Nucl. Acids Res. 7, 417-432.

Peck, L.J. & Wang, J.C. (1983). Energetics of B-to-Z transition in DNA. Proc. natl. Acad. Sci., U.S.A. 80, 6206-6210.

Philip, M., Jamaluddin, M., Sastry, R.V.R. & Chandra, H.S.

(1979). Nucleosome Core histone complex isolated gently and rapidly in 2 M NaCl is octameric. Proc. natl. Acad. Sci., U.S.A. 76, 5178-5182.

Pohl, F.M. & Jovin, T.M. (1972). Salt-induced Co-operative Conformational Change of a Synthetic DNA: Equilibrium and Kinetic Studies with Poly(dG-dC). J. molec. Biol. 67, 375-396.

Prior, C.P., Cantor, C.R., Johnson, E.M., Littau, V.C. & Allfrey, V.G. (1983). Reversible Changes in Nucleosome Structure and Histone H3 Accessibility in Transcriptionally Active and Inactive States of rDNA Chromatin. Cell 34, 1033-1042.

Prunell, A. (1983). Periodicity of Exonuclease III Digestion of Chromatin and the Pitch of Deoxyribonucleic Acid on the Nucleosome.
Biochemistry 22, 4887-4894.

Rattle, H.W.E., Kneale, G.G., Baldwin, J.P., Matthews, H.R., Crane-Robinson, C., Cary, P.D., Carpenter, B.G., Suau, P. & Bradbury, E.M. (1979). Histone Complexes, Nucleosomes, Chromatin and Cell-Cycle Dependent Modification of Histones. In Chromatin Structure and Function, Part B (NATO Advanced Study Institute Series A, Vol. 21b) (ed. C. Nicolini), pp. 451-513.

New York: Plenum.

Record, M.T., Jr., Anderson, C.F. & Lohman, T.M. (1978). Thermodynamic analysis of ion effects on the binding and conformational equilibria of proteins and nucleic acids: the roles of ion association or release, screening, and ion effects on water activity. Quart. Rev. Biophys. 11, 103-178.

Record, M.T. Jr., Mazur, S.J., Melancon, P., Roe, J.-H., Shaner, S.L. & Unger, L. (1981). Double Helical DNA: Conformations, Physical Properties, and Interactions with Ligands. A. Rev. Biochem. 50, 997-1024.

Riemer, S.C. & Bloomfield, V.A. (1978). Packaging of DNA in Bacteriophage Heads: Some Considerations on Energetics. Biopolymers 17, 785-794.

Riley, D. & Weintraub, H. (1978). Nucleosomal DNA is Digested to Repeats of 10 Bases by Exonuclease III. Cell 13, 281-293.

Rill, R. & Oosterhof, D.K. (1982). The Accessibilities of Histones in Nucleosome Cores to an Arginine-specific Protease. J. biol. Chem. 257, 14875-14880.

Roark, E.D., Geoghegan, T.F. & Keller, G.H. (1974). A

Two-Subunit Histone Complex from Calf Thymus. Biochem. Biophys. Res. Commun. 59, 542-547.

Robinson, B.H., Forgacs, G., Dalton, L.R. & Frisch, H.L. (1980). A simple model for internal motion of DNA based upon EPR studies in the slow motion region. J. chem. Phys. 73, 4688-4692.

Rosenberg, J.M., Seeman, N.C., Day, R.O. & Rich, A. (1976). RNA Double-helical Fragments at Atomic Resolution: II. The Crystal Structure of Sodium Guanylyl-3',5'-Cytidine Nonahydrate. J. molec. Biol. 104, 145-167.

Rubin, R.L. & Moudrianakis, E.N. (1975). The F3-F2a1 Complex as a Unit in the Self-Assembly of Nucleoproteins. Biochemistry 8, 1718-1726.

Ruiz-Carillo, A. & Jorcano, J.L. (1979). An Octamer of Core Histones in Solution: Central Role of the H3.H4 Tetramer in the Self-Assembly. Biochemistry 18, 760-768.

Russev, G., Vassilev, L. & Tsanev, R. (1980a). Salt-induced structural changes in core particles. Molec. Biol. Rep. 6, 45-49.

Sakuma, K., Matsumura, Y. & Senshu, T. (1984). Formation of transcribing mononucleosome-eukaryotic RNA polymerase II complexes in vitro as a simple model of active chromatin. Nucl. Acids Res. 12, 1415-1426.

Sandeen, G., Wood, W.I. & Felsenfeld, G. (1980). The interaction of high mobility proteins HMG 14 and 17 with nucleosomes. Nucl. Acids Res. 8, 3757-3778.

Sanders, M.M. (1978). Fractionation of Salt Elution from Micrococcal Nuclease-Digested Nuclei. J. Cell Biol. 79, 97-109.

Sanger, F., Air, G.N., Barrell, B.G., Brown, N.L., Coulson, A.R., Fiddes, J.C., Hutchison, C.A. III, Slocombe, P.M. & Smith, M. (1977). Nucleotide sequence of bacteriophage OX174 DNA. Nature, Lond. 265, 687-695.

Schellman, J.A. (1974). Flexibility of DNA. Biopolymers 13, 217-226.

Schlaeger, E.J., Vantelge, H.J., Klempnau, K.H. & Knippers, R. (1978). Association of DNA-polymerase with nucleosomes from mammalian-cell chromatin.
Eur. J. Biochem. 84, 95-102.

Schroter, H. & Bode, J. (1982). The Binding Sites for Large and Small High-Mobility-Group (HMG) Proteins. Studies on HMG-Nucleosome Interactions in vitro. Eur. J. Biochem. 127, 429-436.

Seeman, N.C., Rosenberg, J.M. & Rich, A. (1976).Sequence-specific recognition of double helical nucleic acids by proteins. Proc. natl. Acad. Sci., U.S.A. 73, 804-808.

Seeman, N.C., Rosenberg, J.M., Suddath, F.L., Kim, J.J.P. & Rich, A. (1976). RNA Double-helical Fragments at Atomic Resolution: I. The Crystal and Molecular Structure of Sodium Adenylyl-3',5'-Uridine Hexahydrate. J. molec. Biol. 104, 109-144.

Serwer, P. & Allen, J.L. (1984). Conformation of Double-Stranded DNA during Agarose Gel Electrophoresis: Fractionation of Linear and Circular Molecules with Molecular Weights between 3 x 10^6 and 26 x 10^6. Biochemistry 23, 922-927.

Shaw, B.R., Herman, T.M., Kovacic, R.T., Beaudreau, G.S. & van Holde, K.E. (1976). Analysis of subunit organization in chicken erythrocyte chromatin. Proc. natn. Acad. Sci., U.S.A. 73, 505-509.

Shaw, J. (1955). Ionic Regulation in the Muscle Fibres of Carcinus maenas. I. The Electrolyte Composition of Single Fibres. J. exptl. Biol. 32, 383-396.

Shaw, P.A., Sahasrabuddhe, C.G., Hodo, H.G. III, & Saunders, G.F. (1978). Transcription of nucleosomes from human chromatin. Nucl. Acids Res. 5, 2999-3012.

Shick, V.V, Belyavsky, A.V., Bavykin, S.G. & Mirzabekov, A.D. (1980). Primary Organization of the Nucleosome Core Particles. Sequential Arrangement of Histones along DNA. J. molec. Biol. 139, 491-517.

Shindo, H. (1980). NMR Relaxation Processes of 31P in Macromolecules. Biopolymers 19, 509-522.

Shindo, H. & McGhee, J.D. (1980). 31P-NMR Studies of DNA in Nucleosome Core Particles. Biopolymers 19, 523-537.

Shore, J.E. & Zwanzig, R. (1975). Dielectric relaxation and dynamic susceptibility of a one-dimensional model for perpindicular-dipole polymers. J. chem. Phys. 63, 5445-5458.

Simpson, R.T. (1978a). Structure of Chromatin Containing

Extensively Acetylated H3 and H4. Cell 13, 691-699.

Simpson, R.T. (1978b). Structure of the Chromatosome, a Chromatin Particle Containing 160 Base Pairs of DNA and All the Histones. Biochemistry 17, 5524-5531.

Simpson, R.T. (1979). Mechanism of a Reversible, Thermally Induced Conformational Change in Chromatin Core Particles. J. biol. Chem. 254, 10123-10127.

Simpson, R.T. & Shindo, H. (1979). Conformation of DNA in chromatin core particles containing poly(dAdT).poly(dAdT) studied by 31P NMR spectroscopy. Nucleic Acids Res. 7, 481-492.

Simpson, R.T. & Stafford, D.W. (1983). Structural Features of a phased nucleosome core particle. Proc. natl. Acad. Sci., U.S.A. 80, 51-55.

Skadrani, E., Mizon, J., Sautiere, P. & Biserte, G. (1972). Etude de la fraction F2b des histones de thymus de veau. Biochimie 54, 1267-1272.

Sobell, H.M. (1980). Structural and Dynamic Aspects of Drug Intercalation into DNA and RNA. In Nucleic Acid Geometry and Dynamics (ed. R.H. Sarma), pp. 289-323. New York: Pergamon.

Sobell, H.M., Tsai, C., Gilberg, S.G., Jain, S.C. & Sakore, T.D. (1976). Organization of DNA in Chromatin. Proc. natn. Acad. Sci., U.S.A. 73, 3068-3072.

Sokolnikoff, I.S. (1939). Advanced Calculus. New York: McGraw-Hill.

Sollner-Webb, B., Camerini-Otero, R.D. & Felsenfeld, G. (1976). Chromatin Structure as probed by nucleases and proteases: evidence for the central role of histones H3 and H4. Cell 9, 179-193.

Sollner-Webb, B., Melchior, W. Jr. & Felsenfeld, G. (1978). DNAase I, DNAase II and Staphylococcal Nuclease Cut at Different, Yet Symmetrically Located, Sites in the Nucleosome Core. Cell 14, 611-627.

Soumpasis, M. (1984). Calculation of the B-to-Z Transition in DNA, From Statistical Mechanics. Proc. natl. Acad. Sci., U.S.A., in press.

Sperling, R. & Wachtel, E.J. (1981). The Histones. Adv. Prot. Chem. 34, 1-60.

Stacks, P.C. & Schumaker, V.N. (1979). Nucleosome dissociation and transfer in concentrated salt solutions. Nucl. Acids Res. 7, 2457-2467.

Stein, A. (1979). DNA Folding by Histones: The Kinetics of Chromatin Core Particle Reassembly and the Interaction of Nucleosomes with Histones. J. molec. Biol. 130, 103-134.

Stein, A., Bina-Stein, M. & Simpson, R.T. (1977). Crosslinked histone octamer as a model of the nucleosome core. Proc. natl. Acad. Sci., U.S.A. 74, 2780-2784.

Stein, A. & Page, D. (1980). Core Histone Associations in Solutions of High Salt. J. biol. Chem. 255, 3629-3637.

Stein, A. & Townsend, T. (1983). HMG 14/17 binding affinities and DNAase I sensitivities of nucleoprotein particles. Nucl. Acids Res. 11, 6803-6819.

Stein, A., Whitlock, J.P. & Bina, M. (1979). Acidic polypeptides can assemble both histones and chromatin in vitro at physiological ionic strength. Proc. natl. Acad. Sci., U.S.A. 76, 5000-5004.

Steinhardt, J. & Reynolds, J.A. (1969). Multiple Equilibria in

Proteins. New York: Academic Press.

Steinmetz, M., Streek, R.E. & Zachau, H.G. (1978). Eur. J. Biochem. 83, 615-628.

Stratling, W.H. (1979). Role of Histone H1 in the Conformation of Oligonucleosomes as a Function of Ionic Strength. Biochemistry 18, 596-603.

Suau, P., Bradbury, E.M. & Baldwin, J.P. (1979). Higher-Order Structures of Chromatin in Solution. Eur. J. Biochem. 97, 593-602.

Suck, D., Manor, D.C. & Saenger, W. (1976). The Structure of a Trinucleoside Diphosphate: Adenylyl-(3',5')-adenylyl-(3',5')-adenosine Hexahydrate. Acta Cryst. B 32, 1727-1737.

Sussman, J.L., Seeman, N.C., Kim, S.-H. & Berman, H.M. (1972). Crystal Structure of a Naturally Occurring Dinucleoside Phosaphate: Uridylyl 3',5'-adenosine phosphate. Model for RNA Chain Folding. J. molec. Biol. 66, 403-421.

Sussman, J.L. & Trifonov, E.N. (1978). Possibility of Nonkinked packing of DNA in chromatin. Proc. natl. Acad. Sci., U.S.A. 75,

103-107.

Sutcliffe, J.G. (1979). Complete Nucleotide Sequence of the Escherichia coli Plasmid pBR322. Cold Spring Harbor Symp. quant. Biol. 43, 77-90.

Svedberg, T. & Pederson, K.O. (1940). The Ultracentrifuge. Cambridge: Oxford University Press.

Swanstrom, R. & Shank, P.R. (1978). X-Ray Intensifying Screens Greatly Enhance the Detection by Autoradiography of the Radioactive Isotopes 32P and 125I. Anal. Biochem. 86, 184-192.

Swerdlow, P.S. & Varshavsky, A. (1983). Affinity of HMG17 for a mononucleosome is not influenced by the presence of ubiquitin-H2A semihistone but strongly depends on DNA fragment size. Nucl. Acids Res. 11, 387-401.

Tao, T. (1969). Time-Dependent Fluorescence Depolarization and Brownian Rotational Diffusion Coefficients of Macromolecules. Biopolymers 8, 609-632.

Tatchell, K. & van Holde, K.E. (1977). Reconstitution of Chromatin Core Particles. Biochemistry 16, 5295-5303.

Tatchell, K. & van Holde, K.E. (1978). Compact oligomers and nucleosome phasing. Proc. natn. Acad. Sci., U.S.A. 75, 3583-3587.

Tatchell, K. & van Holde, K.E. (1979). Nucleosome Reconstitution: Effect of DNA Length on Nucleosome Structure. Biochemistry 18, 2871-2880.

Thoma, F., Koller, T. & Klug, A. (1979). Involvement of histone H1 in the organization of the nucleosome and of the salt-dependent superstructures of chromatin. J. Cell Biol. 83, 403-427.

Thomas, J.O. & Kornberg, R.D. (1975). An octamer of histones in chromatin and free in solution. Proc. natn. Acad. Sci., U.S.A. 72, 2626-2630.

Thomas, J.O. & Oudet, P. (1979). Complexes of the argining-rich histone tetramer (H3)2(H4)2 with negatively supercoiled DNA: electron microscopy and chemical crosslinking. Nucl. Acids Res. 7, 611-623.

Tidor, B., Irikura, K.K., Brooks, B.R. & Karplus, M. (1983). Dynamics of DNA Oligomers. J. biomol. Struct. Dyn. 1, 231-252.

Todd, R.D. & Garrard, W.T. (1977). Two-Dimensional Electrophoretic Analysis of Polynucleosomes. J. biol. Chem. 252, 4729-4738.

Tsaneva, I. (1980). Comparative-Study on the Thermal-Denaturation of Different Nucleosome Preparations. Int. J. Biochem. 11, 211-216.

Tunis, M.-J. B. & Hearst, J.E. (1968). On the Hydration of DNA. I. Preferential Hydration and Stability of DNA in Concentrated Trifluoroacetate Solution. Biopolymers 6, 1325-1344.

Uberbacher, E.C., Mardian, J.K.W., Rossi, R.M., Olins, D.E. & Bunick, G.J. (1982). Neutron scattering studies and modeling of high mobility group 14 core nucleosome complex. Proc. natl. Acad. Sci., U.S.A. 79, 5258-5262.

Uberbacher, E.C., Ramakrishnan, V., Olins, D.E. & Bunick, G.J. (1983). Neutron Scattering Studies of Nucleosome Structure at Low Ionic Strength. Biochemistry 22, 4916-4923.

Urban, M.K., Franklin, S.G. & Zwiedler, A. (1979). Isolation and Characterization of the Histone Variants in Chicken Erythrocytes. Biochemistry 18, 3952-3959.

van Holde, K.E. (1984). Physical Biochemistry, 2nd Ed. Englewood Cliffs: Prentice Hall.

van Holde, K.E. (1986). Chromatin. Heidelberg: Springer-Verlag. (In preparation.)

van Holde, K.E. & Isenberg, I. (1975). Histone Interactions and Chromatin Structure. Acc. chem. Res. 8, 327-335.

van Holde, K.E. & Weischet, W.O. (1978). Boundary Analysis of Sedimentation-Velocity Experiments with Monodisperse and Paucidisperse Solutes. Biopolymers 17, 1387-1403.

van Holde, K.E. & Yager, T.D. (1985). Nucleosome Motion: Evidence and Models. In Chromatin Structure and Function: Proceedings of the 4th Course on Structure and Function of Genetic Apparatus (NATO Advanced Study Institute Series) (ed. C. Nicolini). New York: Plenum. (In press.)

Vassilev, L., Russev, G. & Tsanev, R. (1981). Heterogeneity of nucleosomes upon dissociation with salts. Int. J. Biochem. 13, 1247-1255.

Vologodskii, A.V., Lukashin, A.V., Anshelevich, V.V. & Frank-Kamenetskii, M.D. (1979). Fluctuations in superhelical

DNA. Nucl. Acids. Res. 6, 967-982.

Voordouw, G. & Eisenberg, H. (1978). Binding of additional histones to chromatin core particles. Nature, Lond. 273, 446-448.

Wang, C.H., Willis, D.L. & Loveland, Q.D. (1975). Radiotracer Methodology in the Biological, Environmental, and Physical Sciences. Englewood Cliffs: Prentice-Hall.

Wang, J., Hogan, M. & Austin, R.H. (1982). DNA motions in the nucleosome core particle. Proc. natl. Acad. Sci., U.S.A. 79, 5896-5900.

Wang, J.C. (1982). The Path of DNA in the Nucleosome. Cell 29, 724-726.

Wang, J.H. (1954a). Theory of the Self-Diffusion of Water in Protein Solutions. A New Method for Studying the Hydration and Shape of Protein Molecules. J. Am. chem. Soc. 75, 4755-4763.

Wang, J.H. (1954b). The Self-diffusion Coefficients of Water and Ovalbumin in Aquaeous Ovalbumin Solutions at 10 C. J. Am. chem. Soc. 75, 4763-4765.

Wang, J.H. (1955). The Hydration of Desoxyribonucleic Acid. J. Am. chem. Soc. 77, 258-260.

Watson, J.D. (1976). Molecular Biology of the Gene, 3rd edn. Menlo Park: W.A. Benjamin.

Weber, K. & Osborn, M. (1969). The Reliability of Molecular Weight Determinations by Dodecyl Sulfate - Polyacrylamide Gel Electrophoresis. J. biol. Chem. 244, 4406-4412.

Weintraub, H., Worcel, A. & Alberts, B. (1976). A Model for Chromatin Based upon Two Symmetrically Paired Half-Nucleosomes. Cell 9, 409-417.

Weisbrod, S. (1982). Properties of active nucleosomes as revealed by HMG 14 and 17 chromatography. Nucl. Acids Res. 10, 2017-2042.

Weisbrod, S. & Weintraub, H. (1981). Isolation of Actively Transcribed Nucleosomes Using Immobilized HMG 14 and 17 and an Analysis of a-Globin Chromatin. Cell 23, 391-400.

Weischet, W.O. (1979). On the de novo formation of compact oligonucleosomes at high ionic strength. Evidence for nucleosomal sliding in high salt. Nucleic Acids Res. 7,

291-304.

Weischet, W.O., Tatchell, K., van Holde, K.E. & Klump, H. (1978). Thermal Denaturation of Nucleosome Core Particles. Nucleic Acids Res. 5, 139-160.

Whitlock, J.P. Jr. (1979). Conformation of the Chromatin Core Particle is Ionic Strength-Dependent. J. biol. Chem. 254, 5684-5689.

Whitlock, J.P. Jr. & Stein, A. (1978). Folding of DNA by Histones Which Lack Their NH2-terminal Regions. J. biol. Chem. 253, 3857-3861.

Wilhelm, M.L. & Wilhelm, F.X. (1980). Conformation of Nucleosome Core Particles and Chromatin in High Salt Concentration. Biochemistry 19, 4327-4331.

Wing, R.M., Drew, H.R., Takano, T., Broka, C., Tanaka, S., Itakura, K. & Dickerson, R.E. (1980). Crystal structure analysis of a complete turn of B-DNA. Nature, Lond. 287, 755-758.

Wishborn, E.W. (ed.). (1928). International Critical Tables, Vol. III and V. New York: McGraw Hill.

Wittig, S. & Wittig, B. (1982). Function of a Transfer-RNA Gene Promoter Depends on Nucleosome Position. Nature, Lond. 297, 31-38.

Woessner, D.E. (1962). Nuclear Spin Relaxation in Ellipsoids Undergoing Rotational Brownian Motion. J. chem. Phys. 37, 647-654.

Wolf, B. & Hanlon, S. (1975). Structural Transitions of Deoxyribonucleic Acid in Aquaeous Electrolyte Solutions. II. The Role of Hydration. Biochemistry 14, 1661-1670.

Wong, N.T.N. & Candido, E.P.M. (1978). Histone H3 Thiol Reactivity as a Probe of Nucleosome Structure. J. biol. Chem. 253, 8263-8268.

Woodcock, C.L.F. & Frado, L.-L.Y. (1977). Ultrastructure of Chromatin Subunits during Unfolding, Histone Depletion, and Reconstitution. Cold Spring Harb. Symp. quant. Biol. 42, 43-55.

Wray, W., Boulikas, T., Wray, V. P. & Hancock, R. (1981). Silver Staining of Proteins in Polyacrylamide Gels. Anal. Biochem. 118, 197-203.

Wu, H.-M., Dattagupta, N., Hogan, M. & Crothers, D.M. (1980). Unfolding of Nucleosomes by Ethidium Binding. Biochemistry 19, 626-634.

Yager, T.D. & van Holde, K.E. (1984). Dynamics and Equilibria of Nucleosomes at Elevated Ionic Strength. J. biol. Chem. 259, 4212-4222.

Yemm, E.W. & Willis, A.J. (1954). The Estimation of Carbohydrates in Plant Extracts by Anthrone. Biochem. J. 57, 508-514.

Yuhasz, S.C., Kan, L.-S. & Ts'o, P.O.P. (1984). NMR studies on 31P relaxation mechanisms in trimethylphosphate as a model for nucleic acid phosphodiester linkage. J. Am. chem. Soc., in press.

Zachau, H.G. & Igo-Kemenes, T. (1981). Face to Phase with Nucleosomes. Cell 24, 597-598.

Zama, M., Bryan, P.N., Harrington, R.E., Olins, A.L. & Olins, D.E. (1977). Conformational States of Chromatin. Cold Spring Harb. Symp. quant. Biol. 42, 31-41.

Zayetz, V.W., Bavykin, S.G., Karpov, V.L. & Mirzabekov, A.D.

(1981). Stability of the Primary Organization of Nucleosome core particles upon some conformational transitions. Nucl. Acids Res. 9, 1053-1068.

Zuiderweg, E.R.P., Scheek, R.M., Veeneman, G., van Boom, J.H., Kaptein, R., Ruterjans, H. & Beyreuther, K. (1981). 1H NMR studies of lac-operator DNA fragments. Nucl. Acids Res. 9, 6553-6569.